Characterization of the interaction between high-risk human papillomaviruses and the host protein kinase A pathway.

By

Paul McCormack

A thesis submitted to the University of Birmingham for the degree of

DOCTOR OF PHILOSOPHY

Institute of Cancer and Genomic Sciences

College of Medical and Dental Sciences

University of Birmingham

September 2019

ABSTRACT

High-risk human papillomaviruses (HPV) infect squamous epithelia and cause hyperproliferative lesions that can progress to cancer. During infection, the virus interacts with and regulates the host kinome, which has important implications for viral and cellular protein function. The cyclic AMP (cAMP) dependent protein kinase A (PKA) phosphorylates several viral proteins and altered activity of this pathway may be relevant for oncogenic progression of HPV infections; however, whether the virus modulates the activity of PKA during infection is unclear. Using a bioluminescent resonance energy transfer-based approach, HPV18 replication was consistently associated with increased activity of the PKA pathway, occurring concomitantly with increased levels of cAMP; this was partially dependent on the HPV E5 oncoprotein. Additionally, biochemical analysis showed that the virus interacted with a nuclear regulator of PKA-RII signalling, the A-kinase-anchoring protein 95 (AKAP95). This interaction was mediated by the PSD95/DLG/ZO-1 (PDZ)-binding motif of the E6 oncoprotein, requiring the polarity protein hScrib and PKA. Intriguingly, E6 regulated AKAP95-PKA binding and silencing of the AKAP in a physiological HPV18 replication model showed that it regulated expression of E6 targets Dlg1, hScrib and p53. Thus, E6 targeting of AKAP95 may be relevant for control of nuclear PKA signalling in order to facilitate virus replication.

ACKNOWLEDGEMENTS

I would like to first acknowledge the endless help, support and encouragement from my supervisor Dr Sally Robert over the past five years, both during my time in the laboratory from a wide-eyed and very eager masters student throughout my PhD and in the write-up period. Her constant reminder of the thesis being ‘almost there!’ has been a great source of support and laughter throughout the writing process and I could have not completed the PhD without her. Thanks must also go to my co-supervisor Dr Jo Parish who, despite our disagreements about what constitutes time zero in a BRET assay, has been a great source of encouragement throughout the entire process.

I would also like to acknowledge the help of Professor Jane McKeating and Dr Mandy Diskar who taught me a great deal about PKA during my MRes year and without whom a great deal of this work would not be possible.

Thanks must go to the world’s greatest post-doc Dr Karen Campos-León, not only for her endless help and support in the laboratory but also for being a great friend and excellent karaoke partner in tissue culture. Thank you also to Dr Ieisha Pentland, my partner in crime, for all the laughs, great nights out and help over the past few years. My time in Birmingham would not have been the same without her.

In addition, I would like to acknowledge all the great friends I made in WX1.14 over the years, including Danny who helped me with my Southern blotting when I couldn’t cope with any more radioactivity work in final year but also for being a great friend, as well as the BMedSci student Helena who contributed to the domain mapping experiments, Shabana, Amalia, Rachel, Megan and various others for being a source of laughter.

I would also like to thank all of my friends, notably James, Aaron, Chloe, Anthony, Toni, April, Holly and Iain, who learnt soon enough to stop asking how my cells are and focused instead on sending messages of encouragement when I inevitably complained about an experiment going wrong.

Thanks must also go to all members of the McCormack clan, Ev, Gaz and our Jenny, who provided plenty of encouragement over the years, particularly in the final write-up period.

Finally, I would like to thank my long-suffering partner Martyn who has put up with me spending who knows how many nights at my desk writing, as well as me being grumpy and declining social invitations to write. He has helped keep me sane throughout this entire process and supplied me with sweets and cups of tea; I could not have done this without him.

This thesis is dedicated to all those I have the pleasure of knowing and who have contributed in some way to its completion.

TABLE OF CONTENTS

LIST OF FIGURES

LIST OF TABLES

ABBREVIATIONS

Abbreviation	Definition
AC	Adenylyl cyclase
Ad	Adenovirus
AIS	Adenocarcinoma in situ
AKAP	A-Kinase Anchoring Protein
AMP	Adenosine monophosphate
APS	Ammonium persulphate
ATM	Ataxia telangiectasia mutated
ATP	Adenosine triphosphate
ATR	Ataxia telangiectasia and Rad3-related protein
BSA	Bovine serum albumin
cAMP	Cyclic AMP
CD	Cluster of differentiation
CDK	Cyclin-dependent kinase
cGMP	Cyclic guanosine monophosphate
Chk1	Checkpoint kinase 1
CIN	Cervical intraepithelial neoplasia
COX-2	Cyclooxygenase-2
CRE	cAMP response element
CREB	cAMP response element-binding protein
CTCF	CCCTC-binding factor
DAPI	4’6-Diamidino-2-phenylindole
Dlg1	Discs Large 1
DMEM	Dulbecco’s modified Eagle medium
DMSO	Dimethyl sulfoxide
E. coli	*Escherichia coli*
E6-AP	E6-associated protein
EBV	Epstein-Barr virus
EDTA	Ethylenediaminetetraacetic acid
EGF	Epidermal growth factor
EGFR	EGF receptor
EPAC	Exchange proteins directly activated by cAMP
EV	Epidermodysplasia verruciformis
FBS	Foetal bovine serum
FCS	Foetal calf serum
FH-	Flag/HA-
GAPDH	Glyceraldehyde-3-phosphate dehydrogenase
GDP	Guanosine diphosphate
GFP	Green fluorescent protein
GPCR	G protein-coupled receptor
GST	Glutathione S-transferase (
GTP	Guanosine triphosphate
HCV	Hepatitis C virus
HFK-18	HFK maintaining HPV18 genomes

HFKs	Human foreskin keratinocytes
HIV	Human immunodeficiency virus
hnRNP	Heterogeneous nuclear ribonucleoproteins
HPV	Human papillomavirus
hScrib	Scribble
IARC	International Agency for Research on Cancer
IF	Immunofluorescence
IPTG	Isopropyl-β-d-thiogalactopyranoside
KGFR	Keratinocyte growth factor receptor
KSHV	Kaposi sarcoma-associated herpesvirus
LB	Luria-Bertani
LCR	Long control region
MAPK	Mitogen-activated protein kinase
MCM2	Minichromosome maintenance 2
MLL	Mixed-lineage leukaemia
mRNA	Messenger RNA
ND10	Nuclear domain 10
NIKS	Normal immortalised keratinocytes
NIKS-18	NIKS maintaining HPV18 genomes
ORF	Open reading frame
PBM	PDZ binding motif
PBS	Phosphate-buffered saline
PCNA	Proliferating cell nuclear antigen
PCR	Polymerase chain reaction
PDEs	Phosphodiesterases
PDGFRβ	Platelet-derived growth factor receptor beta
PDZ	PSD95/DLG/ZO-1
PGE2	Prostaglandin E2
PKA	Protein Kinase A
R/C	Regulatory/Catalytic (subunit)
Rb	Retinoblastoma
Rluc	*Renilla* luciferase
RNA	Ribonucleic acid
RSV	Respiratory syncytial virus
SDS-PAGE	Sodium dodecyl sulfate-polyacrylamide gel electrophoresis
ShRNA	Short hairpin RNA
SiRNA	Small interfering RNA
SSC	Saline-sodium citrate
STAT	Signal transducer and activator of transcription
TBE	Tris-Borate-EDTA
TBS	Tris-buffered saline
TBS-T	Tris-buffered saline containing 0.1% Tween 20
TE	Tris-EDTA
TEMED	N,N,N',N'-Tetramethylethylenediamine
TFIID	Transcription factor II D
UT	Untransfected

UV	Ultraviolet
VIN	Vulvar intraepithelial neoplasia
YY1	Yin Yang 1
ZF	Zinc finger

CHAPTER 1 INTRODUCTION

1.1 Virus infection and cancer

The first suggestion that viral infections could lead to the development of cancer came from studies in the early 20th century that showed a filterable agent (later termed Rous sarcoma virus) in cell extracts taken from a chicken tumour could transmit tumour formation to a healthy chicken (Rous, 1911). The first evidence of virus-induced human cancers came from Epstein-Barr virus (EBV). In the 1950s, the British surgeon Denis Burkitt described a childhood tumour while working in East Africa that he suspected was due to a virus being spread by arthropods (Burkitt, 1962). Subsequently, the virologists Tony Epstein and Yvonne Barr established the first cell line from Burkitt's lymphoma and showed that it was possible to observe the virus by electron microscopy (Epstein et al., 1964). Although met with initial scepticism by the scientific community, there is now significant evidence that EBV plays a central role in the development of Burkitt's lymphoma, as well as other malignancies such as nasopharyngeal and post-transplant carcinomas, thus establishing it as the first human tumour virus (reviewed in Javier and Butel, 2012).

Since then, the number of viruses causally associated with human cancers has risen considerably, with seven viruses being defined by the International Agency for Research on Cancer (IARC) as carcinogenic in humans. These include EBV, hepatitis B virus, hepatitis C virus (HCV), Kaposi sarcoma-associated herpesvirus (KSHV), human immunodeficiency virus, type-1 (HIV-1), human T cell lymphotropic virus type-1 and several human papillomavirus types (HPV). In addition to these viruses, bacteria such as *Helicobacter pylori* have also been classified as carcinogenic by IARC. Together, these

infections cause approximately 16% of human cancers (Akram et al., 2017; Chen et al., 2014; Liao, 2006; Plummer et al., 2016). This list is constantly evolving and it is likely that additional agents will be added as evidence accumulates. One such example is the Merkel cell polyomavirus, a small double-stranded DNA virus that has received increasing research attention due to its link with Merkel cell carcinoma, a rare but often fatal cutaneous malignancy (Feng et al., 2009).

These viruses can persist for many years either as a result of integration into the host genome or by expressing viral proteins that segregate the viral genome into daughter cells during cell division, resulting in latent infection. During this time, they can contribute to the carcinogenic process through either direct or indirect mechanisms. Direct-acting tumour viruses such as EBV and HPV encode oncoproteins whose expression leads to the immortalisation and transformation of infected cells. Indirect-acting tumour viruses, such as HIV and HCV, however, cause cancer by other means, including virus-mediated induction of chronic inflammation and immunosuppression (reviewed in Morales-Sánchez and Fuentes-Pananá, 2014). For example, the mechanisms behind HCV-associated carcinogenesis include the acquisition of DNA damage as a result of immune-mediated hepatic inflammation as well as the induction of oxidative stress, both of which are thought to contribute to the development of hepatocellular carcinoma (Tarocchi et al., 2014). HIV contributes towards cancer risk by inducing a state of immunosuppression in the host. This virus-induced immunosuppression is thought to predispose individuals to opportunistic infection(s) by other viruses such as KSHV, which gives rise to a 500-fold increase in the risk of Kaposi sarcoma compared to the general population (Hernández-Ramírez et al., 2017), as well as reducing immune-mediated surveillance and clearance of malignant cells (Borges et al., 2014).

1.2 Human papillomaviruses

1.2.1 Human papillomaviruses

HPVs are a group of small, non-enveloped, double-stranded DNA viruses that belong to the *Papillomaviridae* family and are associated with the development of both benign and malignant lesions at mucosal and cutaneous squamous epithelial sites. There have been more than 210 HPV types identified to date and the complete genome sequence has been determined for more than 180 of these viruses (https://pave.niaid.nih.gov). Despite the large range of HPV types, only a small subset of these viruses have been defined as carcinogenic and are associated with the development of cancer in the anogenital region (e.g. cervical, anal, penile, vulvar, vaginal cancer) as well as in the oropharynx (tonsil and base of tongue) (International Agency for Research on Cancer, 2007). These viruses have also been linked to cancers at other anatomical sites, such as the breast, lung and liver; however, strong causal evidence is lacking (Cheau-Feng et al., 2016; Simoes et al., 2012; Tulay and Serakinci, 2016)

1.2.2 HPV classification

HPV classification is based on the DNA sequence of the L1 open reading frame (ORF) where differences in L1 DNA sequence of 10% or more define a new HPV type, while 2-10% define a subtype and <2% a new variant. This definition came from scientists working on HPV taxonomy and was agreed at the International Papillomavirus Workshop, Quebec 1995. HPVs are classified into one of five genera—alpha (α), beta (β), gamma (γ), mu (μ) and nu (ν)—based on viral genome sequence, tissue tropism and association with disease, and members of the same genus share >60% DNA sequence identity in the L1 ORF (De Villiers et al., 2004; Figure 1.1). The alpha and beta genera contain the largest

number of known HPV types and attract the vast majority of research attention due to their association with cancer.

The alpha genus contains 66 HPV types and is divided into both high- or low-risk mucosal viruses depending on their propensity to cause cancer, as well as low-risk cutaneous viruses commonly associated with benign skin lesions and warts. Of these high-risk mucosal types, the alpha genus contains HPV types 16 and 18 that together cause around 70 to 76% of cervical cancer cases worldwide, with estimated prevalence rates of 57% and 16% for HPV16 and HPV18, respectively (Li et al., 2011). HPV16 is associated with the development of squamous cell carcinomas while HPV18 is linked with the development of adenocarcinomas (Bulk et al., 2006). The remaining cases are associated with infection by one of the other high-risk HPVs. These include the six most frequently encountered after HPV16 and HPV18 in cervical cancers - HPV31, 33, 35, 45, 52 and 58 – as well as other HPV types (e.g. HPV51, 56, 66, 39 and 59) (IARC Working Group, 2012)

The low-risk alpha-HPV types, such as HPV types 6 and 11, are not commonly associated with cancer development but nevertheless carry a small (1-3%) risk of cancer progression (Egawa and Doorbar, 2017). In addition, these viruses cause genital and oral warts as well as recurrent respiratory papillomas that tend to be difficult to treat clinically (Lacey et al., 2006; De Villiers et al., 2004). The beta genus contains 64 virus types that are associated with the development of cutaneous benign lesions, though there is evidence that some of these viruses are carcinogenic in the immunosuppressed (HPV8: Schaper et al., 2005) or co-operate with ultraviolet light in the development of non-melanoma skin cancer (HPV38: Viarisio et al., 2011, 2016). Additionally, individuals with the genetic disorder epidermodysplasia verruciformis (EV) are highly susceptible to infection by beta HPV types, with a significant proportion (up to 70%) of these individuals going on to develop

squamous cell carcinomas of the skin, particularly on sun-exposed sites. EV is a primary immunodeficiency disorder where sufferers have compromised innate and cell-mediated immunity, thought to arise due to mutations in two genes (*EVER1/TCM6* and *EVER2/TCM8*) whose gene products function in zinc metabolism and T cell activation (Lazarczyk et al., 2009; Ramoz et al., 2002). The remaining gamma, mu and nu viruses all target the cutaneous epithelia and are associated with the development of papillomas and warts with no oncogenic potential.

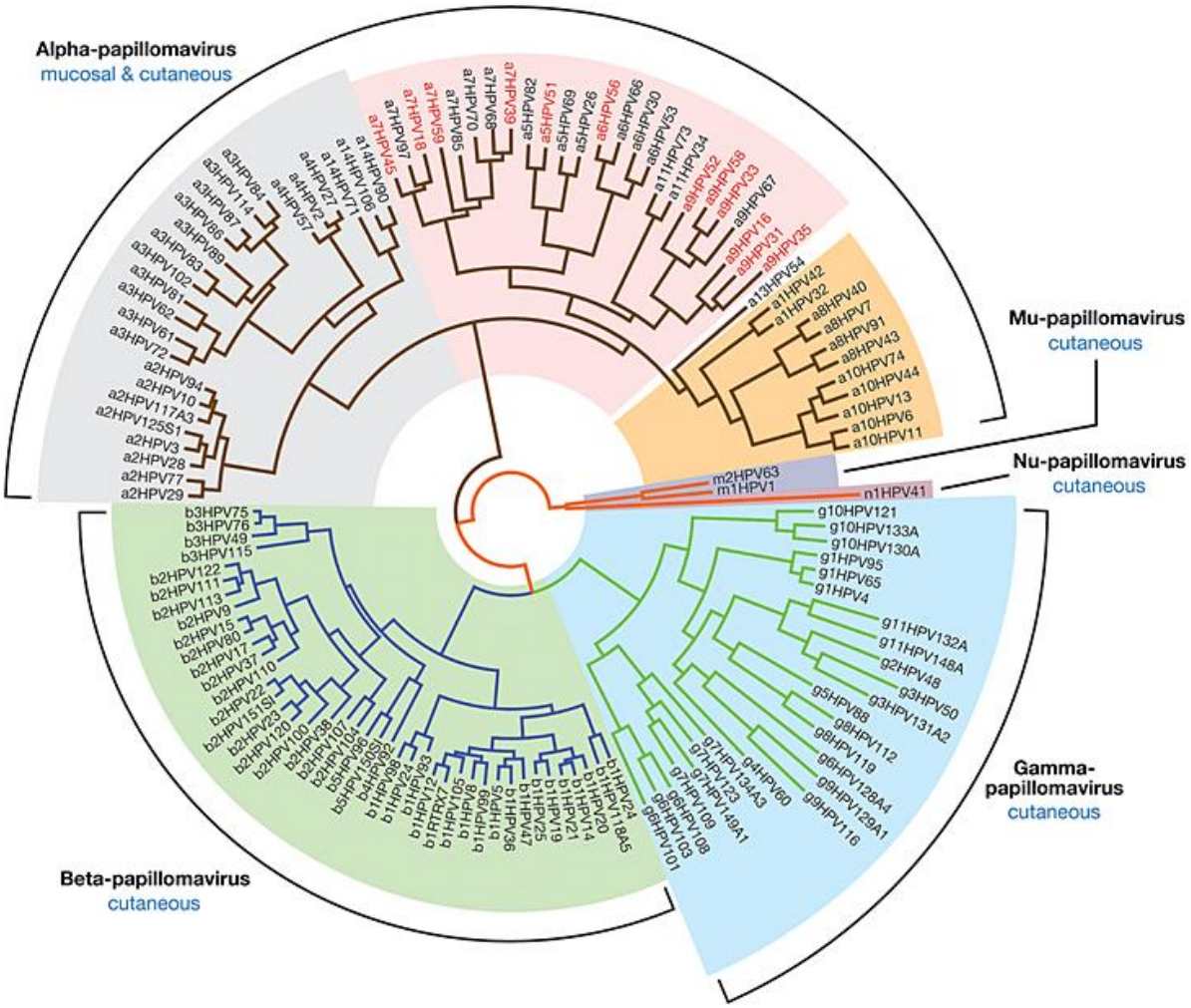

Figure 1.1: HPV phylogenetic tree. HPV types are classified into one of five genera—alpha, beta, gamma, mu and nu—where alpha and beta represent the largest group of HPV types. Within the alpha genus, HPVs can be classified as low-risk cutaneous viruses (grey), low-risk mucosal viruses (orange) or high risk mucosal viruses (pink). Those alpha-types highlighted in red are known carcinogenic virus types while the others are either probably or possibly carcinogenic, in line with the classification by the International Agency for Research on Cancer for group 1, 2A and 2B carcinogens respectively. Image taken from Doorbar et al., 2015.

1.2.3 HPV genome organisation

HPVs contain a double-stranded DNA genome of approximately 8 kb in size, encapsidated by an icosahedral capsid around 50-60 nm in diameter. The viral genome contains both early and late gene regions as well as a non-protein coding region known as the long control region (LCR). The early promoter lies within the E6 ORF, with the late promoter within the E7 ORF. An illustration of the viral genome is given in **Figure 1.2**.

The LCR, sometimes known as the upstream regulatory region, does not encode any known proteins but instead houses the viral origin of replication, the early promoter and a variety of binding sites both for the viral E2 protein and cellular transcription factors, both of which are important for controlling early oncoprotein expression (Hoppe-Seyler and Butz, 1994; Thierry, 2009). The viral genome encodes multiple ORFs, yielding either early or late proteins, so named for the timing of their expression during the viral life cycle. In addition, alternative splicing of these ORFs leads to viral fusion proteins, such as E8^E2 and E1^E4, that have important functions in the viral life cycle. The early region encodes E6, E7, E8, E1, E2, E4 and E5, which play roles in viral transcription, viral genome replication and host cell transformation. Despite its name, E4 expression coincides with the differentiation-dependent aspect of the HPV life cycle. The late region encodes the major (L1) and minor (L2) structural proteins, which together make up the virus coat (Longworth and Laimins, 2004). L2 also has multiple other functions in the viral life cycle, including encapsidation (see section 1.2.4). The viral capsid is an icosahedral capsid composed of 360 copies of the L1 protein arranged into 72 capsomeres, with a variable number of L2 molecules per capsid. The precise number of L2 molecules in each capsid is unclear; however, estimates range from 36 to 72 L2 molecules per capsid depending on the exact HPV type studied (Buck et al., 2008; Finnen et al., 2003).

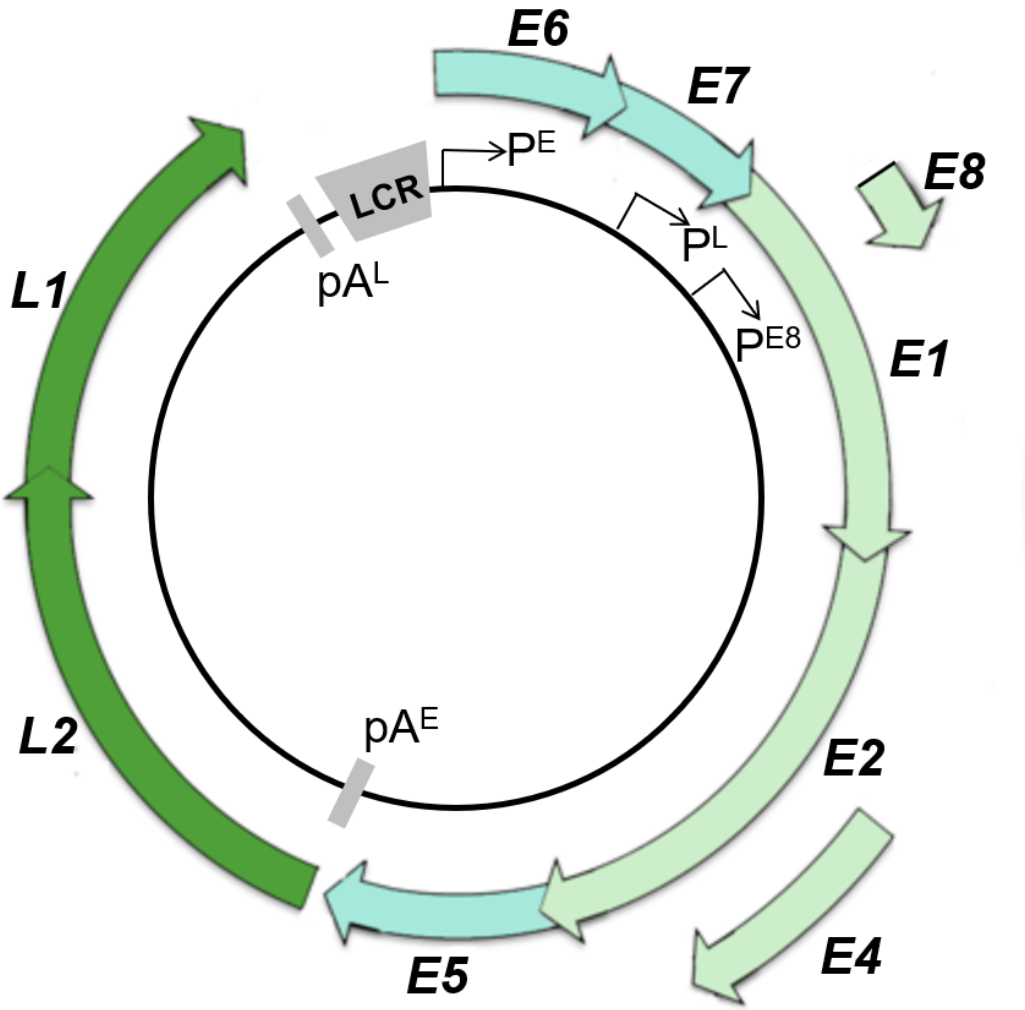

Figure 1.2: HPV genome organisation. The HPV genome is organised into early, late and the LCR. The early region encodes E6, E7, E8, E1, E2, E4 and E5 while the late region encodes the structure proteins L1 and L2. The early promoter (P^E; p105 in HPV18) sits within the E6 ORF and the late promoter (P^L; p811 in HPV18) within the E7 ORF. The promoter P^{E8}, from which the E8^E2 fusion protein is expressed, is contained within the E1 ORF. The early (pA^E) and late (PA^L) polyadenylation sites are shown between the E5 and L2 ORF and L1 and the LCR, respectively. Image from Dr Sally Roberts.

1.2.4 HPV life cycle

The HPV life cycle is closely linked to the differentiation status of the host cell that it infects – the keratinocyte. In a natural infection of the cervix, it is likely that the virus reaches the transformation zone, an area of metaplastic tissue between the squamous epithelium of the ectocervix and the glandular or columnar tissue of the endocervical canal that appears to be particularly susceptible to HPV carcinogenesis – the squamocolumnar junction – following epithelial injury (Elson et al., 2000; Kines et al., 2009). This region contains a discrete population of non-stratified cuboidal cells of embryonic origin that express a junction cell-specific expression profile. It is thought that these junctional cells are progenitors of cervical cancers by the phenotypic similarities between these cells and high-grade cancers (Herfs et al., 2012, 2013; Mirkovic et al., 2015) After the virus reaches this area, it interacts with heparin sulphate proteoglycans such as syndecan-1 via the L1 protein to facilitate internalisation (Joyce et al., 1999; Kines et al., 2009; Shafti-Keramat et al., 2003). This binding event leads to a conformational change in the virus capsid, exposing L1 residues for cleavage by the serine protease kallikrein-8 and resulting in exposure of the amino terminus of L2 (Cerqueira et al., 2015; Richards et al., 2013). Following this, cyclophilin B, a peptidyl-prolyl cis-trans isomerase that is involved in protein folding and maturation (Lang et al., 1987), binds to this exposed region of L2 and induces a further conformational change to reveal a binding site for the proprotein convertase furin (Cerqueira et al., 2015; Day et al., 2008; Richards et al., 2013). These events result in the transfer of the virus to a secondary entry receptor. The identity of this secondary receptor has not been firmly established but attractive candidates include the alpha6-integrin and the tetraspanins cluster of differentiation 9 (CD9), CD63 and CD151,

among others (Evander et al., 1997; Fast et al., 2018; Scheffer et al., 2013; Yoon et al., 2001).

The exact mechanism of virus internalisation is not completely understood and appears to vary between different HPV types. For example, internalisation of HPV16 is dependent on actin polymerisation and tetraspanin-enriched microdomains but is independent of clathrin, caveolin and lipid rafts (Scheffer et al., 2013; Schelhaas et al., 2012; Selinka et al., 2002; Spoden et al., 2008). By contrast, HPV31 is dependent on caveolin and dynamin but independent of clathrin-mediated endocytosis (Smith et al., 2007). Nevertheless, the virus is endocytosed in an asynchronous fashion over a number of hours, with the exact timing depending on the cell cycle stage of the target cell during infection (Broniarczyk et al., 2015).

Following internalisation, the virus is disassembled in the endosomal compartment to L1 and L2-viral DNA complexes. This L2-viral complex is trafficked, via the trans-Golgi network, to the nucleus where, upon breakdown of the nuclear envelope during mitosis, the virus associates with host chromatin (Aydin et al., 2017; Bienkowska-Haba et al., 2012; Calton et al., 2017; DiGiuseppe et al., 2014). Finally, the L2-viral genome accumulates in nuclear domain 10 (ND10) bodies where L2 relocalises the ND10 body proteins Sp100 and Daxx to drive early viral transcription and viral DNA replication (Florin et al., 2002; Stepp et al., 2013)

Replication of viral genomes requires the actions of the viral E1 and E2 proteins. These viral proteins are necessary and sufficient for viral replication and bind to specific binding sites in the viral origin of replication to initiate viral replication (Chiang et al., 1992; Ustav et al., 1991). E2 binds to specific sites in the viral origin of replication and facilitates the binding of E1 by increasing its specificity towards DNA before E2 is then displaced. E1

assembles into a double hexameric helicase and catalyses the melting of the DNA both to allow for access to the cellular replication machinery and to provide a template for the synthesis of viral DNA (Sedman and Stenlund, 1998; Enemark and Joshua-Tor, 2006; Stenlund, 2003). During this process, the virus relies extensively on host factors for viral DNA replication, including replication protein A, proliferating cell nuclear antigen (PCNA), topoisomerase I and the DNA polymerases polα and polϵ (Chojnacki and Melendy, 2018; Loo and Melendy, 2004; Melendy et al., 1995). This initial amplification stage generates around 50 to 100 episomal HPV genomes per cell with minimal viral transcription, which is thought to evade detection by the host immune system (Maglennon et al., 2011; McBride, 2017). This limited viral genome replication is thought to be largely due to expression of the E8^E2 protein, a conserved fusion protein derived from the E8 ORF and E2 C-terminal sequences, which inhibits viral gene expression and genome replication (Dreer et al., 2017). In addition, E2 is involved in the partitioning of viral genomes during mitotic cell division by tethering the virus genome to host chromosomes. A plethora of E2 interactions are thought to anchor the viral genome to host chromosomes, including bromodomain-containing protein 4, mitotic kinesin-like proteins 2, ChlR1 and DNA topoisomerase 2-binding protein 1, ensuring viral persistence in dividing cells (Donaldson et al., 2007; Harris et al., 2017; Parish et al., 2006; You et al., 2004; Yu et al., 2007).

In the next stage of the viral life cycle, the infected cell population expands through the actions of E6 and E7. How exactly this switch from low levels of viral transcription in basal cells to increased oncoprotein expression during differentiation is unclear, however, recent studies have identified a role for the cellular transcriptional regulators CCCTC-binding factor (CTCF) and Yin Yang 1 (YY1). In undifferentiated cells, chromatin looping

between YY1 bound at the viral transcriptional enhancer and CTCF bound at the E2 ORF regulates E6/E7 expression via epigenetic repression of the early promoter. During keratinocyte differentiation, however, there is a decrease in the level of YY1 protein which disrupts this repressive chromatin loop, allowing for increased expression of E6 and E7 (Pentland et al., 2018).

In uninfected cells, basal keratinocytes undergo either symmetrical cell division to produce a daughter cell with the same fate that remains in the basal layer or asymmetrical cell division to produce cells with different fates; one remaining in the basal cell layer with mitotic potential and the other daughter cell entering differentiation, which involves exiting the cell cycle (Koster and Roop, 2007). In HPV-infected cells, the virus subverts this process and pushes post-mitotic differentiating cells back into the cell cycle, delaying differentiation and allowing for amplification of the viral genome to thousands of copies per cell.

One key mechanism by which the virus amplifies its genomes involves the retinoblastoma (Rb) family of proteins. E7 binds to and degrades Rb, as well as the related pocket proteins p105, p107 and p130, via the proteasome. Rb represses the expression of genes required for G1 to S transition via a variety of mechanisms, such as direct binding of Rb to the activation domain of E2Fs, blocking their ability to activate transcription (Flemington et al., 1993). An alternative mechanism exists whereby Rb binds to protein complexes that regulate chromatin structure, such as histone deacetylases, using a binding site distinct from its E2F-binding site. These proteins deacetylate histones bound to gene promoters, promoting the formation of nucleosomes that inhibit transcription (Luo et al., 1998). E7 disrupts Rb-E2F interactions, allowing for constitutive activation of E2F responsive genes, which pushes suprabasal cells back into the cell cycle. Consistent with this, suprabasal

cells prepared from HPV genome containing cultures display markers of cell cycle re-entry such as PCNA and were competent for host DNA replication, even after the onset of differentiation (Cheng et al., 1995). Furthermore, this targeting of pocket proteins is important for the delayed keratinocyte differentiation seen in organotypic rafts derived from HPV genome containing cells, indicating that the virus relies on different E7 functions at different stages of its life cycle (Collins et al., 2005).

This E7-induced premature cell cycle re-entry leads to induction of host defence pathways, including those mediated by the tumour suppressor p53. To overcome this induction of p53, E6 redirects the ubiquitination ability of E6-associated protein (E6-AP), a cellular E3 ubiquitin ligase, towards p53, which is not a natural target of E6-AP, and results in its subsequent proteasomal degradation (Huibregtse et al., 1991; Scheffner et al., 1990, 1992, 1993). E6-mediated degradation of p53 is thought to protect suprabasal cells from apoptosis as a result of E7-induced cell cycle re-entry and appears to contribute to replication of the viral DNA in cells (Flores et al., 2000; Park and Androphy, 2002; Thomas et al., 1999). In addition to causing its degradation, E6 inactivates p53 function by downregulating its ability to activate transcription of p53-dependent promoters (Lechner and Laimins, 1994; McCance *et al.*, 1999; Zimmermann *et al.*, 1999), which also appears to contribute to the maintenance and amplification of viral episomes (Kho et al., 2013; Lorenz et al., 2013; Wang et al., 2009).

Other E6 functions distinct from its p53 targeting ability are also important for the viral life cycle, including its ability to target a subset of cellular proteins containing PSD95/DLG/ZO-1 (PDZ) domains. This targeting ability is mediated by a four amino acid class I PDZ binding motif (PBM) located in the extreme carboxyl terminus of E6 (HPV16: ETQL; HPV18: ETQV) and often results in degradation or mislocalisation of the target

protein (reviewed in James and Roberts, 2016). Disruption of this motif in the context of the complete viral genome impairs cell proliferation, viral genome maintenance and amplification, and late viral protein expression in multiple high-risk viruses (Delury et al., 2013; Lee and Laimins, 2004; Nicolaides et al., 2011). In addition, loss of this targeting ability has also been associated with an increased rate of abnormal mitoses, chromosomal segregation defects and genomic instability in HPV genome containing cells, suggesting it also plays a role in maintaining mitotic integrity of HPV genome containing cells (Marsh *et al.*, 2017). E6-PDZ interactions are also important for controlling E6 protein expression (Kranjec et al., 2016; Nicolaides et al., 2011).

In addition to the functions described above, the virus also depends on other host pathways during its life cycle, including components of the cellular DNA damage response, for viral genome amplification. Multiple high-risk HPV types activate the ataxia telangiectasia mutated (ATM) pathway, a cellular DNA repair pathway that primarily responds to DNA double-strand breaks, in the absence of DNA damage, with virus-induced phosphorylation of multiple ATM substrates throughout keratinocyte differentiation (Moody and Laimins, 2009). This activation is mediated by E7 through the signal transducer and activator of transcription (STAT)-5β protein via the peroxisome proliferator-activated receptor γ; however, E1 can also activate ATM signalling (Hong and Laimins, 2013; Moody and Laimins, 2009; Sakakibara et al., 2011). Use of pharmacological inhibitors showed that the activity of this pathway was not required for the maintenance of the viral episome in undifferentiated cells but was crucial for viral genome amplification during differentiation (Moody and Laimins, 2009). Furthermore, E7 increases the expression of the MRN (MRE11, RAD50, and NBS1) complex proteins, activators of ATM following DNA damage, with at least one of these components (NBS1) required for viral genome

amplification during differentiation (Anacker et al., 2014). Similarly, various other DNA repair factors such as Rad51 and BRCA1, which also function in repairing DNA double-strand breaks, are required for differentiation-dependent viral genome amplification (Chappell et al., 2016). The virus also relies on another DNA damage response pathway during its life cycle – the ataxia telangiectasia and Rad3-related protein (ATR) pathway. This pathway protects the integrity of replicating chromosomes and appears to be required for viral replication, with inhibition of phosphorylation of ATR or checkpoint kinase 1 (Chk1; a downstream target of ATR) inhibiting viral genome amplification during differentiation and, to a lesser extent, viral genome maintenance in undifferentiated cells (Hong et al., 2015).

Another host pathway used by the virus for viral DNA replication and/or amplification involves members of the STAT protein family. STATs were originally discovered for their role in interferon-regulated gene transcription but have since been recognised as mediating cellular responses to a variety of cytokines and growth factors. There are seven STAT family members (STAT1α/β, STAT2, STAT3α/β, STAT4, STAT5A, STAT5B and STAT6) which, although structurally similar, have diverse biological roles and regulate processes ranging from embryonic development and cell differentiation to regulation of the immune response (Konjević et al., 2013). HPV represses STAT-1 expression primarily at the level of transcription, with both E6 and E7 proteins able to inhibit its expression. For E6, this ability depended on its binding to E6-AP. Restoration of STAT-1 in overexpression experiments or by treatment with gamma-interferon, which leads to activation of STAT-1, showed that it contributed to both episomal maintenance in undifferentiated cells and to viral genome amplification during keratinocyte differentiation (Hong et al., 2011). STAT3 has also been shown to contribute to the virus life cycle.

Primary human foreskin keratinocytes (HFKs) maintaining HPV18 genomes displayed increased phosphorylation of STAT3 compared to control cells, with the expression of E6 alone sufficient to drive this phosphorylation via a mechanism involving Janus kinases and the mitogen-activated protein kinase (MAPK) pathway. This occurred independently of E6's ability to degrade p53, bind to E6-AP and interact with PDZ proteins. Further experiments showed that STAT3 was required for expression of E6 and E7 and viral genome maintenance in undifferentiated cells as well as viral genome amplification and expansion of the suprabasal compartment in organotypic raft culture (Morgan et al., 2018). More recent work in HPV positive cervical cancer cells showed that this E6-driven STAT3 activation occurred via the pro-inflammatory cytokine interleukin-6 through a signalling axis composed of Rac1 and NFkB. Furthermore, in these cells, activation of STAT3 contributed to cancer cell proliferation and survival (Morgan and Macdonald, 2019)

The function of E5 during the virus life cycle remained for some years unclear however recent studies using E5 mutant or knockout genomes have begun to unravel a role for this enigmatic protein. Using normal immortalised keratinocytes maintaining HPV16 wild type or E5 knockout genomes, E5 was shown to be involved in suprabasal DNA synthesis (Genther et al., 2003). In a parallel study using primary HFKs maintaining HPV31 wild type or E5 knockout genomes, E5 appeared to contribute to differentiation-dependent viral genome amplification and expression of late viral proteins (Fehrmann et al., 2003). Furthermore, experiments carried out in an HPV18 life cycle model established in primary HFKs showed that E5 contributed to cell cycle progression and unscheduled host DNA synthesis in differentiating keratinocytes, which correlated with activation of the epidermal growth factor receptor (EGFR) in these cells. The same study showed this E5 potentiated activity of EGFR signalling modulated keratinocyte differentiation in a manner dependent

on the keratinocyte growth factor receptor (KGFR), a regulator of the balance between epithelial proliferation and differentiation, and its effector protein kinase B (otherwise known as AKT) in differentiating cells (Wasson et al., 2017). Although largely examined in transient overexpression experiments, E5 also appears to augment other functions of the E6 and E7 oncoproteins (described in section 1.2.6), which may be relevant for the completion of the viral life cycle.

The next stage of the viral life cycle is marked by expression of the E1^E4 protein (otherwise known as E4), a fusion protein derived from first five amino acids of E1 fused to the complete E4 ORF (Doorbar et al., 1986). It is the most abundantly expressed viral protein and its expression coincides with the onset of viral genome amplification in differentiated cells (Peh et al., 2002). Studies in life cycle models showed that its contributions to the viral life cycle, such as regulation of differentiation-dependent viral genome amplification and late gene expression, are common to the high-risk HPV16, HPV18 and HPV31 (Egawa et al., 2017; Wilson et al., 2005, 2007) as well as cottontail rabbit papillomavirus (Peh et al., 2002), although the exact mechanism by which this occurs is unclear. One possibility is through its ability to regulate the cell cycle. HPV16 and 18 E4 have both been shown to induce G_2 arrest by cytoplasmic sequestration of cyclin B/cyclin-dependent kinase (CDK)2 complexes, possibly preventing the phosphorylation of nuclear targets important for cell cycle progression (Davy et al., 2002; Knight et al., 2011; Nakahara et al., 2002). This G2 arrest likely establishes a pseudo-S phase state in which host DNA replication is complete but the cell remains competent for replication, allowing the virus access to the replicative machinery without any competition from host DNA synthesis. Analysis of the motifs required for this arrest, however, showed this G2 arrest only contributed to viral genome amplification in HPV16, and not HPV18

(Egawa et al., 2017; Knight et al., 2011), possibly reflecting important biological differences between these viruses.

In the final stages of the virus life cycle, high levels of the E2 protein suppress E6 and E7 expression, which is important for cellular differentiation, expression of the late viral proteins and eventual production and release of new infectious virions from the uppermost layers of the differentiated epithelium (Bernard et al., 1989). Studies in keratinocytes have suggested that these later phases occur in a multi-step process. Virion assembly begins in the cytoplasm where L1 is assembled into pentameric structures prior to nuclear import mediated by cellular karyopherin proteins, likely aided by additional proteins such as the heat shock protein 70 family members (Bird et al., 2008; Florin et al., 2002b; Nelson et al., 2000). These proteins also appear to be required for incorporation of L2 into the developing capsid by facilitating its nuclear transport (Bordeaux et al., 2006; Florin et al., 2004). The cellular protein nucleophosmin also appears to contribute to the correct assembly of the virus capsid, possibly by acting as a protein scaffold for L1 and L2, although this is not fully understood at present (Day et al., 2015). How the viral genome is then incorporated into the capsid is also unclear. While the majority of viruses contain packaging signals that are recognised by viral proteins to allow for encapsidation of viral DNA, no such sequence has been identified for HPV. *In vitro* experiments have suggested that viral DNA is instead incorporated into the capsid by a size discrimination mechanism. The viral capsid goes through a repeated process of assembly and disassembly, taking in both cellular and viral DNA, until a suitably sized DNA is encountered, leading to the formation of a virion that is resistant to disassembly (Cerqueira et al., 2016). This size discrimination mechanism is consistent with earlier observations that papillomavirus capsids can package a variety of DNA as long as the total size does not exceed 8 kb (the

size of the HPV genome) (Buck et al., 2004; Stauffer et al., 1998). Once the viral DNA has been assembled and packaged, capsid maturation occurs in the naturally occurring redox environment of the uppermost layers of the epithelium, leading to the formation of infectious virions (Conway et al., 2009). There is evidence from an HPV18 life cycle model that expression of E1^E4 in these layers contributes to capsid assembly, infectivity and viral release through an as yet undefined mechanism (Biryukov et al., 2017).

How exactly these infectious virions are released from the upper layers of the differentiated epithelium has not been fully resolved; however, it is generally thought to occur as the result of the sloughing off of cells containing matured virus particles. The role of viral proteins during this process is largely unclear but there is some evidence that E4 may play a role in facilitating viral egress. Both HPV1 and HPV16 E4 interact with cytokeratin proteins and, in the case of HPV16 E4, cause their collapse (Doorbar et al., 1991; Roberts et al., 1993). Furthermore, studies using HPV11 E4 showed that it could alter the morphology of differentiated keratinocytes and cornified cell envelope, leading to a much thinner and fragile cell envelope (Brown and Bryan, 2000; Brown et al., 2006). Together, these data suggest that E4 may facilitate viral release by interfering with the integrity of the uppermost layers of the epithelium, although further studies are required in primary life cycle models to confirm this mechanism.

An illustration of the main steps of the virus life cycle is provided in **Figure 1.3**.

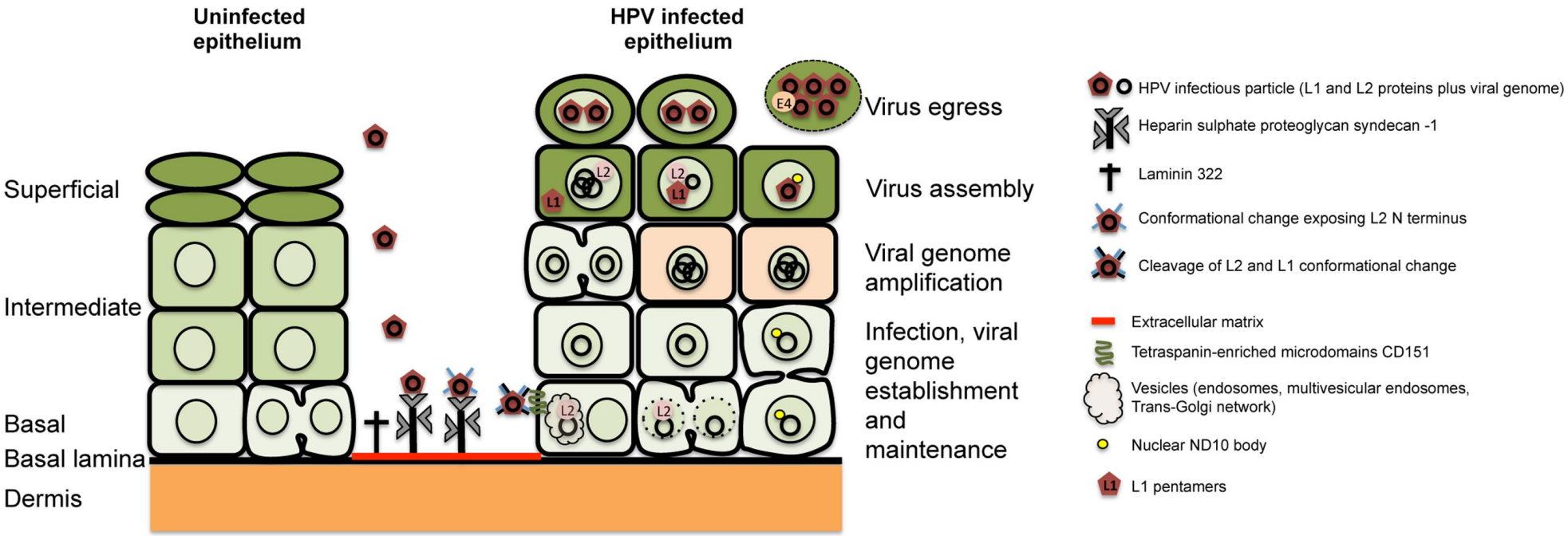

Figure 1.3: HPV life cycle. HPV gains entry to basal keratinocytes in the basal lamina following small microwounds or abrasions where it attaches to the heparin sulphate proteoglycan syndecans-1, resulting in conformational changes of L2 and L1 that results in its attachment to secondary receptors such as cluster of differentiation 151 (CD151) for virus internalisation. The viral genome is then trafficked through cellular vesicles until it reaches nuclear domain 10 (ND10) bodies. Viral DNA is replicated due to the actions of the E1 and E2 as well as various cellular proteins and is maintained as a low copy number episome. In the intermediate layers, E6 and E7 delay differentiation and stimulate cell division to support viral DNA replication, which results in amplification of the viral genome to thousands of copies per cell. In the superficial layers, the structural proteins L1 and L2 are expressed and this is associated with viral coating and release of progenitor virions. Viral release occurs through sloughing off of cells containing matured virus particles, which is thought to be aided by the actions of the E4 protein. Image from Dr Sally Roberts.

1.2.5 Viral transcription

Transcription of the early viral proteins is controlled by the actions of E2 as well as a myriad of host transcription factors. These viral and cellular proteins bind to specific sites in the viral LCR and either activate or repress viral transcription.

The viral LCR is divided into three regions known as the 5' segment, central segment and the 3' segment. The 5' segment contains the nuclear matrix binding region and transcription termination signal, the central segment contains a tissue-specific enhancer and the 3' segment contains the viral origin of replication and the early promoter, which overlaps with the start of the E6 ORF (McBride, 2009; Stünkel and Bernard, 1999). The promoter contains a canonical TATA box that is involved in the recruitment of the general transcription factor II D (TFIID) to the viral LCR, leading to ribonucleic acid (RNA) polymerase II-dependent transcription of viral transcripts with the potential to encode E1, E2, E1^E4, E5, E6, E7 and E8, which are polyadenylated at the early polyadenylation site (Johansson and Schwartz, 2013; Straub et al., 2015; Thierry, 2009).

Also contained within the LCR is a number of E2 binding sites. E2 binds as a homodimer to specific sequences containing the consensus motif ACCGN_4CGGT and recruits cellular factors important for regulation of viral transcription. There are multiple E2 binding sites in the LCR, with most alpha HPVs containing four binding sites (McBride, 2009), and E2 binding to these sites can either activate or repress transcription. For example, at low E2 protein levels, it only binds to E2 binding site 4, activating transcription of early viral genes. However, as levels of E2 protein rise, other binding sites (such as binding sites 1 and 2) become occupied and there is repression of viral transcription (Steger and Corbach, 1997).

E2 binding to these repressive sites regulates the recruitment of host transcription factors important for viral transcription. For example, E2 binding to binding site 1, which is close to the TATA box, blocks the recruitment of proteins of the transcription pre-initiation complex, such as TFIID and TATA-binding protein and E2 binding to binding site 2 results in the displacement of the transcription factors Sp1 and activator protein-1 (AP-1) from their adjacent binding sites in the LCR, repressing viral transcription. These binding sites are bound by E2 with low affinity and are only occupied at high E2 protein levels, indicating that E2 protein expression is an important regulator of viral transcription from the early promoter (Demeret et al., 1994; Tan et al., 1994).

In differentiated cells, late viral transcription occurs from the late promoter within the E7 ORF (p670 in HPV16; p811 in HPV18). The activity of this promoter is dependent on differentiation-specific transcription factors such as the CCAAT-enhancer binding proteins (Gunasekharan et al., 2012) and gives rise to HPV transcripts with the potential to encode E1^E4, E5, L1 and L2 that are polyadenylated at the late polyadenylation site. E1^E4 and E5 containing transcripts however can also be polyadenylated at the early polyadenylation site (Johansson and Schwartz, 2013).

Transcription from the viral genome occurs from only one DNA strand and is polycistronic, giving rise to transcripts with the potential to encode for more than one viral protein. A complex process of alternative splicing of viral transcripts exists, yielding multiple messenger RNAs (mRNAs) that maximises the coding potential of the 8 kb viral genome (reviewed in Graham and Faizo, 2017). For example, the E6 ORF can encode up to four E6* proteins, depending on the exact HPV type. In HPV18, E6*I, the most well studied of the E6* proteins, degrades discs large 1 (Dlg1) and scribble (hScrib) in the absence of full-length E6 (Pim et al., 2009).

There is no evidence that the HPV genome encodes viral microRNAs, small noncoding RNAs involved in the control of various cellular processes, but it is known that the virus alters expression of host microRNAs during the HPV life cycle. One well-studied example is miR-203a-3p, which regulates the balance of proliferation versus differentiation during keratinocyte differentiation. HPV E7 blocks the induction of this microRNA during differentiation via the MAPK/protein kinase C pathway, and this inhibition is important for both episomal maintenance in undifferentiated cells as well as viral genome amplification during keratinocyte differentiation (Melar-New and Laimins, 2010).

1.2.6 HPV oncoproteins

The viral oncoproteins functionally interact during infection, resulting in changes in cellular proliferation and apoptosis, which provide an environment conducive for viral DNA replication. Additional functions of the viral oncoproteins contribute to the immortalisation of HPV genome containing cells and, with the acquisition of oncogenic mutations, these infections may progress to cellular transformation and cancer (**Figure 1.4;** Roberts, 2015). A description of some of these functions is given below.

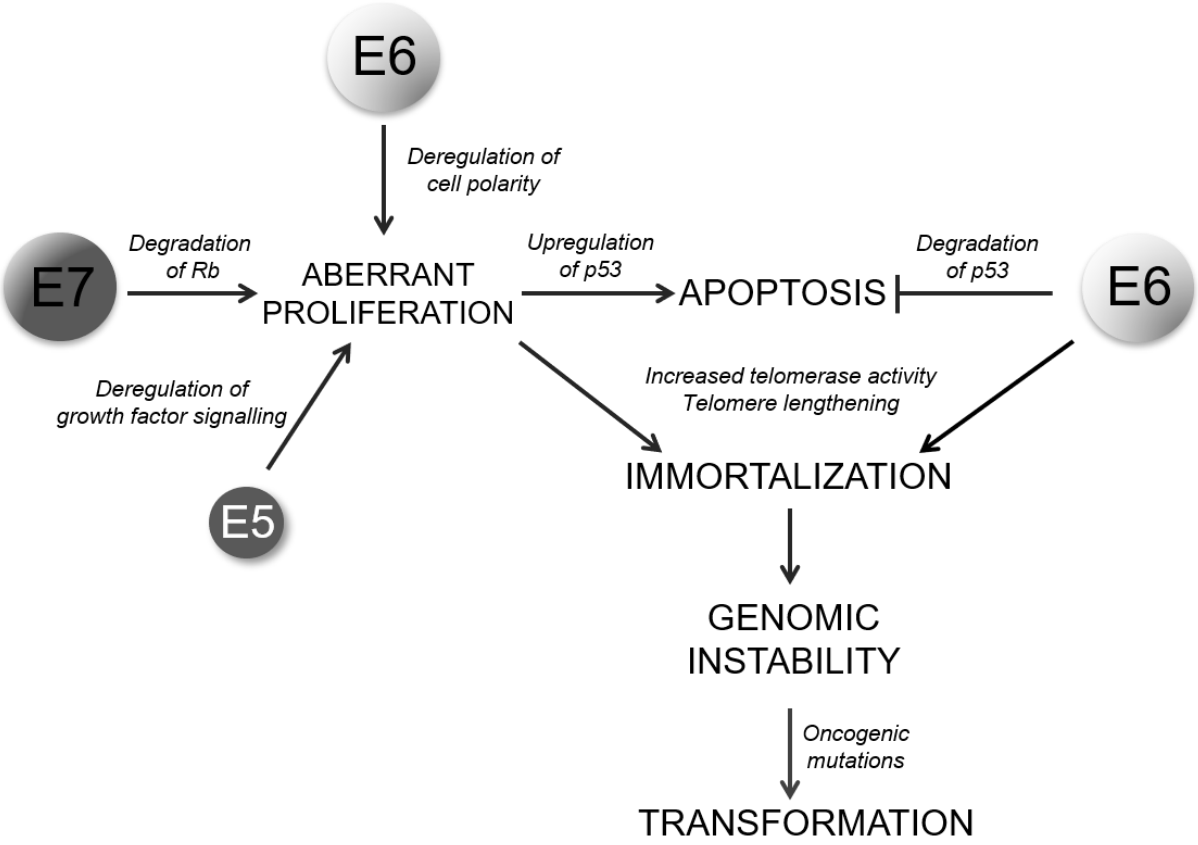

Figure 1.4: Functional interaction of the HPV oncoproteins. The HPV oncoproteins E5, E6 and E7 functionally synergise to promote the aberrant proliferation of cells containing HPV genomes. These interactions result in cellular hyperproliferation through degradation of the retinoblastoma tumour suppressor pathway by viral targeting of the pocket proteins, deregulation of cell polarity proteins (PDZ domain-containing proteins) and deregulation of growth factor signalling. In response to aberrant cell proliferation, the host cell upregulates apoptotic pathways, including those mediated by p53. To ensure cell survival, E6 targets p53 for degradation through the ubiquitin-proteasome system, inactivating the apoptotic response. E6 can also drive cellular immortalisation through modulation of telomerase, leading to the emergence of immortal cells. Continuous expression of the viral oncoproteins through integration of viral DNA into the host genome leads to an unstable host environment, leading to the acquisition of additional oncogenic mutations that lead to cellular transformation. Image taken from Roberts, 2015.

1.2.6.1 E5

The E5 protein is a small, hydrophobic protein expressed by a subset of HPV types that, when overexpressed in fibroblasts appears to localise to the endoplasmic reticulum, Golgi apparatus and to nuclear membranes (Conrad et al., 1993). When expressed in keratinocytes, the natural host cell of HPV, E5 localises primarily to the endoplasmic reticulum (Disbrow et al., 2003).

Unlike bovine papillomavirus type one E5 that interacts with the platelet-derived growth factor receptor beta (PDGFRβ) to drive cell transformation, HPV E5 proteins do not interact with PDGFRβ and are comparatively only weakly transforming in cell culture. Instead, HPV E5 appears to primarily mediate its effects via EGFR (reviewed in DiMaio and Petti, 2013; Müller et al., 2015).

The first evidence of HPV E5 transforming ability came from HPV6 E5, which induced anchorage-independent growth in mouse fibroblasts (Chen and Mounts, 1990). Subsequent work using HPV16 E5 showed that it could also induce cellular transformation of murine fibroblasts, acting synergistically with the EGFR (Leechanachai et al., 1992; Straight et al., 1993). *In vitro* studies showed that E5 can enhance phosphorylation of the EGFR in response to epidermal growth factor (EGF) treatment (Crusius et al., 1998; Straight et al., 1993), induce EGF-dependent cellular proliferation of primary keratinocytes (Bouvard et al., 1994) and enhance the activity of EGF-dependent signalling cascades such as those involving ERK1/2 and protein kinase B in EGF-treated cells (Crusius et al., 1997; Gu and Matlashewski, 1995). Furthermore, E5 also enhances recycling of the EGFR to the plasma membrane and prevents its degradation by modulating membrane trafficking pathways (Straight et al., 1995; Thomsen et al., 2000). Consistent with a role in driving proliferation, transgenic mice expressing HPV16 E5 targeted to basal keratinocytes showed an increased

frequency of epidermal hyperplasia and spontaneous tumour formation, both of which were dependent on EGFR activity (Genther Williams et al., 2005).

In addition to its effects on EGF signalling, E5 potentiates the effects of other HPV oncoproteins. Together with E7, E5 can enhance proliferation of rodent epithelial cells (Leechanachai et al., 1992; Valle and Banks, 1995) and augment the ability of E6 and E7 to immortalise primary human keratinocytes (Stöppler et al., 1996). More recently, E5 has been identified as a novel virus-encoded membrane channel – viroporin - and this channel activity seems to be important for E5-driven mitogenic signalling (Wetherill et al., 2012, 2018). Other functions of E5 include downregulation of major histocompatibility complex surface complexes and reduction of antigen presentation to cytotoxic T cells, allowing for immune evasion of HPV infected cells (De Freitas et al., 2017), stimulation of host DNA synthesis (Straight et al., 1993) and increasing the motility and invasiveness of keratinocyte cell lines (Kivi et al., 2008).

1.2.6.2 E6

E6 proteins expressed by those alphavirus types associated with cancers are small (~15 kDa) proteins that contain two zinc fingers (ZFs) as well as a C-terminal PBM. The ZFs are characterised by Cys-X-X-Cys motifs and mediate its interaction with E6-AP to drive degradation of p53. In addition, the PBM mediates interactions with a variety of cellular proteins containing PDZ domains, generally resulting in degradation or mislocalisation of the target protein. Through these interaction domains, E6 targets a number of cellular pathways involved in the regulation of genome stability, apoptosis, cell morphology and polarity, chromatin remodelling and the immune response, among others (reviewed in Wallace and Galloway, 2015). Additional functions of E6 include the activation of telomerase, the host enzyme responsible for adding repeat sequences to

chromosome ends, which is important for the immortalisation of keratinocytes (Klingelhutz et al., 1996; Liu et al., 2009; Oh et al., 2001).

E6 interactions with p53 and cellular PDZ proteins are discussed below.

1.2.6.2.1 E6 and p53

One of the best-studied E6 interacting partners is the p53 protein. Originally identified in 1979, p53 has become known as the master guardian of the genome and regulates cellular responses to diverse genotoxic insults, such as those arising from DNA damage, hypoxia, oncogenic signalling and nutrient deprivation, among others, and its induction often results in cell cycle arrest or, in the case of irreparably damaged cells, apoptosis or senescence (Vousden and Prives, 2009). In addition to activation as a result of one of the above described stimuli, p53 is also activated upon inappropriate stimulation of DNA synthesis. E7-mediated premature cell cycle re-entry of suprabasal keratinocytes leads to induction of p53, which is targeted by E6 for degradation to prevent apoptosis of HPV genome containing cells.

The mechanism by which E6 degrades p53 involves the host E3 ubiquitin ligase E6-AP. The p53 protein is not a natural target of E6-AP; it only binds to p53 in the presence of E6, leading to its degradation through the proteasome (Huibregtse et al., 1991; Scheffner et al., 1990, 1992, 1993). This degradation effect is only towards nuclear p53, as a p53 mutant that localises predominantly in the cytoplasm is not degraded by E6 (Stewart et al., 2005). While both high and low-risk E6 proteins interact with p53, only high-risk proteins can induce its degradation. This is due to differences in the domains of p53 to which E6 bind; only high-risk E6 proteins bind to the core region of p53, which appears to be required for E6-mediated degradation (Bernard et al., 2011; Li and Coffino, 1996).

In addition to directing its degradation, E6 can also manipulate p53 function by inhibiting its binding to specific DNA sequences. This inhibition correlated with the relative affinity of E6 for p53, with E6 proteins such as those derived from HPV16 shown as a strong binder and potent inhibitor of p53 DNA binding (Lechner and Laimins, 1994). Mechanistically, E6 binding induces a conformational change in the p53 protein that prevents p53-DNA binding and/or disruption of already formed p53-DNA complexes (Thomas et al., 1995).

A second mechanism by which E6 modulates p53 function distinct from degradation is through changes in its localisation. In E6-expressing cells, a subpopulation of p53 is retained in the cytoplasm. While not fully understood, this sequestration may arise either through masking of the nuclear localisation sequence located in the protein's C-terminus or through enhanced nuclear export (Freedman and Levine, 1998; Stewart et al., 2005). The latter hypothesis is supported by findings in HPV positive cervical cancer cell lines that inhibition of nuclear export by the drug leptomycin B, which blocks the formation of several nuclear export complexes, leads to increased nuclear p53 (Freedman and Levine, 1998).

The ability of E6 to target p53 through multiple mechanisms is important not only during the virus life cycle where it contributes to replication of viral DNA and episomal maintenance (Flores et al., 2000; Kho et al., 2013; Lorenz et al., 2013; Park and Androphy, 2002; Thomas et al., 1999; Wang et al., 2009), but it has important implications for cancer development. Loss of p53 likely contributes to the acquisition of additional oncogenic mutations seen during disease progression that would have otherwise been repaired, leading to genomic instability. This is discussed further in section 1.2.7.

1.2.6.2.2 E6 and PDZ domain-containing proteins

Other important E6 interacting partners are those that contain PDZ domains. These proteins often contain multiple PDZ domains as well as other interaction domains (e.g. Src homology 2 domains) and so often act as protein scaffolds. As a result, these proteins can form multiprotein complexes that are involved in diverse cellular functions, including neuronal synapse formation, cellular polarity and proliferation, and survival. Rather unsurprisingly, these proteins are often deregulated during viral infection and during carcinogenesis (reviewed in James and Roberts, 2016).

In the high-risk viruses, E6 binding to PDZ domain-containing proteins occurs via a short peptide sequence (class I PBM) located in the protein's carboxyl terminus. Interestingly, of the ~300 PDZ proteins encoded by the human genome, E6 only targets a subset of approximately 19 proteins (Thomas et al., 2016).

As all high-risk E6 proteins possess a canonical PBM, the ability to target PDZ domain-containing proteins was therefore thought to be a marker of oncogenicity. However, it was recently shown that the several related, albeit non-oncogenic, virus types (such as HPV40) degrade PDZ domain-containing proteins. The authors suggest that, therefore, the ability of E6 to target PDZ domain-containing proteins represent an adaptation to colonise a new ecosystem in the host and this was acquired prior to the oncogenic phenotype (Van Doorslaer et al., 2015).

Although all high-risk E6 proteins contain PBMs, there is variation within this region (HPV16 E6: ETQL; HPV18 E6: ETQV). The first hint that this difference in sequence was biologically relevant came from early studies on the interaction of HPV18 and HPV16 E6 with the PDZ domain-containing proteins Dlg1 and scribble (otherwise known as hScrib). These studies demonstrated that a single valine/leucine residue within the PBM determines

substrate specificity, with HPV18 E6 (PBM: ETQV) binding Dlg1 more efficiently than HPV16 E6, and vice versa, HPV16 E6 (PBM: ETQL) preferring hScrib over Dlg1 (Thomas et al., 2005).

A recent analysis compared the binding profile of the E6 PBM of various virus types, both oncogenic and non-oncogenic, and showed that sequences upstream of the PBM were also important in determining substrate specificity (Thomas et al., 2016). The results from this study showed that while Dlg1 was a major target of all PBMs tested, regardless of oncogenic potential, the interaction with hScrib correlated directly with cancer risk, with interactions detected for all virus types classified as Group I carcinogens by IARC (Thomas et al., 2016).

The ability of E6 to target PDZ domain-containing proteins is important for several stages of the virus life cycle. Loss of this PDZ targeting ability in various experimental systems has shown it to play a role in cell proliferation, mitotic integrity, viral genome maintenance and amplification, and late viral protein expression (Lee and Laimins, 2004; Nicolaides *et al.*, 2011; Delury *et al.*, 2013; Marsh *et al.*, 2017). Furthermore, some of these PDZ targets, such as hScrib, are important for regulating E6 protein expression, further highlighting the importance of this E6 function (Kranjec et al., 2016; Nicolaides et al., 2011). Interestingly, there appears to be some co-operation between E6's p53 and PDZ targeting ability, with depletion of p53 improving episomal maintenance in cells lacking the PBM (Brimer and Vande Pol, 2014). This is intriguing as E6 mutants defective for PDZ targeting still target p53 as efficient as the wild type protein, which may suggest that at least one of the targets of the E6 PBM feeds into a cellular pathway controlled by p53 (Brimer and Vande Pol, 2014; Nguyen et al., 2003).

This motif likely also plays a key role in HPV-driven transformation and cancer development, with studies showing this targeting ability to be important for the transforming ability of E6 both *in vivo* and *in vitro*. Studies in immortalised keratinocytes showed that the E6 PBM contributed to an epithelial to mesenchymal-like phenotype with concomitant changes in the actin cytoskeleton and adherens junctions, all of which are features of the transformed phenotype in keratinocytes (Watson et al., 2003). In addition, this motif has been linked to anchorage-independent growth in both mouse and human tonsillar keratinocytes and contributes to the inhibition of apoptosis in epithelial cells (James et al., 2006; Spanos et al., 2008). Furthermore, studies in transgenic mice showed that the E6 PBM contributes to epithelial hyperplasia, with mice expressing a ΔPDZE6

developing fewer and smaller tumours compared to those expressing a wild type E6 protein (Shai et al., 2007).

Little is known about which of the E6 PDZ targets are important for HPV-associated carcinogenesis. In normal cervical keratinocytes expressing E7, oncogenic Ras (Ras^{G12V}) and an E6 protein unable to degrade PDZ proteins, short hairpin RNA (shRNA)-mediated depletion of hScrib, MAGI1 or PAR3 increased anchorage-independent growth, with a combined knockdown inducing anchorage-independent growth to the same level as the wild type E6. Combined knockdown of hScrib, Dlg1 and Dlg4 had the same effect. Analysis of tumorigenicity in nude mice showed that combined knockdown of MAGI1 and hScrib or Dlg1, Dlg4 and hScrib enhanced tumour growth more than the individual shRNAs but not to the level of wild type E6. Interestingly, however, triple knockdown of MAGI, hScrib and PAR3 led to tumour growth at a higher rate than that of wild type E6. Together, these data indicate that multiple targets of the E6 PBM are relevant for HPV-associated cervical carcinogenesis (Yoshimatsu et al., 2017)

A description of two of the most well studied E6-PDZ interactors, Dlg1 and hScrib, is given below.

1.2.6.2.2.1 E6 and Dlg1

The first E6-PDZ target identified was the human homologue of the *Drosophila* discs large 1 tumour suppressor protein, Dlg1 (Kiyono *et al.*, 1997; Gardiol *et al*., 1999). Dlg1 contains three PDZ domains and is the founding member of the membrane-associated guanylate kinase homologs protein family (Hough et al., 1997). Much of what is known about Dlg function comes from a series of studies carried out in *Drosophila* where it was shown to localise to septate junctions (Woods and Bryant, 1991). Mutation of Dlg results

in neoplastic growth of imaginal discs, epithelial structures that give rise to adult body structure during *Drosophila* development. These studies showed that Dlg is required for the correct organisation of the cytoskeleton, for the proper localisation of membrane proteins and for establishing epithelial polarity in the fly (Woods et al., 1996).

Interestingly, the human homologue of Dlg shares approximately 60% homology and has the same localisation as its *Drosophila* counterpart (Lue et al., 1994), raising the suggestion that it plays a similar function in human cells. Indeed, changes in Dlg1 expression and localisation are seen in various cancer types, including cervical cancer, and its loss may contribute to neoplastic transformation through changes in tissue architecture (Mantovani et al., 2001; Sugihara et al., 2016; Watson et al., 2002).

The E6-Dlg1 interaction results in degradation of the nuclear, phosphorylated form of the protein (Kiyono *et al.*, 1997; Gardiol *et al*., 1999). It is much more efficiently degraded by HPV18 E6 than by HPV16 E6 (Thomas et al., 2005). There is some contention in the literature of the exact ubiquitin ligase involved in this degradation, with some studies stating this occurs in an E6-AP independent fashion (Pim et al., 2000; Sterlinko Grm and Banks, 2004), while others suggest functional E6-AP is required (Kuballa et al., 2007).

Changes in Dlg1 localisation has been reported during cervical cancer progression, with loss of Dlg1 at sites of cell to cell contact associated with a concomitant increase in cytoplasmic Dlg1 in high-grade cancers (reviewed in Roberts et al., 2012). Total cellular levels of Dlg1 are also reduced in high-grade cancers. As the vast majority of cervical cancers contain HPV DNA, and oncogenic HPVs are known to target Dlg1 for degradation, it is tempting to speculate that these changes may represent an important step during HPV associated cervical carcinogenesis (Watson et al., 2002). However, HPV negative cervical cancer cell lines also display reduced levels of Dlg1, suggesting that

alternative mechanisms may also regulate Dlg1 expression in cancer (Mantovani et al., 2001). It is plausible that the presence of oncogenic HPV genomes enhances Dlg1 degradation but this is yet to be proven.

1.2.6.2.2.2 E6 and hScrib

hScrib is the human homologue of the *Drosophila* scribble protein. It is a member of the leucine-rich repeat and PDZ family of proteins, with 16 leucine-rich repeats and four PDZ domains (Murdoch et al., 2003). hScrib localises to the basolateral membrane of polarised epithelial cells where it colocalises with Dlg1 (Dow et al., 2003; Nakagawa et al., 2004).

In *Drosophila,* loss and/or mutation of scribble results in mislocalisation of apical proteins and adherens junctions to the basolateral cell surface due to changes in localisation of the apical transmembrane protein Crumbs (Bilder and Perrimon, 2000), and results in cells that are overgrown and profoundly disorganised (Bilder et al., 2000). Using a *Drosophila* system containing mutant scribble combined with overexpression of the human homologue, hScrib was shown to functionally restore defects in differentiation, tissue architecture and polarity induced by the mutant fly protein (Dow et al., 2003), leading to the idea that both *Drosophila* and human proteins act as tumour suppressors.

Analysis of hScrib during cervical cancer progression showed a dramatic loss at the protein level in samples derived from HPV positive invasive cancers compared to control tissue. Furthermore, immunohistochemical analysis was only able to detect a faint signal in the uppermost layers of the epithelium. This is in contrast to control tissue where it was localised to sites of cell to cell contact (Nakagawa et al., 2004)

In an analogous way to HPV18 E6's apparent preference towards Dlg1, HPV16 E6 targets and degrades hScrib more efficiently via E6-PDZ interaction. The same study showed that

E6 could abrogate hScrib's inhibition of cell immortalisation in a co-operation assay using oncogenic Ras, suggesting that this degradation event may contribute towards cell immortalisation during the viral life cycle (Thomas et al., 2005).

1.2.6.2.2.3 Regulation of the E6 PBM

A canonical PKA phosphorylation motif (R/K-R/K-X-S/T) overlaps with the E6 PBM from several high-risk viruses, including HPV18 and HPV16, with the amino acid (serine or threonine) at position -3 being the phosphoacceptor (Kühne et al., 2000). In HPV18 E6, phosphorylation of threonine at position 156 by PKA blocks E6-PDZ interactions by steric hindrance (Zhang et al., 2007), preventing E6-mediated degradation of Dlg1 (Kühne et al., 2000). In addition to regulating E6-PDZ interactions, PKA phosphorylation allows for E6 interactions with non-PDZ proteins such as 14-3-3 family members (Boon and Banks, 2012).

Studies in keratinocytes maintaining HPV18 genomes in which the E6 protein cannot be phosphorylated by PKA showed increased growth of HPV genome containing cells and a more hyperproliferative phenotype on organotypic raft culture compared to cells maintaining wild type HPV genomes (Delury et al., 2013). In addition, this loss of kinase recognition has also been associated with enhanced morphological transformation of keratinocytes (Watson et al., 2003), suggesting that changes in E6 phosphorylation may be relevant for disease progression.

In addition to the above regulation by PKA, the E6 PBM is also subject to modulation by oxidative stress or the DNA damage response. Experiments done in cervical cancer cells showed that the induction of either process resulted in phosphorylation of E6. Depending on the exact stimulus, this phosphorylation occurred via the ATM/ATR pathway and was

primarily mediated by Chk1, although checkpoint kinase 2 was involved to a lesser extent via activation of PKA. This was associated with an inhibition of p53 transcriptional activity on some p53-responsive promoters, linking the DNA damage response to control of the E6 PBM and its p53 targeting ability (Thatte et al., 2018).

Recent evidence has suggested that the presence of this PKA site contributes to E6's recognition of cellular PDZ proteins. Mutation of HPV18 E6 sites crucial for PKA phosphorylation reduced the number of PDZ proteins to which E6 could bind. In contrast, the generation of a PKA recognition motif in HPV66 and HPV40 E6 proteins, which have PBMs but not PKA recognition sites, increases PDZ recognition. While it would be assumed that acquisition of a PKA recognition site would limit E6-PDZ interactions through changes in phosphorylation, it appears instead that this contributes to the promiscuity of the E6 PBM (Sarabia-Vega and Banks, 2019).

1.2.6.3 E7

High-risk E7 proteins are approximately 18 kDa in size, have no known enzymatic activity and, like E6, target and modify the function of various cellular proteins during infection. E7 proteins contain at their amino-terminus sequence similarity to the conserved regions 1 and 2 of adenovirus E1A and simian virus 40 large T, and a carboxyl zinc-binding site, consisting of two CXXC domains separated by 29 to 30 amino acids. Loss of E7 in an HPV18 life cycle model has shown it to contribute to viral DNA amplification and production of infectious virus during differentiation (McLaughlin-Drubin et al., 2005). This viral DNA amplification defect is also evident in life cycle models of HPV16 and HPV31 (Flores et al., 2000; Thomas et al., 1999). In all of these life cycle models, it does not appear to contribute to the maintenance of viral episomes (Flores et al., 2000; McLaughlin-Drubin et al., 2005; Thomas et al., 1999)

E7 appears to be the major transforming protein in standard mouse-based cell transformation assays, showing morphological transformation in NIH-3T3 mouse fibroblasts and, together with oncogenic Ras, baby rat kidney cells. For this, E7 regulates a myriad of host processes, including the cell cycle, transcription, cell death/survival, DNA damage/repair and cellular differentiation, among others (Roman and Munger, 2013; Yeo-Teh et al., 2018).

The best characterised E7 interaction is that of the Rb tumour suppressor and the related pocket proteins, p107 and p130, and is described below.

1.2.6.3.1.1 E7 and the pocket proteins-E2F complex

The interaction with the Rb tumour suppressor and the related pocket proteins, p107 and p130, is one of the best characterised E7 interactions. These interactions occur via a conserved LXCXE motif in the N-terminus of the protein and serve to induce host DNA synthesis in post-mitotic, differentiating keratinocytes (Lee et al., 1998; Münger et al., 1989).

This family of proteins negatively regulates cell cycle progression from G_0 into G_1 and then into S phase. The expression of these pocket proteins varies throughout the cell cycle, with Rb constitutively expressed throughout all stages of the cell cycle, p107 expressed largely in S phase and p130 in G_0 (Classon and Dyson, 2001). In differentiating epithelium, there is also variation in expression; Rb and p107 are localised to the basal and suprabasal keratinocytes, with p130 confined to the uppermost differentiated layers (Roman, 2006; Zhang et al., 2006).

The mechanism by which the pocket proteins control cell cycle progression involves, at least in part, the E2F family of transcription factors. Their expression is low in quiescent

cells but is induced as cells move through G1/S. There are eight E2F genes encoding nine major proteins, with three (E2F1, E2F2, and E2F3a) considered activating E2Fs based on experiments that showed they activate transcription when overexpressed and two (E2F4 and E2F5) considered repressive factors. E2F6, E2F7 and E2F8 do not contain the sequences required for transactivation or binding to pocket proteins and therefore are pocket protein-independent regulators of transcription (Iaquinta and Lees, 2007).

In normal cells, the transcriptional activity of E2Fs 1-5 is regulated largely by their interactions with the pocket proteins, with pocket protein binding thought to inhibit transcription by two mechanisms. These mechanisms include masking the key residues required for transcriptional activation and by recruiting repressor complexes to E2F-responsive promoters. In $G_{0/1}$, the repressive E2Fs are complexed with p107 and p130 proteins and associate with E2F-responsive genes to repress their transcription. Similarly, the activating E2Fs are bound by Rb, inhibiting their ability to activate transcription. As cells enter the cell cycle, there is induction of cyclin-CDK activity, which leads to phosphorylation of the pocket proteins, with subsequent disruption of pocket protein-E2F complexes (Iaquinta and Lees, 2007; Trimarchi and Lees, 2002). In the case of the activator E2Fs, this relief of inhibition leads to binding of E2Fs to target promoters where they activate transcription (Trimarchi and Lees, 2002).

In high-risk HPV genome containing cells, E7 binds to the pocket proteins via its LXCXE motif and targets them for proteasomal degradation via the cullin-2 ubiquitin ligase complex in a manner dependent on the host protease calpain (Münger et al., 1989; Boyer et al., 1996; Chellappan et al., 1992; Darnell et al., 2007; Huh et al., 2007). As a result, the inhibitory effect of the pocket proteins on E2Fs is lost and E7-expressing cells show induction of various E2F-responsive genes involved in host DNA synthesis and cell cycle

re-entry, such as PCNA and cyclins A and E in differentiating cells (Cheng et al., 1995; Demeter et al., 1994). This is consistent with the data from an HPV16 life cycle model that showed that E7-mediated induction of host suprabasal synthesis required pocket protein binding, although this was independent of Rb degradation (Collins et al., 2005). E7 proteins from low-risk HPVs can associate with Rb but this interaction does not lead to induction of E2F-responsive genes, although they can still degrade p130 (Dyson et al., 1989; Zhang et al., 2006).

There is conflicting evidence whether targeting of Rb is important for cellular transformation, with studies in various experimental systems showing that transformation correlates with Rb binding (Heck et al., 1992) but others showing that it is not essential (Jewers et al., 1992).

1.2.7 HPV and cancer

Oncogenic HPV infection accounts for approximately 600,000 annual cases of cancer of the cervix, oropharynx, anus, vulva and vagina, with the vast majority (70%+) of these cancers being associated with HPV16 or HPV18 infection (de Martel et al., 2017; Plummer et al., 2016). In the cervix, HPV16 tends to be associated with the development of squamous cell carcinomas while HPV18 is largely associated with adenocarcinomas (Bulk et al., 2006). The risk factors for the development of HPV associated cancer in HPV infected individuals have not been fully defined but may include long term (~6+ years) use of the combined oral contraceptive pill and smoking (Dempsey, 2008; Vaccarella et al., 2006). The exact mechanisms by which these factors contribute to cancer risk are unknown but presumably involve suppression of the immune system, leading to viral persistence, or through smoking-induced acquisition of DNA damage.

The role of oncogenic HPVs in the development of cervical cancer has received much research attention and this multistep process is fairly well defined. This process involves initial infection, virus persistence, the development of a pre-cancerous lesion and cancer. Of note, although high-risk HPV is an incredibly common infection, with an estimated global prevalence of up to 25%, the vast majority of these infections are cleared by the host immune system within two years, with only around 10% of infected individuals at risk of cervical cancer (Bruni et al., 2010; Velfhuijzen et al., 2010).

Cervical cancer features a well-defined pre-malignant phase that is amenable to clinical examination by cytology and/or histology based examination of cervical tissue. These pre-malignant changes represent a range of histological abnormalities, ranging from grade one cervical intraepithelial neoplasia (CIN1) whose features include mild dysplasia confined to the basal one-third of the epithelium to CIN3, which features severe dysplasia, may be present throughout the epithelium and is considered to be carcinoma in situ/pre-cancer. Persistent infection is considered to be a key factor for the later development of cervical cancer, with several studies highlighting that women who harboured persistent oncogenic HPV were significantly more likely to go on to develop cervical neoplasia than those who were infected with different oncogenic type sequentially or those who cleared the infection (Cuschieri et al., 2005; Kjaer et al., 2002; Wallin et al., 1999).

In those with persistent infection, a critical event in the carcinogenic process is the integration of the viral genome into host DNA. This integration event can occur by one of two mechanisms, either a single viral genome can integrate into host DNA or multiple copies of the viral genome integrate into host DNA, and provides HPV genome containing cells a growth advantage through increased expression of early viral proteins (Jeon et al., 1995; McBride and Warburton, 2017). There are several mechanisms by which integration

drives early protein expression, including disruption of the E2 ORF. Loss of E2 protein alleviates its repressive effect on the early promotor, which drives early oncoprotein expression (Nishimura et al., 2000). An alternative mechanism is one by which progressive methylation of E2 binding sites 1 and 2 occurs during carcinogenesis, promoting the binding of E2 to binding site 4 and leading to upregulation of early viral transcripts with the potential to encode E6 and E7 (Leung et al., 2015). Various other mechanisms may also be relevant during carcinogenesis, including the formation of a virus-host super-enhancer, with the viral genome integrating adjacent to and synergising with a cellular enhancer, driving E6/E7 expression (Dooley et al., 2016).

As described in section 1.2.4, expression of the E6 and E7 oncoproteins disrupt a number of host pathways, including those dependent on p53 and Rb, and this is important for multiple aspects of the viral life cycle. Although this increased expression of E6 and E7 is likely a driving force in progression from CIN1 to cervical cancer (Daniel et al., 1997; Liu et al., 2018), additional cellular insults are required for cancer progression. One key mechanism underlying progression is the induction of host genomic instability. For example, cells expressing E6 and E7 override growth arrest mediated by DNA damaging agents (Song et al., 2002), induce numerical and structural chromosomal abnormalities (Duensing and Münger, 2002) and prevent the repair of DNA lesions by impairing the activity of cellular DNA damage response pathways (Khanal and Galloway, 2019). It is thought that mechanisms such as these contribute to the acquisition of the additional oncogenic hits needed for cell transformation. Consistent with this, recent evidence has shown that mutational load correlates with the degree of cancer risk, highlighting the important role that these additional oncogenic events play during disease progression (Gillison et al., 2019; Litwin et al., 2017; Tian et al., 2019).

1.2.8 HPV prevention

There are currently three licensed vaccines against HPV marketed by the pharmaceutical companies Merck and GlaxoSmithKline – Cervarix, Gardasil and Gardasil9. These vaccines contain L1 virus-like particles derived from several HPV types, produced either in yeast or baculovirus expression systems, and confer immunity through the generation of high titres of virus neutralising antibodies that appear to be stable over time (David et al., 2009; Mariani and Venuti, 2010; Villa et al., 2006).

Cervarix is a bivalent vaccine that offers protection against both high-risk HPV16 and HPV18. Gardasil is a quadrivalent vaccine that offers protection against HPV16 and HPV18 in addition to the low-risk HPV6 and HPV11 viruses that are associated with the development of genital warts and recurrent respiratory papillomatosis (Lacey et al., 2006). Gardasil9, which has since replaced Gardasil in vaccination programmes, confers protection against seven high-risk virus types as well as HPV6 and HPV11. The exact composition of these vaccines, including manufacturing components and adjuvants, is described in Harper and DeMars, 2017. All vaccines are approved from nine years of age with a two-dose schedule up to the age of 13 (Cervarix) or 14 (Gardasil and Gardasil9). In the UK, the HPV vaccination programme has been available through the NHS to girls ages 12 and 13 since 2008, with a catch-up scheme up to the age of 25. The recommended dose schedule is two doses but in individuals older than 15, the recommended schedule is 3 doses administered at months 0, 1 or 2 and 6. While the studies required for their regulatory approval assessed a variety of clinical endpoints, only a selection of the primary endpoints are described briefly here. A full description of the study endpoints can be found in the referenced European Medicines Agency public assessment reports.

The efficacy of Cervarix was assessed in two placebo-controlled, double-blind, clinical studies, including a total of 19,778 women aged 15 to 25. These studies demonstrated significant protection against CIN1 and CIN2+ disease associated with *de novo* infection by HPV16 and HPV18, as well as protection against persistent infection by these viral types for up to 12 months (European Medicines Agency, 2007). Long term follow up studies showed that this protective effect was evident at least up to 9.4 years post-vaccination (Naud et al., 2014). More recent data from Scotland tracking 138,392 women who received the bivalent vaccine at ages 12 or 13 reported a significant reduction in all grades of CIN disease at age 20, equating to a vaccine efficacy of >80%, as well as showing herd immunity against high-grade disease in unvaccinated women in the cohort offered vaccination (Palmer et al., 2019).

The efficacy of Gardasil was shown in four placebo-controlled double-blind, randomised clinical studies, including a total of 20,541 women. These studies demonstrated that Gardasil provided protection against CIN1-3, adenocarcinoma in situ (AIS), vulvar intraepithelial neoplasia (VIN) and genital warts associated with *de novo* HPV6, 11, 16 and/or 18 infections throughout the duration of the study. The efficacy of the vaccine against the combined incidence of persistent infection, genital warts, vulvar and vaginal lesions, CIN of any grade, AIS and cervical cancer related to these HPV types was 88.7%, with an efficacy rate of 84.7% for HPV16 or HPV18 alone. The duration of immunity following three doses of Gardasil has been shown for up to 14 years post-vaccination (European Medicines Agency, 2017a).

Analysis of the efficacy and long term effectiveness of Gardasil9 against HPV6, 11 16 and 18 showed that, in 16 to 26-year-old women, the vaccine was 92.2% effective in preventing HPV16 and 18 related CIN2/3, AIS and cervical cancer. For HPV6, 11, 16 or

18 related diseases, the vaccine was 96.0% effective for CIN or AIS, 100% for VIN2/3, 100% for vaginal intraepithelial neoplasia and 99.0% for genital warts. In women 24 to 45 years of age, combined efficacy against HPV6, 11, 16 and 18 associated disease was 88.7%. Finally, in men aged 16 to 26, efficacy against HPV6, 11, 16 and 18 associated disease was 74.9% for AIN 2/3, 100.0% for penile intraepithelial neoplasia grades 1-3 and 89.3% for genital warts. This protection appears to be stable long term as a review of data from 2,084 women over 12 years showed no cases of high-grade CIN. In addition, long term extension studies showed no cases of high-grade intraepithelial neoplasia nor genital warts up to 11.5 years in both sexes (European Medicines Agency, 2017b).

As of September 2019, the HPV vaccine will be given to boys aged 12 and 13 in England, Northern Ireland and Wales, and boys aged 11 and 12 in Scotland on a two-dose schedule. There are also calls for the vaccine to be made available to all men and boys up to the age of 25, matching the coverage available to girls and women on the NHS.

1.3 The cyclic AMP (cAMP)-PKA signalling axis

1.3.1 Cell signalling overview

Cell signalling describes a complex network of communication events that allow cells to respond to changes in their environment. Signalling molecules that cannot bypass the cell membrane provoke their effect by binding to receptors on the cell surface. These are therefore known as first messenger molecules and are often peptides or peptide hormones. Once the signalling molecule binds to its receptor, the receptor undergoes a conformational change that ultimately results in the generation of a second messenger molecule that mediates the effects of the peptide inside the cell.

1.3.2 cAMP signalling overview

Cyclic adenosine monophosphate (cAMP) was the first second messenger to be discovered and was identified during work to elucidate the mechanism underlying the hyperglycaemic actions of adrenaline and glucagon in the liver (Akileswaran et al., 2001; Sutherland et al., 1968). Since then, cAMP has been shown to mediate the effects of numerous hormones via G-protein coupled signalling in mammals. In addition, cAMP is present in all kingdoms where it regulates diverse processes such as mammalian gene transcription and virulence in pathogenic bacteria and fungi (Gancedo, 2013; McDonough and Rodriguez, 2011).

In mammalian cells, activation of the cAMP signalling pathway occurs following the binding of an extracellular ligand to its respective G protein-coupled receptor (GPCR) which, through G proteins, regulate the activity of the adenylyl cyclases (AC), a family of enzymes that generate cAMP from adenosine triphosphate (ATP). The effects of cAMP are mediated through three main effector proteins: the cAMP-dependent protein kinase A (PKA), exchange proteins directly activated by cAMP (EPACs) and cyclic nucleotide-gated ion channels. The level of cAMP within cells is also regulated by another set of enzymes known as phosphodiesterases (PDEs), which break down cAMP into adenosine monophosphate (AMP), as well as through a-kinase anchoring proteins (AKAPs) that act as signalling hubs that compartmentalise these signalling events (Wong and Scott, 2004).

1.3.3 Adenylyl cyclases

There are two families of AC enzymes expressed in mammalian cells, which are either soluble or transmembrane-associated. Soluble AC has two heterologous catalytic domains in the N-terminus with several putative regulatory domains in the C-terminus, including an autoinhibitory domain (Buck et al., 1999; Chalopuka et al., 2006). In addition to this

full-length protein, there is a splice variant containing just the catalytic domains (Jaiswal and Conti, 2001). The activity of both the full length and the splice variant soluble AC is stimulated by bicarbonate and calcium ions and regulates processes mediated by changes in these ions in diverse cells and tissues, including the testis and sperm, kidney and eye, among others (Litvin et al., 2003; Tresguerres et al., 2011).

There are nine known isoforms of transmembrane ACs (I-XI), which share a common structure of two transmembrane and two cytoplasmic regions. Each transmembrane region contains six membrane-spanning domains linked to each other by cytoplasmic domains (Hurley, 1999). These transmembrane ACs are characterised into one of four different groups depending on how they are regulated; group I consists of Ca^{2+}-stimulated ACs 1, 3 and 8; group II of Gβγ-stimulated AC 2, 4 and 7; group III of Giα (an inhibitory Gα protein)/Ca^{2+}-inhibited AC5 and 6, while group IV contains forskolin-insensitive AC9 (Sadana and Dessauer, 2009).

The mechanism of cAMP synthesis involves the conversion of ATP to cAMP. This is a cyclisation reaction of ATP with the simultaneous release of inorganic phosphate (otherwise known as inorganic phosphate) (Eckstein et al., 1981; Gerlt et al., 1980). Degradation of cAMP occurs through the actions of PDEs that catalyse the hydrolysis of the 3'-phosphodiester bond on the ribose sugar, converting cAMP to AMP (Ashman et al., 1963; Skoyles and Sherry, 1992). A schematic of cAMP generation and degradation is shown in **Figure 1.5.**

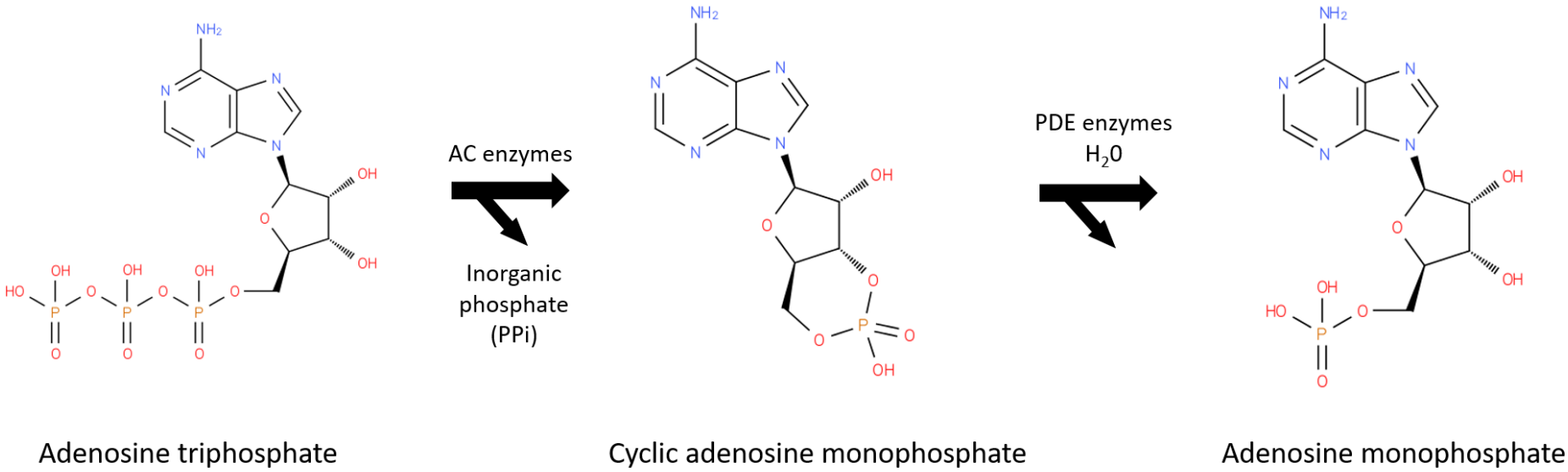

Figure 1.5: cAMP metabolism. Cyclic AMP is formed by the actions of the adenylyl cyclase (AC) family of enzymes, which convert ATP to cAMP. Mechanistically, this is a cyclisation reaction where there is displacement of inorganic phosphate by nucleophilic attack of the 3'-OH atom towards the inorganic phosphate, resulting in a change of configuration. Inorganic phosphate is then released (PPi). Degradation of cAMP to AMP is mediated by phosphodiesterase enzymes (PDEs), which catalyse the hydrolysis of phosphodiester bonds. The structural images were taken from the Chemical Entities of Biological Interest database where the ID numbers were ATP: 15422, cAMP: 17489 and AMP: 16027.

1.3.4 G protein-coupled receptors and G proteins

The first step in the cAMP signalling pathway is the activation of GPCRs and their associated guanine nucleotide binding proteins (i.e. G proteins). GPCRs are the largest family of proteins in the mammalian genome with more than 1000 human GPCRs identified to date. It is thought that around 80% of all known hormones and neurotransmitters signal through GPCRs (Lesch and Manji, 1992). Examples of GPCR-mediated signalling include those that regulate heart contractility (β1-adrenergic receptor: Madamanchi 2007; McGraw & Liggett 2005) and brain function (dopamine receptor: Girault & Greengard 2004). Structurally, GPCRs share a common structure of seven hydrophobic transmembrane domains, an extracellular amino terminus and an intracellular carboxyl terminus. Despite this conserved structure, individual GPCRs can have unique combinations of cell signalling activities, with multiple G protein subtypes and G protein independent signalling pathways contributing to these functions (Rosenbaum et al., 2009). Accordingly, GPCRs have been implicated in regulating diverse physiological functions, such as vision, thyroid function, hormone secretion and fertility, and have also been linked to cancer development (Schoneberg et al., 2004). A general overview of GPCR activation is given below.

When the GPCR is inactive, the guanosine diphosphate (GDP) bound alpha subunit (Gα) and a G protein beta and gamma heterodimeric complex (Gβγ) exist as a multi-protein complex bound to GDP, which may or may not be associated with the GPCR. On ligand binding to the GPCR, there is a conformational change in the intracellular domain of the GPCR that leads to the exchange of GDP for guanosine triphosphate (GTP) on Gα. This binding of GTP results in the dissociation of Gα from this G protein complex, activating multiple downstream effectors. Of note, activated Gα subunits bind to and induce a

conformational change in ACs, resulting in their activation and upregulation of cAMP synthesis (Hurley, 1999). Other effector molecules include calcium and potassium ion channels, phospholipase C and other kinases. Similarly, the Gβγ subunit interacts with various downstream effectors, including ACs, potassium channels and the β-adrenergic receptor kinase (Logothetis et al., 1987; Tuteja, 2009). The Gβγ subunit can also activate the Gα subunit (Rondard et al., 2001). Finally, inactivation of GPCR signalling occurs via the GTPase activity of the Gα subunit, hydrolysing GTP to GDP, leading to its reassociation with Gβγ, stopping the signal (**Figure 1.6**).

GPCRs do not solely exist in 'on' or 'off' configurations, but instead adopt a range of confirmations depending on their association with other ligands and receptors, other signalling molecules and/or regulatory proteins (Geppetti et al., 2015). In addition to this, GPCRs can be spontaneously active and show ligand-independent activity, otherwise known as constitutive receptor activity, which contributes to the basal activity of cell signalling cascades (Costa et al., 1992; Schütz and Freissmuth, 1992).

1.3.5 Phosphodiesterases

Phosphodiesterases are a superfamily of enzymes that catalyse the hydrolysis of the cyclic phosphate bond in cAMP and cyclic guanosine monophosphate (cGMP) nucleotides, generating AMP and GMP. There are at least 11 PDE families, comprising five dual specific PDEs (PDEs 1-3, 10 and 11), three cAMP-specific PDEs (PDEs 4, 7 and 8) and three cGMP specific PDEs (PDEs 5, 6 and 9). The general structure of these proteins is a transmembrane helix in the N-terminus responsible for subcellular localisation, two regulatory domains (consisting *inter alia* of an autoinhibitory domain, phosphorylation site, ligand binding and effector binding sites), a catalytic domain and a C-terminal

anchoring domain (Azevedo et al., 2014). This anchoring domain is involved in targeting PDEs to distinct subcellular locales.

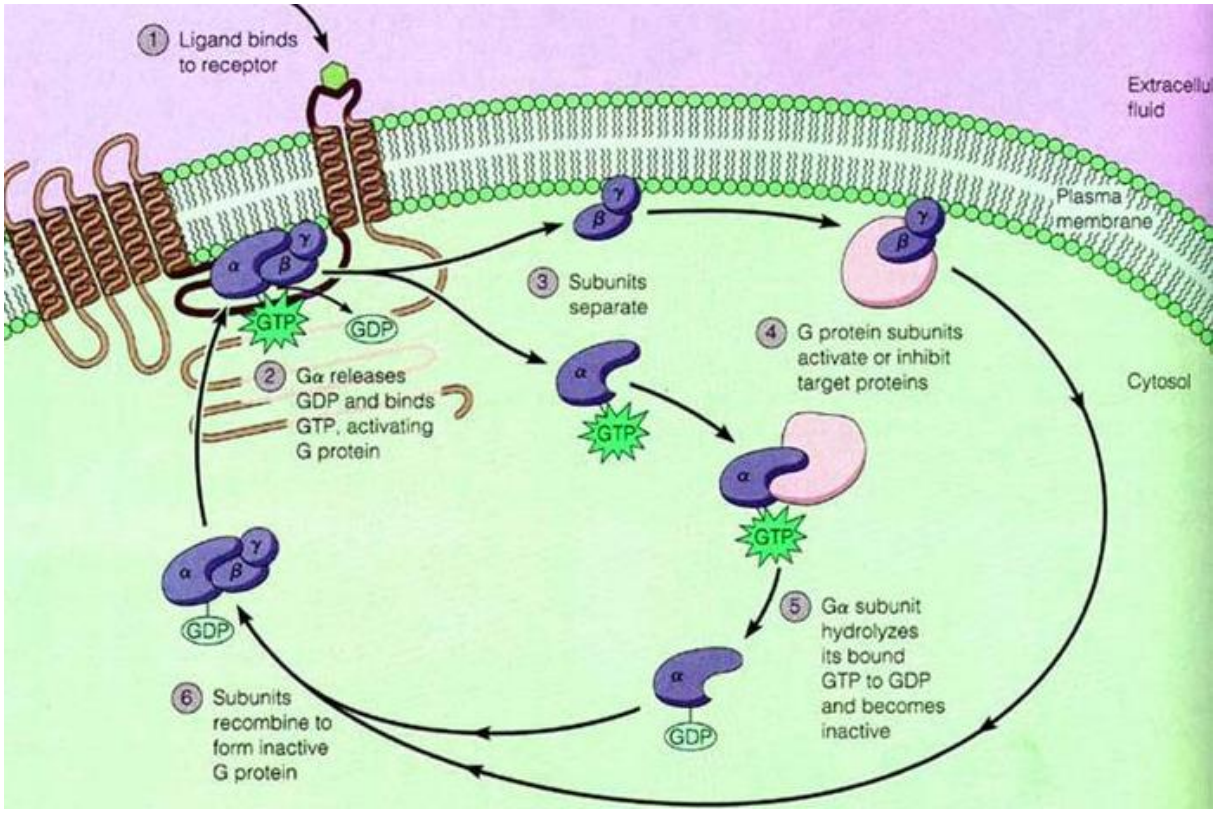

Figure 1.6. GPCR cycle. The first step in activation of G-protein coupled receptor signalling begins with ligand binding to its receptor (Step 1), which results in the exchange of GDP for GTP on the Gα subunit, with subsequent separation of the subunits to G_{α} or a $G_{\beta\gamma}$ dimer (Steps 2 and 3). These activated G protein subunits then interact with their target proteins (Step 4). Cessation of signalling occurs when the GTP bound to the Gα is hydrolysed by the intrinsic GTPase activity of Gα (Step 5), leading to the reassociation of Gα and Gβγ subunits (Step 6), terminating the signal. Image taken from SilvaBio, 2009.

The PDE families are derived from 21 different genes and classified into the above groups based on amino acid sequence, regulatory properties and mechanisms of catalysis. PDEs 1-4 are expressed in most cells, with PDE3 and 4 providing the bulk of the cAMP hydrolysis. The other PDEs are likely only expressed in select cell populations where they regulate critical functions therein (Francis et al., 2011).

The activity of these enzymes is regulated by AC and guanylyl cyclases through different effector proteins and feedback networks, ensuring appropriate cAMP and cGMP levels for cell signalling networks. While the main mechanism for lowering cAMP/cGMP levels is through inactivation by hydrolysis of the phosphodiester bond, additional mechanisms such as changes in the localisation of the cyclic nucleotide into the extracellular environment and into adjacent cells have also been reported, although these likely only contribute to small changes in cAMP levels (Barber and Butcher, 1981; Cheng et al., 2010; Norris et al., 2009).

1.3.6 Protein Kinase A

Protein kinase A is a heterotetrameric protein kinase composed of two catalytic (C) subunits and two regulatory (R) subunits. There are two isoforms of PKA that differ in the identity of their R subunits (RI, RII), giving rise to either type I or type II holoenzymes (PKA-RI, PKA-RII) (Corbin et al., 1975; Reimann et al., 1971). There are various differences between the R subunits, including amino acid conservation (although they share 75% identity overall), molecular weight, isoelectric point and cAMP binding. Despite this, both regulatory subunits have the same general structure and contain a docking and dimerization domain in the N-terminus through which PKA can dimerise and interact with AKAPs (see 1.3.8). This is followed by an inhibitor site, either a pseudosubstrate for RI or substrate site for RII, that prevents activation of the catalytic

subunit, as well as two cAMP binding domains. While there are several differences in the biology of these regulatory subunits, there are two important differences; firstly, the PKA-RI holoenzyme more readily activated by cAMP than the -RII holoenzyme in both *in vivo* and *in vitro* experiments (Cummings et al., 1996; Dostmann et al., 1990), and RII subunits are autophosphorylated by the catalytic subunit, while the RI subunit is not (Langeberg and Scott, 2015).

The regulatory (RIα, RIβ, RIIα, RIIβ) and catalytic (Cα, Cβ, Cγ, and PRKX) subunits exist as multiple isoforms, with major differences in tissue expression, biochemical and physical properties of these subunits (Scott, 1991; Tasken et al., 1993; Clegg et al., 1988; Jahnsen et al., 1986; Lee et al., 1983; Scott et al., 1987). Despite this variation, no apparent preferential expression with any of the catalytic subunit isoforms with RI or RII has been found (Beebe et al., 1990)

The canonical mechanism for activation of PKA by cAMP was that after the generation of cAMP from GPCR signalling, activation of PKA occurs on cAMP binding to two sites on each regulatory subunit (sites A and B). When PKA is inactive, only the B site is exposed and available for cAMP binding. Following binding to this site, there is an intramolecular conformational change that allows binding of cAMP to site A. Once two molecules of cAMP are bound to each regulatory subunit, the catalytic subunits are liberated from the regulatory subunits and can phosphorylate their target proteins on serine or threonine residues within the PKA consensus sequence RRXS/T (Dostmann et al., 1990; Taylor et al., 1990). Additional analyses, however, have shown that there is more to this activation mechanism than first thought. Using X-ray scattering techniques under physiological concentrations of the holoenzymes, the addition of cAMP resulted in only partial dissociation of the subunits, with full dissociation requiring the presence of a substrate as

well as cAMP (Vigil et al., 2004). In addition, for the RII holoenzyme, autophosphorylation of the catalytic inhibitor sequence was required for cAMP-induced PKA dissociation, with subsequent dephosphorylation by a currently unknown PDE required for reassociation of the subunits (Isensee et al., 2018).

Deactivation of PKA has been less well studied but is thought to occur as a result of PDE binding to the cAMP binding domains of the regulatory subunits and likely involves allosteric communication between the two cAMP binding sites. In this model, PDE-mediated removal of cAMP from site A results in destabilisation of the intervening structure between the two cAMP sites such that the allosteric effects of site A on site B are lost, resulting in loss of cAMP binding at that site (Guo and Zhou, 2016). As a result, the R subunit, now free of cAMP, binds to the catalytic subunit, displacing the PDE and leading to reassociation of the holoenzyme complex and termination of the cAMP signal (Moorthy et al., 2011)

1.3.7 Other effectors of cAMP signalling

1.3.7.1 Exchange proteins directly activated by cAMP

For over 30 years, the widely held notion was that with the exception of cyclic nucleotide-gated ion channels (see 1.3.7.2), the effects of cAMP were mediated exclusively by PKA. In 1998, however, a new family of cAMP effectors was discovered – the EPACs. There are two EPAC proteins in humans (EPAC1 and EPAC2) which were originally thought to only act as guanine nucleotide exchange factors for the Ras-like GTPases Rap1 and Rap2, however, additional studies showed them to act as docking stations for additional proteins for the co-ordination of diverse signalling events (Grandoch et al., 2010; Kawasaki et al., 1998; de Rooij et al., 1998). These proteins are targeted to various subcellular locales, including the plasma membrane, cytoplasm and nuclear

membrane, and are involved in a wide array of physiological processes such as calcium handling, cell proliferation and differentiation and gene transcription (Grandoch et al., 2010).

EPACs consist of two structural domains - the N-terminal regulatory region containing two cAMP binding sites and the C-terminal catalytic region which confers guanine nucleotide exchange factor activity - connected by a central switchboard or hinge region. In the absence of cAMP, EPACs are kept in an autoinhibitory state whereby the N-terminal region folds over the C-terminal region, blocking the active site. On cAMP binding, however, there is an intramolecular conformational change such that this autoinhibition is lost and the two regions hinge away from one another, opening up the active site (Rehmann et al., 2008; De Rooij et al., 2000; Tsalkova et al., 2009). As a result, the catalytic region interacts with the target Rap protein and facilitates the exchange of GDP for GTP (De Rooij et al., 2000).

As these proteins are regulated by cellular cAMP concentrations, they have been widely used as genetically encoded sensors to measure intracellular cAMP levels in real-time. A description of this, as well as other sensors used to measure cAMP and PKA activity in cells, is provided in section 1.3.9.

1.3.7.2 Cyclic nucleotide-gated ion channels

Cyclic nucleotide-gated ion channels are a family of cation channels that transduce signalling events important for visual and olfactory function. These channels generally comprise four monomers, each containing six transmembrane helices, of which the first four form the voltage-sensing domain of the channel and the last two forming the central pore. These channels are directly regulated by the binding of the cyclic nucleotides cAMP

and cGMP to the final helical structure and, as a result, lead to depolarization of the cell membrane through the movement of sodium and potassium ions. Mechanistically, the binding of the cyclic nucleotide to the channel, in its closed conformation, gives rise to an allosteric conformational change in the linking region between the four helices that make up the voltage-sensing domain, opening up the channel and allowing for movement of ions (Gofman et al., 2014; Goulding et al., 1994; Kaupp and Seifert, 2002; Matulef and Zagotta, 2003).

1.3.8 A-Kinase Anchoring Proteins

The specificity of PKA signalling is exquisitely controlled by a combination of cellular factors, including interactions with a family of host proteins known as AKAPs. This family of proteins was first discovered as contaminants of purified PKA-RII subunits but have since been shown to be a structurally diverse protein family, unified by their ability to bind to PKA and precipitate catalytic activity (Pidoux and Taskén, 2010).

The first AKAP to be discovered was the microtubule-associated protein-2, which was found to be phosphorylated by PKA in lysate derived from brain microtubule preparations (Vallee et al., 1981). Since then, the number of AKAPs identified has risen dramatically, largely due to the widespread use of the modified Far Western blot technique known as the RII overlay. This technique, popularised by Lohmann *et al*, has been used extensively to investigate novel RII-binding AKAPs and is possible because the vast majority of AKAPs retain their PKA binding activity after transfer to a nitrocellulose membrane. In this technique, proteins are separated in two dimensions: first by isoelectric focusing in one dimension and then by sodium dodecyl sulfate-polyacrylamide gel electrophoresis (SDS-PAGE) based separation in the second. The membrane is then incubated with radiolabelled PKA-RII to identify RII binding proteins (Lohmanntt et al., 1984). Alternative methods

have also been used to identify cellular AKAPs, including yeast two-hybrid approaches and bioinformatic screens based on algorithms designed to identify binding motifs (Burgers et al., 2015). To date, more than 70 AKAPs have been identified (Suryavanshi et al., 2018).

The AKAP-PKA interaction is mediated through a 14 to 18 amino acid amphipathic helical structure that binds to the docking and dimerization domain of PKA. Both nuclear magnetic resonance spectroscopy and analysis of crystal structures of AKAP-PKA complexes have shown that the PKA regulatory subunits dimerise at the N-terminus and this is necessary for AKAP binding. Furthermore, the docking and dimerization domain consists of an antiparallel dimer that forms into a cross helix shape, providing a binding surface for the AKAP (Gold et al., 2006; Kinderman et al., 2006; Newlon et al., 2001; Pidoux and Taskén, 2010).

In addition to this PKA binding domain, AKAPs contain additional sequences that target these complexes to distinct subcellular locales, including the Golgi apparatus and the nucleus (Wong and Scott, 2004). Accordingly, PKA activity has been detected at these sites (Clister et al., 2019; Li et al., 2003; Zippin et al., 2004).

While these sequences target the AKAP-complex to the correct subcellular compartment, it is thought that protein-protein interactions at that site fine-tune the positioning of the AKAP towards it substrates (Carnegie and Scott, 2003). For example, AKAP79 localises to postsynaptic membranes in neurons through a targeting sequence that binds to acidic phospholipids and is selectively bound to glutamate receptor, calcium and potassium ion channels through protein-protein interactions (Dodge and Scott, 2000).

AKAPs further contribute to cAMP-PKA signalling by binding additional signalling molecules and forming multiprotein complexes important for regulation of signalling events. For AKAP79, in addition to binding PKA, it binds to protein kinase C and the calcium/calmodulin-dependent phosphatase, PP2B. These binding partners contribute to the functional diversity of signalling events mediated by the AKAP, where distinct combinations of AKAP79 binding partners dictate what signalling network the AKAP79 complex participates in as well as regulating what substrates are targeted by the complex (Hoshi et al., 2003, 2005).

Together, the data shows that AKAPs co-ordinate multiprotein signalling hubs capable of directing PKA to discrete subcellular sites where the kinase can act on its substrates, providing specificity to the cAMP-PKA signalling pathway.

1.3.9 Imaging-based measurement of cAMP and PKA

Up until the early 1990s, measurements of cAMP were made by conventional biochemical methods, including antibody-dependent competition assays, however, these experiments only gave information about total cAMP levels in pooled cellular populations at a single point in time. Although serial measurements could be taken to give an overall picture of cAMP changes over time, these experiments had limited spatiotemporal resolution and there was no information at that time of what was happening at a cellular level. As a result, the prevailing hypothesis at the time was that after generation by ACs, cAMP diffused freely into the cytoplasm where it was actioned by its effectors in the cytoplasm. Through the use of various genetically encoded biosensors, it is now known that cAMP signalling is highly organised into distinct cellular compartments, shaped by AKAPs and PDEs, to form signal transduction hubs (Beavo and Brunton, 2002; Paramonov et al., 2015).

The first widely used set of sensors were based on Förster resonance energy transfer (FRET). FRET involves the non-radiative energy transfer between a pair of donor and acceptor fluorophores, which is dependent on the intramolecular distance between the two fluorophores. All FRET sensors work in a similar fashion and generally have three domains: a sensor domain to which the molecule under study binds and the two fluorophores that make a FRET pair. The binding of the molecule under study to the sensor domain leads to a conformational change in the structure of the sensor, changing the distance between the donor and acceptor fluorophores. This change in distance is interpreted as a change in FRET efficiency (Paramonov et al., 2015). The first successful FRET sensor used to measure cAMP was based on PKA and featured the *ex vivo* labelling of catalytic subunits with fluorescein and the regulatory subunits with rhodamine, introduced into cells via microinjection (Adams et al., 1991). Binding of cAMP to the sensor resulted in dissociation of the holoenzyme such that fluorescein and rhodamine were no longer in close proximity, resulting in changes in FRET efficiency (Adams et al., 1991). Microinjection techniques are however laborious and technically challenging, spurring on the development of a variety of other genetically encoded sensors that could be introduced into cells by transfection (Zaccolo et al., 2000).

Although these PKA based sensors were instrumental in our understanding of cAMP dynamics, they all shared some common shortfalls, which were largely due to the mechanism of action of PKA. For example, as activation of PKA leads to a dissociation of the regulatory and catalytic subunits, one might expect the reassembled holoenzyme to incorporate non-FRET subunits present in the cell, which may negatively affect FRET efficiency in long term experiments (Paramonov et al., 2015; Rich et al., 2014). These sorts of problems led to the development of unimolecular FRET sensors based on EPAC

proteins (DiPilato et al., 2004; Nikolaev et al., 2004; Ponsioen et al., 2004). All EPAC sensors contain a cAMP binding domain and the two fluorophore probes. Binding of cAMP to its binding site in the EPAC proteins result in a change in the sensor confirmation, accompanied by changes in FRET efficiency. These sensors have several advantages over the multiprotein probes. For example, as all domains are on one molecule, only transfection of one plasmid construct is needed and, as compared to the multiprotein sensors, the activation kinetics are much more favourable and have a faster response to cAMP. Apart from EPAC FRET sensors, other sensors based on AKAPs have been developed to measure cAMP and PKA at specific subcellular sites (Paramonov et al., 2015).

FRET approaches are associated with several problems both due to the physical properties of FRET but also the technology used to measure FRET. One particular issue is that the fluorescent proteins used as a label are sensitive to environmental changes, such as pH, ionic concentrations and temperature (Leavesley and Rich, 2018). In addition, FRET requires an external light source for the fluorescence transfer, which can lead to photobleaching (Xie et al., 2011). To circumvent these problems, sensors based on bioluminescent resonance energy transfer (BRET) have been developed. BRET does not require an external light source to excite the donor fluorophore and so does not suffer from the problems associated with FRET, such as photobleaching, light scattering or autofluorescence. Other advantages to BRET-based approaches include low background signal and high signal to noise ratio, facilitating data analysis. This BRET approach has been used in this thesis to measure cAMP and PKA in keratinocytes and has been described in more detail in section 3.2.1.

1.3.10 Viruses and cAMP-PKA signalling

Several viruses have been reported to interact with the cAMP-PKA pathway, including HCV, HIV and respiratory syncytial virus (RSV). A brief summary of these virus interactions is given below.

HCV activates cAMP response element (CRE)-dependent transcription in hepatoblastoma Huh-7 cells through the non-structural NS2 protein. Interestingly, levels of transcripts whose stability is regulated by cAMP were also decreased in a manner dependent on NS2 expression. The data suggest that NS2 affects the stability of these mRNAs either via changes in intracellular cAMP or through modulation of one of the proteins involved in regulating the cAMP pathway (Kim et al., 2007). Furthermore, through a complex composed of two of the other viral structural proteins, NS3 and NS4, the virus also inhibits the activity of PKA and PKA-mediated phosphorylation of cAMP response element-binding protein (CREB), a downstream PKA target that is involved in mediating cAMP-dependent changes in gene transcription, by regulating ATP turnover (Aoubala et al., 2001). Further evidence for a role of the cAMP-PKA pathway in the HCV life cycle came from studies on viral entry and infectivity. Using a mixture of Huh-7 and primary human hepatocytes, these studies suggested a role for the PKA-RII holoenzyme in HCV internalisation; inhibition of PKA activity led to a re-organisation of receptors involved in HCV entry. Further inhibitor studies showed that PKA was also involved in regulating viral infectivity, although the precise mechanism was not elucidated. Finally, HCV infection was shown to increase cAMP levels, with a concomitant increase in phosphorylation of PKA substrates (Farquhar et al., 2008). Together, these data suggest that HCV targets cAMP-PKA by multiple mechanisms to regulate expression of host mRNAs, virus release and transmission

The cAMP-PKA pathway is also important during the HIV-1 life cycle. Using purified HIV-1 virions, the catalytic subunit of PKA has been shown to be incorporated into virus particles where it regulates viral infectivity in permissive cells (Cartier et al., 2003). Furthermore, HIV-1 infection increases cAMP levels in T cells *in vitro*, resulting in activation of the PKA pathway, which appears to be mediated by the viral glycoprotein 120 envelope protein (Hofmann et al., 1993; Nokta and Pollard, 1991; Masci et al., 2003). This activation of cAMP may have dual and opposite functions, however, with some studies showing changes in cAMP to be detrimental by decreasing anti-HIV T cell responses while others have shown it to be protective through limiting replication of viral DNA, inhibiting viral entry into cells or by decreasing viral spread. It is likely therefore that the functional consequence of cAMP depends on the exact stage of infection (Moreno-Fernandez et al., 2011).

Respiratory syncytial virus (RSV), a major cause of respiratory infection in young children and high-risk adults, also interacts with the cAMP-PKA pathway. RSV infection is associated with disruption of the airway epithelial barrier by triggering disassembly of tight junctions. Induction of cAMP by forskolin and/or cAMP analogues protected against RSV-induced disassembly of tight junctions in epithelial cells through a PKA-dependent mechanism. In these cells, inhibition of PKA by the kinase inhibitor H89 reversed the forskolin-induced stabilisation of epithelial tight junctions, confirming that PKA was involved in this stabilisation and not one of the other cAMP effector proteins. Mechanistically, this protective effect was due to stabilisation of adherens and tight junction structures, inhibition of RSV-induced rearrangement of the cytoskeleton and inhibition of viral mRNAs and viral transmission in airway epithelial monolayers (Rezaee et al., 2017). Another cAMP target, EPAC2, is also involved in the life cycle of RSV.

Pharmacological inhibition and small interfering RNA (siRNA) knockdown experiments showed that EPAC2 was involved in RSV replication, production of infectious viral progeny and virus-induced upregulation of proinflammatory cytokines, such as monocyte chemoattractant protein-1 and interleukin-6 (Choi et al., 2018).

1.3.11 HPV and PKA

HPV interacts with multiple host signal transduction pathways during the viral life cycle to facilitate viral DNA replication and amplification, including PKA.

The functions of several viral proteins are regulated by PKA phosphorylation. HPV E2 proteins are critical regulators of viral genome maintenance and viral persistence through binding to host chromosomes. For HPV8, a beta HPV type associated with cutaneous lesions, the E2 protein requires the residues R250 and S253 for this chromosomal association, with the S253 residue being phosphorylated (Sekhar et al., 2010). Using an *in vitro* phosphorylation prediction software, S253 was predicted to be phosphorylated by PKA, and this was confirmed using activators and inhibitors of PKA activity. Treatment of cells with forskolin showed an increased number of cells with E2 bound to mitotic foci, showing that PKA activity regulated the chromosomal binding function of E2. Finally, this study showed that PKA phosphorylation of E2 occurred in S phase, increased the half-life of the E2 protein and promoted E2 binding to chromosomes from S phase through mitosis (Sekhar and McBride, 2012). The E4 protein from diverse HPV types (HPV1, 11 and 16) has also been reported to be phosphorylated by PKA (Bryan et al., 2000; Grand et al., 1989; Wang et al., 2009b). Although the consequence of this phosphorylation event on E4 function is unknown, it does not result in a change in localisation of the protein (Bryan et al., 2000). E4 phosphorylation by ERK results in enhanced binding of the protein to the

host keratin network so it is tempting to speculate the PKA phosphorylation may regulate E4 function through an as yet unidentified manner (Wang et al., 2009b).

The virus also encodes proteins that regulate the activity of the PKA pathway. HPV16 E5 induces the expression of cyclooxygenase-2 (COX-2), which leads to increased secretion of the main COX-2 product, prostaglandin E2 (PGE2). As a result, PGE2 induces the expression of the PGE2 receptor subtype EP4, increasing levels of cAMP. The induction of the EP4 receptor was shown to be due to the activity of the PKA pathway, resulting in increased phosphorylation of CREB and subsequent CREB binding to a variant CRE in the EP4 promoter, and was important for E5-induced colony formation and VEGF secretion in cervical cancer cells (Oh et al., 2009). In addition, the same authors showed that the activity of this COX-2-PGE2-induced PKA pathway was involved in E5 inhibition of hydrogen peroxide-induced apoptosis by regulating the expression of the pro-apoptotic Bax and Bak proteins (Oh et al., 2010).

As described in section 1.2.6.2.2.3, PKA phosphorylation regulates multiple aspects of E6 function. E6 through its C-terminal PBM targets a subset of host PDZ domain-containing proteins, a function which is regulated by phosphorylation at the overlapping PKA recognition site. Experiments in an HPV18 life cycle model showed that loss of PKA recognition was associated with increased cell proliferation in monolayer cells and, on organotypic raft culture, a more hyperproliferative phenotype (Delury et al., 2013). In addition, loss of PKA recognition in immortalised keratinocytes was associated with epithelial to mesenchymal transition (Watson et al., 2003). These data, together with that described in section 1.2.6.2.2.3, suggest that changes in PKA phosphorylation may be relevant for oncogenic progression of HPV infections. In addition, phosphorylation of the E6 PBM allows for interactions with the host 14-3-3 family members. A full functional

analysis of the consequences of this interaction is lacking but initial experiments have shown it to contribute to E6 protein levels (Boon and Banks, 2012). Given that 14-3-3 family members are involved in diverse cellular processes, such as cell cycle regulation, apoptosis and signal transduction, and have been implicated in cancer initiation and progression, E6 binding may, therefore, be relevant during the oncogenic progression of HPV infections (Hermeking and Benzinger, 2006; Neal and Yu, 2010).

1.3.12 AKAP95

AKAP95 is an RII-specific AKAP and is one of two AKAPs found in the nucleus, the other being the splicing factor SFRS17A (AKAP17A). In addition to localising to the nucleus, AKAP95 has also been localised to the nuclear matrix (Akileswaran et al., 2001), nucleolus and mitotic chromatin, although the latter two are somewhat contentious with some studies not finding such a localisation (Collas et al., 1999; Landsverk et al., 2001; Marstad et al., 2016). SFRS17A binds to both RI and RII subunits, colocalises with the catalytic subunit in nuclear speckles in immunofluorescence experiments and is involved in splicing of alternative splicing of the *E1A* minigene in a manner dependent on its ability to bind to PKA (Jarnæss et al., 2009). AKAP95 is the founding member of the AKAP95 family of proteins, characterised by the presence of two ZFs (Castello et al., 2012). Other members of this family include HA95, a homologue of AKAP95 that does not bind to PKA regulatory subunits (and therefore is not an AKAP) but binds to the catalytic subunit directly (Martins et al., 2000; Ørstavik et al., 2000) and ZNF326, a largely uncharacterized protein thought to regulate alternative splicing (Close et al., 2012).

The domain structure of AKAP95 is shown in **Figure 1.7** and contains a nuclear matrix targeting sequence (amino acids 110-1140), a bilateral nuclear localisation sequence (290-306), a nuclear localisation sequence (368-377), two ZFs (392 to 414; 481 to 501) and a binding site for PKA-RII (572-589).

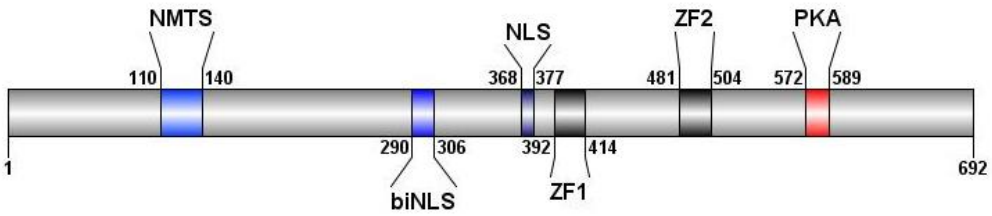

Figure 1.7: AKAP95 structure. AKAP95 contains a nuclear matrix targeting sequence (NMTS), bilateral nuclear localisation sequences (biNLS), a nuclear localisation sequence (NLS) two zinc fingers (ZF1 and ZF2) and a binding site for PKA-RII subunits (PKA). Image generated using Dog 2.0 software.

Consistent with the scaffold function of AKAPs, AKAP95 binds to a multitude of cellular proteins, including heterogeneous nuclear ribonucleoproteins (hnRNPs) M, K, H, F, D and U proteins through the N-terminal 100 amino acids (Hu et al., 2016), the p68 RNA helicase via the nuclear matrix targeting sequence (Akileswaran et al., 2001) and PKA-RII through the PKA binding site in the C-terminus, with amino acid isoleucine (I) at position 582 being the critical residue for this binding (Carr et al., 1992). AKAP95 participates in various cellular functions including cell cycle control, regulation of transcription and RNA metabolism, and has been implicated in human conditions such as regulation of head size and autism (Jarnæss et al., 2009), cleft palate (Yang et al., 2006) and cancer (Liu et al., 2015; Zhao et al., 2015).

Figure 1.8 provides an overview of several known AKAP95 functions. These include providing a scaffold for the minichromosome maintenance 2 (MCM2) protein loading onto the pre-replication complex during DNA replication (Eide et al., 2003), recruitment of condensin complexes onto chromosomes and regulation of chromosomal condensation (Collas et al., 1999; Steen et al., 2000), protein-protein interactions with cyclins D and E (Arsenijevic et al., 2004, 2006) and nuclear targeting of p90 ribosomal S6 kinase 1 (RSK1; Gao et al., 2012). Recently, AKAP95 has also been shown to regulate transcription and splicing (Hu et al., 2016; Jiang et al., 2013). Descriptions of some of AKAP95-dependent processes are given below.

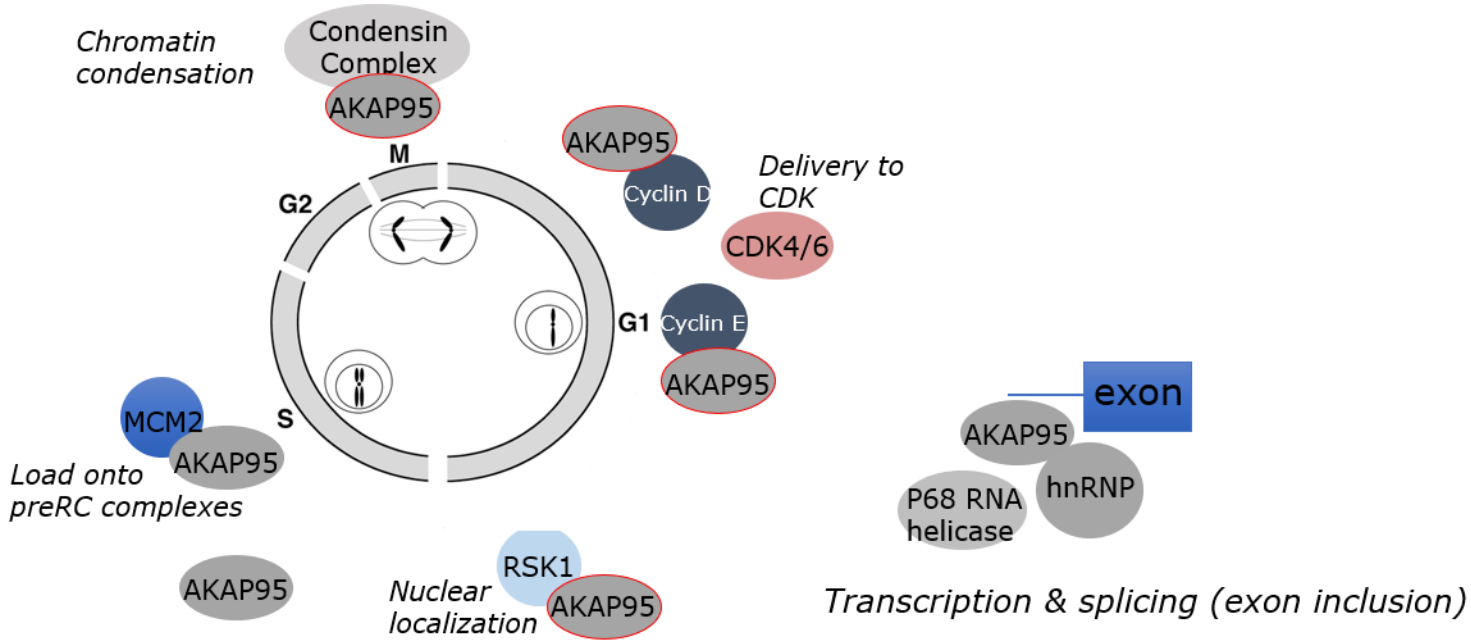

Figure 1.8: Overview of AKAP95 functions. AKAP95 regulates multiple cellular processes, including loading of MCM2 onto pre-replication complexes (preRC), targeting of condensin complex proteins and regulation of chromatin condensation, regulation of cyclin D and cyclin E complexes and nuclear targeting of p90 ribosomal S6 kinase 1 (RSK1). A role for AKAP95 in transcription and splicing has recently been identified. A description for some of these processes is given in the text. The red circles around AKAP95 for some of these functions indicates a requirement for PKA/PKA activity during the indicated process.

1.3.12.1 AKAP95, mitosis and cell cycle control

AKAP95 regulates mitotic and cell cycle events through interactions with various proteins, including members of the condensin complex, MCM2 and cyclins D and E.

AKAP95 is involved in multiple stages of chromosomal condensation by acting as a targeting molecule for condensin proteins, a group of large proteins involved in chromosome assembly and segregation during mitosis. At the onset of mitosis, a population of AKAP95 is redistributed onto chromatin following the breakdown of the nuclear envelope. Depletion of this chromatin-bound AKAP95 prevented chromosomal condensation in cervical cancer cells (HeLa), which was due to an inability to recruit members of the condensin complex, such as hCAP-D2/Eg7, onto chromatin (Collas et al., 1999; Steen et al., 2000). Domain mapping experiments showed that AKAP95 binding to chromatin required residues 387-450 and ZF1, although ZF2 rescued chromatin binding in a mutant AKAP95 protein with a compromised ZF1. The residues required for chromosomal condensation were within 387-569, including both ZFs, and this region was sufficient for recruitment of condensin proteins to chromatin. Interestingly, the PKA binding domain of AKAP95 was not involved in the onset of chromosomal condensation but PKA activity was required for maintenance of condensed chromosomes (Eide et al., 2002). The fact this PKA activity is required may suggest that the kinase phosphorylates subunits of the condensin complex or other structural proteins involved in the maintenance of condensed chromatin during mitosis (Landsverk et al., 2001).

The AKAP95-MCM2 interaction was found by a yeast two-hybrid approach aiming to identify novel AKAP95 interacting partners and was confirmed using both glutathione S-transferase (GST) pull-down and co-immunoprecipitation experiments from chromatin. This interaction was mapped to residues 1-195 of AKAP95 and disruption of this

interaction through incubation of HeLa cell nuclei with a 1-195 AKAP95 peptide dramatically inhibited both the initiation and elongation phases of DNA replication *in vitro*. This occurred via changes in MCM2, with depletion of AKAP95 resulting in a loss of nuclear MCM2 protein. Accordingly, rescue experiments using a recombinant AKAP95 protein restored nuclear MCM2 levels. Disruption of the AKAP95-PKA interaction did not impair either stage of DNA replication but inhibition of PKA activity negatively affected the initiation of DNA replication. Together, the data suggest that AKAP95 regulates DNA replication by anchoring MCM2 in the nucleus and that PKA activity is important for initiation but not elongation stages of DNA replication. How this might occur is not yet clear but as activation of PKA is required for S phase progression by phosphorylation of Cdc6, AKAP95 may target PKA to the nucleus to facilitate this phosphorylation event. Alternatively, there may be a nuclear pool of PKA catalytic subunits that are involved in phosphorylating nuclear substrates for progression of mitosis (Eide et al., 2003).

Another set of proteins under the control of AKAP95 is the D and E type cyclins, cyclins D1, D2, D3 and E1 (Arsenijevic et al., 2004, 2006). These proteins are important regulators of cell cycle progression that, when bound to their respective cyclin-dependent kinases, drive the phosphorylation of various downstream substrates important for cell cycle progression, including other cyclins, condensins and lamin proteins (which are involved in nuclear envelope breakdown at mitosis) (Lodish et al., 2007). Co-immunoprecipitation experiments using both endogenous and overexpressed proteins showed that AKAP95 bound all D-type cyclins and the association was specific, with AKAP95 not binding known binding partners of cyclin D proteins, CDK4 or $p27^{kip1}$. Surprisingly, these protein complexes were regulated by CDK4 levels, with overexpression of CDK4 in cells displacing AKAP95 from cyclin D3 complexes (Arsenijevic et al., 2004).

Later experiments showed that AKAP95 mediates the binding of the PKA-RII holoenzyme to cyclin D3, although this interaction was not regulated by levels of cAMP (Arsenijevic et al., 2006). In the same study, AKAP95 was shown to also interact with cyclin E1 and was displaced by its catalytic partner CDK2. Similar to the cyclin D3 experiments, AKAP95 also mediated PKA-RII binding to cyclin E1 and was unaffected by changes in cAMP (Arsenijevic et al., 2006).

1.3.12.2 AKAP95, transcription and splicing

AKAP95 was first assumed to be involved in transcriptional regulation by virtue of its binding to the nuclear matrix and the p68 RNA helicase, a DEAD-box protein implicated in cellular processes such as initiation of transcription and assembly of the spliceosome (Akileswaran et al., 2001). More recent experiments showed that AKAP95 was a novel binding partner of DPY30, a common subunit of the mixed-lineage leukaemia (MLL) family of histone-3 methyltransferases, which are responsible for histone H3 lysine 4 (H3K4)-mediated chromatin modifications and transcriptional activation. AKAP95 binding to MLL-DPY30 complexes directly enhances the methyltransferase activity of the MLL complex and drives expression of a chromosomal reporter gene, occurring concomitantly with increased levels of di- and tri-methylation of H3K4, epigenetic marks generally associated with transcriptional activation (Sims and Reinberg, 2006). This transcriptional stimulation requires the N-terminal 100 amino acids and AKAP95 binding to DPY30. Functional analysis of this interaction in mouse embryonic stem cells showed that AKAP95 regulated a common set of genes as DPY30, such as those involved in early development, in retinoic acid-treated cells (Jiang et al., 2013).

In addition to its role in retinoic acid-mediated gene transcription in mouse ES cells, AKAP95 also regulates transcription and RNA processing through its interaction with

hnRNPs (Hu et al., 2016). These proteins control the maturation of newly formed RNAs (pre-mRNAs) into mRNAs through processes such as alternative splicing, stabilisation of the mRNA during cellular transport and control of translation (Geuens et al., 2016; Martinez-Contreras et al., 2007). Through mass spectroscopy-based analysis and subsequent validation by co-immunoprecipitation experiments, AKAP95 was found to interact with several RNA processing factors through its N-terminus, including multiple hnRNP proteins (hnRNP M, K, H, F, D and U). Use of various AKAP95 mutant proteins combined with AKAP95 knockdown or overexpression experiments showed that the N-terminal 100 residues and ZFs are involved in splicing in a minigene splicing system. The ability of AKAP95 to regulate splicing was further demonstrated using an endogenous target of hnRNP F, one of the novel AKAP95-interacting hnRNPs; exon 11 of the *FAM126A* transcript. Treatment of cells with either shRNA or siRNA against AKAP95 resulted in skipping (reduced inclusion) of exon 11 of the transcript, which depended on the integrity of the ZFs. Finally, this analysis showed that AKAP95 binds to the introns immediately upstream of the exons that it regulates and loss of AKAP95 functionally mimics the loss of hnRNP F, U and H proteins, suggesting that AKAP95 selectively co-ordinates with hnRNP proteins to regulate alternative splicing (Hu et al., 2016)

1.4 Hypothesis and Aims

In order for the virus to successfully replicate in squamous epithelia, HPV alters the milieu of the infected keratinocyte to one that supports the viral replication process. This involves interaction with the host's kinome to modify viral protein function and/or host protein function. HPV proteins are phosphorylated by a variety of kinases but they can also modulate the activity of signal transduction pathways, as is the case with E5 and EGF signalling (Straight et al., 1995; Watson et al., 2003), or E4 and SRPK1 activity (Prescott et al., 2014). Another signalling pathway that is intimately involved in the infectious cycle is PKA, and whilst several HPV proteins are known PKA substrates (E2, E4, E6), it is not clear if or how the virus modulates PKA signalling activity during infection. Moreover, when the effects of PKA signalling on the function of the E6 PBM are considered, reduced PKA activity might promote morphological transformation (Watson et al., 2003) whereas increased activity may lead to increased viral DNA integration (Delury et al., 2013). Deregulation of this host pathway could, therefore, be an independent risk factor for progression of high-risk HPV infections.

Therefore, it was hypothesised that high-risk HPV modulates the activity of the PKA pathway to support the infectious cycle and that this virus-host interaction has a consequence on HPV protein function.

Therefore, the aims of this thesis are:

1. Determine if HPV18 modulates the activity of the PKA pathway using a bioluminescent resonance energy transfer approach to study PKA activation in a physiologically relevant system composed of the natural host cells of the virus – the keratinocyte (Chapter 3).

2. To identify and characterize the association between HPV proteins and host factors involved in the regulation and control of PKA signalling – AKAP95-HPV18 E6 (Chapter 4).

3. Investigate the functional importance of the HPV18 E6-AKAP95 interaction in cells maintaining HPV18 genomes and/or expressing E6 (Chapter 5).

CHAPTER 2 MATERIALS AND METHODS

2.1 Cell culture

2.1.1 General information

All cell culture work was carried out in a HEPA-filtered laminar flow hood. Surfaces were wiped with 70% industrial methylated spirit. Work with HPV genome containing keratinocytes was approved by the Health and Safety Executive (reference number GM67/05.1).

2.1.2 Cell growth conditions

NIH-3T3 J2 cells (hereafter called J2 cells) were maintained in Dulbecco's modified Eagle medium (DMEM), HEPES modification (Sigma-Aldrich, Gillingham, UK), supplemented with 4 mM L-glutamine (Sigma-Aldrich) and 10% (vol/vol) Gibco adult bovine serum (ThermoFisher Scientific, Paisley, UK) HeLa, HEK293T (hereafter 293T) and C33A cells were grown in DMEM, HEPES modification, supplemented with 4 mM L-glutamine and 10% (vol/vol) foetal calf serum (FCS) (All Sigma-Aldrich). Primary HFKs were maintained in Gibco Keratinocyte-Serum Free Media supplemented with 20 µg/ml bovine pituitary extract and 0.1 ng/ml human recombinant EGF (ThermoFisher Scientific). Establishment of HPV18 genome containing cell lines (HFK-18) by transfection of the HPV18 genome into HFKs was carried out by previous members of Dr Roberts' laboratory (Delury et al., 2013; Wilson et al., 2007; see **Figure 2.1**) and maintained as described in section 2.1.3.

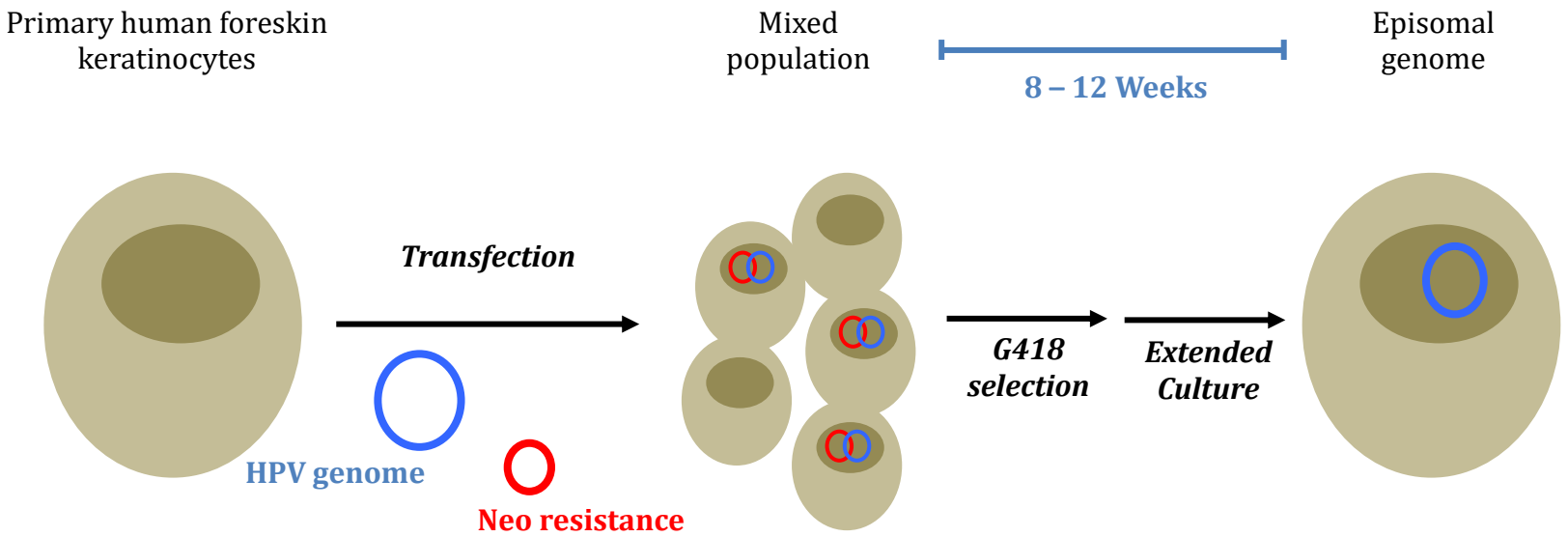

Figure 2.1. Generation of primary human foreskin keratinocytes maintaining HPV18 genomes. Low passage human foreskin keratinocytes were co-transfected with plasmids encoding the HPV18 genome and neomycin (neo) resistance. One day after transfection, transfected cells were seeded onto a layer of γ-irradiated J2-3T3 cells and grown for 8 days in the presence of G418 antibiotic in E medium containing EGF. Emerging colonies were then pooled and expanded on irradiated J2-3T3 cells.

2.1.3 Maintenance of HPV18 genome containing lines

Growth and maintenance of HPV genome containing lines are described fully in Wilson et al., 2005. Untransfected normal immortalised keratinocytes (NIKS) were a kind gift of Professor Paul Lambert, University of Wisconsin-Madison, USA, and NIKS containing HPV18 genomes (NIKS-18) were established by Dr S Roberts and Dr G Knight (unpublished). NIKS cells were maintained in F media, composed of 3:1 DMEM: Ham's F12 media, 5% foetal bovine serum (FBS), 24 μg/ml adenine, 8.4 ng/ml cholera toxin, 10 ng/ml EGF, 2.4 μg/ml hydrocortisone and supplemented with 5 μg/ml insulin before use. HPV18 genome containing HFKs were maintained in E media (see 2.1.4).

These cell lines were grown on a layer of γ-irradiated J2 cells. For this, J2 cells were grown to 80% confluency, harvested by trypsinisation and resuspended at $2x10^6$ cells/ml, before irradiation with 30 Gray using a Caesium-137 radiation source (Biomedical Services Unit, University of Birmingham, UK). Irradiated J2 cells were plated out in the required media at a concentration of $2x10^6$ per 10 cm tissue culture plate (Falcon, ThermoFisher Scientific) and allowed to settle for at least two hours or overnight before the addition of HPV18 genome containing cells. Plates were shaken gently to allow for even distribution of cells and maintained in E media containing 10% (vol/vol) foetal calf serum (Sigma-Aldrich; Wilson *et al.*, 2007; see 2.1.4). Irradiated J2 cells were stored at 4°C for a period not exceeding one week.

2.1.4 Preparation of E media

To prepare two litres of E media, the following components were mixed: 1200 ml DMEM HEPES modification, 640 ml Ham's F12 nutrient mixture (ThermoFisher Scientific), 20 ml of 100X cocktail (see section 2.1.5), 40 ml of 100X penicillin/streptomycin

(ThermoFischer Scientific), 100 ml FBS (Sigma-Aldrich), 2 ml 1000X Cholera toxin (ICN Biomedical, California, USA) and 2 ml 1000X hydrocortisone (Sigma-Aldrich). Following mixing, the media was filter sterilised through a 0.22 µm vacuum filter system (Corning, ThermoFisher Scientific) and was supplemented with 5 ng/ml EGF before use. HyClone™ FBS (ThermoFisher Scientific) was used for E media and batch tested to ensure adequate growth of HPV18 genome containing cells.

2.1.5 Preparation of 100X cocktail

Preparation of 200 ml of 100X cocktail was by mixing the following components: 20 ml of 0.18 M adenine, 20 ml of 5 mg/ml insulin, 20 ml of 5 mg/ml transferrin and 20 ml of $2x10^{-8}$ triiodo-L-thyronine in phosphate-buffered saline (PBS; 137 mM sodium chloride, 2.7 mM potassium chloride, 10 mM disodium phosphate and 1.8 mM monopotassium phosphate). All chemicals were purchased from Sigma-Aldrich. The cocktail was filter sterilised and frozen at -20°C prior to use.

2.1.6 Cell passage

Cells were passaged once they reached 80-85% confluency. For this, the media was removed and plates washed with PBS. Cells were detached by use of TrypLE solution (ThermoFisher Scientific) with incubation at 37°C. Trypsin was neutralised with serum-containing media or soybean trypsin inhibitor (0.25 mg/ml soybean trypsin inhibitor (Invitrogen, ThermoFisher Scientific) in PBS). This solution was then transferred to a centrifuge tube and the dish washed with additional media or PBS to gather any remaining cells. Cells were triturated to ensure a single cell suspension and counted using a

haemocytometer if desired. After centrifugation at 201 *x g* for five minutes in an Eppendorf 5810 centrifuge, cells were resuspended and plated at the desired density.

2.1.7 Organotypic raft cultures

Organotypic raft cultures were prepared by Dr Sally Roberts (Wilson and Laimins, 2005). Briefly, $2x10^6$ keratinocytes were grown on a collagen plug containing $2x10^6$ non-irradiated J2 fibroblasts. After 96 hours, or sooner if the media on the plug turned yellow one day after media change, the plug was lifted onto a wire mesh and the underneath flooded with E media lacking EGF to create a liquid-air interface. Media was changed every two days and the rafts were harvested after 13 days. Harvesting was by flooding the dish with 3% formaldehyde in culture media prior to embedding in paraffin and sectioning by Propath UK Ltd, Hereford, UK.

2.1.8 Cell freezing

Cells were frozen down routinely to maintain stocks. For this, cells were processed as above for cell passage and after centrifugation, resuspended to $1\text{-}2x10^6$ cells/ml in freezing media (9:1 ratio media: dimethyl sulfoxide (DMSO)). Primary keratinocytes were frozen in cell media with 10% FCS containing 20% (vol/vol) glycerol or 10% (vol/vol) DMSO. One millilitre of cell solution was placed in cryovials (Greiner Bio-One, Stroudwater, UK) and stored at -80°C in a Nalgene Mr Frosty system. Long-term storage was in the vapour phase of liquid nitrogen.

2.1.9 Cell thawing

Cells were removed from liquid nitrogen and allowed to thaw briefly in a water bath set to 37°C. The cell solution was transferred dropwise to a universal tube containing 10 ml media, before centrifugation at 201 *x g* for five minutes. Cells were then resuspended in fresh media and plated out at the required density. Alternatively, thawed cells were added directly to a cell culture dish containing media.

2.2 Cell Biology

2.2.1 Cell fixation and permeabilization for immunofluorescence staining

Cells were plated directly onto coverslips and allowed to adhere. Coverslips were washed twice in PBS before fixation. For methanol fixation, coverslips were treated with cold methanol (-20°C) for ten minutes before permeabilization in cold acetone for one minute. For paraformaldehyde fixation, coverslips with treated with 4% paraformaldehyde for ten minutes before permeabilization in 0.1% Triton X-100 in PBS for ten minutes. After fixation, coverslips were washed in PBS and left either in PBS at 4°C for short-term storage or left to air dry and stored at -20°C.

2.2.2 Agitated low-temperature epitope retrieval

For immunofluorescence staining of sections from organotypic raft culture, formalin-fixed and paraffin-embedded slides were deparaffinised and rehydrated by sequential immersions in xylene, absolute ethanol and then water, followed by agitated low-temperature epitope retrieval (Watson et al., 2002). For this, raft sections were incubated in epitope retrieval buffer (1 mM ethylenediaminetetraacetic acid (EDTA),

0.01% Tween 20, pH 8.0) at 65°C overnight with stirring. Once cooled, slides were processed as described in section 2.2.3 for immunostaining.

2.2.3 Indirect immunofluorescence (IF) staining

Fixed cells were blocked in IF blocking buffer (20% heat-inactivated normal goat serum and 0.1% (wt/vol) bovine serum albumin (BSA) fraction V (Sigma-Aldrich) in PBS) for at least one hour before incubation with the primary antibody in blocking solution overnight at 4°C. All staining procedures were carried out in a humidified chamber to prevent evaporation of the antibody. Cells were washed three times in PBS under agitation before incubation with the appropriate Alexa Fluor™ species-specific secondary antibody for one hour at 37°C. Cells were washed a further three times before incubation in PBS containing the DNA stain 4'6-Diamidino-2-phenylindole (DAPI) for five minutes before being mounted onto microscope slides using Fluoroshield (Sigma-Aldrich). Slides were stored at -20°C. Images were captured using a Nikon Eclipse E600 microscope and associated software.

2.2.4 Plasmid DNA transfection

For transfection into 10 cm plates, cells were seeded at $3x10^6$ and, the following day, transfected using 5-10 µg plasmid DNA using X-tremeGene DNA transfection reagent (Roche, Sussex, UK) or linear polyethyleneimine (Sigma-Aldrich) at a ratio of 1:3 DNA to reagent. Cells were processed as required for downstream assays at 48 hours post-transfection.

2.2.5 Plasmid DNA transfection for Bioluminescence Resonance Energy Transfer

One day prior to transfection, established cell lines (i.e. all cells bar parental primary keratinocytes) were plated at a density of $2x10^4$ cells/well in a Nunc™ white bottomed 96 well plate (ThermoFisher Scientific) and transfected using X-tremeGene DNA transfection reagent at a ratio of 1:3 DNA to reagent. Cells were transfected with 200 ng of plasmid DNA encoding PKA isoform I (PKA-I: *Renilla* luciferase (Rluc)-RIα and green fluorescent protein (GFP)-Cα), PKA isoform II (PKA-RII: Rluc-RIIα and GFP-Cα) or 100 ng encoding the cAMP target EPAC. Control cells expressing only *Renilla* luciferase (100 ng) were included to determine background as well as non-transfected cells.

For the oncoprotein identification experiments, cells were also transfected with constructs expressing HPV18 E5 (kindly provided by Dr Andrew Macdonald, University of Leeds), E6 and E7, alongside the BRET sensors.

For transfection into parental primary keratinocytes, cells were seeded at $3\text{-}4x10^5$ in a six-well plate and transfected with 2 µg PKA-I/II or 1 µg EPAC using TransIT-Keratinocyte Transfection Reagent at a ratio of 1:1.5 DNA to reagent (Mirus Bio LLC, Madison, USA). After 24 hours, these cells were harvested by trypsin and plated out at $2x10^4$ cells/well in 96 well plates. BRET was performed 48 hours after transfection. In all transfections, total DNA was kept equivalent by transfecting empty vector.

2.2.6 Bioluminescence Resonance Energy Transfer

Bioluminescence resonance energy transfer was carried out as described elsewhere (Prinz et al., 2006). Briefly, 48 hours post-transfection, media was removed, and the cells rinsed twice in PBS. Cells were then incubated with 5 µM in 50 µl luciferase substrate in PBS

(Coelenterazine 400a, Biotium, UK) either in the presence or absence of the cAMP-elevating agent forskolin (final concentration: 10 μM). To quantify BRET, light emission was measured at 410 nm wavelength ± 80 nm bandpass for the donor luciferase and a 515 nm wavelength ± 30 nm bandpass for the GFP acceptor using a PheraStar high throughput plate reader (BMG LabTech, Ortenberg, Germany). The emission from non-transfected (NT) cells was subtracted and the BRET signal calculated as (emission (515 nm–NT 515 nm)/(emission (410 nm–NT 410 nm)). All reagents were a generous gift of Dr Mandy Diskar, University of Birmingham, or purchased commercially. Graphs and statistical analysis were carried out on GraphPad Prism 5 (San Diego, USA).

Unless otherwise stated in the figure legends, statistical analyses (Student's t-tests) were conducted to compare control cells with those expressing either HPV18 oncoproteins or the complete viral genome. Statistical significance was denoted by inclusion of the following in the figures: ns demonstrates non-significance at the level of $p=0.05$, * denotes $p<0.05$, ** denotes $p<0.01$ and *** denotes $p<0.001$.

2.2.7 CRE-luciferase assays

C33A cells were seeded into a six-well plate as described in section 2.25 and, after 24 hours, were transfected with 100 ng of CRE-luciferase reporter alongside 100 ng each of the expression vectors indicated in the figure legends using X-tremeGene DNA transfection reagent at a ratio of 1:3 DNA to reagent. Total DNA was kept equivalent by transfecting empty vector plasmid. After 48 hours, cells were harvested in 200 μl of passive lysis buffer and quantification of relative light units was determined using the Stop & Glo reagent system (Promega, Wisconsin, USA). Statistical analyses were carried out as described above in section 2.2.7.

2.2.8 Preparation of lentiviral particles

Lentiviral particles were prepared by transfecting second-generation TRIPZ shRNA constructs, along with packaging and envelope constructs, into 70-80% confluent 293T cells. Constructs were obtained from Dharmacon as a set of three shRNA sequences targeted against AKAP95. Transfection was performed using 9 µg shRNA construct, 4.5 µg pMDG.2 (encoding the vesicular stomatitis virus envelope protein) and 6.75 µg psPAX2 (encoding the packaging proteins Gag, Pol, Rev and Tat from HIV-1) using a 3:1 ratio of linear polyethyleneimine to DNA. After incubation for 30 minutes at room temperature, the transfection complex was added to the cells. At 48 and 72 hours post-transfection, cell media was harvested, filtered through a 0.45 µm filter and stored at -80°C before use. Typically, one ml of filtered media was used to infect one well of a six-well plate.

ShRNA AKAP95 sequences were: ShAKAP95 1: 5'-TTCATAACCTTGCCAGCTG-3', ShAKAP95 2: 5'-AAATTGTCATCTCCTTCCA-3' or ShAKAP95 3: 5'-TAGATTACAGCATATTCTG-3'. The TRIPZ control non-targeting construct was provided by Dr Clare Davies, University of Birmingham, and contains the shRNA sequence 5'-CTTACTCTCGCCCAAGCGAGAG-3'.

2.2.9 Lentivirus infection

Cells were seeded in a six-well dish such that they were 70% confluent at the time of infection. Cell media was removed and replaced with fresh media containing 8 µg/ml hexadimethrine bromide (otherwise known as polybrene), before the addition of media containing lentiviral particles. For spin-infection, six-well plates were wrapped in saran

wrap and cells were then centrifuged at room temperature at 804 *x g* for 90 minutes in a fixed bucket centrifuge (Eppendorf 5810). Lentivirus particle-containing media was then removed, the cells washed with PBS, and then complete media added to cells. After 48 hours, cells were re-plated in 10 cm dishes and underwent drug selection by addition of puromycin until the uninfected cells had died, typically 0.5-1 µg/ml puromycin over a period of four to five days. A kill curve was established for each cell line used such that all uninfected cells are dead by day four or five. The plasmid pHIV-szGreen was used a positive control for infection (kindly provided by Dr Clare Davies, University of Birmingham). Induction of the shRNA was triggered by the addition of doxycycline into the cell media. Cells were maintained in normal growth media containing tetracycline free serum.

2.2.10 Crude subcellular fractionation

Crude fractionation of cells was done using the REAP method, as previously described (Suzuki et al., 2010). Cells were washed in ice-cold PBS and scraped from the tissue culture dish into a 1.5 ml microcentrifuge tubes in 1 ml PBS. After a brief centrifugation at top speed in a tabletop microfuge (21,130 *x g*) for 10 seconds to collect the cells, the supernatant was removed and the cells triturated five times in 900 µl ice-cold 0.1% NP-40. Three hundred µl of this lysate was removed for the whole cell sample to which 100 µl 4X Laemmli sample buffer containing 5% (vol/vol) β-mercaptoethanol was added. The remaining 600 µl was centrifuged for 10 seconds as above and 300 µl removed for the cytoplasmic fraction, to which 100 µl of Laemmli sample buffer was added. The pellet was then resuspended in 1 ml ice-cold 0.1% NP-40 and centrifuged as above, and the supernatant discarded. The pellet was then resuspended in 180 µl of Laemmli sample

buffer (nuclear fraction). Nuclear and whole-cell fractions were sonicated once at 30% amplitude for 10 seconds using a Microson ultrasonic cell disrupter (Misonix, New York, USA). All samples were then heated at 95°C for five to 10 minutes prior to SDS-PAGE.

2.2.11 Subcellular fractionation

Subcellular fractionation was carried out using the ProteoExtract Subcellular Proteome Extraction Kit (Merck, Watford, UK) as per manufacturer's instructions. All solutions were supplemented with protease and phosphatase inhibitors and buffer III was also supplemented with benzonase. All buffers were used cold except for buffer IV, which was used at room temperature as it contains SDS. Briefly, monolayer cells were washed twice with Tris-buffered saline (TBS; 50 mM Tris-HCl and 150 mM sodium chloride in PBS) before incubation with 1 ml buffer I for 10 minutes at 4°C, which was then transferred to a pre-cooled Eppendorf tube (fraction one: cytosol). Next, 1 ml buffer II was added to the monolayer cells and incubated at 4°C for 30 minutes before being transferred to an Eppendorf tube (fraction two: membrane/organelle associated). Five hundred µl buffer III containing benzonase was then added to cells and incubated at 4°C for 10 minutes before the supernatant was transferred to a pre-cooled Eppendorf tube (fraction three: nuclear). Finally, 500 µl room temperature buffer IV was added to the cell monolayer and the dish swirled to collect any residual material, before collecting in a Eppendorf (fraction four: cytoskeletal). For Western blot analysis of these fractions, 15 µl of each was added to 15 µl Laemmli buffer containing 5% (vol/vol) β-mercaptoethanol, boiled at 95-100°C for five to 10 minutes before loading onto a polyacrylamide gel.

2.3 Southern blotting

2.3.1 Isolation of DNA

Cells were washed in PBS and resuspended in lysis buffer (400 mM sodium chloride, 10 mM Tris (pH 7.4), 10 mM EDTA) and RNase A added to a final concentration of 400 µg/ml. Lysates were mixed and incubated at 37°C for 60 minutes before the addition of 50 µg/ml proteinase K and 0.2% (vol/vol) SDS, and incubated at 37°C for 2-3 hours or overnight. Cellular DNA was then sheared by passing the cell lysate through a blunted 20-gauge needle.

DNA isolation was by phenol-chloroform extraction. This was performed by the addition of 6 ml phenol/chloroform/isoamyl alcohol in a ratio of 25:24:1 before repeated inversion of the tube and centrifugation at 537 *x g* for five minutes. The upper aqueous layer was retained and the extraction was repeated. Finally, the aqueous layer was extracted with 6 ml chloroform/isoamyl alcohol in a ratio of 24:1. DNA was precipitated by the addition of two volumes of ethanol and one-tenth volume of 3 M sodium acetate (pH 5.2), and incubated overnight at -20°C. The following day, samples were centrifugated at 537 *x g* for 30 minutes and the DNA pellet was washed twice with 70% ethanol, before centrifugation as above. After removal of the supernatant, the DNA was left to air dry at room temperature and resuspended in sterile Tris-EDTA buffer (TE buffer; 10 mM Tris-HCl and 0.1 mM EDTA, pH 8.0). DNA concentration was determined by the nucleic acid setting on a Nanodrop spectrophotometer (ThermoFisher) with TE buffer as a blank.

2.3.2 Digestion of DNA

Five micrograms of purified DNA were digested with restriction enzymes overnight at 37°C in a total volume of 20 µl. For HPV18, *Eco*RI will linearize the HPV18 genome while *Bgl*II will not cut the HPV18 genome. Reactions were set up with *Dpn*I to digest any residual bacterial DNA from the HPV18 plasmid before overnight incubation at 37°C. DNA was resolved on a 0.8% (wt/vol) agarose gel prepared in Tris-Borate-EDTA buffer (TBE; 45 mM Tris-HCl, 45 mM boric acid and 1 mM EDTA) containing 0.2 µg/ml ethidium bromide overnight at 50 V. To enable quantification of viral genome copy number, purified HPV18 DNA was used to prepare copy number standards equivalent to 5, 50 and 500 genome copies per cell.

2.3.3 Transfer of DNA to a nylon membrane

Once electrophoresis had finished, loading and digestion quality of the DNA was checked by viewing the gel under ultraviolet (UV) light (Gene Flash UV lightbox, Syngene, UK). The gel was then washed twice in 250 mM HCl for 30 minutes each at room temperature, before two washes in 400 mM sodium hydroxide (NaOH) under gentle agitation.

For transfer of the DNA to the nylon membrane, a tray was prepared using 1 L of 400 mM NaOH with a glass plate placed on the tray. A 24 x 33 cm sheet of Whatman™ paper was soaked in NaOH and placed on the glass plate, both ends submerged in NaOH. Bubbles were removed by rolling a pipette over the paper, and then three more layers of Whatman™ paper added. The agarose gel was flipped and placed on top of the paper, with the loading wells facing downwards. Bubbles were removed as above. A 20 x 22.5 cm Gene Screen Plus nylon membrane was soaked in NaOH, and placed on top of the gel,

followed by four layers of the Whatman™ paper. Finally, paper towels were placed on top, covering the paper, to ensure there were no gaps between stacks. Another glass plate was placed on top alongside a weight. Saran wrap was then used to ensure the top and bottom layers of Whatman™ papers did not touch. This was left overnight.

The following day, the positions of the wells were marked onto the nylon membrane. The DNA was cross-linked to the membrane using a Stratalinker UV crosslinker in crosslink mode. The membrane was then soaked in 2X saline-sodium citrate (SSC) buffer (30 mM trisodium citrate and 300 mM sodium chloride, pH 7.0) and sorted at -20°C in saran wrap.

2.3.4 Preparation of the radiolabelled DNA probe

To make the radiolabelled HPV18 probe, the pGEMII-HPV18 plasmid (a kind gift of Frank Stubenrauch, University of Tubingen) was digested with *Eco*RI to release the HPV18 complete genome and the digest resolved on a 1% (wt/vol) agarose gel. The released viral genome of ~8000 bps was cut out of the gel with a clean scalpel and the DNA extracted using a QIAquick gel extraction kit (see section 2.4.3). Fifty nanograms of purified DNA was then diluted with TE buffer to a final volume of 14 µl and denatured by boiling at 95°C for five minutes before incubation on ice for a further five minutes. To this, 5 µl oligonucleotide labelling buffer (1 mg/ml random deoxynucleotide primers, 1 M HEPES, pH 6.6), 1.5 µl nuclear grade BSA and 1.5 µl Klenow polymerase was added, followed by 30 µC of radiolabelled deoxynucleotide (^{32}P-dCTP, EasyTides, PerkinElmer). The reaction was incubated for several hours in a lead container at room temperature. Unincorporated deoxynucleotide was removed by purification on an Illustra Probe Quant G-50 microcolumn and the radiolabelled DNA probe used immediately or stored at -20°C.

2.3.5 Hybridisation of radiolabelled probe to DNA

To prepare the hybridisation buffer, 2X hybridisation solution (5X SSC: 750 mM sodium chloride and 75 mM M trisodium citrate (pH 7.0)), 10X Denhardt's solution (0.2% (wt/vol) Ficoll 400, 0.2% (wt/vol) polyvinylpyrrolidone), 0.2% (wt/vol) BSA fraction V and 20% (wt/vol) dextran sulphate) were mixed. The hybridisation solution was mixed 1:1 with deionized formamide and SDS added to a final concentration of 0.1% (wt/vol). Two hundred µl of a 10 mg/ml solution of salmon sperm was prepared by boiling at 100°C before incubation on an ice/water slurry for two minutes. This was then added to 10 ml hybridisation buffer (pre-hybridisation buffer).

The membrane was rolled tight in a nylon gauze and placed in a hybridisation canister and rotated such that the membrane unrolled inside the canister, DNA facing outwards. Ten millilitres pre-hybridisation buffer (containing the salmon sperm) was then added to the canister and this was rotated for one hour at 42°C. This was then removed and replaced by 10 ml hybridisation buffer containing the radiolabelled DNA probe and boiled salmon sperm, before being incubated at 42°C overnight with rotation.

2.3.6 Stringency washes

The membrane was rinsed in buffer one (600 mM sodium citrate, 300 mM sodium chloride and 0.1% (wt/vol) SDS, pH 7.0) before two 15 minutes washes in the same buffer. Then, the membrane was washed twice in buffer two (150 mM sodium citrate, 75 mM sodium chloride and 0.1% (wt/vol) SDS pH 7.0) followed by a further two washes in buffer three (30 mM sodium citrate, 15 mM sodium chloride and 0.1% (wt/vol) SDS, pH 7.0). All washes were at room temperature. Finally, the membrane was washed at 55°C in buffer

four (30 mM sodium citrate, 15 mM sodium chloride and 0.1% (wt/vol) SDS, pH 7.0). The membrane was then wrapped in saran wrap and exposed to x-ray film with an intensifying screen at -80°C.

2.4 Molecular methods

2.4.1 Polymerase Chain Reaction (PCR)

For the preparation of the GST-HPV18 E6 fusion protein, pGEMII-HPV18 was used to amplify the complete HPV18 E6 ORF. This plasmid contains the complete HPV18 genome cloned into the pGEMII vector at the *Eco*RI site at residue 2440. DNA was amplified using Phusion® High-Fidelity DNA Polymerase (New England Biolabs (NEB), Hitchin, UK) in a 20 µl reaction containing 200 µM dNTPs, 0.5 µM forward and reverse primers, 20 ng plasmid DNA and 1 U of DNA polymerase. Amplification was performed on an Applied Biosciences thermal cycler using a 10-minute hot start at 98°C followed by 35 cycles of 30 seconds at 75°C, 30 seconds at 70°C and two minutes at 72°C. The final extension step was 10 minutes at 72°C before hold at 4°C.

The primers used to amplify the E6 ORF were forward 5'-G TAA TGA ATT CTG GCG CGC TTT GAG GAT CCA ACA-3' and reverse 5'-GTATTGAATTC TTA TAC TTG TGT TTC TCT GCG-3'. These primers were designed to introduce an *Eco*RI digestion site, shown underlined, and were synthesised by AltaBioscience, Birmingham, UK.

2.4.2 Agarose gel electrophoresis

DNA was resolved by 1-1.5% (wt/vol) agarose gel electrophoresis in a horizontal Mini-Sub® tank (Bio-Rad, London, UK). Agarose powder was dissolved by boiling in TBE

buffer in a microwave and allowed to cool at approximately 50-60°C before casting. DNA was mixed with Midori Green Nucleic Acid Stain (Geneflow, Lichfield, UK) prior to loading alongside a 1 kb DNA ladder for size determination (Invitrogen). Alternatively, ethidium bromide was added to the gel at a final concentration of 0.2 µg/ml and gels run at 80-110 volts until finished. DNA bands were visualised under UV light per section 2.3.3.

2.4.3 Gel Purification of DNA

After resolution of DNA fragments by agarose gel electrophoresis, bands were excised and purified using the QIAquick Gel Extraction Kit (Qiagen) according to the manufacturer's instructions. Briefly, the band was cut out of the gel using a clean scalpel and placed in solubilisation buffer for 10 minutes at 50°C to melt the agarose, following which one volume of isopropanol was added. This was then applied to a QIAquick DNA binding column and centrifuged for one minute at 16, 000 *x g* in a tabletop centrifuge. The column was washed by adding 750 µl wash buffer, centrifuged as above, and DNA eluted by applying 30-50 µl TE buffer and collected by a further centrifugation step. Eluted DNA was stored at -20°C.

2.4.4 Restriction enzyme digestion

For the preparation of the pGEX-2T plasmid, restriction enzyme digestion of vector DNA was carried out using 5-10 µg DNA with 10-20 units of *Eco*RI in a total volume of 20-50 µl, as per manufacturer's instructions. Digestion was carried out at 37°C for at least two hours or overnight. To verify digestion, an aliquot was analysed using agarose gel electrophoresis, as described above (section 2.4.2).

2.4.5 Alkaline Phosphatase treatment of DNA

For sticky end cloning, the 5' terminal phosphate groups were removed from DNA using alkaline phosphatase (NEB) as per manufacturer's instructions. Briefly, digested DNA was incubated with a one-tenth volume of reaction buffer and then one to five units of alkaline phosphatase as per manufacturer's instructions. The solution was incubated at 37°C for one hour before inactivation at 65°C for 15 minutes.

2.4.6 DNA ligation

Following restriction enzyme digestion, samples were heat inactivated prior to ligation by a ten-minute incubation at 65°C before being placed on ice. Ligation of HPV18 E6 and pGEX-2T plasmids were carried out using a vector to insert ratio of 1:3, 1:5 and 1:10 with T4 DNA ligase as described by the manufacturer overnight at 16°C (NEB). DNA was then transformed into bacteria, as described in section 2.5.2.

2.5 Bacterial methods

2.5.1 General information

The *Escherichia coli (E. coli)* DH5α strain was used as a host for the growth of all plasmids for bacterial transformation and preparation of plasmid DNA. BL21 or Rosetta 2 DE3 pLysS strains were used for expression of GST fusion proteins. Agar plates were made using Luria-Bertani (LB) medium (1% (wt/vol) bacto-tryptone, 0.5% (wt/vol) bacto-yeast extract and 1% (wt/vol) sodium chloride) supplemented with agar. After autoclaving, the agar solution was boiled in a microwave and allowed to cool to approximately 50-60°C before the addition of antibiotics. Typical concentrations were ampicillin 100 µg/ml, kanamycin 50 µg/ml, chloramphenicol 34 µg/ml and zeocin 25 µg/ml. Approximately

20-30 ml agar was added to 10 cm bacterial dishes and allowed to set and dry in a microbiological safety hood under aseptic conditions. Plates were stored at 4°C for a maximum of six weeks.

2.5.2 Bacterial transformation

E. coli cells were thawed on ice and 30-50 µl added to a pre-cooled Eppendorf tube. Plasmid DNA was then added to the tube and incubated on ice for 30 minutes, heat shocked at 42°C for 45 seconds then placed back on ice for two minutes. Five hundred µl LB was then added per tube and placed on a shaker set to 200 revolutions per minute for one hour. Two hundred µl cell solution was then streaked out onto the relevant agar plate with the appropriate antibiotic. The remainder of the cell solution was stored at 4°C for further plating, as needed. After overnight incubation at 37°C, single colonies of bacteria were picked and used to inoculate 10 ml LB media with antibiotic for generation of small cultures. These small cultures were then diluted into a larger 200-300 ml culture if desired. Both were incubated overnight at 37°C with shaking before use.

2.5.3 Long-term storage of transformed bacteria

One ml transformed bacteria from an overnight culture was added to 500 µl sterile 50% (vol/vol) glycerol solution in a cryovial, mixed thoroughly, and stored at -80°C.

2.5.4 Preparation of plasmid DNA

Preparation of plasmid DNA for transfection was as per manufacturer's instructions using the PureLink® HiPure Plasmid Maxiprep Kit (Invitrogen), except the final ethanol precipitation step was extended to 45 minutes at 4°C. DNA was eluted into 250-500 µl TE

buffer. DNA concentration was determined by the nucleic acid setting on a Nanodrop spectrophotometer with TE buffer as a blank.

2.5.5 Expression of recombinant proteins

Purified DNA was used to transform BL21 or Rosetta 2 competent cells (Stratagene, California, USA), as above. After overnight incubation of a 10-20 ml culture with antibiotics, this was transferred to 0.5-2 litre LB culture containing 2% glucose and incubated at 37°C to an optical density measured at 600 nm (OD_{600}) of 0.6-0.8. Induction was by addition of 0.4 mM isopropyl-β-d-thiogalactopyranoside (IPTG) and incubated with shaking at 37°C for three to four hours, or overnight at 15-20°C with 0.1 mM IPTG. Cells were pelleted by centrifugation (5000 *x g*, 4°C, 15 minutes) and froze at -80°C prior to processing. GST-AKAP95 was a kind gift of Professor Kjetil Tasken, University of Oslo. GST-HPV11E6 and GST-HPV16E6 were kind gifts of Dr Miranda Thomas and Professor Lawrence Banks, International Centre for Genetic Engineering and Biotechnology, Trieste.

2.5.6 Purification of recombinant GST proteins

Bacteria were thawed gently on ice and resuspended in bacteria lysis buffer (50 mM HEPES (pH 7.5), 2% Triton X-100 in PBS) supplemented with 5 mg/ml lysozyme. Bacteria were then sonicated on ice. For purification of GST-AKAP95, sonication was one period of 15 seconds on at 20% amplitude. For GST-HPV18 E6, sonication was for three periods of 10-20 seconds on and 40 seconds off at 20% amplitude. Lysates were then cleared by high-speed centrifugation at 10,000 *x g* for 15 minutes. Soluble recombinant protein was then immobilised on glutathione *S*-agarose beads with rotation at 4°C

overnight prior to extensive washing in lysis buffer. Soluble GST proteins were prepared by subsequently eluting the GST protein into lysis buffer containing 50 mM reduced glutathione at pH 8. Soluble proteins were then dialysed overnight in storage buffer (25 mM HEPES (pH 7.5), 200 mM sodium chloride, 20% (vol/vol) glycerol). Alternatively, beads were resuspended in an equal volume of PBS containing 50% glycerol and 1% Triton X-100. Recombinant proteins were stored at -20°C.

2.5.7 GST pull-down from cell lysates

Cells were lysed in E1A buffer (50 mM HEPES (pH 7.5), 250 mM sodium chloride and 0.1% NP-40) before end-over-end incubation with GST fusion proteins overnight at 4°C. After overnight incubation, pre-washed GST beads were added where appropriate for at least two hours at 4°C. For GST fusion proteins already bound to the beads, the fusion proteins were added directly to the cell lysate. After extensive washing (5+) in lysis buffer, the beads were resuspended in an equal volume of 2X Laemmli buffer supplemented with 5% (vol/vol) β-mercaptoethanol, boiled at 95°C for 10 minutes and loaded onto SDS-PAGE gels for Western blotting, as described in section 2.6.2.

2.5.8 Plasmid DNA constructs for interaction mapping

To map the HPV18 E6-interacting domains on AKAP95, a series of AKAP95 mutants in the pcDNA3 background were used, encoding FLAG/HA (FH-) tagged proteins at the amino terminus. These mutants were FH-AKAP95(1-692), FH-AKAP95(101-692), FH-AKAP95(1-210), FH-AKAP95(211-692), FH-AKAP95(1-340), FH-AKAP95(341-692), FH-AKAP95(I582P) and FH-AKAP95(ZF C>S) and were kind

gifts of Professor Hao Jiang (Hu et al., 2016). FH-AKAP95(I582P) contains a mutation that renders it unable to bind to PKA and the ZF C>S mutant cannot bind to DNA.

Similarly, mutant HPV18 E6 constructs were used to map the AKAP95 binding site on E6. These mutants were wild-type HPV18 E6, Arg153Leu or Thr156Glu mutants, and have been described elsewhere (Watson et al, 2003). Replacement of arginine at amino acid 153 with leucine destroys the PKA recognition sequence (RRXS/T) and this mutant E6 no longer responds to PKA signalling and can degrade PDZ substances in a PKA independent manner (LeuE6; Kühne et al., 2000). The threonine residue at residue 156 lies within the PBM of HPV18 E6 and the hydroxyl oxygen of this residue is involved in E6-PDZ interactions. Substitution by glutamic acid inhibits binding to the PDZ substrate Dlg1 and inhibits its degradation *in vitro* (GluE6; Gardiol *et al*., 1999). An additional mutant was used in which the last four amino acids that make up the E6 PBM have been deleted by insertion of two translation termination codons at positions 155 and 156 (ΔPDZE6; Delury et al., 2013).

2.6 Protein biochemistry

2.6.1 Bradford assay

Protein concentrations were determined by the Bradford method. A standard curve was first established using a Bio-Photometer (Eppendorf, Stevenage, UK) using serial dilutions of BSA (Sigma-Aldrich) ranging from 2 mg/ml to 0.125 mg/ml, diluted with Bio-Rad Protein Assay Reagent (Hemel Hempstead, UK), as per manufacturer's instructions. Sample protein concentration was determined by comparison to the standard curve.

2.6.2 Co-immunoprecipitation

Cells were harvested directly in E1A lysis buffer and co-immunoprecipitations performed as described in Parish et al., 2006. Briefly, the cell lysate was sonicated for 10 seconds at 30% amplitude. After centrifugation to remove insoluble material, lysates were incubated overnight at 4°C with 4-5 µg of the indicated antibody before incubation with Protein A/G Sepharose™ beads (Sigma-Aldrich) for at least two hours at 4°C. The beads were washed extensively in wash buffer (100 mM Tris-HCl (pH 8.0), 150 mM sodium chloride, 0.5% NP-40 and 2 mM dithiothreitol) and co-immunoprecipitating proteins detected by Western blotting.

2.6.3 SDS-PAGE

Samples were lysed in urea lysis buffer (8 M urea, 150 mM sodium chloride, 2 mM Tris-HCl (pH 7.2), protease and phosphatase inhibitors) unless otherwise indicated, sonicated once at 30% amplitude for 10 seconds, and cleared by high-speed centrifugation, 16,000 $x\,g$ for 15 minutes at 4°C. A total of 20-30 µg total protein was prepared for electrophoresis by addition of 2X Laemmli buffer supplemented with 5% (vol/vol) β-mercaptoethanol and boiled at 95-100°C for five to 10 minutes on a hot plate. Protein samples were resolved on a polyacrylamide separating gel (350 mM Tris-HCl buffer (pH 7.8), 10-15% (wt/vol) polyacrylamide (37.5:1, acrylamide: bis-acrylamide), 1% (wt/vol) SDS, 0.5% (wt/vol) ammonium persulphate (APS) and 0.08% (vol/vol) N,N,N',N'-Tetramethylethylenediamine (TEMED)). A layer of 100% isopropanol was added to the gel once poured to ensure a smooth surface. Once set, the isopropanol was removed, the gel washed with water and a stacking gel (120 mM Tris-HCl buffer (pH 6.8), 4.5% (wt/vol) polyacrylamide, 1% (wt/vol) SDS, 0.5% (wt/vol) APS and 0.125% (vol/vol)

TEMED) poured and an appropriate comb added to the gel and allowed to set. Once set, the electrophoretic apparatus was flooded with cold running buffer (25 mM Tris-HCl, 192 mM glycine, 0.1% (wt/vol) SDS, pH 8.3) and the comb removed. Wells were then washed with running buffer before samples were added to wells. Electrophoresis was performed using the Bio-Rad Mini-Protean® system at 20-30 mA for 1-2 hours or until the protein marker had reached the end of the gel.

2.6.4 Western blotting

Following protein separation by SDS-PAGE, proteins were transferred to nitrocellulose membranes (Pall Corporation, Portsmouth, UK) in a Trans-Blot transfer tank (Bio-Rad) flooded with transfer buffer (25 mM Tris-HCl, 192 mM glycine, 20% (vol/vol) methanol, pH 8.3) set at 15-25 mA for overnight transfer or 350 mA for three hours. To assess transfer, membranes were stained with the reversible protein stain Ponceau S (0.1% (wt/vol) Ponceau S stain in 5% (vol/vol) acetic acid) to visualise protein bands, before subsequent de-staining by washing in several changes of TBS containing 0.1% Tween-20 (TBS-T: 50 mM Tris-HCl and 150 mM sodium chloride, 0.1% Tween-20, pH 7.6). Membranes were then incubated on a rocking platform with blocking buffer (5% (wt/vol) dried skimmed milk powder in TBS-T or 5% (wt/vol) BSA in TBS-T for phosphor-antibodies) for at least 60 minutes before incubation with primary antibody (**Table 2.1**) in blocking buffer overnight on a rocking platform. Protein loading was assessed by blotting for glyceraldehyde-3-phosphate dehydrogenase (GAPDH). Following incubation with the primary antibody, membranes were washed four times for 10-15 minutes each in TBS-T before incubation with the appropriate species-specific secondary antibody prepared in blocking buffer. After 1-hour incubation at room temperature and

four additional washes, the membrane was developed by enhanced chemiluminescence and signals captured on X-ray film (GE Healthcare, Amersham, UK) or using the Fusion FX digital chemiluminescence detection system (Vilber Lourmat, Collégien, France).

Table 2.1: Table of antibodies

Antibody	Clone/ID	Manufacturer	Species	WB dilution	IF dilution
DLG1	NAG	(Roberts et al., 2007)	Rabbit	1/200	-
hScrib	C20	Santa Cruz	Goat	1/2000	-
p53	DO-1	(Stephen et al., 1995)	Mouse	1/100	1/50
GAPDH	6C5	Santa Cruz	Mouse	1/5000	-
Cytokeratin 18	CK5	Sigma	Mouse	1/1000	-
E-Cadherin	610182	BD Biosciences	Mouse	1/1000	-
GRB2	C7	Santa Cruz	Mouse	1/200	-
HPV18 E6	G7	Santa Cruz	Mouse	1/100	-
HPV18 E7	8E2	Abcam	Mouse	1/1000	-
PKA-RI	18/PKA(RI)	BD Biosciences	Mouse	1/1000	-
PKA-RII	40/PKA(RII)	BD Biosciences	Mouse	1/1000	-
PKA-Cα	C20	Santa Cruz	Rabbit	1/1000	-
Phospho-PKA C (Thr197)	4781S	Cell Signalling Technology	Rabbit	-	1/100
Phospho-PKA substrates	9621	Cell Signalling Technology	Rabbit	1/1000	-
AKAP95	A301-062A	Bethyl Laboratories Inc.	Rabbit	1/2000	1/200
Cyclin D1	H295	Santa Cruz	Rabbit	1/1000	-
Flag	M2	Sigma	Mouse	1/1000	-
HA	HA.11	Covance	Mouse	1/1000	-

CHAPTER 3 INVESTIGATING THE EFFECT OF HPV18 ON THE ACTIVITY OF THE PROTEIN KINASE A SIGNALLING PATHWAY

3.1 Introduction

Human oncogenic viruses, including HPV, interact with and remodel host signalling pathways to facilitate viral DNA replication and drive host cell transformation, and these interactions are important for the oncogenic progression of viral infections. The HPV E6 and E7 oncoproteins have been reported to interact with as many as 243 cellular proteins, regulating up to 153 different signal transduction pathways, including the host cAMP-dependent PKA pathway (Zhao et al., 2011). This pathway is important for several aspects of the HPV life cycle, including regulation of viral protein function, and changes in PKA signalling may be relevant during disease progression, as discussed in section 1.3.11 of the introduction to this thesis.

Given that PKA is important for multiple aspects of the HPV life cycle and changes in the activity of the pathway may be relevant for oncogenic progression of HPV infections, we were interested in understanding whether the virus is able to manipulate cAMP and/or PKA signalling in squamous epithelium keratinocytes, the natural target of the virus. For this, an assay based on BRET was used to investigate both cAMP and PKA signalling in living cells. This assay allows for real-time evaluation of cAMP and PKA dynamics based on changes in protein subunit interactions (described in detail in section 3.2.1). Using this assay, there was increased activity of the kinase in NIKS harbouring HPV18 episomes compared to control NIKS, suggesting that HPV18 replication can modulate this signalling

pathway (unpublished data from the Roberts and McKeating laboratories). NIKS have been used to model life cycle events of various oncogenic HPVs (Flores et al., 1999; Nakahara and Lambert, 2007) but they are a spontaneously immortalised human keratinocyte line. As primary squamous keratinocytes are the natural target cell of the virus, it was, therefore, important to investigate the HPV-PKA axis in physiologically relevant cells.

3.2 Results

3.2.1 Bioluminescence Resonance Energy Transfer sensors to study PKA activity

To understand whether HPV18 can manipulate PKA activity, BRET-based biosensors were used to examine PKA dynamics in intact cells. This assay uses *Renilla* luciferase (Rluc)-tagged regulatory subunits (i.e. Rluc-PKA-RI or -RII) and a GFP-tagged catalytic subunit (GFP-Cα) as the energy donor and acceptor respectively. Co-transfection of these sensors allows for recombinant expression of the PKA holoenzyme in cells with known subunit concentration (Prinz et al., 2006).

When the regulatory and catalytic subunits are assembled as a holoenzyme (i.e. PKA is inactive), there is energy transfer from Rluc-PKA-R subunit to GFP-Cα (410 to 515 nm). On PKA activation by cAMP, the holoenzyme dissociates and this leads to an increase in intra-molecular distance between the donor and acceptor components of the biosensor, resulting in a loss of energy transfer to GFP-Cα. As such, changes in energy transfer to GFP-Cα can be used to study PKA activation.

Changes in cAMP levels can also be examined using this technique by using the known cAMP target, EPAC. In a similar fashion to the PKA biosensors, the EPAC sensor contains

both the luciferase donor and GFP acceptor at opposing termini and, following an increase in cAMP, the intra-molecular distance between the sensors increases, leading to a change in energy transfer to the GFP moiety.

A diagram of these biosensors is shown in **Figure 3.1,** with **Figure 3.2** describing the changes in energy transfer under low and high cAMP levels. Note that lower BRET ratios (515 nm/410 nm) represent activation of that particular sensor.

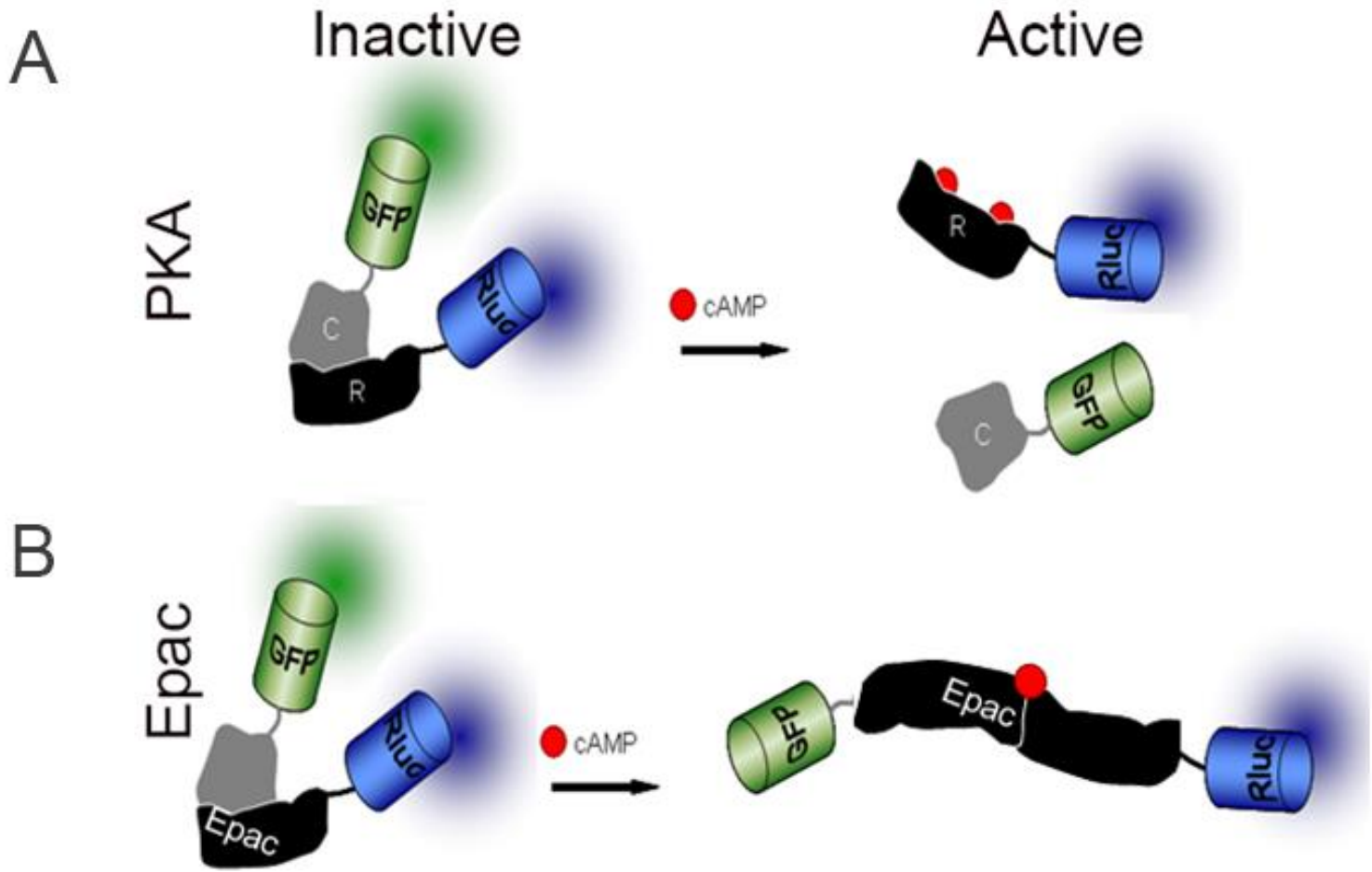

Figure 3.1: Genetically encoded bioluminescent sensors to examine PKA and cAMP signalling in living cells. The *Renilla* luciferase bioluminescent donor (Rluc) and green fluorescent protein (GFP) are fused to the regulatory and catalytic subunits of PKA (A), or different domains of EPAC (B), respectively. Energy transfer occurs when these sensors are in close proximity (1-10 nm). PKA or EPAC activation leads to a conformational change such that there is increased distance between sensors, with an associated decrease in BRET ratio

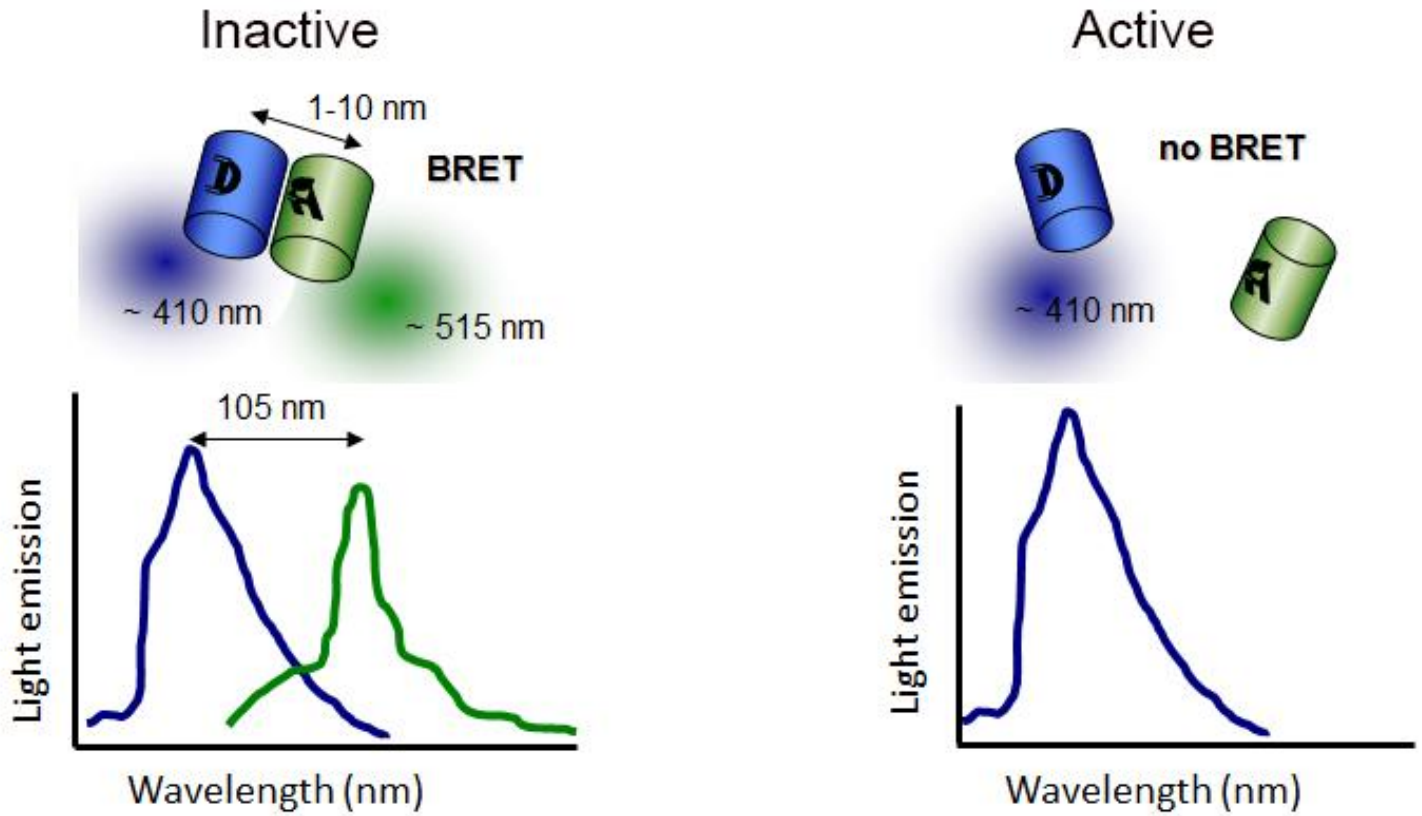

Figure 3.2: Intra-molecular distance dictates energy transfer to GFP acceptor molecules during BRET. When PKA/EPAC is inactive (low cAMP levels), the Rluc-tagged donor (D) is in close proximity (1-10 nm) to the GFP-acceptor (A) and there is energy transfer between the donor and acceptor, resulting in light emission measurable at both 410 nm and 515 nm. When cAMP levels are high, there is an increase in intra-molecular distance such that there is no longer energy transfer from the donor to the acceptor moiety. This results in the light emission from the donor solely being detected.

3.2.2 HPV18 replication in normal immortalised keratinocytes is associated with changes in PKA activity

It was first confirmed whether HPV18 replication in NIKS cells affected the activation of the PKA sensors in the absence of any exogenous stimulation. As shown in **Figure 3.3A**, HPV18 replication did not significantly affect the activity of the PKA-RI sensor (NIKS 0.187 ± 0.0188 and NIKS-18 0.167 ± 0.0157, p=0.07); however, there was increased activity of the PKA-RII sensor (NIKS 0.202 ± 0.007 and NIKS-18 0.108 ± 0.006, p=<0.01). To correlate this PKA-RII activation with cAMP, the activity of the EPAC cAMP sensor was then determined. Interestingly, HPV18 replication also increased the activity of cAMP sensor EPAC (NIKS 0.206 ± 0.021 and NIKS-18 0.116 ± 0.009, p=0.03), which may suggest that the increased PKA-RII activity seen in HPV18 genome containing cells is driven by changes in cAMP. Visualising these data as a fold change showed that NIKS maintaining HPV18 genomes showed an approximate 1.2-fold, 1.9-fold and 1.8-fold increase in activity of the PKA-RI, -RII and cAMP sensors, respectively, compared to control NIKS (data not shown).

Next, whether HPV18 affected the activity of the PKA pathway upon chemical induction of cAMP levels was examined. For this, forskolin was used to increase the activity of adenylate cyclases, leading to an increase in cellular cAMP **(Figure 3.3 B).** Here, viral replication was associated with increased activity of both PKA sensors: PKA-RI (NIKS 0.149 ± 0.024 and NIKS-18 0.087 ± 0.004, p=<0.01) and PKA-RII (NIKS 0.148 ± 0.003 and NIKS-18 0.045 ± 0.004, p=<0.001). Furthermore, replication of the virus was also associated with increased activity of the cAMP sensor (NIKS 0.147 ± 0.017 and NIKS-18 0.085 ± 0.131, p=<0.001). Expressed as a fold change, replication of the HPV18 genome

was associated with a 1.6-fold, 3.3-fold and 1.8-fold increase in activity of the PKA-RI, -RII and cAMP sensors (data not shown).

These data suggest that HPV18 replication is associated with increased activity of PKA-RI, -RII and cAMP biosensors. Under both unstimulated and stimulated conditions, this increased activity is greatest for the -RII subunit, which may suggest that HPV preferentially activates the RII isoform during viral replication in NIKS cells.

3.2.3 Identification of a transfection reagent for primary human foreskin keratinocytes

While a variety of keratinocyte lines, including NIKS, have been used to study HPV in the laboratory, they are not a truly physiological model system to study HPV life cycle events. For example, NIKS are near diploid, containing 47 chromosomes due to additional long arm of chromosome 8, and express wild type p53 (Allen-Hoffmann et al., 2000). In addition, there are various differences in how the virus interacts with NIKS compared with primary HFKs. For example, infection by HPV16 pseudovirions in NIKS was approximately 400-fold more efficient than in HFKs (Griffin et al., 2013), which is consistent with earlier studies that showed NIKS cells to be more permissible for HPV31b infection than HFKs (Ozbun, 2002). Furthermore, NIKS are a spontaneously immortalised cell line so one must be aware of the underlying genetic changes in these cells, which may not be present in primary HFKs. These examples clearly illustrate the importance of using an appropriate culture system to study HPV. It was, therefore, important to examine whether HPV18 regulates PKA in a physiologically relevant system established in primary human keratinocytes, the natural host cell of the virus.

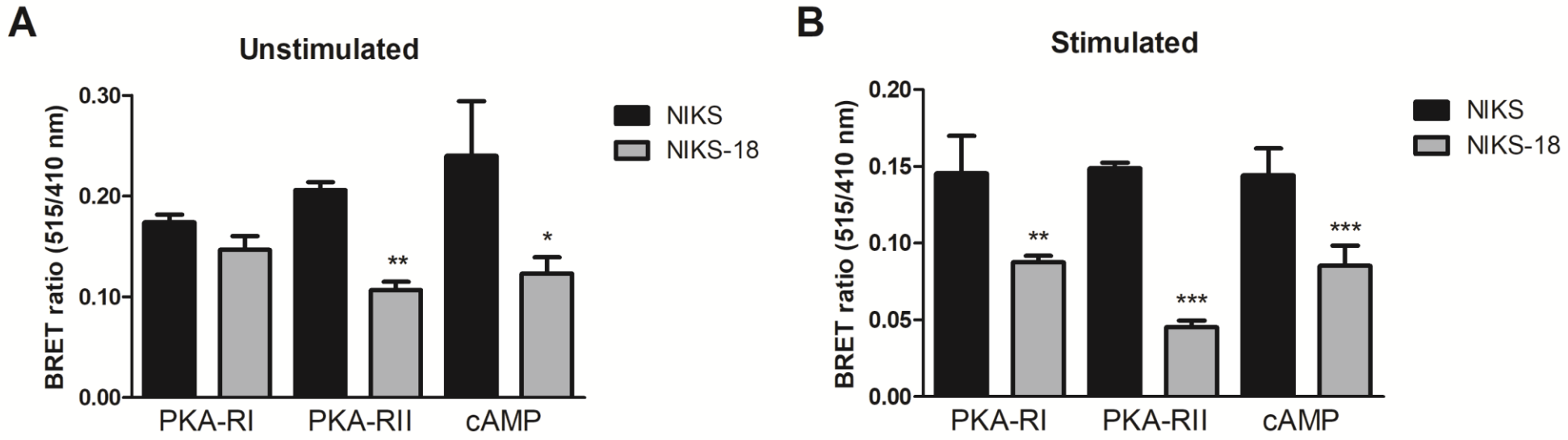

Figure 3.3: Normal immortalised keratinocytes maintaining HPV18 genomes show altered PKA activation. NIKS or NIKS cells containing HPV18 genomes (NIKS-18) cells were transfected with PKA or cAMP biosensors. The activity of these biosensors was determined 48 hours later by bioluminescent resonance energy transfer in the absence (unstimulated) or presence (stimulated) of the cAMP elevating agent forskolin. Data ±SEM taken from three independent experiments. Statistical significance was determined by Student's t-test comparing NIKS to NIKS-18 cells where * denotes $p<0.05$, ** denotes $p<0.01$ and *** denotes $p<0.001$.

For this, it was first important to find a transfection reagent for primary HFKs suitable for high-level expression of the PKA/cAMP biosensors as HFKs are traditionally quite difficult to transfect. HFKs grown in monolayer culture were transfected with a GFP encoding plasmid (pMAX-GFP) using a variety of commercially available transfection reagents and assayed by fluorescence microscopy for GFP expression 48 hours later to determine transfection efficiency. Rate of transfection was judged by determining the percentage of cells that were GFP positive. As shown in **Figure 3.4,** Mirus Keratinocyte provided the highest transfection efficiency of the reagents tested with minimal effects on cell morphology and viability. Several of the other reagents, including Viromer Red and Mirus 20:20, resulted in very poor transfection efficiencies and cell viability. Additionally, these reagents disturbed the ability of these cells to form the traditional cobblestone appearance of primary keratinocytes. Further optimisation of the Mirus Keratinocyte reagent provided a DNA to reagent ratio for maximum transgene expression but with low cell toxicity (1:1.5; data not shown).

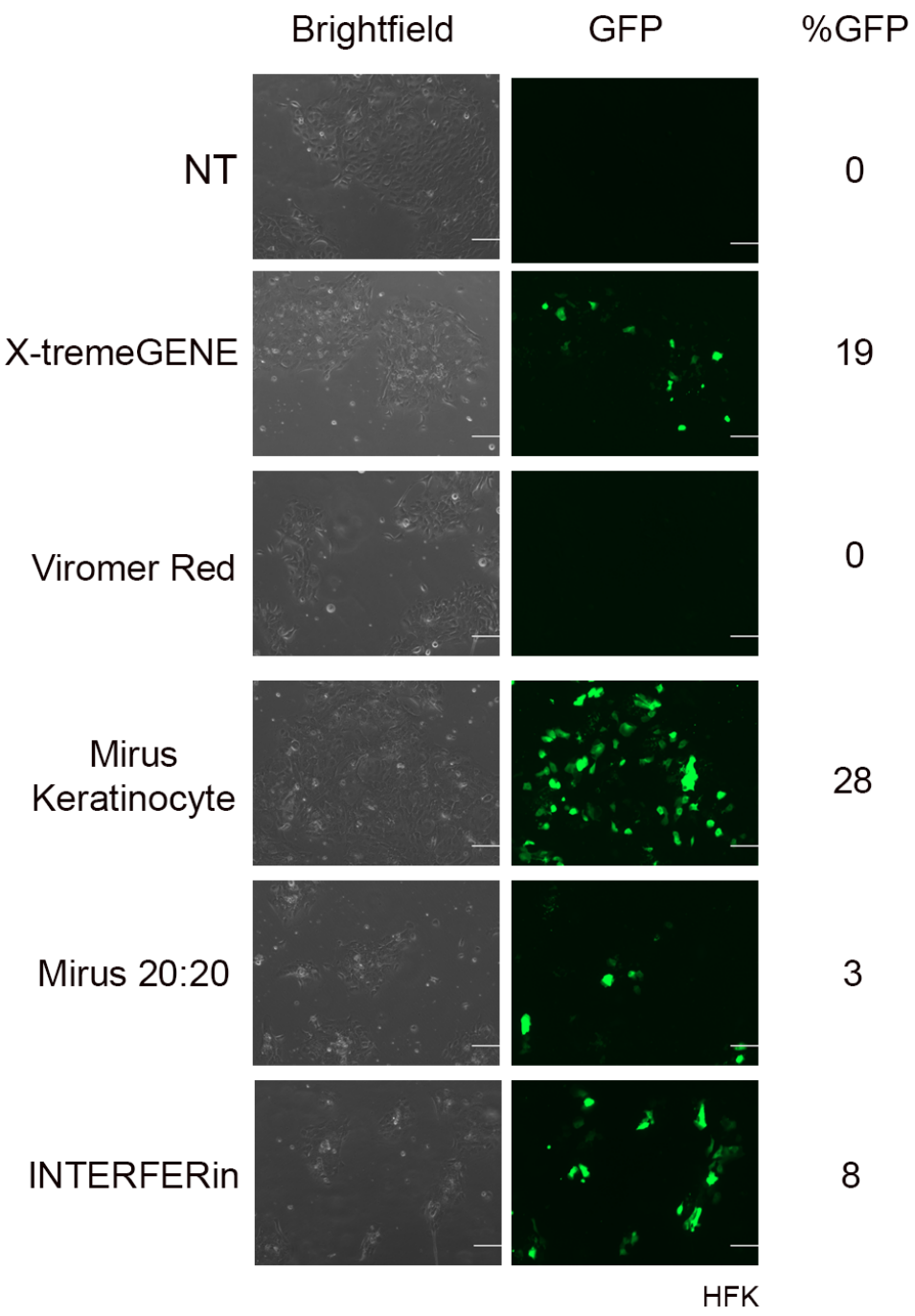

Figure 3.4: Identification of a transfection reagent suitable for primary human foreskin keratinocytes. Primary HFKs were plated out in a six-well plate and transfected with a GFP expression vector using the indicated reagents as per manufacturer's instructions. GFP expression was assayed by fluorescence microscopy and morphology examined under phase contrast. NT: not transfected. Scale bar: 10 μm. Percentages represent transfection efficiency as determined by the 'Find Maxima' method on ImageJ to count GFP positive cells.

3.2.4 HPV18 replication in a primary human foreskin keratinocyte grown to low passage also associated with changes in PKA activity

Having identified a suitable transfection reagent, the BRET experiments were then carried out in donor matched HFK and HFK cells maintaining HPV18 genomes (Wilson et al., 2007). It has been reported that oncogenic HPV episomes, including HPV18, in primary keratinocyte donors are sometimes reduced upon cell passage concomitant with the integration of viral DNA into the host DNA (Delury et al., 2013; Lace et al., 2011), an event that is linked to malignant progression of infections (Burk et al., 2017). Therefore, changes to PKA activity by HPV might contribute to this progression. To examine this, the BRET assay was carried out in HPV18 genome containing cells grown to both low (HFK-18 LP) and high cell passages (HFK-18 HP).

In **Figure 3.5 A**, for foreskin donor one (top row), HPV18 replication in cells cultured to low cell passages displayed slightly increased activity of the PKA-RI sensor compared to control cells (HFK 0.157 ± 0.024 and HFK-18 LP 0.110 ± 0.022), although this did not reach significance (p=0.06). For PKA-RII, there was increased activity of the biosensor in HFK-18 LP cells (HFK 0.164 ± 0.014 and HFK-18 LP 0.046 ± 0.021, p=<0.01), which occurred concomitantly with a significant increase in cAMP sensor activity (HFK 0.311 ± 0.031 and HFK-18 LP 0.200 ± 0.026, p=<0.01). In cells stimulated with forskolin **(Figure 3.5 B)**, there was a significant decrease in PKA-RI sensor activity with HPV18 replication (HFK 0.134 ± 0.024 and HFK-18 LP 0.193 ± 0.012, p=0.02); however, significant increases in PKA-RII (HFK 0.148 ± 0.014 and HFK-18 LP 0.060 ± 0.012, p=0.01) and cAMP sensor (HFK 0.285 ± 0.031 and HFK-18 LP 0.166 ± 0.015, p=<0.01) activity were detected in cells maintaining HPV18 genomes.

In the second foreskin donor (bottom row, **Figure 3.5**), replication of the HPV18 genome in unstimulated cells (**panel C**) was associated with increased activity of all biosensors; PKA-RI (HFK 0.198 ± 0.012, HFK-18 LP 0.136 ± 0.006, p=<0.05), PKA-RII (HFK 0.168 ± 0.014 and HFK-18 LP 0.095 ± 0.001, p=<0.01) and cAMP (HFK 0.304 ± 0.014, HFK-18 LP 0.173 ± 0.011, p=<0.01). After stimulation with forskolin (**panel D**), there was no significant effect of HPV18 replication on PKA-RI activity (HFK 0.129 ± 0.021 and HFK-18 LP 0.104 ± 0.036 (p=>0.05). However, viral replication was associated with significant increases in PKA-RII (HFK 0.087 ± 0.016 and HFK-18 LP 0.041 ± 0.012, p=<0.01) and cAMP sensor activity (HFK 0.171 ± 0.017 and HFK-18 LP 0.130 ± 0.01, p=<0.05).

The data obtained in unstimulated LP cells showed that HPV18 replication was associated with small changes in PKA-RI activity but a more marked increase in PKA-RII and cAMP activity, which was statistically significant in both donor backgrounds. On stimulation with forskolin, there was a small increase in PKA-RI activity in one foreskin donor but no change in the other donor, possibly suggesting a donor-specific effect of HPV18 on PKA-RI activity. Consistent with the unstimulated data, there is a significant activation of both PKA-RII and cAMP activity in cells treated with forskolin. Thus, the data show a consistent activation of PKA-RII and cAMP in LP cells maintaining HPV genomes.

3.2.5 HPV18 replication in primary human foreskin keratinocytes grown to high passage also display alterations in PKA and cAMP activity

In unstimulated HFKs derived from donor one grown to high passage **(Figure 3.6 A),** replication of the HPV18 genome had no effect on the PKA-RI (HFK 0.157 ± 0.024 and HFK-18 HP 0.101 ± 0.023, p=0.06) or PKA-RII sensor (HFK 0.164 ± 0.014 and HFK-18

HP 0.135 ± 0.017, p=0.09). HPV18 replication was associated with increased activity of the cAMP sensor (HFK 0.311 ± 0.031 and HFK-18 HP 0.194 ± 0.011, p=<0.01).

After stimulation of the cells with forskolin **(Figure 3.6 B),** there was no significant activation of the PKA-RI sensor in cells maintaining HPV18 genomes (HFK 0.147 ± 0.014 and HFK-18 HP 0.102 ± 0.022, p=0.1). However, the activity of the PKA-RII (HFK 0.166 ± 0.018 and HFK-18 HP 0.079 ± 0.014, p=0.04) and cAMP (HFK 0.285 ± 0.031 and HFK-18 HP 0.128 ± 0.0135, p=<0.01) sensors was significantly increased in cells maintaining viral genomes.

In the second foreskin donor, in unstimulated cells **(Figure 3.6 C),** the presence of the HPV18 genome did not significantly affect the activity of the PKA-RI sensor (HFK 0.198 ± 0.01 and HFK-18 HP 0.144 ± 0.01, p=0.07). In contrast, viral replication significantly increased the activity of both PKA-RII (HFK 0.168 ± 0.03 and HFK-18 HP 0.103 ± 0.02, p=<0.01) and cAMP sensors (HFK 0.304 ± 0.02 and HFK-18 HP 0.163 ± 0.03, p=<0.001).

In cells treated with forskolin (**Figure 3.6 D**), replication of HPV18 DNA did not affect the activity of the PKA-RI sensor (HFK 0.129 ± 0.03 and HFK-18 HP 0.086 ± 0.02, p=0.08), however significant activation of both the PKA-RII (HFK 0.087 ± 0.02 and HFK-18 HP 0.046 ± 0.01, p=0.01) and cAMP (HFK 0.171 ± 0.01 and HFK-18 HP 0.106 ± 0.03, p=0.01) sensors were detected in these cells.

In unstimulated HP cells, there is no activation of PKA-RI in cells containing HPV18 genomes but small changes in PKA-RII activity in one foreskin donor. In both donors, replication of HPV18 DNA was associated with significant increases in cAMP sensor activity. In cells stimulated with forskolin, there is no activation of PKA-RI but significant activation of PKA-RII in both donor backgrounds, occurring concomitantly with significant increases in cAMP sensor activity.

Taken together, the data from LP and HP cells showed marked activation of PKA-RII, albeit less so in the HP cells, and a variable response to HPV18 DNA replication for PKA-RI activity. In all foreskin donors, under both unstimulated and stimulation conditions, HPV replication was associated with increased cAMP activity.

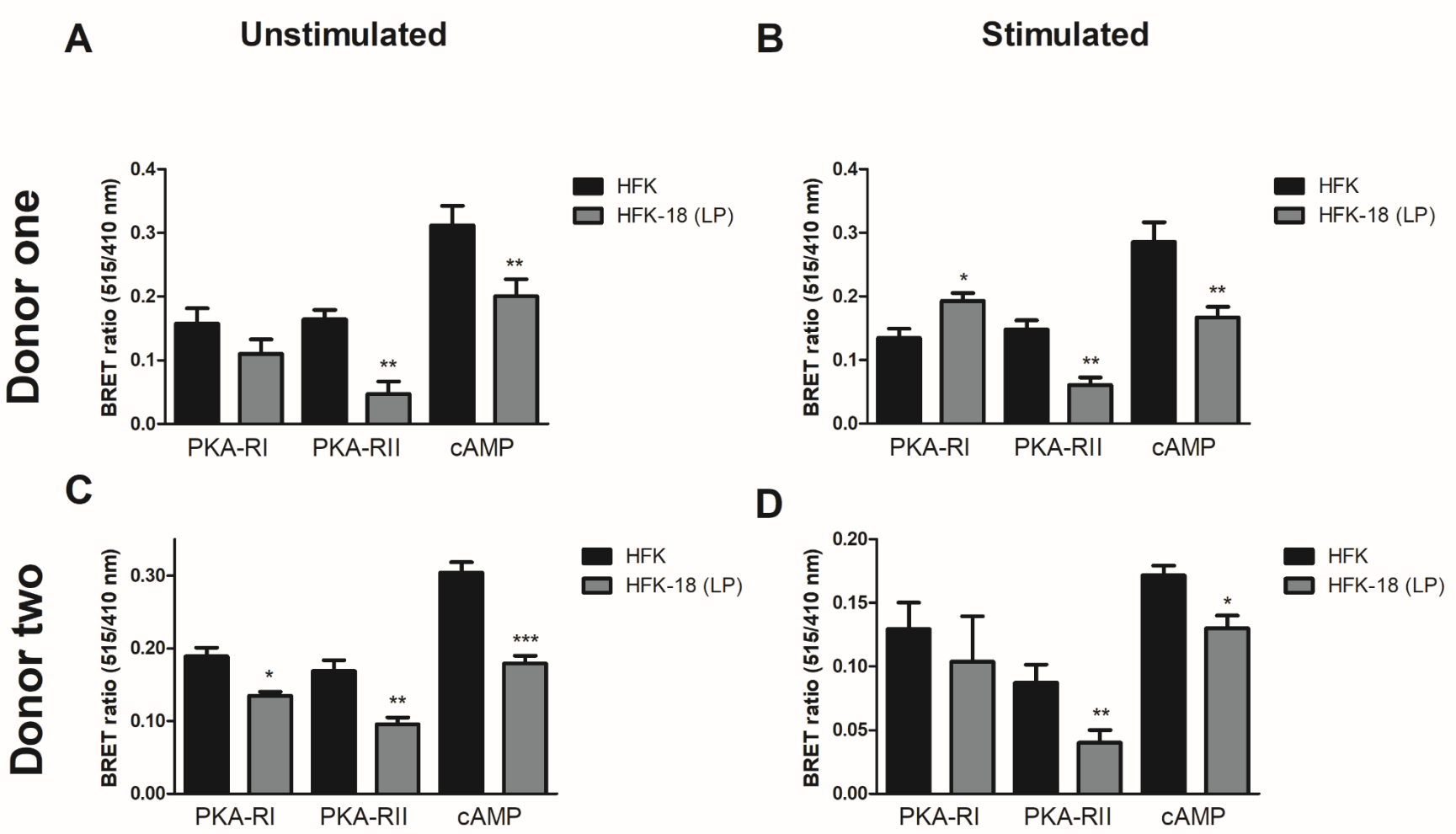

Figure 3.5: HPV18 replication in low passage primary human foreskin keratinocytes regulates PKA activity. HFK or HFK-18 cells from two foreskin donors were transfected with PKA or cAMP biosensors. The activity of these biosensors was determined 48 hours later by bioluminescent resonance energy transfer in the absence (unstimulated; A, C) or presence (stimulated; B, D) of the cAMP elevating agent forskolin. Data ±SEM taken from three independent experiments. Statistical significance was determined by Student's t-test comparing HFK to HFK-18 cells where * denotes $p<0.05$, ** denotes $p<0.01$ and *** denotes $p<0.001$.

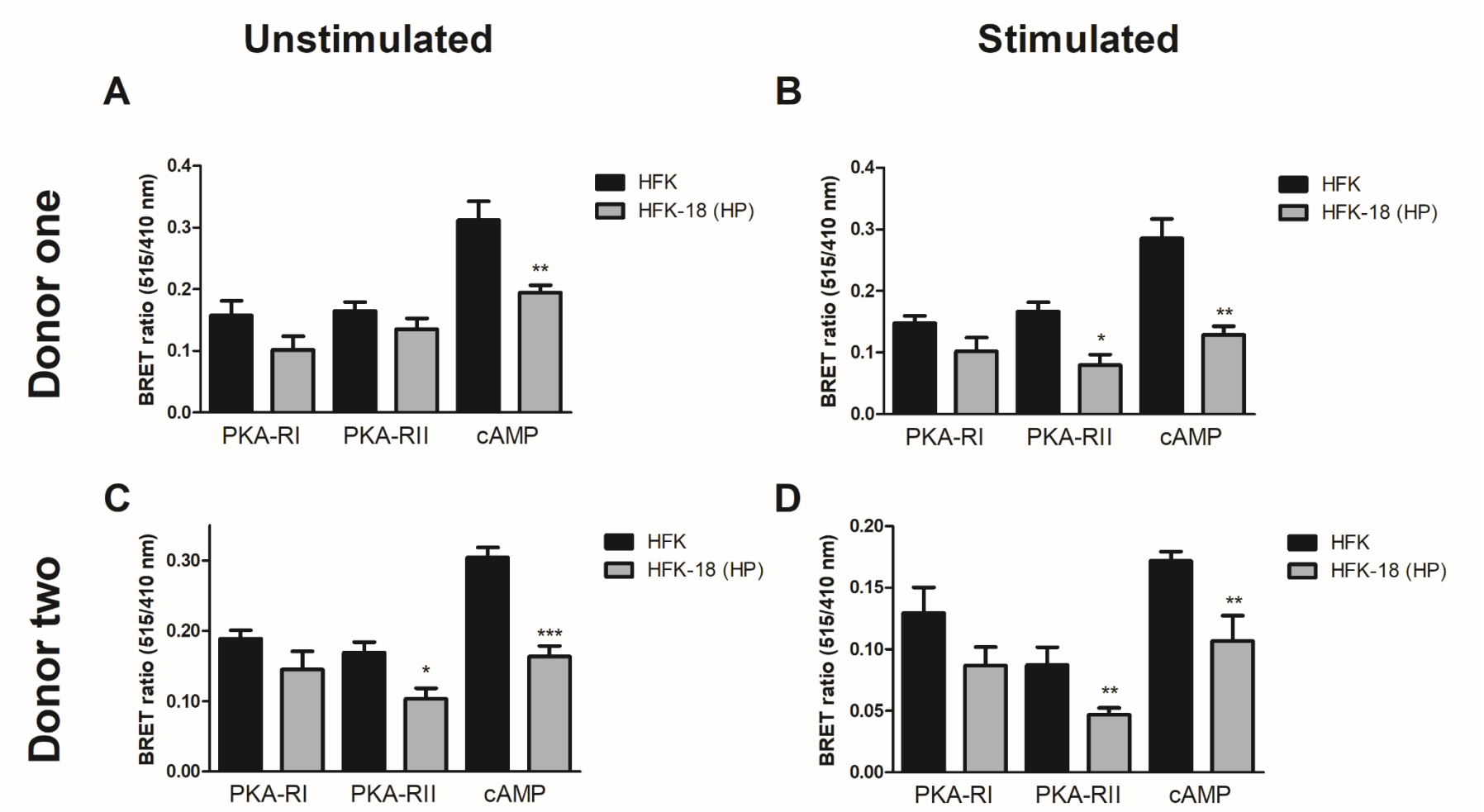

Figure 3.6: HPV18 replication in high passage primary human foreskin keratinocytes regulates PKA and cAMP activity. HFK or HFK-18 cells from two foreskin donors were transfected with PKA or cAMP biosensors. The activity of these biosensors was determined 48 hours later by bioluminescent resonance energy transfer in the absence (unstimulated; A, C) or presence (stimulated; B, D) of the cAMP elevating agent forskolin. Data ±SEM taken from three independent experiments. Statistical significance was determined by Student's t-test comparing HFK to HFK-18 cells where * denotes $p<0.05$, ** denotes $p<0.01$ and *** denotes $p<0.001$.

3.2.6 Both episomal and integrated HPV18 genomes regulate PKA activity

The data in HFKs presented thus far showed that viral replication was associated with changes in PKA and cAMP sensor activity in cells maintaining HPV18 genomes grown to both low and high cell passage. The main difference between these cells is that the increased activity of PKA-RII was less marked in HP cells, which may reflect changes in the physical state of viral DNA in these cells. The HPV18 genome containing cells used for the low passage BRET analysis were all below passage 10 (p<10) and high passage were beyond passage 15 (p>15). To examine the physical status of the viral genome, DNA was extracted from cells from the two different foreskin donors by phenol-chloroform extraction and digested with either *Eco*RI, which linearizes the HPV18 genome, or *Bgl*III, which does not cut the HPV18 genome but will cut host DNA, prior to Southern blot analysis. Residual input DNA was digested with *Dpn*I. The Southern blot for data from donor one (top row, **Figures 3.5** and **3.6**) is shown in **Figure 3.7** and donor two (bottom row, **Figures 3.5** and **3.6**) shown in **Figure 3.8.**

In **Figure 3.7,** episomal forms of the HPV18 DNA migrate as supercoiled (SC) and open circle (OC) forms in the presence of the non-cutter *Bgl*II, and as a linear 8 kilobase (kb) band upon digestion with the single cutter *EcoR*I. The intensity of the bands begin to diminish around passage 10 and continues to do so until passage 13 where they are no longer visible. This suggests that in these cells the viral genome is maintained as an episome to passage 10 but then these episomes are gradually lost upon extended cell passage (>p13). In addition, there are faint bands at approximately 6 kb at p13 and p15 cells cut with *Eco*RI that may represent a virus-host junction in these cells (see black arrowhead in **Figure 3.7).** Similarly, in **Figure 3.8**, the HPV18 genome is episomal and

detected up to passage 9 before a gradual loss of episomes up to passage 13. No viral episomes were detected from passage 16 to 21. In addition, there are higher molecular bands, evident in cells grown to passage 8-10, that may represent concatemeric forms of the HPV genome (indicated by black arrowhead). The SC band is very faint in these cells, indicating that the major proportion of episomes are in the form of open/relaxed circles.

Taken together, the Southern blot data shows that, in both foreskin donors, cells grown to low passage ($p<10$) contain episomal HPV18 genomes and these episomes are lost with extended cell culture and the viral DNA has become integrated into the host. Thus, in the BRET analyses, the LP cells contain episomes and HP cells contain lack or have reduced episomes and contain HPV integrants.

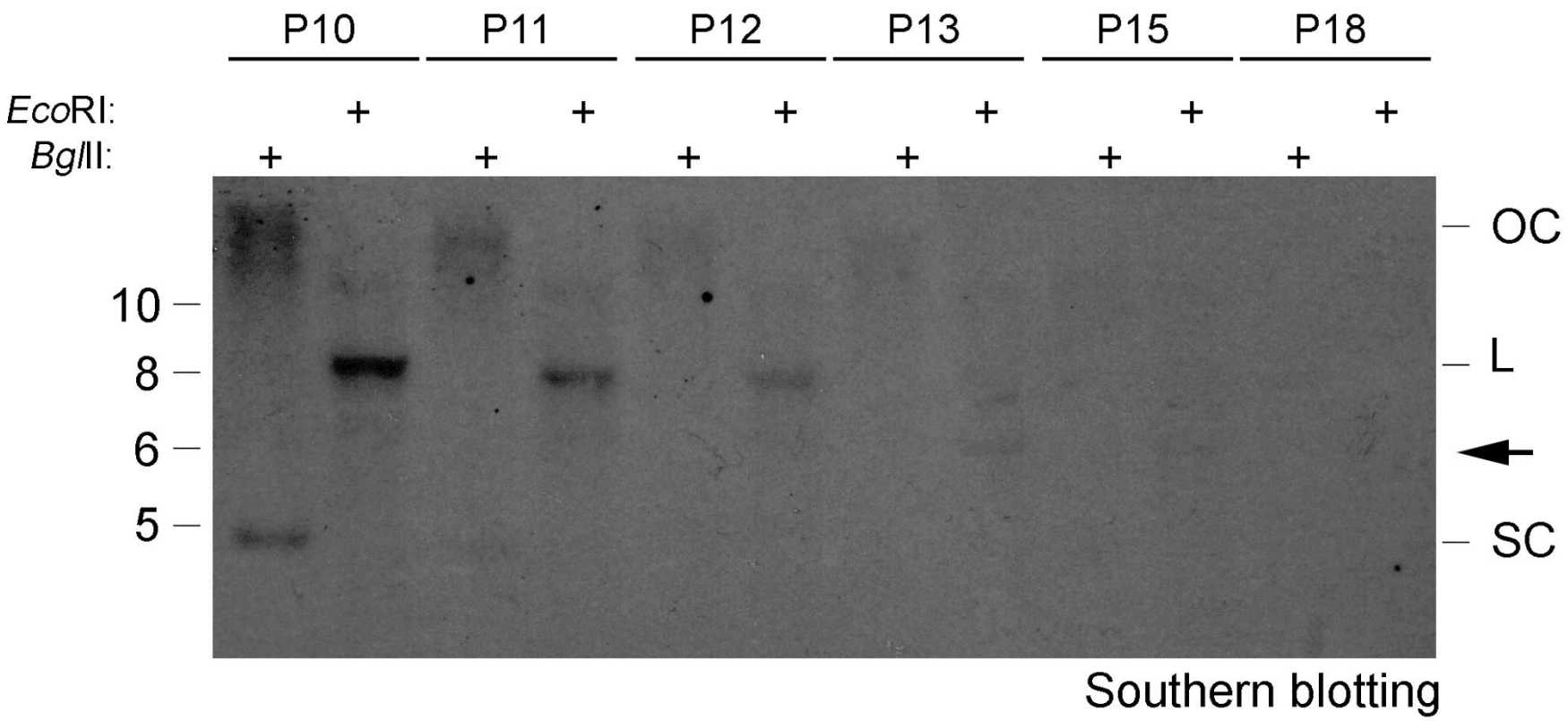

Figure 3.7: Detection of HPV18 genome status by Southern blotting in donor one BRET series. DNA was extracted from HPV18 genome containing HFKs grown to the indicated passages, prior to digestion with either *Eco*RI or *Bgl*II to analyse the physical status of the HPV genome. OC: open circle. L: linear. SC: supercoiled. Southern blotting was performed by Mr Dhananjay Evans, PhD student. The molecular weight (kilobase) is indicated on the left.

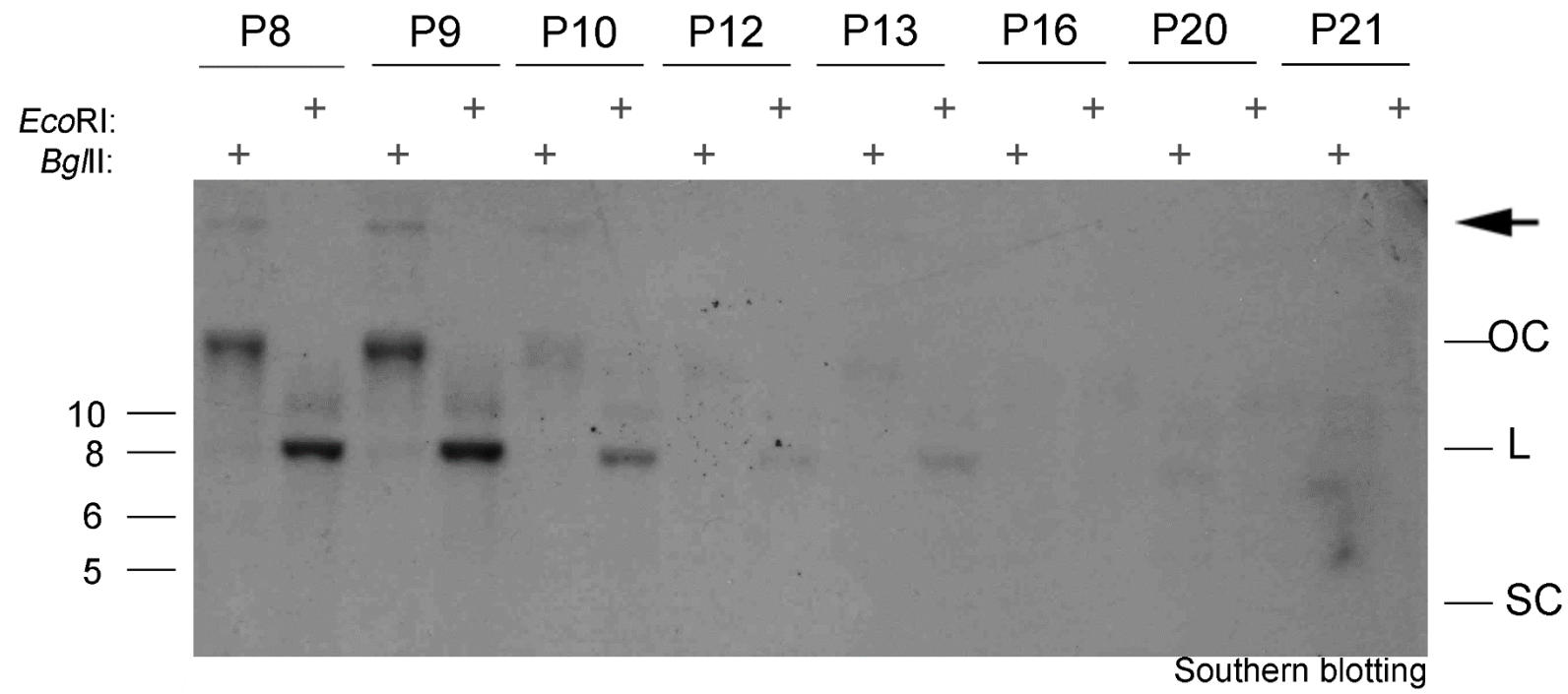

Figure 3.8: Detection of HPV18 genome status by Southern blotting in donor two BRET series. DNA was extracted from HPV18 genome containing HFKs grown to the indicated passages, prior to digestion with either *Eco*RI or *Bgl*II to analyse the physical status of the HPV genome. OC: open circle. L: linear. SC: supercoiled. Southern blotting was carried out by Mr Dhananjay Evans, PhD student. The molecular weight (kilobase) is indicated on the left.

3.2.7 HPV18 genome containing cells display increased phosphorylation of PKA substrates

To correlate the increased activity of the PKA-RII and cAMP sensors with activation of the PKA pathway, lysates derived from HFK or HFK-18 cells were examined for expression of phosphorylated PKA substrates. This antibody detects proteins that contain a phosphorylated serine or threonine with arginine residues at positions -3 and -2 within the PKA recognition motif RRXS*/T*. **Figure 3.9** demonstrates that replication of HPV18 DNA is associated with increased phosphorylation of PKA substrates, with the black arrowheads in the figure representing substrates that are increased in expression in the HFK-18 cells. Interestingly, the increased expression of some of these substrates (for example, the bands at approximately 80, 46 and 25 kDa) were seen in lysates derived from both donors. Similar results were obtained using an independent antibody that detects proteins a phosphorylated serine or threonine residue with arginine at the -3 position (data not shown). Together, these data suggest that the virus induces phosphorylation of a common set of PKA substrates during viral replication, although the exact identity of these substrates cannot be identified from these blots alone.

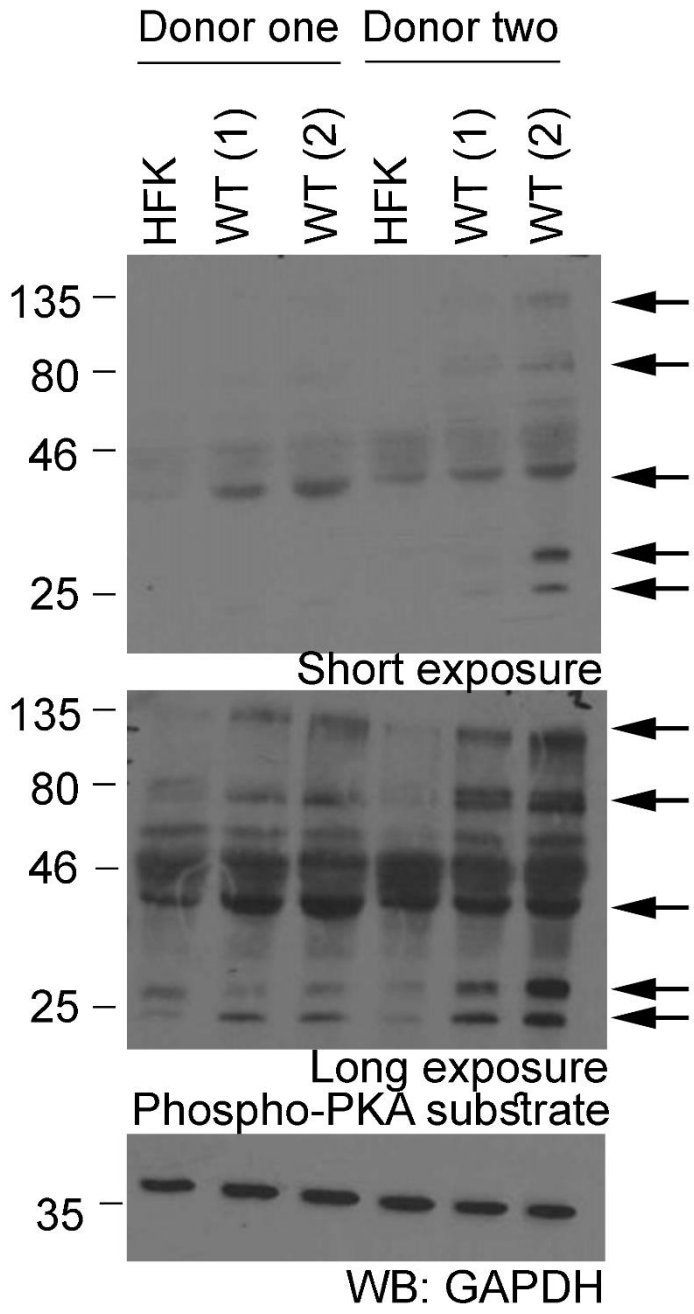

Figure 3.9: Increased expression of phosphorylated PKA substrates in HFK cells maintaining HPV18 genome. Lysates from donor matched HFK or HFK-18 cells were probed for expression of phosphorylated PKA substrates using an antibody that detects phosphorylated serine or threonine residues within the consensus PKA recognition sequence. Note that WT(1) and WT(2) represent independently prepared HFK-18 lysates. Arrowheads represent increased phosphorylated substrates in HFK-18 cells.

3.2.8 PKA-RI and -RII subunit expression in HFK-18 cells

As discussed in section 1.3.6 in the introduction to this thesis, the main function of the PKA regulatory subunits is to inhibit the activation of the catalytic subunits. This has been best exemplified by patients with Carney Complex, a multiple neuroendocrine tumour disease state featuring inactivating mutations in the gene encoding PKA-RI (*PRKAR1A*), giving rise to upregulated PKA catalytic activity. Furthermore, loss of PKA-RI leads to upregulation of cyclin D1 expression, which is thought to contribute to tumour development (Nadella and Kirschner, 2005; Porter et al., 2001). On the other hand, PKA-RI expression is increased in various cancer cell lines and primary tumours where it is associated with poor prognosis, and knockdown of PKA-RI induces growth arrest, apoptosis and changes in cell morphology in cancer cell lines (Neary et al., 2004), suggesting dual roles for this regulatory subunit.

To understand whether the changes in PKA activity seen in the BRET experiments were due to changes in expression of the regulatory subunits, lysates were prepared directly from the 96 well plates used for BRET experiments and assayed for regulatory subunit protein expression. **Figure 3.10** shows that there is no change in expression of the PKA-RI subunit in the presence of the viral genome in either low or high passage cells, either unstimulated or stimulated with the cAMP elevating agent forskolin (indicated by +), compared to HFK cells. Expression of PKA-RII appeared to be increased in cells maintaining HPV18 genomes in cells grown both to low and high cell passages, compared to donor matched HFK cells; however, this was not reproducible in subsequent experiments. These data indicate that the presence of the HPV18 genome does not affect protein levels of the PKA-RI or -RII subunits.

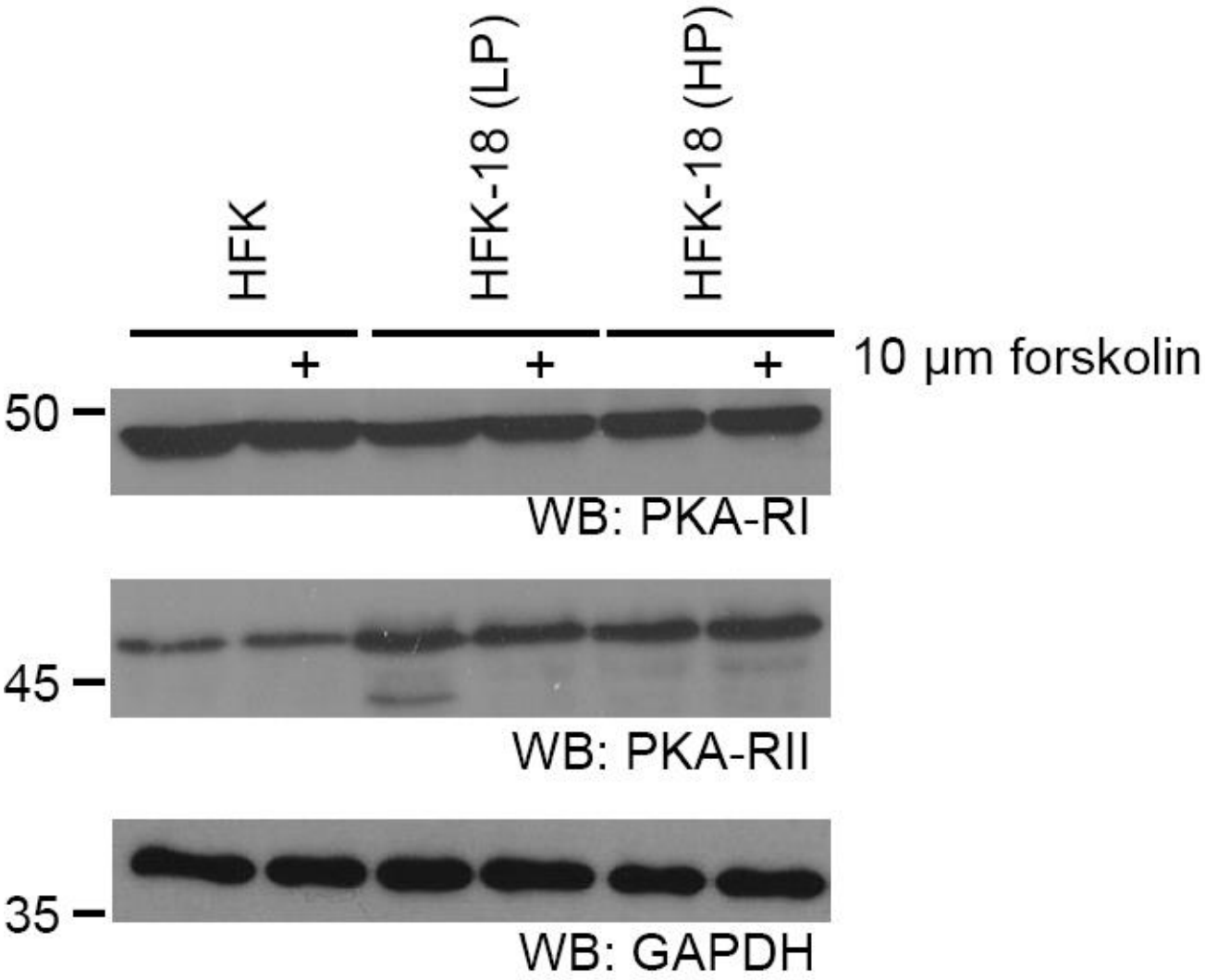

Figure 3.10: PKA-RI and -RII expression under both unstimulated and forskolin-stimulated conditions in cells grown to low or high cell passage. Lysates derived from foreskin donor one were examined for expression of PKA-RI and PKA-RII subunits under both unstimulated and forskolin-stimulated (indicated by +) conditions. Data representative of two independent experiments.

Next, to examine whether changes in localisation underpinned the observed changes in PKA sensor activity, the subcellular distribution of PKA-RI and -RII subunits was examined by immunofluorescence in HFK and HFK-18 cells. The data in **Figure 3.11** show that in HFK cells, localisation of PKA-RI is diffusely cytoplasmic with some areas of intense staining at the nuclear membrane (white arrowheads). In cells maintaining HPV18 genomes, there are no major differences in subcellular localisation of PKA-RI; staining is still diffusely cytoplasmic with an area of intense staining surrounding the nucleus (white arrowheads). For PKA-RII, staining is also diffusely cytoplasmic in HFK cells; however, some cells show increased signal adjacent to the nucleus that may represent association with the Golgi apparatus (red arrowheads; Dohrman *et al.*, 1996). In addition, several cells (indicated by white arrowheads) contain bright nuclear PKA-RI foci. In HFK-18 cells, there is no gross redistribution of PKA-RII; there are still bright PKA-RII nuclear foci and a bright signal adjacent to the nucleus, albeit this is less apparent in these cells. Although not quantified, the HFK-18 cells appear to contain more PKA-RII foci per nucleus.

These data revealed no gross redistribution of PKA regulatory subunits in cells maintaining HPV18 genomes compared to control HFK cells. There may be an increased number of PKA-RII foci per nucleus in cells containing HPV18 genomes, although this requires further investigation. It would be also prudent to examine using antibodies against the E1 and E2 proteins whether these increased nuclear foci represent viral replication factories (Swindle et al., 1999).

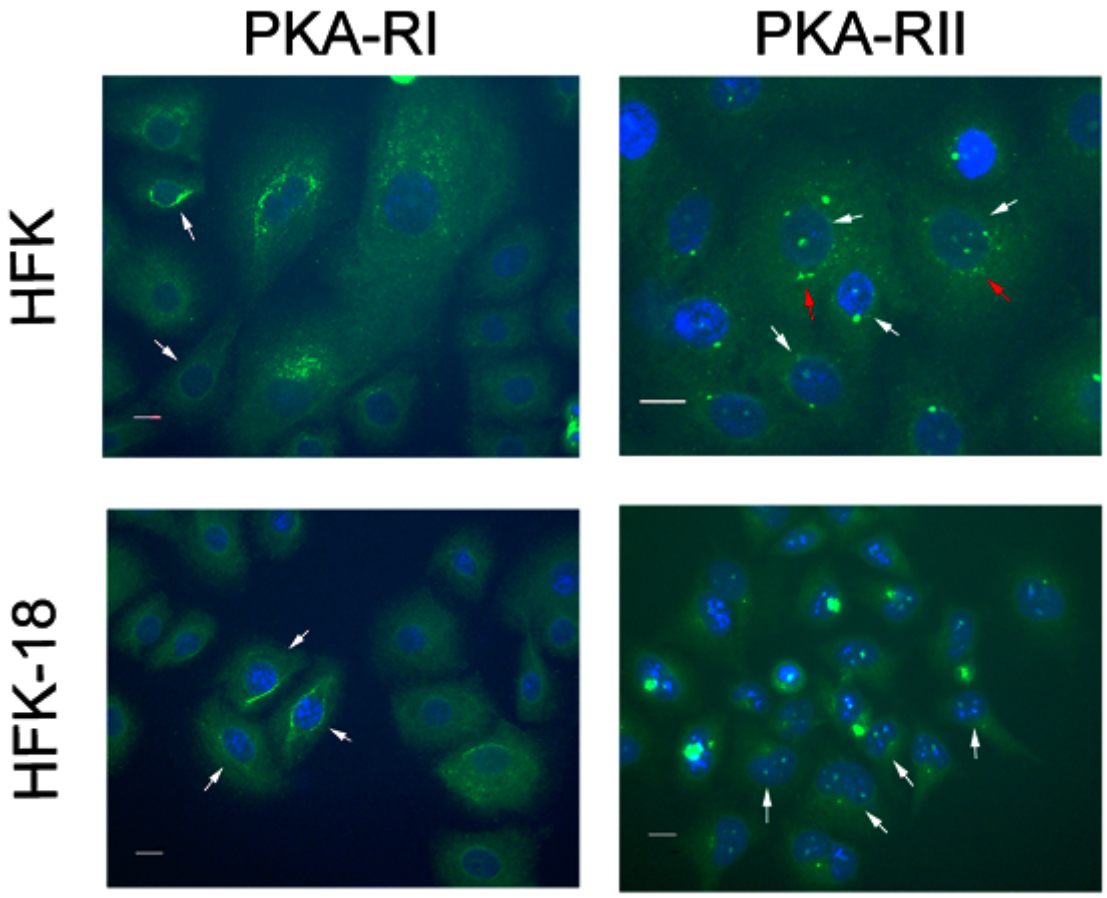

Figure 3.11: PKA-RI and -RII subcellular localisation in HFK and HFK-18 cells. HFK and HFK-18 cells were fixed as described in 4% paraformaldehyde and processed for indirect immunofluorescence using antibodies specific for PKA-RI or PKA-RII subunits. The nuclei are identified by DAPI staining. Scale bar: 10 µM.

3.2.9 HPV18 E5 regulates PKA-RI activity

To determine how HPV18 manipulates PKA activity, it was important to identify which of the HPV proteins were involved. Since other viruses have shown that manipulation of this pathway is often via the virus oncoproteins, the BRET assay was repeated in HPV negative C33A cervical cancer cells transfected with, either alone or in combination, E5, E6 or E7 expression vectors.

First, whether E6 or E7, alone or together, contributed to changes in PKA activity was examined. As illustrated in **Figure 3.12 A**, in the absence of cAMP stimulation, there were no significant changes in PKA or cAMP activity in cells expressing E6, E7 or E6E7, compared to empty vector control. Similarly, in **Figure 3.12 B**, in cells pre-treated with forskolin, there were no significant alterations in PKA or cAMP sensor activity in cells expressing E6, E7 or E6E7 compared to control cells.

Next, whether E5 contributed to PKA and/or cAMP activity was tested using a GFP-tagged E5 protein kindly provided by Dr Andrew Macdonald, University of Leeds. In **Figure 3.13 A**, there were no significant alterations in PKA or cAMP sensor activity in vehicle-treated cells expressing GFP-E5 compared to control cells expressing a GFP plasmid. Interestingly, however, when cells were pre-treated with forskolin (**Figure 3.13 B**), there was significant activation of the cAMP sensor (Control 0.12 ± 0.021 and E5 0.07 ± 0.01, $p=0.01$). In addition, the activity of PKA-RI was also significantly increased (Control 0.08 ± 0.01 and E5 0.05 ± 0.01, $p=0.04$) but without any concomitant change in PKA-RII sensor activity. These data suggest that E5 is able to selectively modulate PKA-RI via cAMP.

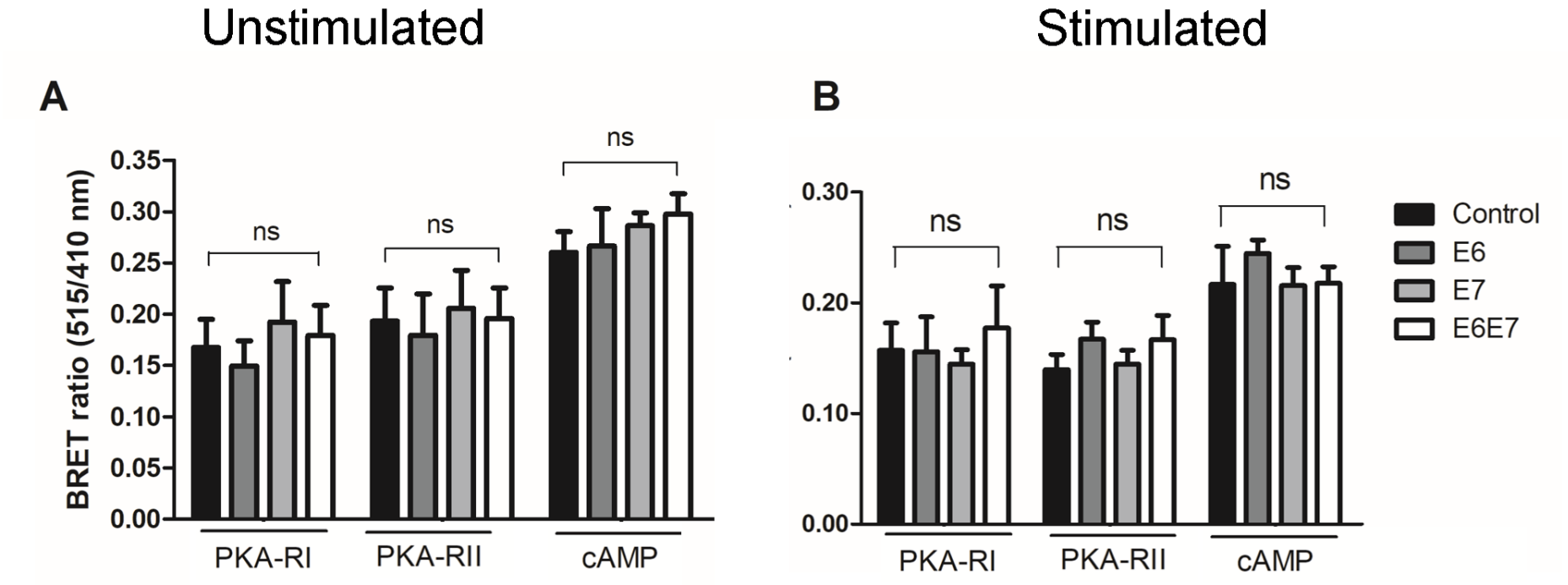

Figure 3.12: HPV18 E6 and E7 do not regulate PKA activity. C33A cells were transfected with empty vector (control), E6, E7 or E6E7 expression plasmids, as indicated, as well as BRET biosensors. The activity of these biosensors was determined 48 hours later by bioluminescent resonance energy transfer in the absence (unstimulated) or presence (stimulated) of the cAMP elevating agent forskolin. Data ±SEM taken from three independent experiments. Statistical significance was determined using the Student's t-test; ns indicates non-significance at a cut off of p=0.05.

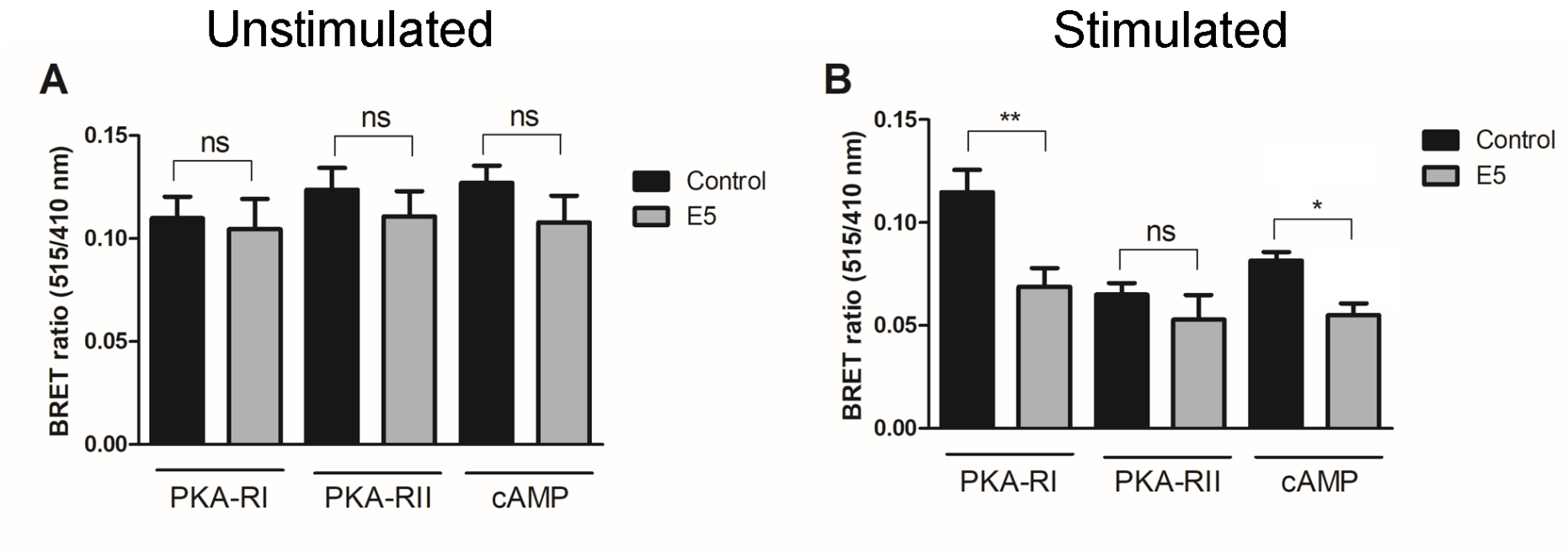

Figure 3.13: HPV18 E5 regulates cAMP concentration and PKA-RI activity. C33A cells were transfected with GFP or GFP-E5 expression vectors, as indicated, as well as BRET biosensors. The activity of these biosensors was determined 48 hours later by bioluminescent resonance energy transfer in the absence (unstimulated) or presence (stimulated) of the cAMP elevating agent forskolin. Data ±SEM taken from three independent experiments. Statistical significance was determined by Student's t-test comparing E5-expressing cells to control cells where ns indicates a non-significant result at the cut off of $p=0.05$, * denotes $p<0.05$ and ** denotes $p<0.01$.

3.2.10 HPV18 E5 regulates PKA-RI-induced cAMP response element-luciferase activity

It was next of interest to determine whether the E5 associated increases in cAMP and PKA-RI sensor activity seen in the BRET assay were functionally relevant. For this, the activity of a CRE-luciferase reporter was measured in C33A cells expressing GFP or GFP-E5 alongside the different PKA subunits (RI, RII, Cα) under both vehicle and forskolin-treated conditions. This reporter contains the firefly luciferase gene under the control of a multimerised CRE located upstream of a minimal promoter. Elevation of intracellular cAMP results in CREB binding CRE, leading to luciferase expression (Lazzeroni et al., 2013).

First, the induction of the CRE-reporter was examined in C33A cells treated either with vehicle or forskolin to ensure that the sensor responds to changes in cAMP. These data (**Figure 3.14**) show that addition of forskolin was associated with an approximate 140-fold increase in CRE-luciferase sensor activity relative to unstimulated cells, indicating that the sensor responds to forskolin-stimulated induction of cAMP. The large error bars under stimulated conditions likely represent the wide variation in CRE-luciferase activity recorded in these cells.

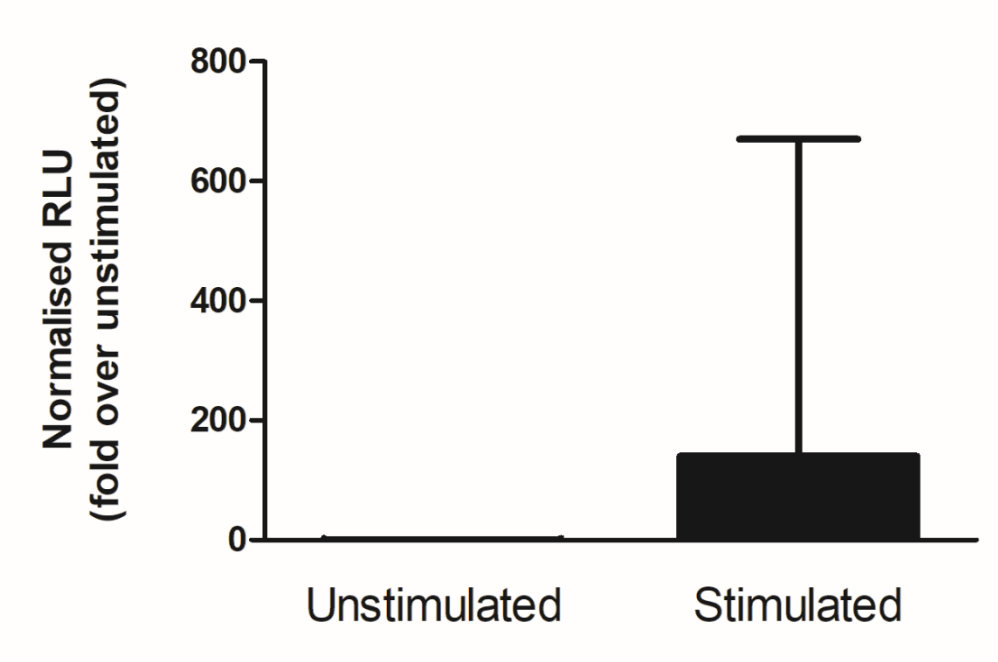

Figure 3.14: Stimulation of CRE-luciferase activity in forskolin-stimulated C33A cells. C33A cells were transfected with a CRE-luciferase expression plasmid and, after 48 hours, were treated with vehicle (unstimulated) or forskolin (stimulated) and assayed for CRE-luciferase activity by luciferase assay. Data normalised to corresponding untransfected cells. RLU: relative luciferase units.

In **Figure 3.15 A**, in vehicle-treated cultures, transfection of the RI regulatory unit did not strongly induce luciferase expression (~19-fold over untransfected (UT) cells), but co-transfection of the complete PKA-RI holoenzyme (PKA-RI and Cα) resulted in an approximate 800-fold increase in luciferase expression compared to UT cells. Transfection of the catalytic subunit alone (Cα) resulted in an ~250-fold increase in luciferase expression. Transfection of the RII regulatory unit alone or the complete PKA-RII holoenzyme (PKA-RII and Cα) did not strongly induce luciferase expression (all <30-fold compared to UT cells). Similarly, expression of E5 alone did not result in significant activation of the CRE-luciferase sensor (~10-fold compared to UT). Interestingly, co-expression of E5 with either the complete PKA-RI holoenzyme or Cα alone resulted in a significant decrease of luciferase expression to 150-fold and 52-fold over UT, respectively, which equates to about an 80% repression (PKA-RI and Cα 791-fold over UT, E5, PKA-RI, Cα 150-fold over UT; Cα 251-fold over UT and E5, Cα 52-fold over UT). There was no effect on the activity of the CRE reporter in the presence of the other PKA subunits, suggesting a specific impact of E5 on the PKA-RI holoenzyme.

Similar results were obtained in cells pre-treated with forskolin, albeit the magnitude of luciferase expression was much greater in these cells, as expected (**Figure 3.15 B**). In these experiments, co-transfection of the complete PKA-RI holoenzyme resulted in an approximate 4600-fold induction of luciferase expression over UT cells, which was heavily repressed to ~1300-fold over UT in cells expressing E5 (~70% repression). In addition, expression of Cα alone resulted in ~1700-fold induction of luciferase expression, which decreased to ~250-fold when expressed with E5 (~85% repression). All other transfections produced comparatively little luminescent signal of <250-fold of UT levels.

Together, these data show that E5 negatively regulates the ability of PKA-RI and Cα to activate the CRE-luciferase reporter.

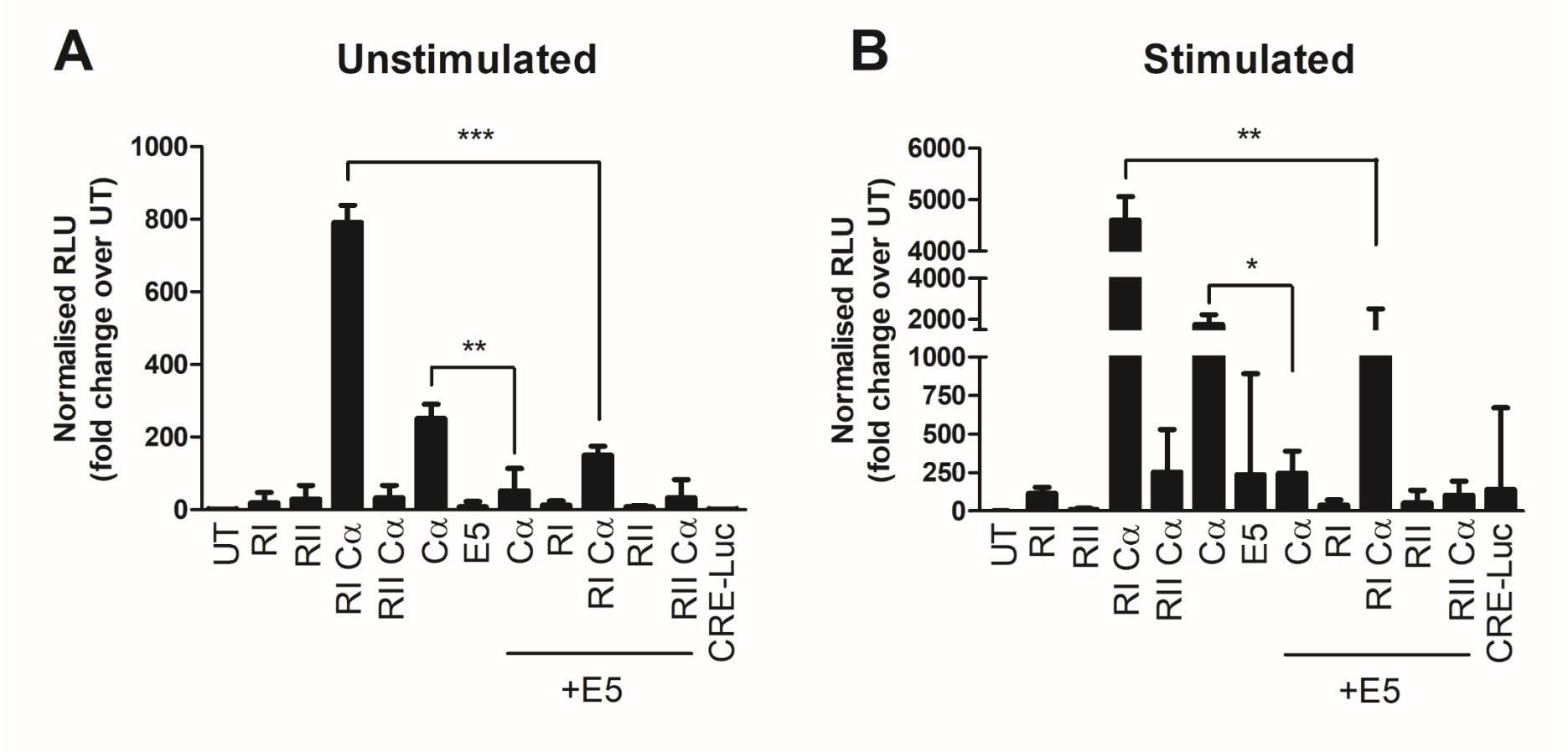

Figure 3.15: HPV18 E5 regulates PKA-RI and Cα dependent CRE-luciferase transcription. C33A cells transfected with the indicated expression vectors alongside CRE-luciferase DNA were assayed for luminescence 48 hours post-transfection in the absence (panel A: unstimulated) or presence (panel B: stimulated) of the cAMP elevating agent forskolin. Data ±SEM taken from three independent experiments. UT: untransfected. RI: PKA-RI. RII: PKA-RII. Cα: PKA-Cα. CRE-Luc: CRE-luciferase. Statistical significance was determined using the Student's t-test between the indicated conditions where * denotes $p<0.05$, ** denotes $p<0.01$ and *** denotes $p<0.001$.

3.3 Discussion

The ability of HPV to modulate host signalling pathways during infection is critical for the viral life cycle as it provides an environment conducive to viral DNA replication. The host pathway mediated by the cAMP-dependent PKA is an important regulator of multiple aspects of the virus life cycle, including regulation of oncoprotein function (see section 1.3.11). For example, PKA phosphorylation of the E6 PBM negatively regulates its interactions with cellular PDZ domain-containing proteins, whilst allowing for interactions with proteins that only recognise the phosphorylated form of the E6 PDZ, such as 14-3-3 family members. In addition, changes in PKA signalling may also be important for the oncogenic progression of HPV infections; loss of PKA recognition of E6 in an HPV18 life cycle model is associated with increased growth of HPV genome containing cells and a more hyperproliferative phenotype on raft culture. In addition, loss of kinase recognition is associated with enhanced morphological transformation of keratinocytes.

Details of whether the virus can manipulate the activity of this pathway directly during its infectious cycle, which may be of relevance for viral replication, are lacking. In this chapter, cAMP and PKA signalling dynamics were investigated in HPV18 life cycle models established in immortalised (NIKS) and primary epidermal keratinocytes harbouring complete HPV genomes.

Using genetically encoded cAMP and PKA biosensors in immortalised and primary cells harbouring HPV18 genomes, the presence of the viral genome as an episome (unintegrated) was consistently associated with increased levels of cAMP, as measured by increased activity of the EPAC biosensor, as well as increases in PKA-RII activity. Notably, these changes were consistent between the two life cycle models and between

different primary keratinocyte donors, suggesting a physiologically relevant effect. Changes were also observed for PKA-RI but these were far less marked and not always consistent between the models or between foreskin donors. In accordance with the BRET results, we also detected an increased number of phosphorylated PKA substrates in HFK cells maintaining HPV18 genomes in two donor backgrounds, suggesting that the BRET assay results are indicative of *in vivo* phosphorylation events. This is the first demonstration to our knowledge of changes in PKA signalling activity in a physiological model of the HPV18 infectious cycle.

Furthermore, in the HPV18 model based in primary keratinocytes, grown to a higher cell passage, viral episomes were severely reduced and most likely the viral DNA had integrated. Experience from the Roberts laboratory and others have shown that upon extended cell culture wild type HPV18 genomes can eventually integrate, mimicking a viral mechanism in oncogenic progression. Integration leads to increased levels of E6 and E7 and often the loss of expression of other viral factors, such as E2. In these cells, BRET assays showed retention of increased cAMP signalling and PKA-RII activity, although the magnitude of these changes was not as great as the low passage cells.

Microarray profiling in cells overexpressing PKA-RI or -RII subunits showed that these regulatory units dictated the balance between cellular proliferation and differentiation, with PKA-RI overexpression upregulating the expression of genes associated with cell growth and -RII with differentiation (Cheadle et al., 2008). It would, therefore, be interesting to examine PKA and cAMP signalling dynamics upon activation of the productive cycle of the virus by keratinocyte differentiation.

The functional consequence of this increased PKA activity is not yet clear so future experiments should concern themselves with identifying differentially phosphorylated

PKA substrates in HFK versus HFK-18 cells. For example, using antibodies directed against phosphorylated PKA substrates to co-immunoprecipitate PKA phosphoproteins from cell lysates, mass spectrometry approaches such as liquid chromatography-tandem mass spectrometry combined with titanium dioxide enrichment of phosphoproteins will likely provide a starting point to unravel the HPV phosphoproteome (Hamaguchi et al., 2015; Imamura et al., 2017). As HPV is known to induce the phosphorylation of various cellular proteins, such as those involved in DNA damage response signalling and cell communication networks (e.g. STATs), during its life cycle, these experiments will be important for the further identification of host proteins required for the HPV infectious cycle.

Unpublished data from the Roberts' laboratory has shown that there is selective downregulation of PKA-RI, but not PKA-RII, subunits in HeLa cervical cancer cells, (McCormack, Roberts, unpublished data). Changes in PKA-RI subunit expression are seen in individuals with the neuroendocrine tumour condition, the Carney Complex, which features inactivating mutations in *PKA-RI*, leading to dysregulated PKA signalling and tumour development. In addition, RI null mouse embryonic fibroblasts show constitutive PKA activity and become immortalised in a manner that appears to be dependent on upregulation of D-type cyclins (Kirschner et al., 2000; Nadella and Kirschner, 2005). Thus, changes in PKA-RI expression may be relevant for the progression of HPV infections or maintenance of the transformed phenotype. Consistent with the constitutive upregulation of PKA activity in cells lacking PKA-RI, BRET data in HeLa cells showed a dramatic increase in PKA and cAMP sensor activity compared to both primary HFKs and those containing HPV18 genomes (McCormack, MRes thesis). Together, these data suggest that

the virus differentially interacts with the PKA pathway at certain stages of the virus life cycle.

To understand whether HPV oncoproteins were contributing to the changes in PKA and cAMP activity, the BRET assay was repeated in cells expressing the viral oncoproteins E5, E6 or E7, either alone or in combination. Although overexpression of one or two viral oncoproteins is unlikely to faithfully recapitulate the situation in cells containing the complete viral genome, it was interesting to note that E5 expression increased the activity of both cAMP and PKA-RI biosensors, without any noticeable change in PKA-RII activity. There were no noticeable changes in cells expressing E6 or E7, either alone or in combination. While the effect of transfecting all of the viral oncoproteins, alone or in combination, into cells was not examined due to time constraints, it may be that the full repertoire of viral oncoproteins (or at least alternative combinations than those examined here) is required to phenocopy the results observed in cells maintaining the whole viral genome. The fact we did not observe the same PKA activation pattern during these overexpression experiments may suggest that this is the case.

An alternative explanation is that these overexpression experiments do not recapitulate the proper timing of oncoprotein expression during *in vivo* viral replication or the functional interactions that occur between viral proteins. For example, there is evidence that E5 interacts with E6 and E7 functions by enhancing cell proliferation and immortalisation of keratinocytes, raising the possibility that functional interactions between the viral oncoproteins are relevant for how the virus interacts with host cells (reviewed in Müller et al., 2015). Furthermore, these experiments were done in HPV negative cancer cells that were already transformed and may therefore not respond to changes in PKA signalling in the same manner as primary keratinocytes. Overexpression of the viral oncoproteins in

primary human keratinocytes, therefore, would likely determine the identity of the viral protein responsible for the alterations in PKA signalling seen in this chapter.

Although the results presented here are in contrast to previously published reports of higher basal cAMP levels in cells expressing HPV16 E5 (Oh et al., 2009), the BRET results following forskolin stimulation are consistent with the ability of E5 to increase cAMP levels compared to control cells. At present, there is no literature comparing cAMP production in cells expressing HPV16 and HPV18 E5, so we cannot exclude that these results represent an important difference in HPV biology or may have arisen due to differences in experimental methods. Nevertheless, the finding that E5 leads to increased cAMP concentrations and PKA-RI activity in forskolin-stimulated cells indicates that the virus is able to modulate cAMP signalling with a bearing on PKA activation in C33A cells.

PKA is the main downstream mediator of cAMP gene regulation responses in mammalian cells. In this process, the binding of cAMP to PKA results in kinase activation, with subsequent liberation of PKA catalytic subunits. These subunits then translocate to the nucleus and phosphorylate target proteins such as the transcription factor CREB at serine-133. Phospho-CREB recruits the transcriptional coactivator CREB-binding protein/p300 to cyclic response elements on target genes, which modify gene expression by regulating chromatin and interacting with various proteins of the general transcriptional machinery (Chrivia et al., 1993; Della Fazia et al., 1997; Gonzalez and Montminy, 1989).

To understand whether E5 can regulate this process by modulating cAMP and PKA-RI activity, the activity of a CRE-luciferase reporter was assessed in cells expressing E5 together with the various PKA subunits. These experiments showed that in both vehicle and forskolin-treated C33A cells, the complete PKA-RI holoenzyme, and to a lesser extent the catalytic subunit alone, is required for activation of the CRE-luciferase reporter.

Furthermore, this luciferase signal was heavily repressed in cells expressing HPV18 E5, suggesting that E5 negatively regulates PKA-RI-dependent activation of CRE-luciferase transcription. The fact that this result occurred under both vehicle and forskolin treatment conditions was unexpected given that no significant changes in cAMP or PKA-RI activity were seen in vehicle-treated E5-expressing cells in the BRET assay, although this may reflect differences in sensitivity between the two assays.

Intriguingly, these data do not agree with a previous report that suggested E5 drives CRE-luciferase expression in C33A cells in a PKA and CREB dependent manner, although that study used a variant CRE sequence (CGTCA) derived from the EP4 promoter (Oh et al., 2009). In fact, using a CRE-luciferase construct that contains the canonical CRE sequence (TGACGTCA), the data described in this thesis showed that E5 clearly has the opposite effect and can suppress PKA-dependent CRE-luciferase transcription. How this occurs is unclear. One would imagine that if E5 increases cAMP and in doing so activates PKA then the downstream effect would be further activation of CRE-luciferase expression in E5-expressing cells compared to control, rather than a significant repression of luminescent signal.

The data in this chapter add to the growing knowledge of HPV18 E5 biology. As described in section 1.2.4, data from an HPV18 life cycle model established in primary HFKs showed that loss of E5 had no detectable effect in basal keratinocytes; however, there was a significant impact in suprabasal cells. In these cells, E5 contributed to cell cycle progression and unscheduled host DNA synthesis in suprabasal cells, correlating with activation of EGFR in these cells. There was no impact of loss of E5 on viral genome amplification nor late protein expression with keratinocyte differentiation. The same study showed that this E5 driven EGFR activity regulated keratinocyte differentiation through

modulation of KGFR signalling. Accordingly, blockade of KGFR rescued the differentiation phenotype associated with loss of E5 expression (Wasson et al., 2017).

To establish the functional consequence of E5-mediated regulation of PKA-RI activity, future experiments using cAMP antagonists to selectively inhibit PKA-RI signalling (e.g. Rp-8-Br-cAMPS) in HFKs containing wild type and E5 knockout viral genomes would provide insight into the importance of this novel E5-host interaction. These experiments could include analysis of the impact of PKA-RI signalling on known E5 cellular functions (such as examination of suprabasal cell cycle re-entry and host DNA synthesis) as well as gene expression profiling to identify genes downstream of E5 and PKA-RI that may act as novel regulators of the HPV18 life cycle.

Overall, the data presented in this chapter showed that HPV18 replication in model systems established in primary and immortalised keratinocytes demonstrated marked changes in PKA-RII and cAMP signalling, which was associated with increased phosphorylation of PKA substrates. These changes were not due to overt changes in changes in expression or localisation of the PKA regulatory subunits. Furthermore, overexpression experiments in HPV negative cervical cancer cells (C33A cells) showed that HPV18 E5 induced PKA-RI and cAMP sensor activity. Initial functional analysis of this interaction using a CRE-luciferase reporter showed that E5 negatively regulated the ability of the complete PKA-RI holoenzyme to activate CRE-luciferase transcription. Future experiments using specific PKA-RI inhibitors in HFK cells maintaining wild type and E5 knockout genomes will likely provide information as to the functional consequence of this interaction.

CHAPTER 4 INTERACTION OF HPV18 E6 AND A-KINASE ANCHORING PROTEIN 95

4.1 Introduction

The data presented in the previous chapter demonstrated that PKA activity was modulated in human keratinocytes that both maintain HPV18 genomes and support the productive virus life cycle upon differentiation. In addition, PKA activity is also altered in HPV18 positive HeLa cervical cancer cells, which harbour integrated forms of the viral genome. Notably, the changes in PKA activity occurred concomitantly with changes in cellular cAMP concentration.

The downstream effects of cAMP signalling are finely tuned by the actions of AKAPs, cellular proteins that assemble PKA and other effector proteins to discrete cellular microdomains, forming multiprotein scaffolds that action cAMP signalling. The first indication that cAMP signalling undergoes such organisation came from Hayes and colleagues who showed that a number of GPCR activators elevated cAMP to similar levels but produced distinct cellular responses (Hayes et al., 1980). This was underscored by work where FRET-based sensors targeted to different subcellular locales displayed different responses to cAMP elevating agents, suggesting that cAMP responses were spatiotemporally regulated in cells (Di Benedetto et al., 2008; Zaccolo et al., 2000). In these cellular compartments, cAMP is actioned upon by either PKA-RI or -RII holoenzymes where each PKA isoform phosphorylates a discrete set of substrates (Wong and Scott, 2004; Zaccolo and Pozzan, 2002). While the vast majority of AKAPs

preferentially bind to RII subunits, there is a growing list of AKAPs that bind to RI, and some that are dual specific (reviewed in Torres-Quesada et al., 2017).

In addition to PKA, the macromolecular scaffold structures organised by AKAPs contain a variety of other proteins, including other protein kinases, PDEs that degrade the cAMP signal, and protein phosphatases that remove phosphate groups from phospho-substrates. Taken together, the AKAP based scaffolds direct PKA to its substrates and convey tight spatiotemporal control to cAMP signalling (Langeberg and Scott, 2015).

In order to successfully propagate in squamous epithelium, HPV interacts with and modulates many signalling pathways to create an environment conducive for viral replication. Modulation of the signal transduction pathway is often through an association between an HPV protein and a factor in the pathway and can involve either inhibition of a pathway (e.g. STAT-1; Hong et al., 2011), or activation (e.g. ATM; Moody and Laimins, 2009). Therefore, one approach taken to investigate further the interaction between HPV and PKA signalling was to determine whether the virus interacted with any of the components of the signal transduction pathway. This investigation identified a novel interaction between HPV18 E6 and the nuclear PKA-anchoring protein AKAP95.

4.2 Results

4.2.1 AKAP95 may be a conserved E6 target

Given that HPV18 modulates PKA activity and this is concomitant with changes in cAMP levels, we were interested to see if the virus interacted with other components of the PKA pathway. To examine this possibility, published mass spectroscopy databases of HPV protein-interacting partners were scrutinised for PKA pathway components. These databases included host interactions with diverse E2 (Muller et al., 2012), E6 (Gulbahce et

al., 2012; Rozenblatt-Rosen et al., 2012; White et al., 2012a) and E7 proteins (White et al., 2012b), as well as the online VirHostNet and virusMINT databases (Cesareni et al., 2002; Navratil et al., 2009).

While the regulatory or catalytic subunits of PKA were not represented in this mass spectroscopy analysis, a potential interaction between E6 and the nuclear PKA-anchoring protein AKAP95 was found for alpha-HPV types 18, 45 and 52 – all defined as group 1 carcinogens by IARC (**Table 4.1).** Interestingly, these data did not suggest a potential interaction of E6 and AKAP95 between other high-risk alpha-types tested (HPV16 and HPV33), even when complexes were analysed in the presence of the proteasome inhibitor MG132. A separate mass spectroscopic screen suggested that HPV16 E7 may bind to AKAP95, which may indicate that there are type-specific differences in AKAP95 binding (**Table 4.1**). AKAP95 was not found in complexes containing the low-risk alpha type HPV6. However, several E6 proteins from beta-HPV types were included in the mass spectroscopic analysis and the E6 proteins of HPV17a and HPV38, both types linked to causing non-melanoma cutaneous malignancies, were complexed with AKAP95. Together, the mass spectroscopic analyses suggest that E6 from diverse HPV types may bind to AKAP95, including HPV18.

4.2.2 Optimisation of GST-AKAP95 purification

To investigate whether AKAP95 was a novel interacting partner of HPV18 E6, it was first expressed recombinantly as a GST fusion protein. Full-length human AKAP95 cloned into pGEX-KG was a kind gift of Professor Kjetil Tasken, University of Oslo, and transformed into BL21 competent *E. coli* cells. A small-scale (~10 ml) pilot experiment was first carried out to test induction of GST-AKAP95 upon addition of IPTG. After induction at 37°C for three hours, a band corresponding to the calculated molecular weight of

GST-AKAP95 (131 kDa) can be seen on a Coomassie-stained gel, indicating successful induction of GST-AKAP95 **(Figure 4.1)**

HPV protein	Genus	Species	HPV type(s)	Detected in vehicle control treated cells	Detected in MG132 treated cells	Reference	Clinical manifestations
E6	Alpha	7	18 45	Y	Y	White *et al*., 2012	High risk—malignant mucosal lesions
	Alpha	9	52	Y	Y	White *et al*., 2012	High risk—malignant mucosal lesions
	Beta	2	17a 38	Y	Y	White *et al*., 2012	Most frequently causing cutaneous lesions. Associated with EV.
E7	Alpha	9	17	NA	NA	Gulbache *et al*., 2012	High risk—malignant mucosal lesions

Table 4.1: AKAP95 may be a common binding partner of E6 proteins from diverse HPV types. Scrutiny of published E6-mass spectroscopic databases identifies AKAP95 as a potential binding partner. AKAP95 binders are shown. Non-AKAP95 binders include E6 from HPV types 16, 33, 6b, 2a, 57, 8, 20, 25, 98, 76, 92. Data taken from the indicated sources. EV: epidermodysplasia verruciformis.

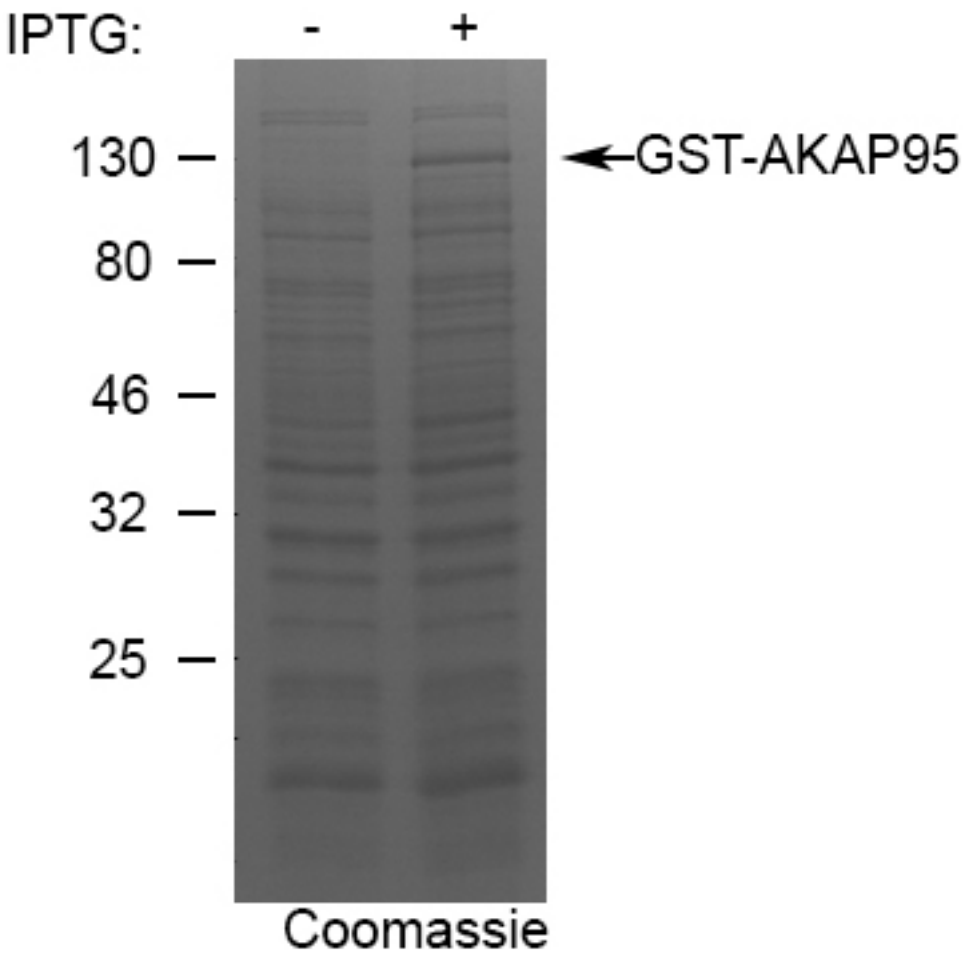

Figure 4.1: Induction of GST-AKAP95 by IPTG. Coomassie-stained SDS-PAGE gel of equal densities of *E.coli* transformed with a GST-AKAP95 plasmid before IPTG induction (-IPTG) and after IPTG induction for 3 hours (+IPTG). The position of GST-AKAP95 is marked by an arrow.

Having shown that GST-AKAP95 is expressed in *E. coli*, it was then necessary to define the purification conditions. Using a larger ~50 ml culture of *E. coli*, cells were lysed in PBS containing 2% Triton-X100 and insoluble material removed by high-speed centrifugation. Insoluble material was then solubilised directly in an equal volume of Laemmli buffer containing β-mercaptoethanol. The soluble fraction was incubated overnight with glutathione beads, washed, and then the fusion protein was eluted from the beads by sequential incubations in reduced glutathione. Equal volumes of all samples were examined for the presence of GST-AKAP95 by Coomassie staining. As shown in **Figure 4.2 A**, the addition of IPTG results in the production of a ~131 kDa band corresponding to the expected molecular weight of GST-AKAP95 and this is absent in the uninduced lane. After separation of soluble and insoluble fractions, GST-AKAP95 appeared in both fractions. Equal amounts of the reduced glutathione eluate were analysed for GST-AKAP95; however, no appreciable GST-AKAP95 could be seen on the Coomassie-stained gel.

Given the robust induction of GST-AKAP95 by IPTG, purification was then tested in a much larger one-litre culture of *E. coli* (**Figure 4.2 B**). Again, GST-AKAP95 was found in both soluble and insoluble fractions after lysis in PBS buffer containing 2% Triton-X100. This attempt resulted in appreciable levels of GST-AKAP95 on the Coomassie-stained gel, indicating that a larger bacterial culture was sufficient to purify recombinant AKAP95. Various other attempts were made to improve the yield of purified GST-AKAP95, such as varying incubation temperature and IPTG concentration; however, there were no marked increases in GST-AKAP95 yield. Different *E. coli* strains were also tested as AKAP95 contains codons not commonly used in *E. coli* (Rosano and Ceccarelli, 2009), however, this did not make a substantial improvement in GST-AKAP95 yield (data not shown).

For this reason, subsequent purifications were done using at least one-litre cultures of *E. coli*. Sonication times were also varied to improve the release of GST-AKAP95 from insoluble inclusion bodies but this often resulted in a lack of binding of GST-AKAP95 to the glutathione beads, possibly due to degradation of the fusion protein (data not shown).

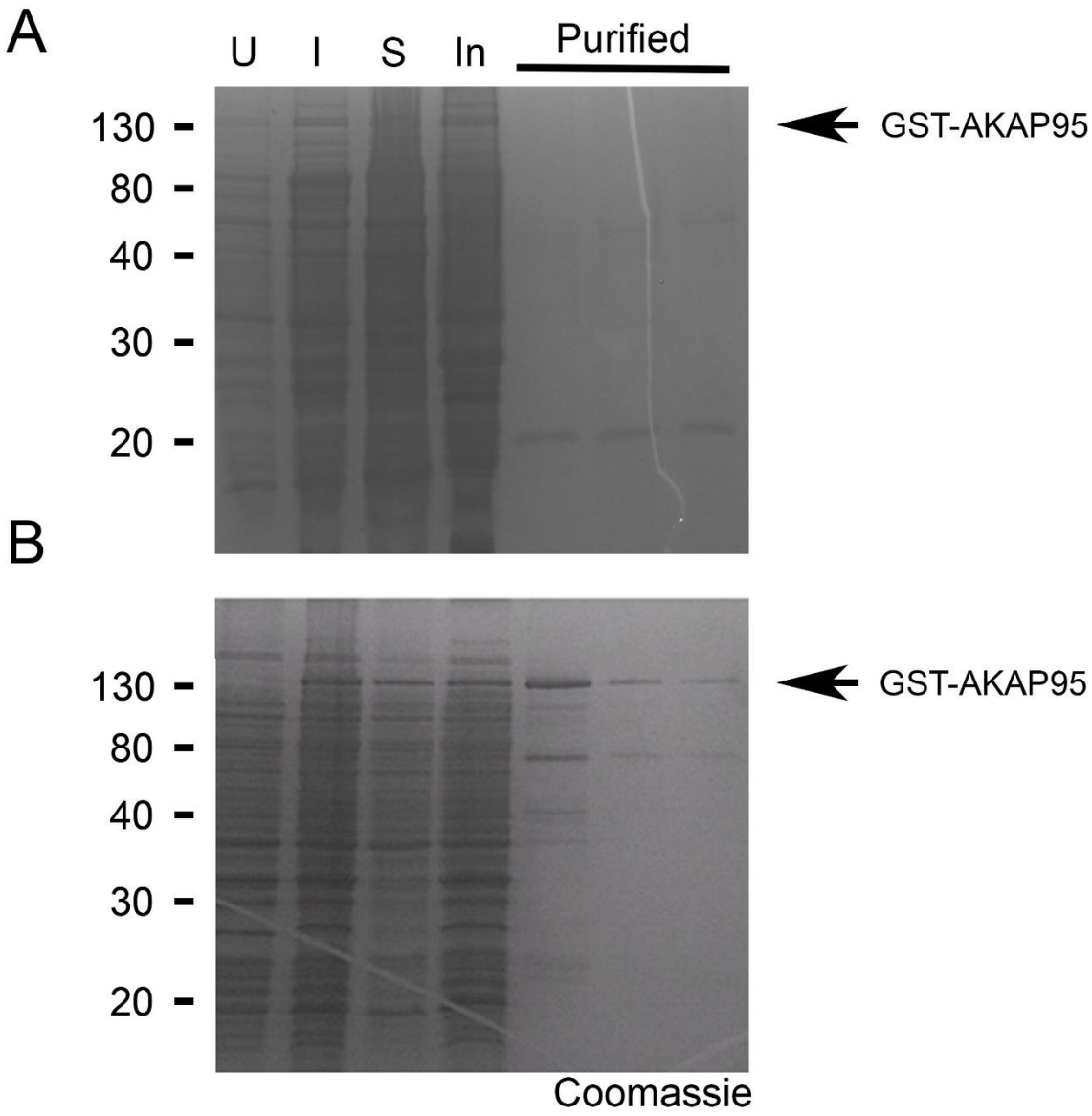

Figure 4.2: Optimisation of GST-AKAP95 purification from *E. coli*. Coomassie stained gel of lysates of BL21 *E. coli* expressing GST-AKAP95 induced with IPTG for three hours at 37° C and glutathione-purified eluates. **Panel A** represents 50 ml culture and **B** represents 1 L culture. GST-AKAP95 is marked by arrows. U: uninduced, I: induced; S: soluble, In: insoluble. Purified represents reduced glutathione eluate.

4.2.3 Optimisation of GST-HPV18 E6 purification

In order to perform GST-E6 pull-down assays, HPV18 E6 was expressed recombinantly as a GST fusion protein (GST-HPV18 E6). The complete coding sequence of HPV18 E6 was PCR amplified from the plasmid pGEM2-HPV18, which contains the whole HPV18 genome, and ligated into an appropriately prepared pGEX-2T vector to form pGST-HPV18 E6. BL21 *E. coli* cells were transformed with this plasmid and used to express the fusion protein.

When overexpressed in *E. coli*, recombinant E6 can be found in bacterial inclusion bodies, even when fused to GST or MBP tags, which often provide solubility to the fusion protein (Nominé et al., 2001, 2006; Verma et al., 2013). Indeed, GST-HPV18 E6 is insoluble in 1-2% Triton-X100, concentrations commonly used in GST protein purification (**Figure 4.3**). Initial attempts to solubilise GST-HPV18 E6 in 2% Triton-X100 involved lowering IPTG concentration and induction temperatures, heat shock prior to induction (Thomas and Baneyx, 1996), as well as the addition of ethanol to the broth, both of which mimic the heat shock response (Chhetri et al., 2015). However, these methods failed to significantly enhance the purification of soluble GST-HPV18 E6.

Recombinant HPV18 E6 in *E. coli* associates with bacterial membranes and/or inclusion bodies, which makes purification using traditional methods technically challenging (Miranda Thomas, personal communication). As an alternative method to improve protein extraction, cells were subjected to a sonication trial. Cells expressing GST-HPV18 E6 were lysed in 2% Triton-X100, sonicated at a fixed amplitude for various periods of time and then soluble extracts examined for GST-HPV18 E6. As shown in **Figure 4.4 A**, several short rounds of sonication were required to extract GST-HPV18 E6 (~46 kDa) from bacterial inclusion bodies. Longer sonication periods resulted in a failure of the

fusion protein to bind to the glutathione beads (data not shown). Therefore, several short periods (three rounds of 10 seconds) of sonication were used for future GST-E6 purifications.

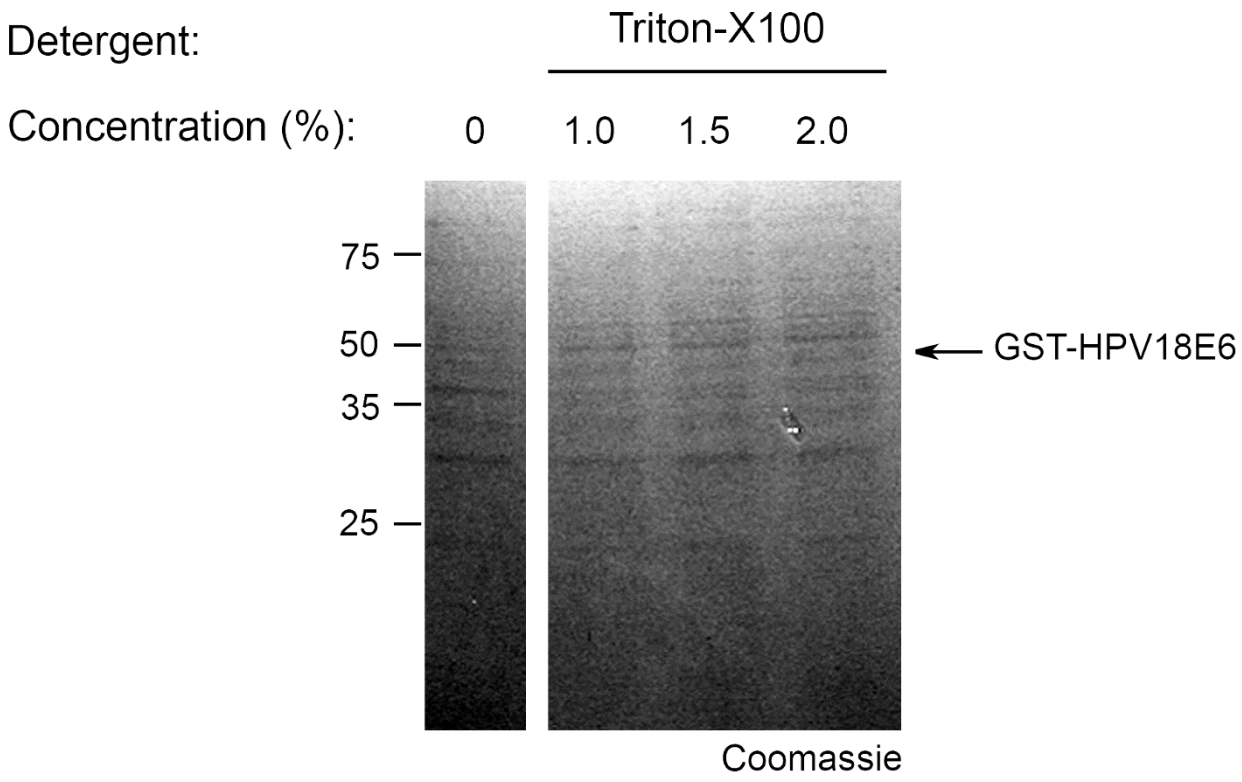

Figure 4.3: GST-HPV18 E6 is insoluble in PBS containing 2% Triton-X100. BL21 *E. coli* expressing GST-HPV18 E6 were grown in liquid culture before induction with IPTG for three hours at 37℃. Cells were harvested in PBS and Triton-X100 added to the indicated concentrations. After removal of insoluble material by centrifugation, equal volumes of soluble extracts were electrophoresed, and total protein stained by Coomassie. The position of GST-HPV18 E6 is shown by an arrowhead. Note this gel is a cropped image from **Figure 4.4.**

The ability of the detergent *n*-lauryl sarcosine (otherwise known as sarkosyl) to solubilise GST-HPV18 E6 was also investigated. Sarkosyl has been used to solubilise cysteine-rich ZF domain-containing proteins, such as E6, and is known to disrupt aggregates that are insoluble in NP-40 and Triton-X100 based buffers (Park et al., 2011; Tao et al., 2010). GST-HPV18 E6 was expressed in *E. coli* and lysed in PBS, before the addition of sarkosyl or Triton-X100 as indicated in **Figure 4.4 B**. The addition of up to 2% sarkosyl resulted in a greater amount of total solubilised protein, including GST-HPV18 E6, compared to Triton-X100, suggesting that this detergent could be used in purification. However, large-scale purification from a one-litre culture using sarkosyl was technically challenging due to the high viscosity of the lysate, likely due to the efficient release of *E. coli* DNA. As substantial amounts of DNase and lengthy sonication times were required to reduce this viscosity to workable levels, it was preferable to extract GST-HPV18 E6 by sonication in a 2% Triton-X100 based buffer as this provided sufficient recombinant protein for GST pull-down assays. Taken together, these experiments have refined the purification protocol for GST-HPV18 E6.

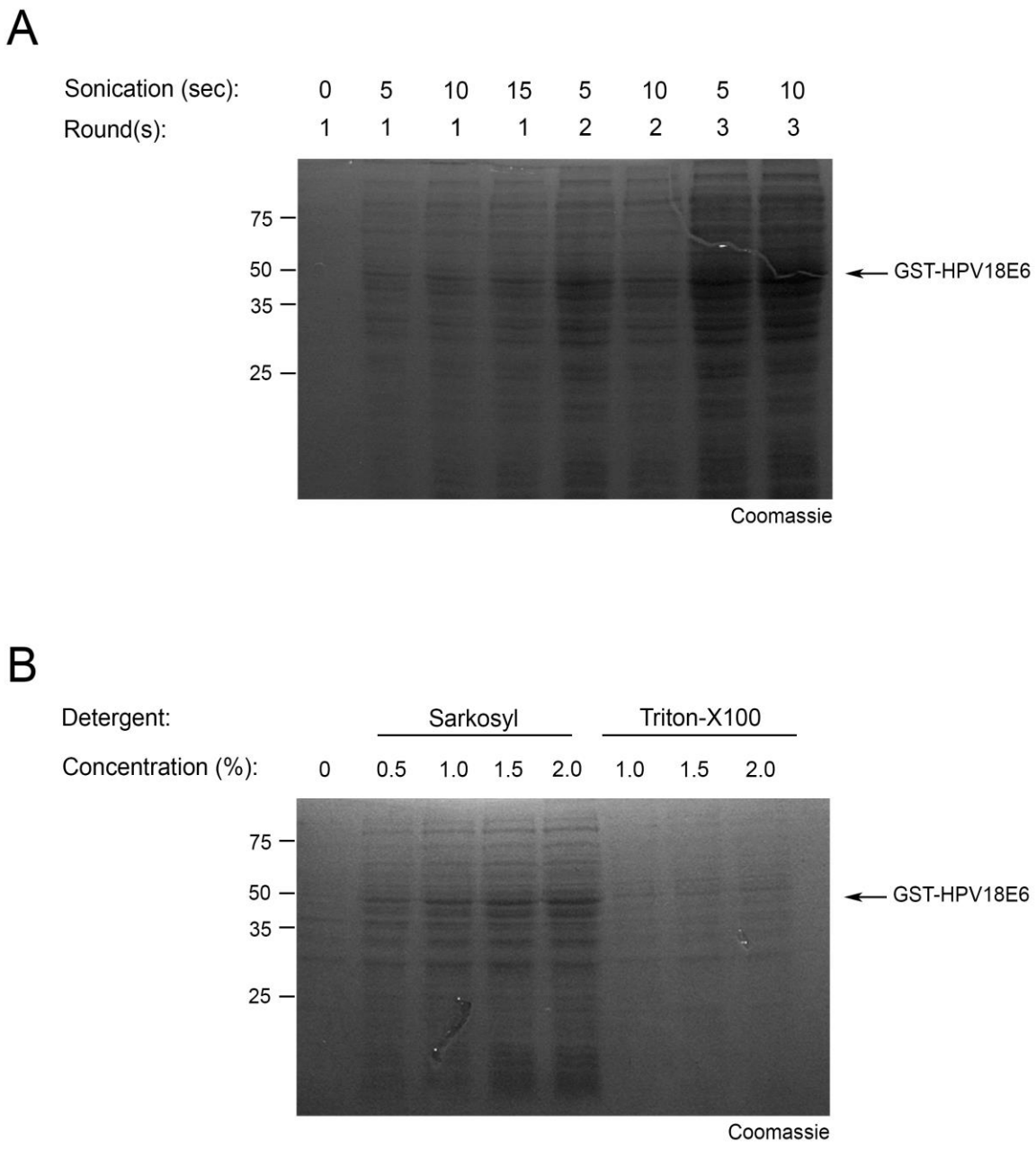

Figure 4.4: Optimisation of sonication and detergent extraction of GST-HPV18 E6. BL21 *E. coli* expressing GST-HPV18 E6 were grown in liquid culture before induction with IPTG for three hours at 37℃. **Panel A**: Cells were harvested in PBS buffer containing 2% Triton-X100, before sonication as indicated. Soluble extracts were examined for GST-HPV18 E6. **B:** Cells were harvested in PBS and the indicated detergent was added to the final concentrations shown. After removal of insoluble material, equal volumes of soluble extracts were electrophoresed and total protein stained by Coomassie. The position of GST-HPV18 E6 is shown.

4.2.4 Expression of GST-AKAP95 and GST-HPV18 E6

To verify the binding of HPV18 E6 to AKAP95, both proteins were expressed as GST-fusion proteins and purified on glutathione Sepharose™ beads using the optimised protocols outlined in sections 4.2.2 and 4.2.3. Both GST-AKAP95 and GST-HPV18 E6 migrated at their expected molecular weight by SDS-PAGE: GST-AKAP95 131 kDa and GST-HPV18 E6 46 kDa and were recognised by antibodies specific to the individual proteins **(Figure 4.5)**.

Although it is generally thought that soluble recombinant proteins are functional as misfolded proteins tend to precipitate, numerous reports have suggested that soluble fusion proteins may, in fact, show very little biological activity compared to native protein (reviewed in Nominé et al., 2001). To verify that the recombinant AKAP95 and E6 proteins were folded correctly, they were examined for binding to known interacting partners from cell lysates. GST-AKAP95 and GST-HPV18 E6 were incubated separately with cell lysate derived from C33A cells. GST-AKAP95 was examined for its ability to bind to cyclin D1 and p53 was used as a known GST-HPV18 E6 target, alongside GST as a negative control (Lechner and Laimins, 1994; Arsenijevic *et al.*, 2004). Western blotting of the washed precipitate showed that the recombinant proteins were able to bind their known endogenous targets **(Figure 4.6)**. Together, these data suggest that both GST-AKAP95 and GST-HPV18 E6 were likely to be folded correctly and able to interact with known targets.

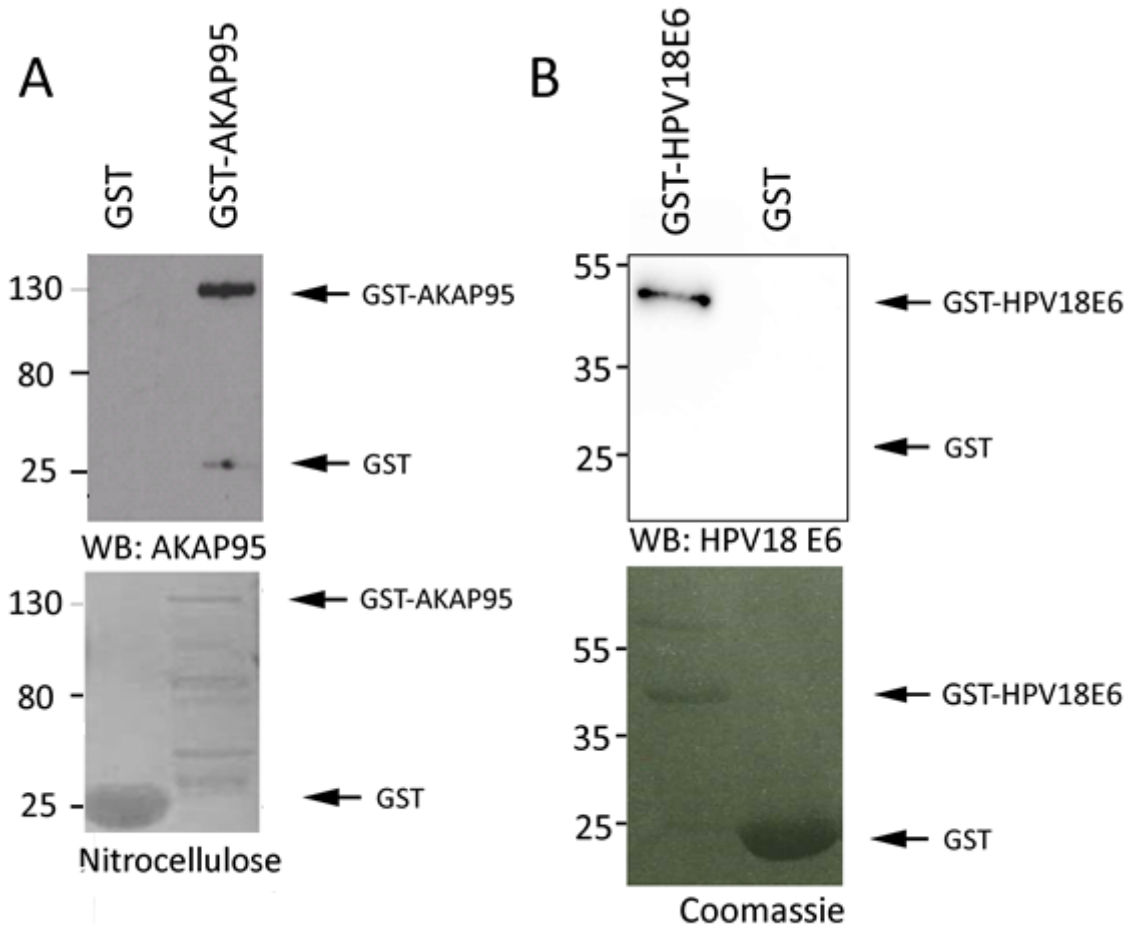

Figure 4.5: Recombinant GST-AKAP95 and GST-HPV18 E6 proteins are recognised by specific antibodies. The indicated GST or GST-fusion proteins were electrophoresed and immunoblotted with antibodies specific to AKAP95 (panel A; polyclonal) and HPV18 E6 (panel B; monoclonal).

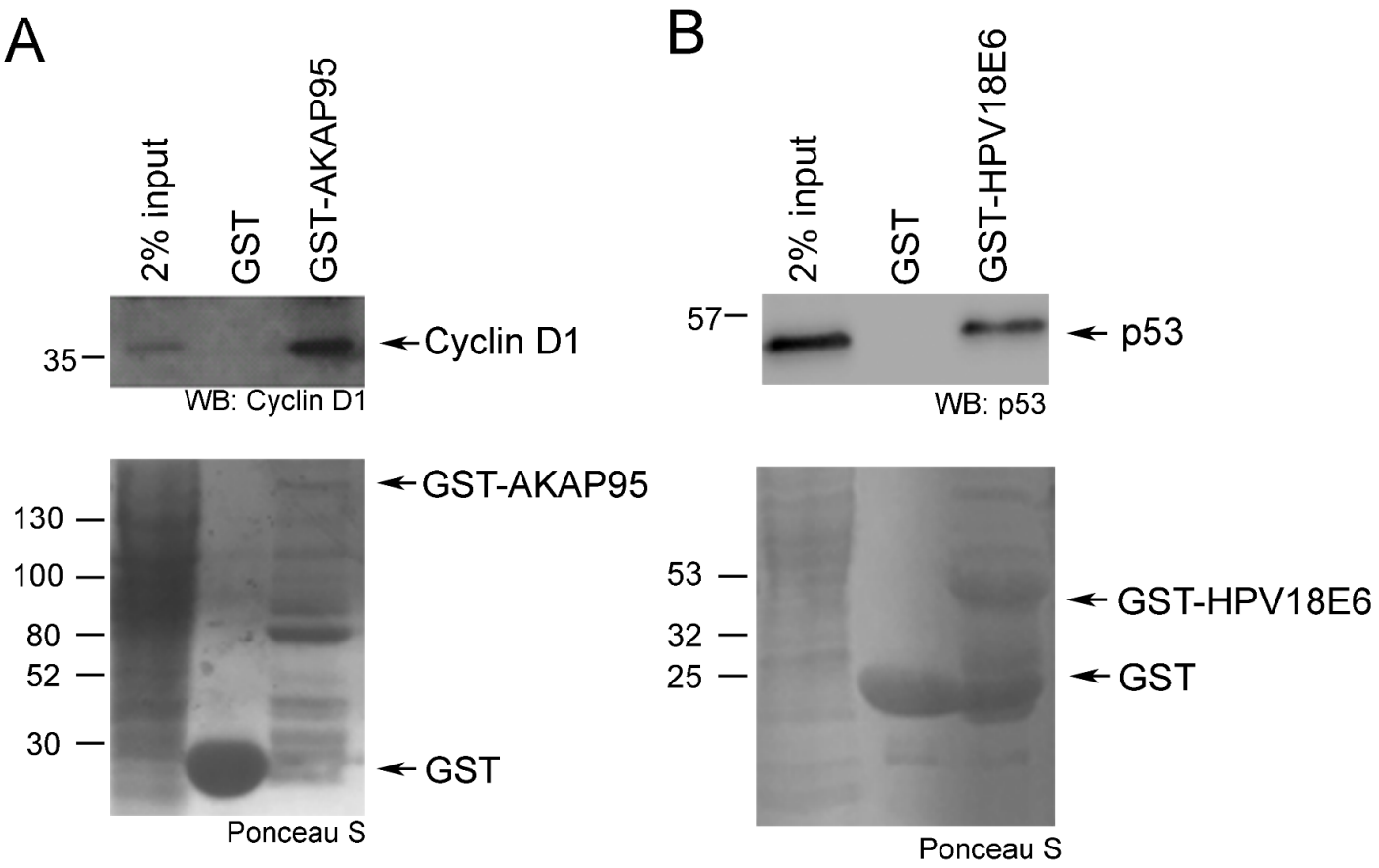

Figure 4.6: Recombinant GST-AKAP95 and GST-HPV18E6 proteins bind to endogenous targets from cell lysate. Purified GST or the indicated GST-fusion protein was incubated with lysate derived from C33A cells. **Panel A** represents an immunoblot using an anti-cyclin D antibody. **Panel B** represents an immunoblot for p53. The lower portion of each panel shows the Ponceau S stained membrane from the immunoblots. The GST fusion proteins are indicated by arrowheads.

4.2.5 AKAP95 and HPV18 E6 interact *in vitro*

Having shown that the GST-fusion proteins bound known protein targets, they were then assayed for their ability to bind to endogenous E6 or AKAP95 protein from cell lysates in a GST pull-down assay. Crude nuclear fractions were prepared from HeLa and C33A cervical cancer cell lines. Purified GST-AKAP95 bound to glutathione Sepharose™ beads, was incubated with nuclear lysate from HeLa cervical cancer cells, which expresses E6 from integrated HPV18 DNA, alongside GST as a negative control. Similarly, purified GST-HPV18 E6 was incubated with nuclear lysate from C33A (HPV negative) cells as a source of endogenous AKAP95 protein. (Nuclear extract was used to enrich for endogenous AKAP95 as it is thought to be expressed at a relatively low level.). After thorough washing of the beads, interacting proteins were detected by Western blotting and the results are shown in **Figure 4.7**. GST-AKAP95 pulled down HPV18 E6 from HeLa cell lysate (**Figure 4.7 A**) and GST-HPV18 E6 precipitated endogenous AKAP95 from C33A lysate (**Figure 4.7 B**). In both cases, the interactions were specific as GST pulldowns were negative or contained a very low level of the proteins.

Next, whether GST-AKAP95 can precipitate E6 from primary HFKs maintaining episomes of HPV18 genomes was examined. In **Figure 4.8**, a lysate was prepared from HFKs harbouring HPV18 episomes and this was incubated with purified GST or GST-AKAP95 proteins. While a small amount of E6 was isolated by the control GST protein, there was a significant enrichment of E6 complexed with GST-AKAP95, suggesting that in a physiologically relevant primary keratinocyte model of HPV18 infected cells GST-AKAP95 interacts with HPV18 E6 expressed from intact HPV18 genomes. Taken together, these data show that HPV18 E6 and AKAP95 interact *in vitro* in lysates derived

from cervical cancer cells as well as in a physiologically relevant system of the HPV18 life cycle.

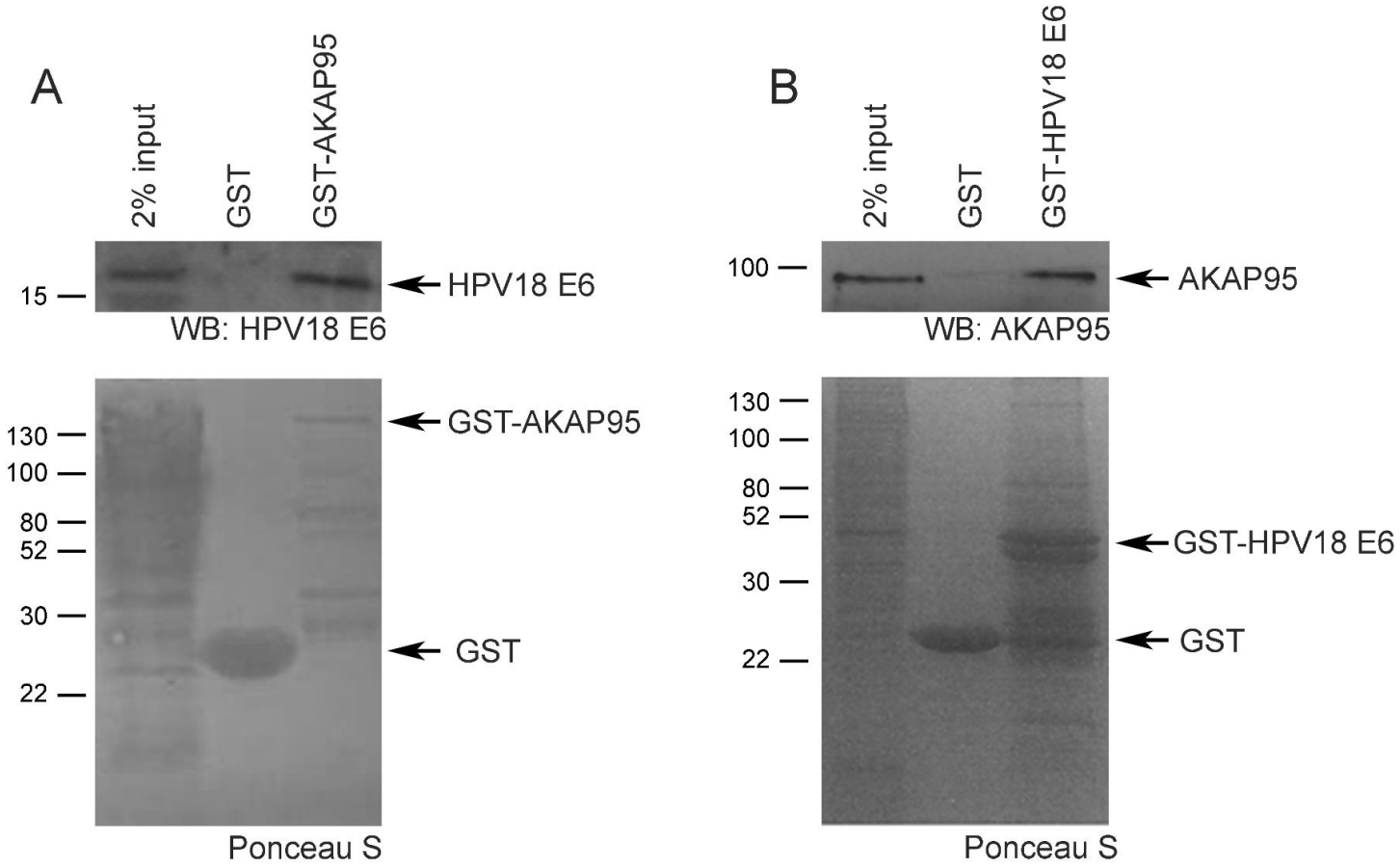

Figure 4.7: HPV18 E6 and AKAP95 interact *in vitro* by GST pull down assay. **A**: Purified GST-AKAP95 was incubated with HeLa nuclear lysate and Western blotted for HPV18 E6. Top panel represents Western blot for AKAP95 and bottom panel the corresponding Ponceau S stained membrane to demonstrate loading of GST proteins. **B**: Purified GST-HPV18 E6 was incubated with C33A nuclear cell lysate and Western blotted for AKAP95. Top panel represents Western blot for AKAP95 and bottom the corresponding Coomassie gel to demonstrate loading of GST proteins. Data representative of three independent experiments.

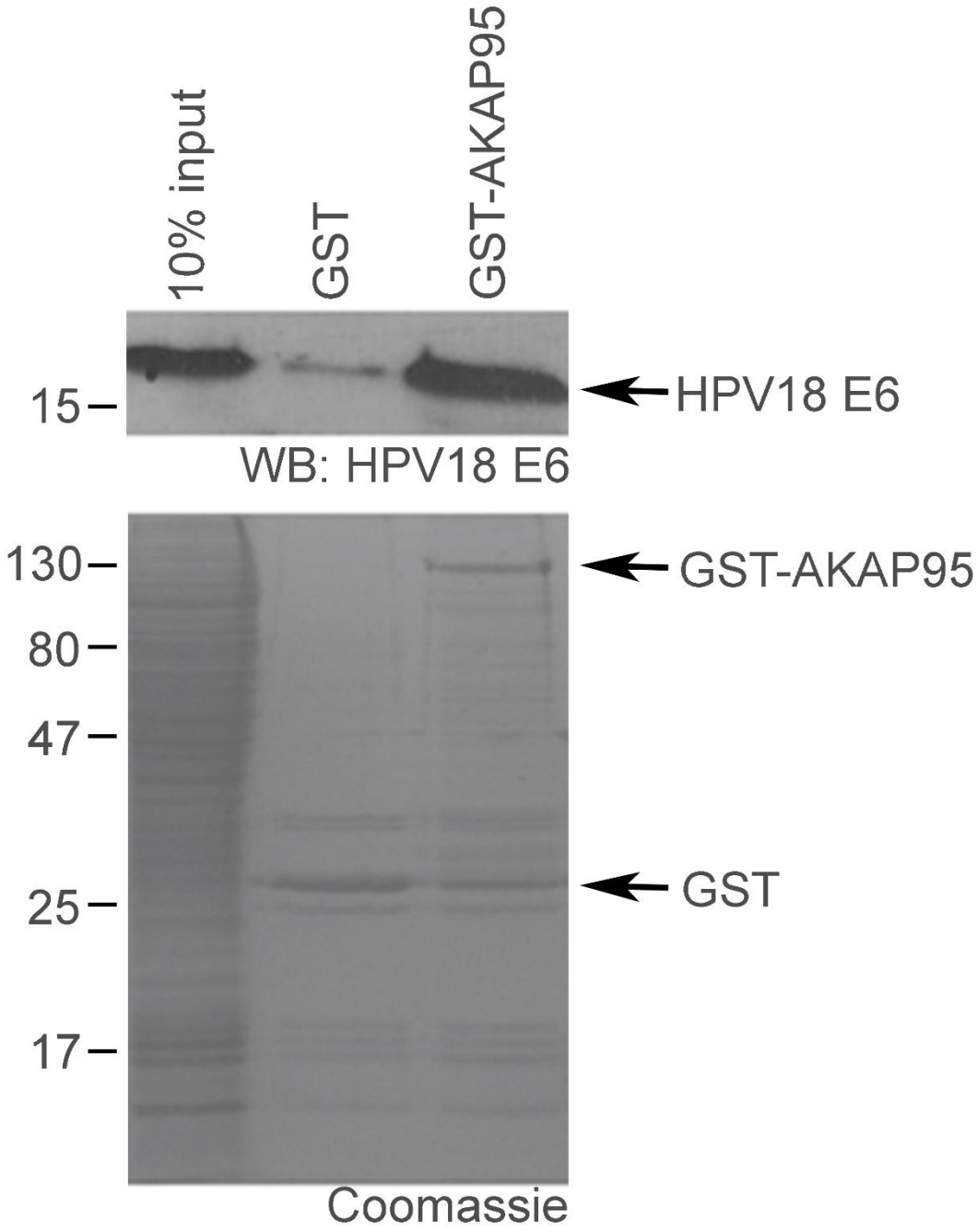

Figure 4.8: GST-AKAP95 interacts with endogenous E6 from primary human foreskin keratinocytes maintaining HPV18 genomes. Purified GST or GST-AKAP95 fusion proteins were incubated in lysate derived from primary human foreskin keratinocytes maintaining HPV18 genomes. Co-purifying proteins were detected by immunoblotting using an antibody specific for HPV18 E6. The lower Coomassie stained gel demonstrates loading of GST-proteins. Representative of two independent experiments.

4.2.6 AKAP95 binds to HPV18 E6 and not HPV16 or HPV11 E6.

While the E6-interaction mass spectroscopy data indicated that several high-risk alpha- and beta-HPV types could bind to AKAP95, neither HPV16 E6 nor the low-risk HPV6 E6 appeared in this analysis, even under conditions that inhibited the proteasome. These data could indicate that E6 binding to AKAP95 is type-specific. To determine whether HPV16 E6 could bind to AKAP95, GST-E6 fusion proteins were prepared from HPV16 **(Figure 4.9 A)**, as well as a low-risk type HPV11 **(Figure 4.9 B)** and examined alongside HPV18 for their ability to bind to endogenous AKAP95 from C33A cell lysate.

The data shown in **Figure 4.9A** demonstrates that AKAP95 binding is restricted to HPV18 E6, as there is no appreciable binding of AKAP95 to GST-HPV16 E6 under these conditions. To understand whether there are differences in AKAP95 binding between low and high-risk E6 proteins, this experiment was then repeated using GST-HPV11 E6. While purification of GST-HPV11 E6 from *E. coli* was much more technically challenging and resulted in a lower yield of purified protein, the interaction data presented in **Figure 4.9B** shows that there is no appreciable binding of AKAP95 to GST-HPV11 E6 fusion protein. These data suggest that binding of AKAP95 is specific to HPV18 in these experimental conditions.

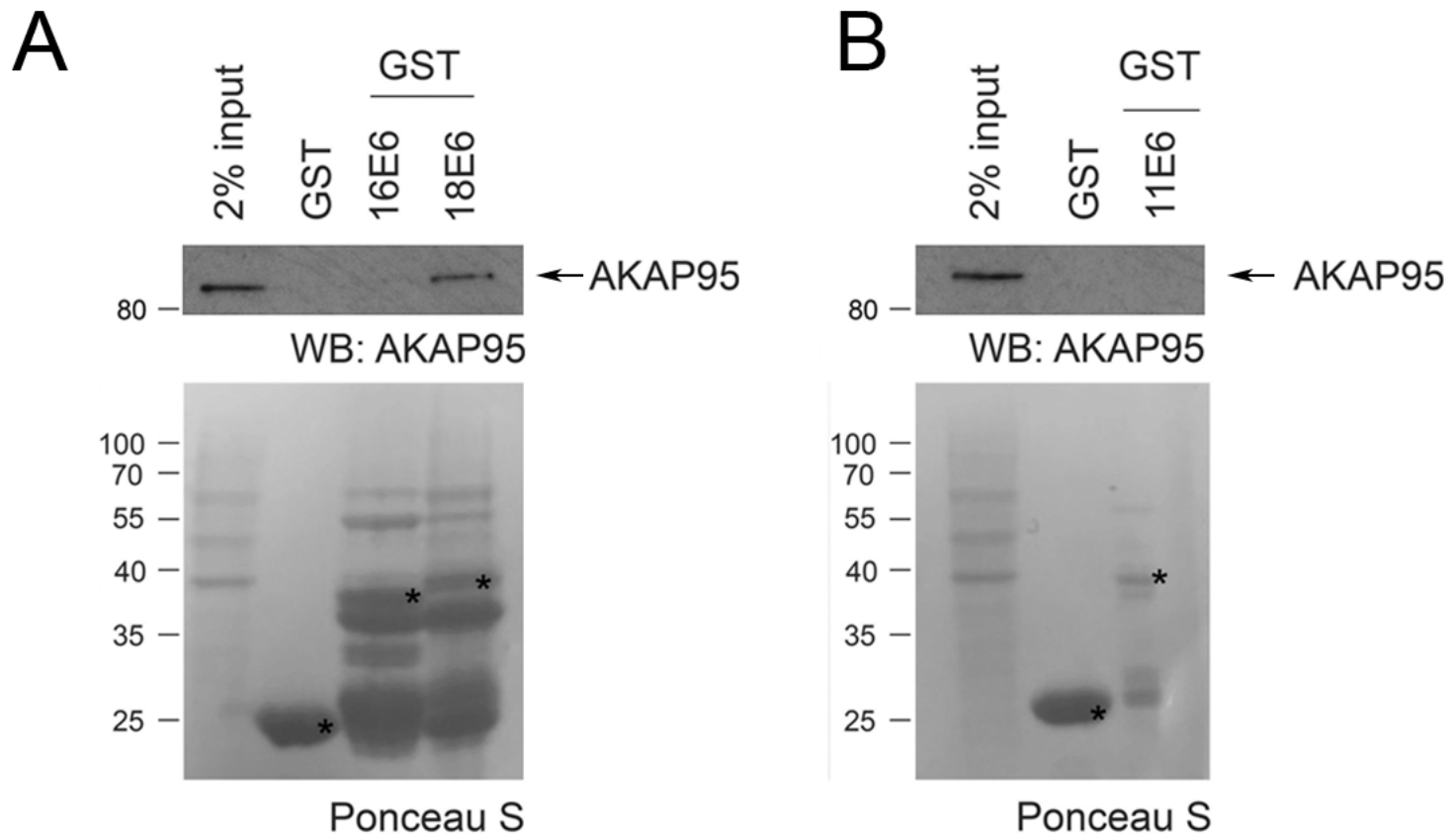

Figure 4.9: GSTE6 fusion proteins of HPV16 and HPV11 do not interact with AKAP95. Purified GST or GST E6 proteins as indicated were incubated with C33A lysate overnight, and after thorough washing of the beads, co-purifying AKAP95 was examined by Western blotting using an AKAP95-specific antibody. **Panel A** represents incubation of GST, GST-HPV16E6 or -HPV18E6. **Panel B** represents incubation with GST or GST-HPV11E6. The lower Ponceau S stained membrane demonstrates loading of GST proteins (indicated by *). Input represents 2% of cell lysate used in pull down reactions. Arrows represent full length proteins. Note that all blots were taken from the same gel.

4.2.7 HPV18 E6 and AKAP95 interact *in vivo*

Having shown that HPV18 E6 and AKAP95 interact *in vitro* by GST pull-down assays, it was important to show that this interaction occurs in intact cells by co-immunoprecipitation. This was done using antibodies specific to AKAP95 and HPV18 E6 to co-immunoprecipitate endogenous proteins from cell lysates. Endogenous co-immunoprecipitations were used to avoid the potential pitfalls of protein overexpression, including mislocalisation of overexpressed protein in a different cellular compartment to endogenous protein and to avoid the potential interference of epitope tags. In the first instance, HeLa cells were used as GST-AKAP95 was able to bind to E6 expressed from the integrated HPV18 genome. As shown in **Figure 4.10**, incubation of HeLa nuclear lysate with a monoclonal antibody directed against HPV18 E6 (left panel) co-immunoprecipitated endogenous AKAP95. The reverse co-immunoprecipitation was also possible; incubation of HeLa lysate with an AKAP95 specific polyclonal antibody co-immunoprecipitated endogenous E6 (right panel). Neither protein was co-immunoprecipitated by a species matched IgG control. Short exposure of the film is shown in **Figure 4.10 A**, while a longer exposure is shown in **Figure 4.10 B**. Interestingly, there are additional lower molecular weight bands detected by the HPV18 E6 antibody in both E6- and AKAP95-immunoprecipitates (indicated by arrowheads). Some of these may be breakdown products, but some might be spliced products of the E6 ORF (HPV18 E6*I, E6*II). Taken together, these data show that the E6-AKAP95 complex exists *in vivo* in HPV18-positive HeLa cervical cancer cells.

It was then important to determine whether this interaction occurs in a physiologically relevant model of the HPV life cycle. For this, a lysate was prepared from HFK-18 cells and AKAP95 and E6 immunoprecipitates isolated. The data presented in **Figure 4.11**

shows that in this physiological model endogenous AKAP95 and E6 are present in a complex *in vivo*.

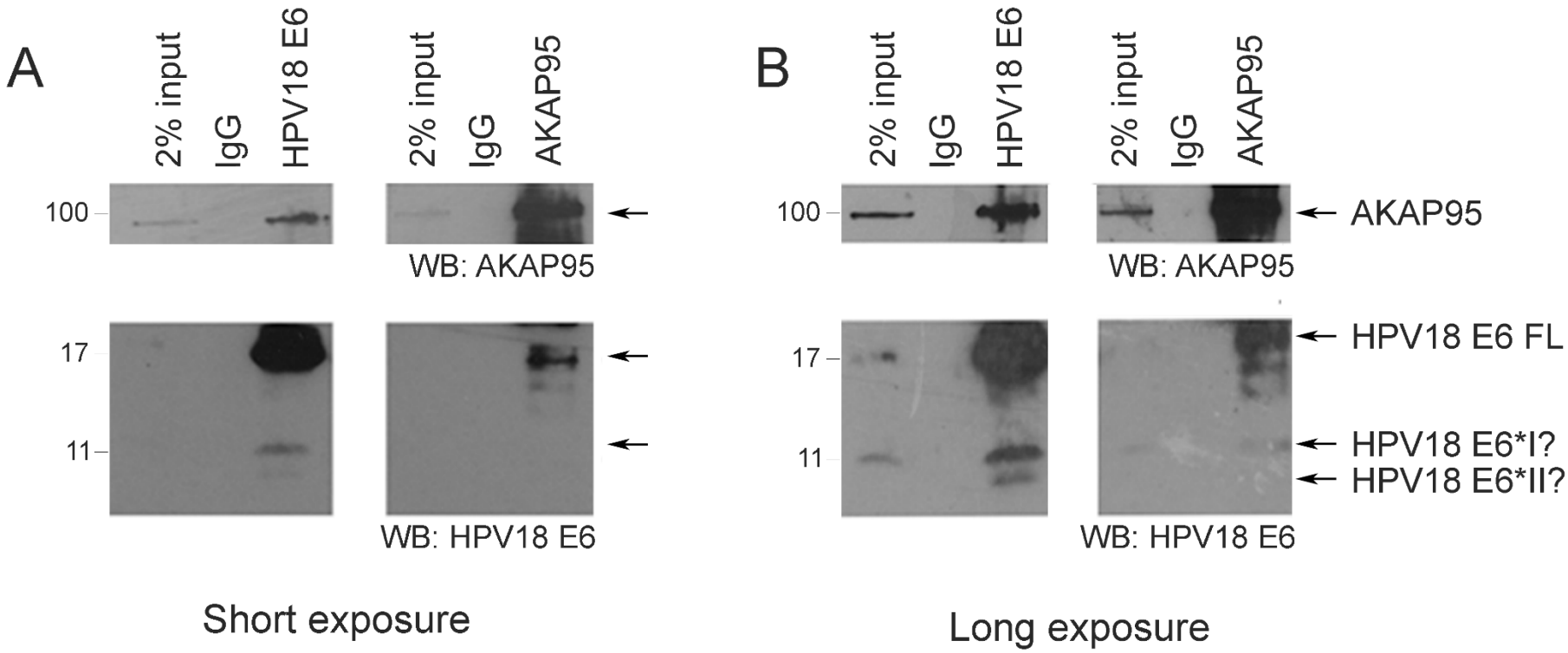

Figure 4.10: Reciprocal co-immunoprecipitation of HPV18 E6 and AKAP95 in HeLa cells HeLa nuclear lysate was immunoprecipitated with the indicated antibodies and the interacting proteins determined by immunoblotting. **Panel A** represents a short exposure while **panel B** is a long exposure. Smaller E6-specific products may represent a spliced product of the E6 ORF (E6*I/E6*II). Data shown representative of three independent experiments. FL: full length.

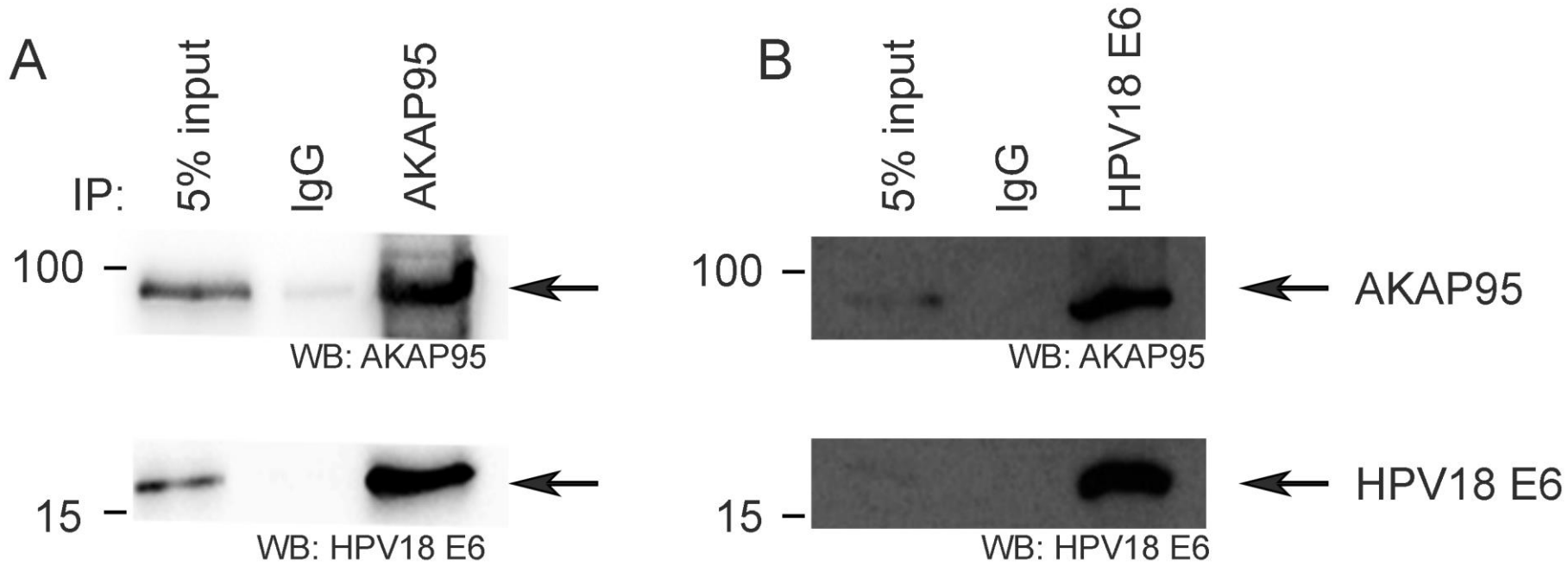

Figure 4.11: Interaction of HPV18 E6 and AKAP95 in primary HPV18 genome containing cells. Lysate derived from HFK-18 cells was immunoprecipitated using either specific anti-AKAP95 (A) or anti-HPV18E6 (B) antibodies, or control IgG. Co-immunoprecipitating proteins were resolved and detected by Western blotting using the indicated antibodies. Input is 5% of total lysate used for co-immunoprecipitation. Data shown representative of three independent experiments. Arrows represent full length proteins.

4.2.8 Mapping the AKAP95 interacting domains of E6

To map the HPV18 E6 residues involved in the interaction with AKAP95, a series of E6 mutants were used. In the first instance, since the Roberts group studied E6–PDZ interactions (Watson *et al.*, 2003; Delury *et al.*, 2013; Marsh *et al.*, 2017) and several E6 mutants were available that contained mutation of the E6 PBM and the overlapping PKA recognition sequence, these were investigated for AKAP95 binding. A class I PBM exists at the extreme C-terminus of E6 (^{155}ETQV^{158}). The threonine residue at 156 is critical for binding PDZ substrates, including Dlg1. PKA phosphorylation of the threonine residue in the E6 PBM disrupts binding with PDZ targets but the phospho-sequence forms a platform for binding 14-3-3 proteins (Boon and Banks, 2012; Kühne et al., 2000). The replacement of the threonine with glutamic acid acts as a phospho-mimic (T156E; GluE6) and disrupts binding to Dlg1. Thus, this mutant is impaired for targeting of PDZ domain-containing proteins (Gardiol *et al*., 1999). Whether this GluE6 mutant is functional in binding to 14-3-3 proteins is unknown. Mutation of a key arginine in the PKA recognition motif (Arg^{153}-X-X-Thr^{156}; R153L, LeuE6) abrogates phosphorylation of the E6 PBM (i.e. it is no longer a substrate for PKA) and therefore E6 binds to and degrades PDZ domain-containing proteins in a PKA independent manner (Kühne et al., 2000).

The location of these mutations in the HPV18 E6 protein is illustrated in **Figure 4.12.**

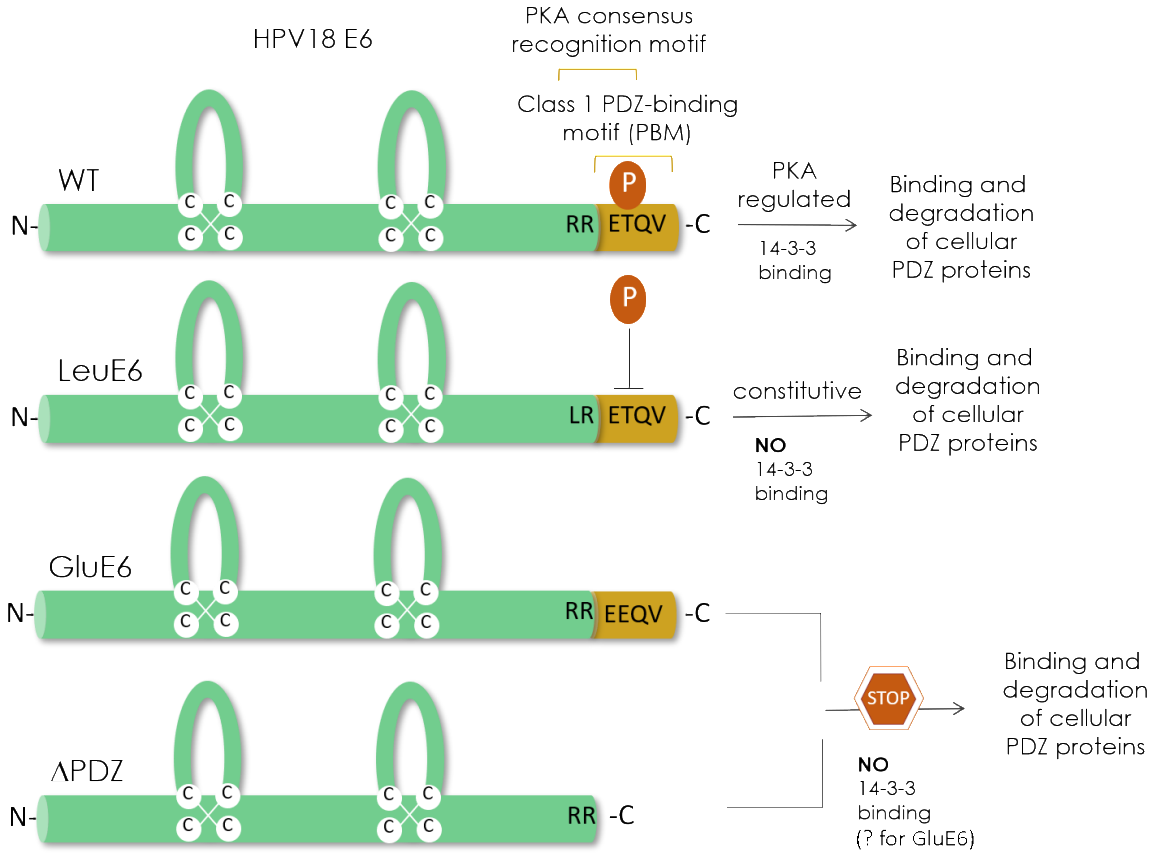

Figure 4.12: HPV18 E6 mutant proteins used in this study. The wild type HPV18 E6 protein contains at its extreme carboxyl terminus a class I PDZ binding motif (PBM) through which it binds cellular PDZ domain-containing proteins. Phosphorylation of the overlapping PKA consensus recognition motif negatively regulates E6-PDZ interactions while allowing for phospho-E6-dependent interactions with 14-3-3 proteins. The LeuE6 mutant contains a R153L substitution that destroys the PKA recognition motif, allowing for constitutive (PKA-independent) binding of E6 to cellular PDZ proteins. The GluE6 mutant contains a T156E substitution that impairs E6 recognition of PDZ proteins and the ΔPDZ protein contains two translational termination codons at positions 155 and 156, removing the entire E6 PBM; these two mutant proteins cannot bind to cellular PDZ domain-containing proteins. Image from Dr Sally Roberts.

To determine whether the ability of E6 to recognise PDZ proteins or to be phosphorylated by PKA was important for the E6-AKAP95 interaction, these E6 mutants were expressed in 293T cells and examined for their ability to bind to GST-AKAP95 in GST pull-down experiments. 293T cells were chosen for these experiments as they are easily transfectable by inexpensive transfection reagents and have been used to profile HPVE6-PDZ interactions (Belotti et al., 2013). The data shown in **Figure 4.13** highlights several important pieces of data. First, HPV18 E6 interacts with GST-AKAP95 in this cell background. Second, the substitution of the threonine residue for glutamic acid in the E6 PBM, which abrogates E6-PDZ interactions, compromises AKAP95 binding. Finally, the destruction of the PKA phosphorylation site does not affect E6-AKAP95 binding. These results suggest that the ability of E6 to bind to AKAP95 does not depend on the integrity of the PKA phosphorylation site that overlaps with the E6 PBM but rather the ability of E6 to target cellular PDZ domain-containing proteins.

To confirm that the E6-AKAP95 interaction depended on the ability of E6 to target cellular PDZ proteins, a second mutant E6 mutant defective for PDZ targeting was tested. This mutant (ΔPDZE6) contains two translation termination codons at positions 155 and 156, deleting the four residues that make up the E6 PBM (Delury et al., 2013).

Similar to the GluE6 mutant, the ΔPDZE6 mutant shown in **Figure 4.14** does not bind to GST-AKAP95.

Together, these results indicate that the E6 PBM is crucial in mediating the E6-AKAP95 interaction.

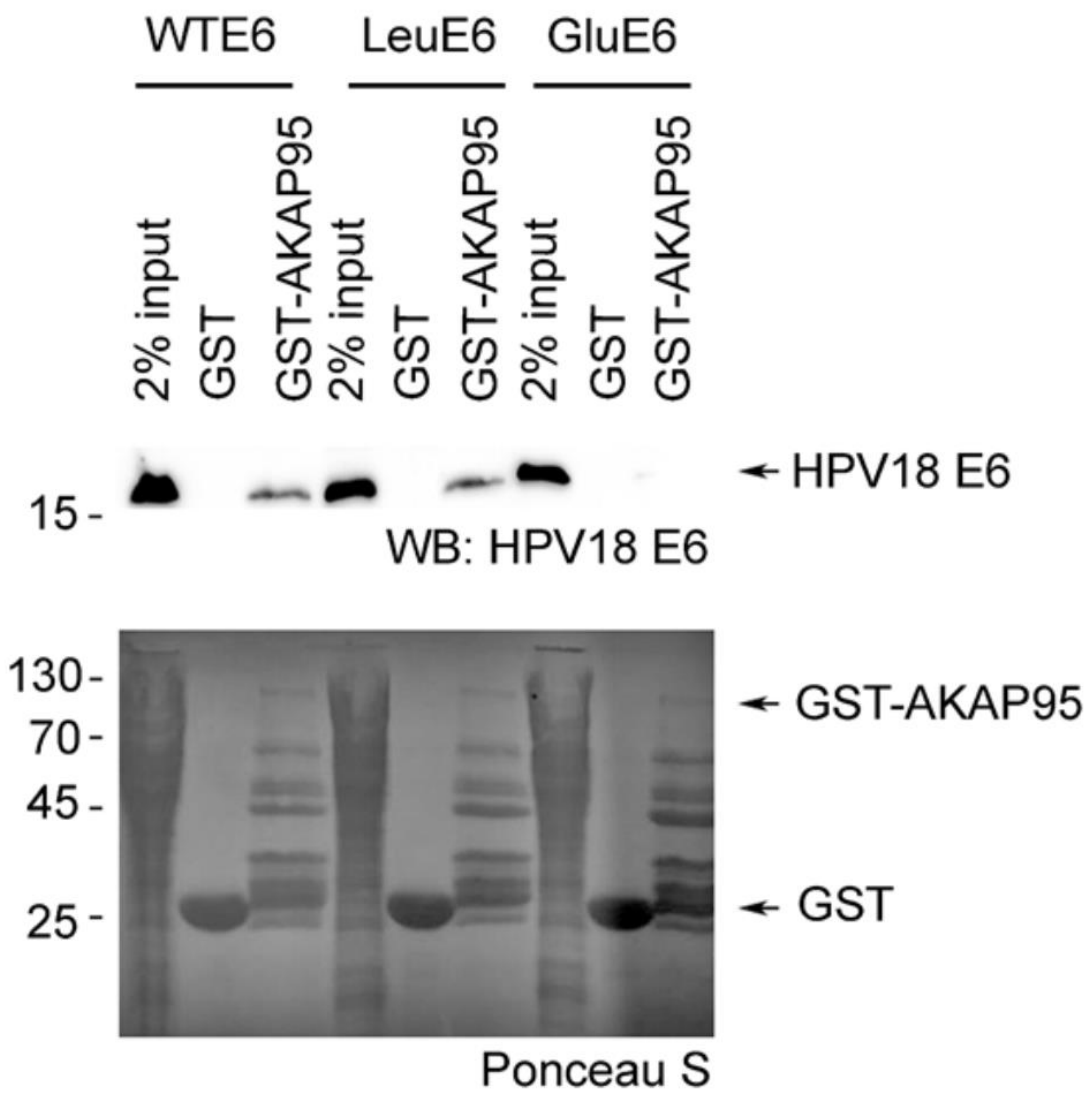

Figure 4.13: The E6 PDZ binding motif mediates the E6-AKAP95 interaction. Purified GST or GST-AKAP95 were incubated with cellular lysate derived from 293T cells expressing the indicated E6 mutants. Co-purifying proteins were separated by electrophoresis and residual E6 examined by Western blotting with a specific antibody. The top panel represents the HPV18 E6 immunoblot, while the lower panel demonstrates loading of the GST fusion proteins. Representative of three independent experiments.

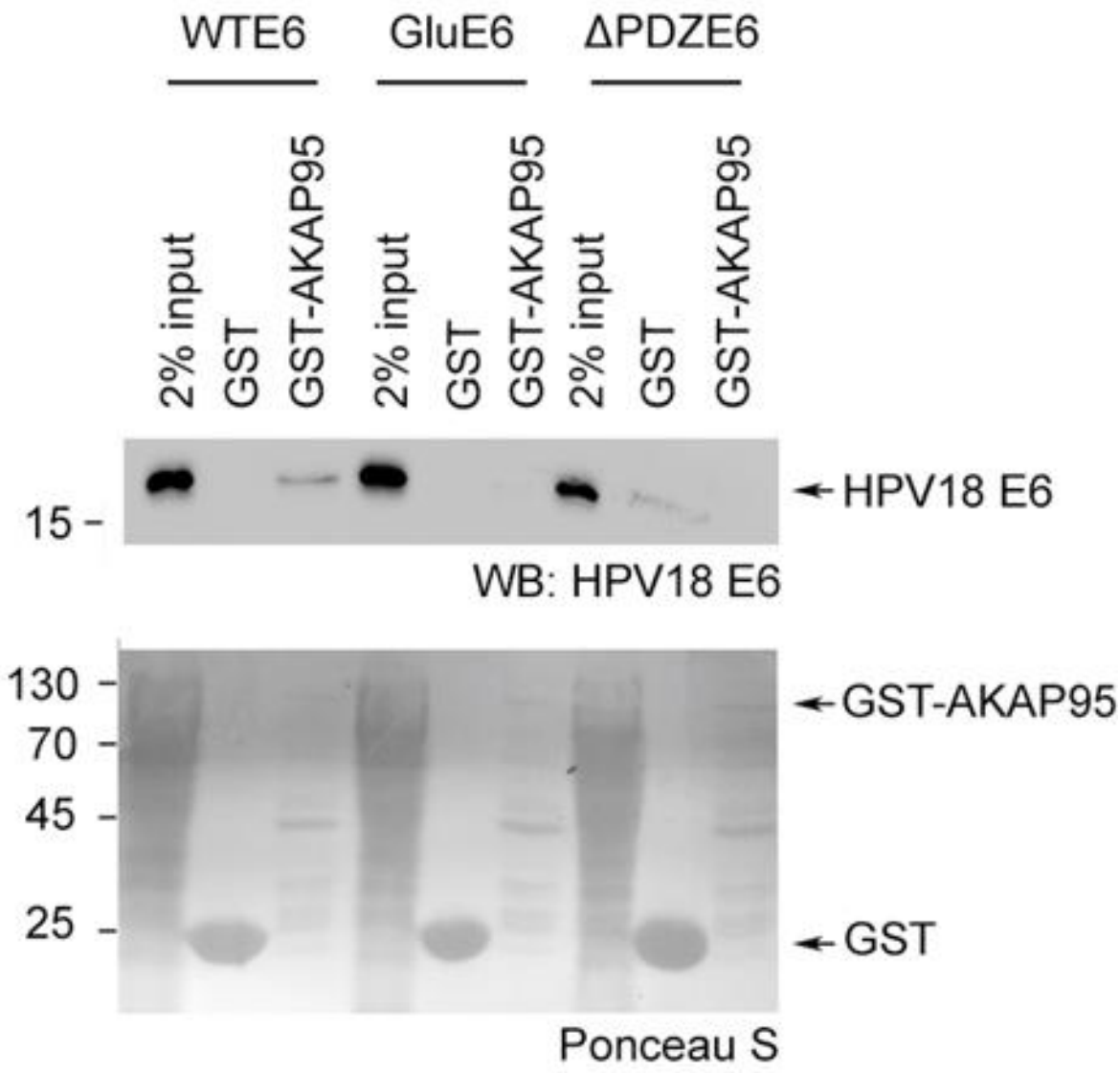

Figure 4.14: Loss of E6-PDZ targeting compromises the E6-AKAP95 interaction. Purified GST or GST-AKAP95 was incubated with cellular lysate derived from 293T cells expressing the indicated E6 mutants. Co-purifying proteins were separated by electrophoresis and GST-AKAP95 bound E6 examined by Western blotting with a specific antibody. The top panel represents the HPV18 E6 immunoblot, while the lower panel demonstrates loading of the GST fusion proteins. Representative of three independent experiments.

4.2.9 AKAP95 binds to the cellular PDZ domain-containing protein hScrib

The finding that the E6-AKAP95 interaction was dependent on the integrity of the E6 PBM was surprising since the AKAP95 sequence does not contain any appreciable PDZ domain structure when analysed by the MoDPepInt Server, an online resource that analyses protein sequence for the presence of SH2, SH3 and PDZ domains (Kundu et al., 2014). Given that E6 has been shown to bind to at least 20 cellular PDZ domain-containing proteins through this binding motif (reviewed in James and Roberts, 2016), it is possible that the E6-AKAP95 interaction is mediated by interaction(s) with cellular PDZ proteins. With this in mind, a published mass spectroscopy database of AKAP95-binding partners was scrutinised for PDZ domain-containing proteins that are known targets of the E6 PBM (López-Soop et al., 2017; **Table 4.2**).

Analysis of the database highlighted potential interactors of AKAP95 with three PDZ domain-containing proteins: hScrib, ZO-1, and ZO-2. Of note, ZO-2 has been previously shown to interact with hScrib in polarised epithelial cells and ZO-1 is a known binding partner of ZO-2 (Bauer et al., 2010; Itoh et al., 1999; Métais et al., 2005). Given the considerable number of unique peptides (10) detected for hScrib in the AKAP95-mass spectroscopy data, it was important to first determine whether or not hScrib was a true binding partner of AKAP95. hScrib and two other PDZ proteins known to be E6 targets, Dlg1 and MAGI-1 but were not represented in the AKAP95-mass spectroscopy data, were expressed as HA- or Flag-tagged proteins in 293T cells and binding to GST-AKAP95 determined by GST pull-downs. As shown in **Figure 4.15,** GST-AKAP95 interacted specifically with HA-hScrib and not HA-Dlg1 or FLAG-MAGI, suggesting that hScrib was a novel AKAP95 interacting partner. Therefore, these data suggest the interaction between HPV18 E6 and AKAP95 is not direct but mediated by the polarity protein hScrib.

Protein	Unique peptides	Observable peptides
Scribble (hScrib)	10	127
Tight junction protein ZO-1	2	141
Tight junction protein ZO-2	2	97

Table 4.2: AKAP95-PDZ potential interactors. Scrutiny of published AKAP95 mass spectroscopic databases identifies a variety of cellular PDZ domain-containing proteins as potential binding partners. Data taken from Lopez-Soop *et al*., 2017. ZO: Zonula occludens.

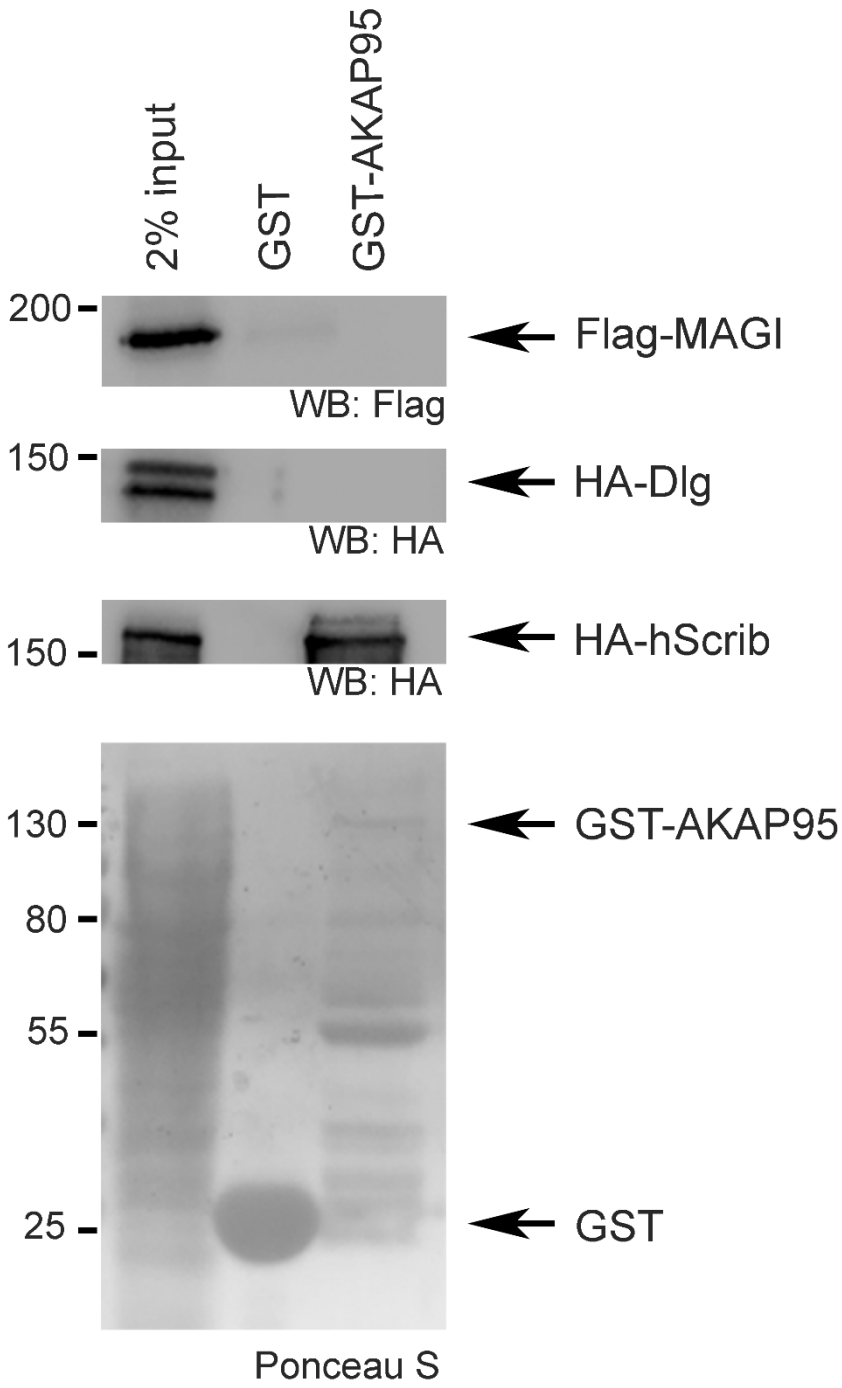

Figure 4.15: hScrib is a novel AKAP95 binding partner. Purified GST or GST-AKAP95 was incubated with cellular lysate derived from 293T cells expressing the indicated expression vectors. Co-purifying proteins were separated by electrophoresis and detected by Western blotting using the indicated antibodies. The top panels represent the immunoblots, while the lower panel demonstrates loading of the GST fusion proteins. Representative of three independent experiments.

4.2.10 The HPV18 E6 PBM is required for AKAP95 binding *in vivo*

To further verify that there was an E6 complex containing AKAP95 *in vivo* and this was dependent on the integrity of the E6 PBM, E6 was immunoprecipitated from primary HFKs maintaining either the wild type HPV18 genome or a mutant genome carrying a deletion of the E6 PBM (ΔPDZE6; Delury *et al.*, 2013) and immunoblotted for AKAP95 and hScrib. As shown in **Figure 4.16**, only in wild type E6 containing HPV18 genomes was AKAP95 detected in the E6 immunoprecipitates and this was absent in immunoprecipitates isolated from the ΔPDZ cells, suggesting that the E6 PBM is crucial for the *in vivo* association of this protein complex. Supporting this is the finding that only wild type E6-immunoprecipitates also contain hScrib, consistent with our model that suggests E6 targeting of hScrib is required for assembly of the E6-AKAP95 protein complex in cells.

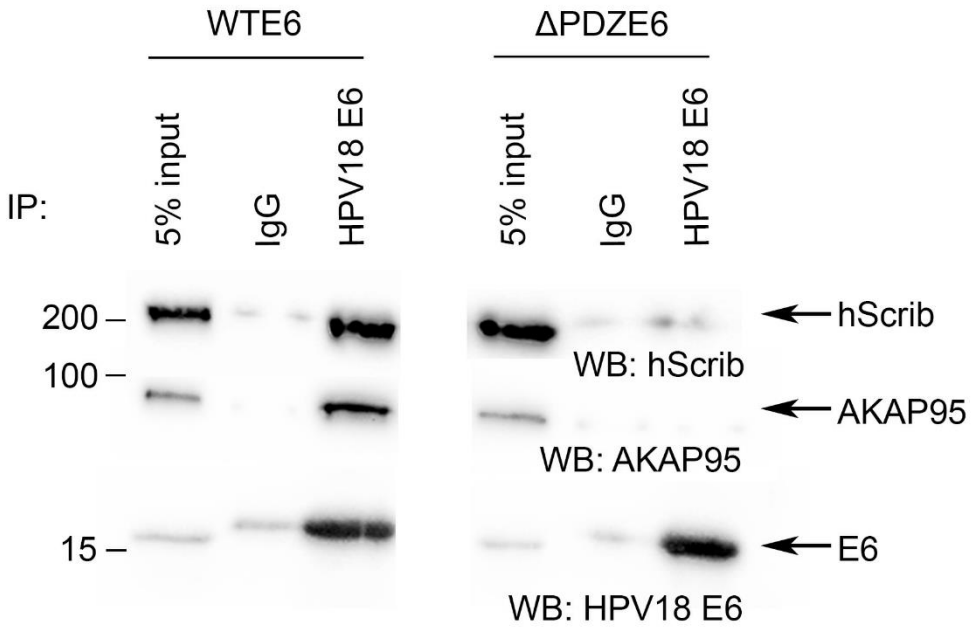

Figure 4.16: The interaction of HPV18 E6, AKAP95 and hScrib depends on an intact E6 PBM *in vivo.* E6 was immunoprecipitated from primary human foreskin keratinocytes maintaining either wild type (WTE6) or ΔPDZ genomes and examined for binding to AKAP95 and hScrib by Western blotting. Representative of two independent experiments.

4.2.11 Mapping the interacting domains of AKAP95 on E6

Next, to map the interacting regions on AKAP95 responsible for binding to HPV18 E6, a GST pull-down based approach using various FLAG-HA-tagged AKAP95 mutants was used. The AKAP95 mutants were expressed in 293T cells and their ability to interact with GST-HPV18 E6 examined by GST pull-downs and Western blotting.

In the first instance, two mutants were used to define whether the E6-interacting site was on the N-terminal (residues 1-340) or C-terminal (residues 341-692) domains of AKAP95. The results shown in **Figure 4.17** indicate that both amino and carboxyl termini of AKAP95 bind to GST-HPV18 E6, suggesting that multiple regions of AKAP95 are required for interaction. Therefore, to better define the E6-interacting region(s), various other mutants were then tested for binding E6 in GST pull-down experiments.

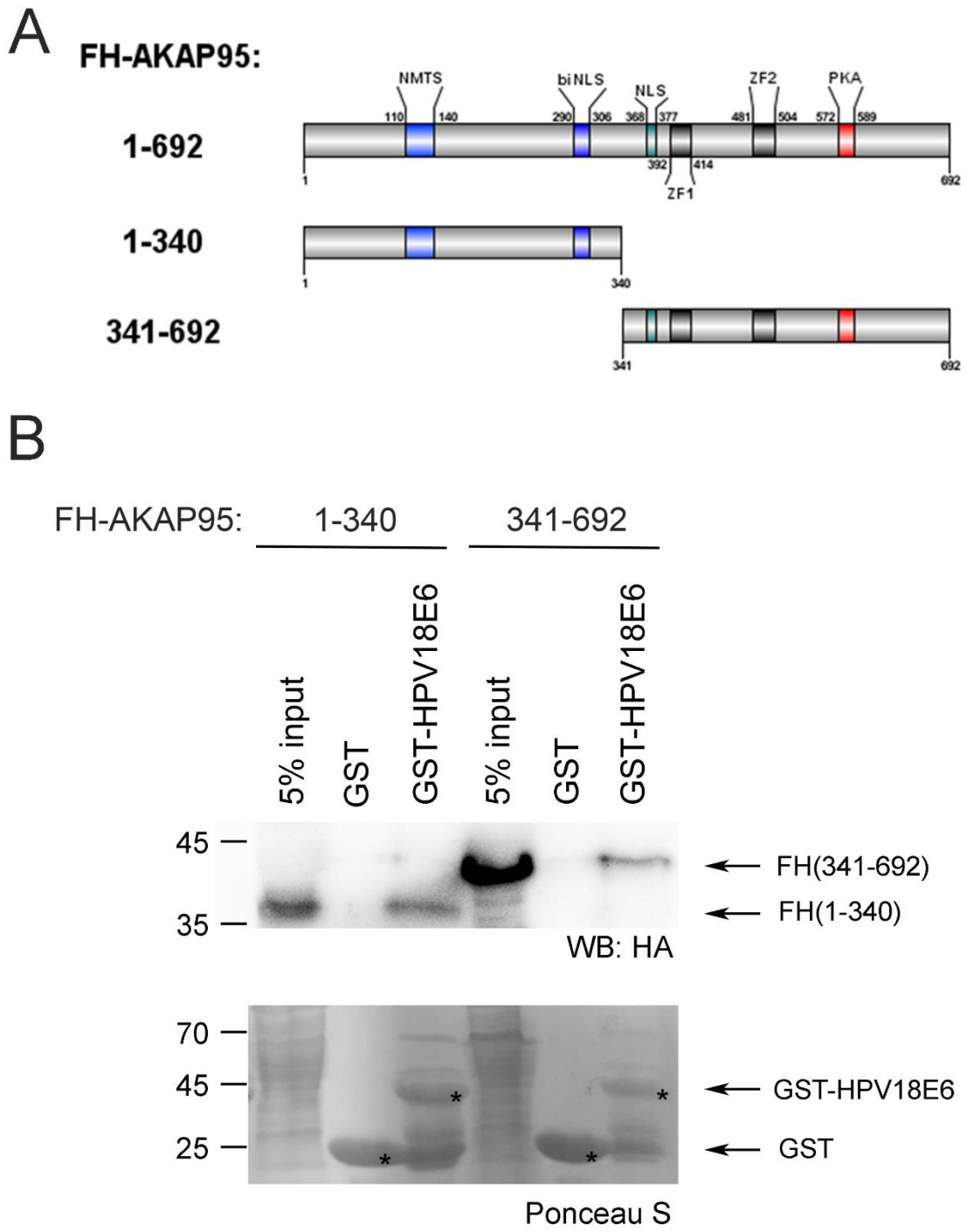

Figure 4.17: Both amino and carboxyl termini of AKAP95 are required for E6 interaction. Panel A: schematic of the AKAP95 mutants used in the GST pull down. **Panel B:** purified GST or GST-HPV18E6 was incubated with cellular lysate derived from 293T cells expressing the indicated FH-AKAP95 mutants, alongside GST as a negative control. Co-purifying proteins were separated by electrophoresis and detected by Western blotting using the indicated antibody. The top panels represent the immunoblots, while the lower panel demonstrates loading of the GST and GST fusion proteins (also indicated by *). Representative of three independent experiments.

4.2.11.1 E6 binds to amino acids 1-100 in the amino terminus of AKAP95

The GST pull-down experiments were repeated using expression vectors encoding fragments within amino acids (aa) 1-340. Fragments covering aa 1-210, 211-692 and 101-692 were expressed in 293T cells and their binding to GST-HPV18 E6 examined in pull-down experiments. As shown in **Figure 4.18**, GST-HPV18 E6 binds strongly to aa 1-210 while a lesser interaction is seen with a fragment covering amino acids 211-692. There is no appreciable interaction with 101-692. These data suggest that the amino acids 1-100 are involved in mediating the interaction with HPV18 E6.

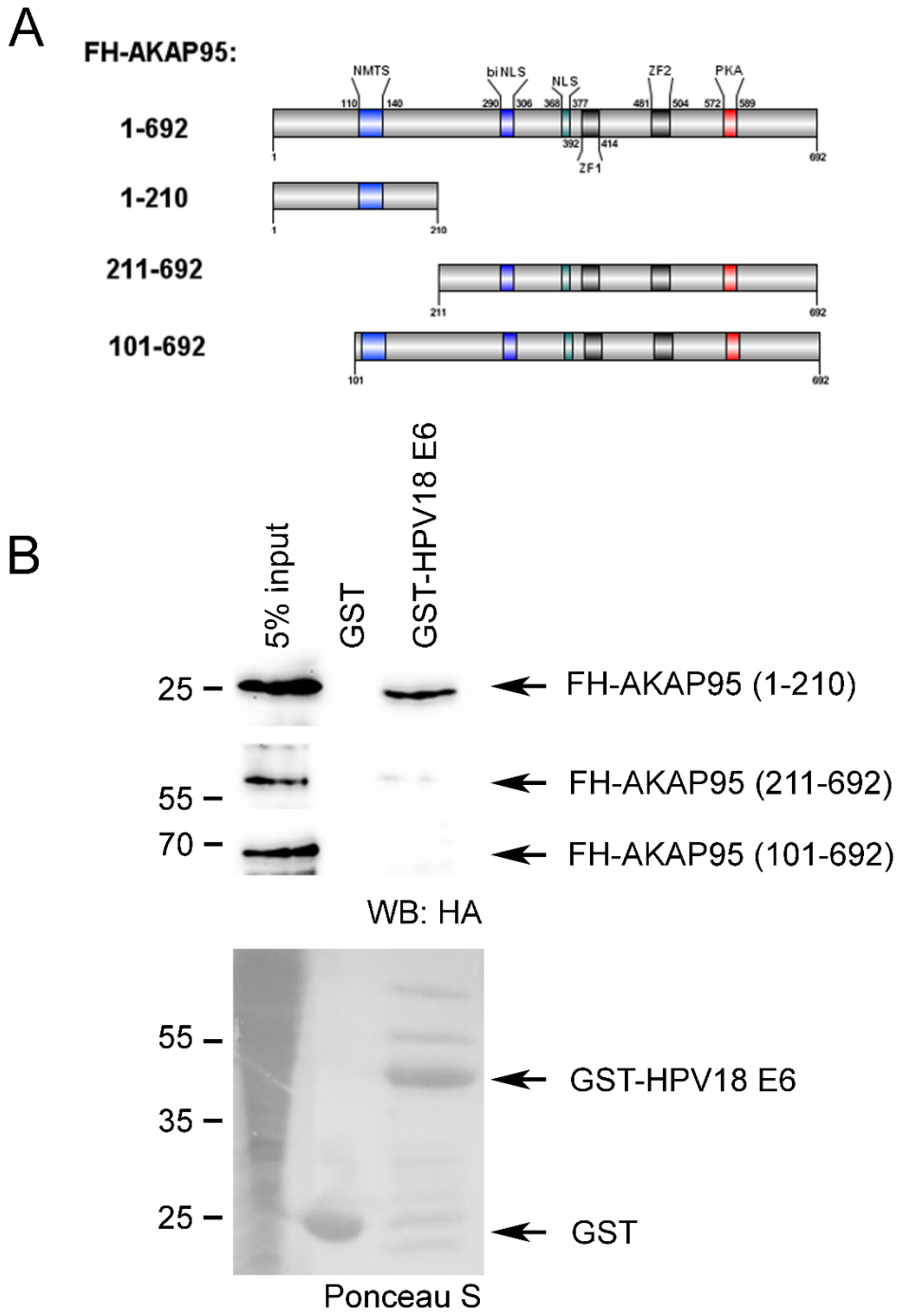

Figure 4.18: The amino terminal 100 amino acids primarily bind to GST-E6. Panel A: schematic of the full length and AKAP95 mutants used in the GST pull down. **Panel B** : purified GST or GST-HPV18E6 were incubated with lysate derived from 293T cells expressing the indicated FH-AKAP95 fragments. Co-purifying proteins were separated by electrophoresis and detected by Western blotting using an antibody against the HA tag. The top panel represents the immunoblots, while the lower panel demonstrates loading of the GST fusion proteins. Representative of two independent experiments.

4.2.11.2 The PKA binding site on AKAP95 is required for the E6-AKAP95 interaction

Embedded within the carboxyl terminus of AKAP95 is a binding site for PKA-RII and point mutation at this site at position 582 (I582P) disrupts the AKAP95-RII interaction (Carr et al., 1992). To understand whether AKAP95 binding to PKA is important in mediating the E6-AKAP95 interaction, GST-E6 pull-down experiments were carried out using both wild type and I582P expression vectors. The data presented in **Figure 4.19** shows that GST-HPV18 E6 binds to wild type AKAP95 but binding is abrogated in the presence of the I582P point mutation, suggesting that the ability of AKAP95 to bind to PKA is important in mediating the E6-AKAP95 interaction.

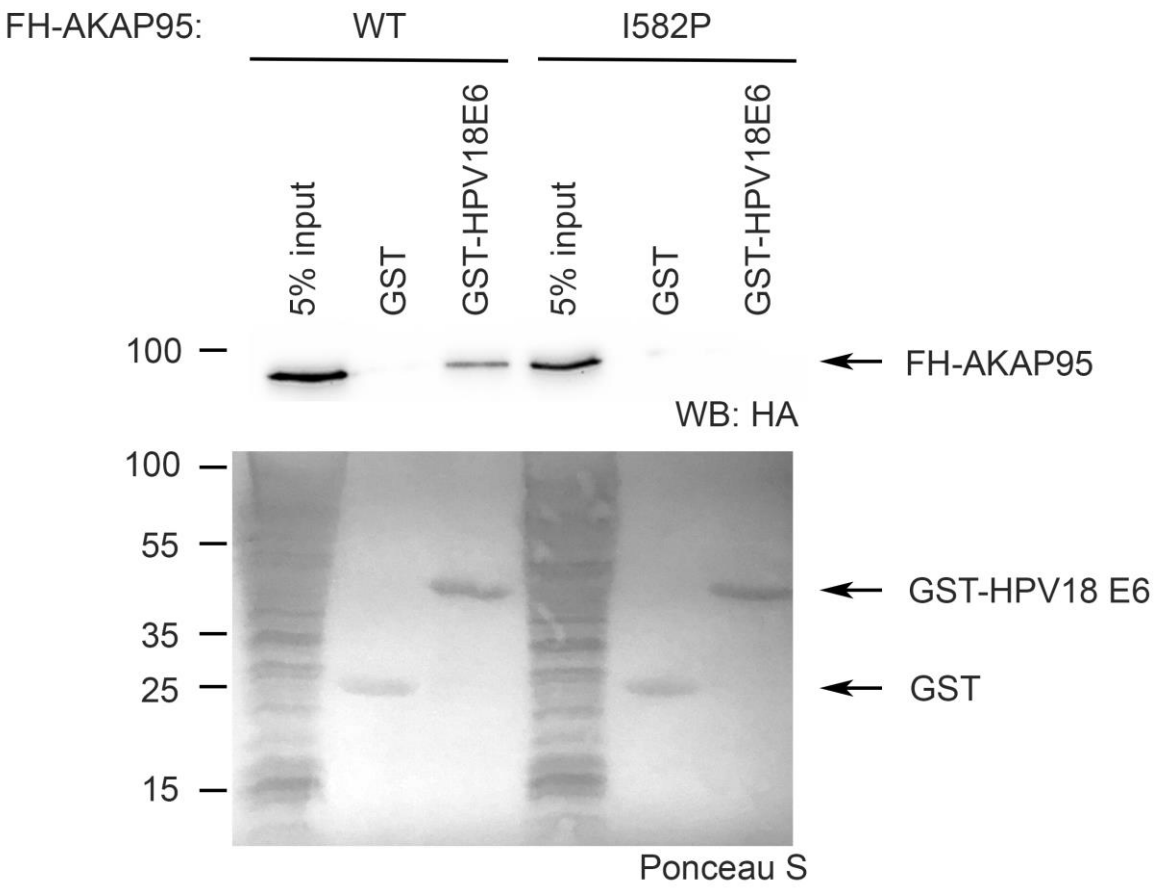

Figure 4.19: The PKA-binding ability of AKAP95 is important for its interaction with E6. Purified GST or GST-HPV18E6 were incubated with lysate derived from 293T cells expressing either the FH-wild type or FH-I582P AKAP95 mutant. Co-purifying proteins were separated by electrophoresis and detected by Western blotting using an antibody against the HA tag. The top panel represents the immunoblots, while the lower panel demonstrates loading of the GST fusion proteins. Representative of three independent experiments.

4.2.11.3 AKAP95 zinc fingers are not important for its interaction with E6

Also within the carboxyl terminus of AKAP95 are two ZFs that are important for its interaction with DNA. To determine whether the ZFs were necessary for AKAP95 binding to E6, the GST-HPV18 E6 pull-downs were repeated with either the wild type protein or a mutant containing Cys to Ser mutations (ZF C-S) in both ZF domains to abrogate its DNA binding ability. The data shown in **Figure 4.20** indicates that disruption of the ZFs does not impair the ability of AKAP95 to bind to E6, with the mutant protein actually binding E6 more efficiently than wild type AKAP95.

The binding to HPV18 E6 by the various AKAP95 mutants is summarised in **Figure 4.21**.

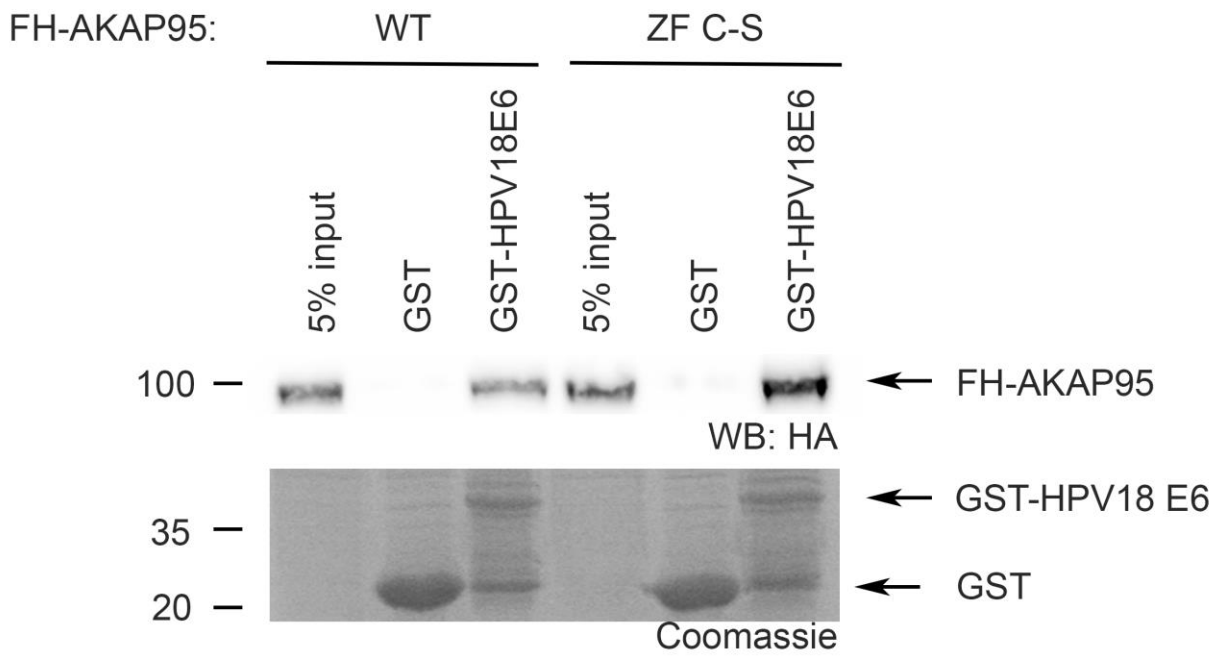

Figure 4.20: Disruption of both AKAP95 zinc fingers does not impair the AKAP95-E6 interaction. Purified GST or GST-HPV18E6 were incubated with lysate derived from 293T cells expressing either the FH-wild type or FH-ZFC-S AKAP95 mutant. Co-purifying proteins were separated by electrophoresis and detected by Western blotting using an antibody against the HA tag. The top panel represents the immunoblots while the lower panel demonstrates loading of the GST fusion proteins. Representative of two independent experiments.

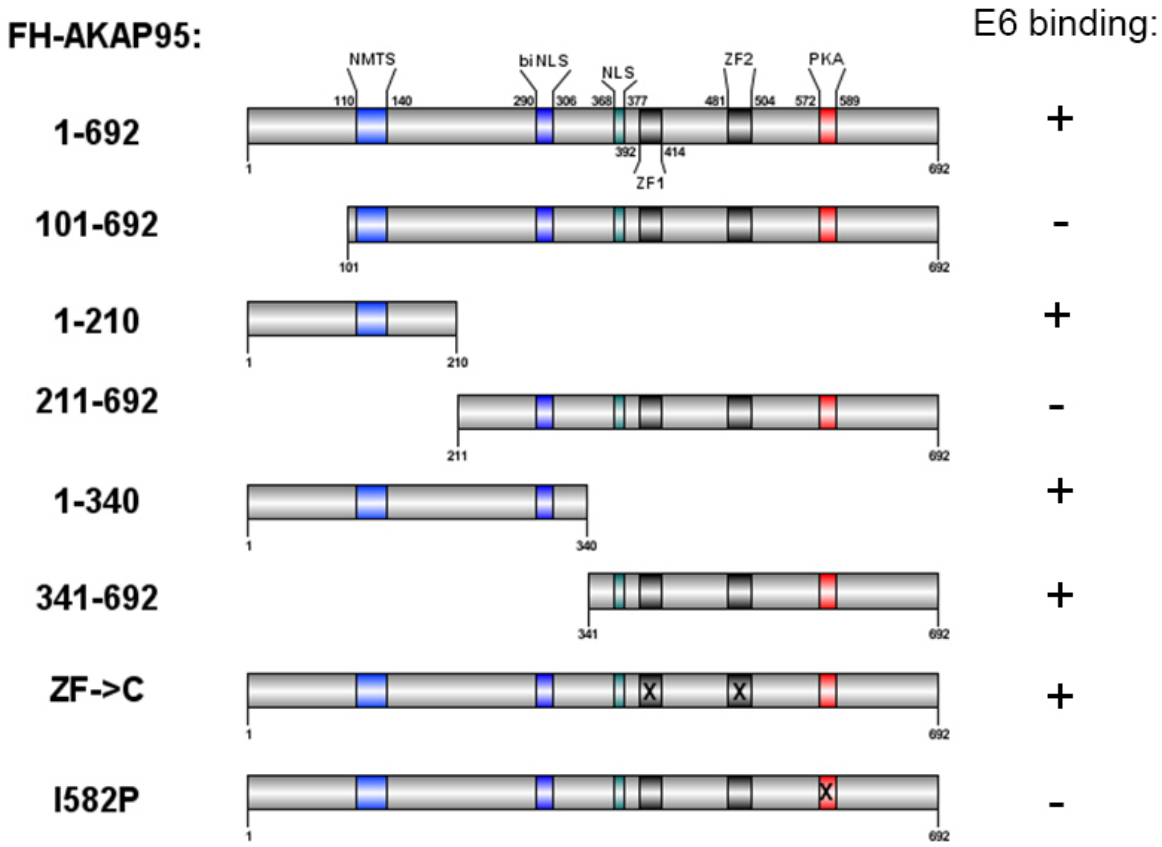

Figure 4.21: Schematic of the AKAP95 domains required for its interaction with E6. The various full length FLAG/HA-tagged AKAP95 mutants are shown with all known domains marked. The column labelled 'E6 binding' highlights binding to GST-HPV18E6 in GST pull down assays where '+' indicates binding and '-' indicates no binding. NMTS: nuclear matrix targeting sequence. BiNLS: bilateral nuclear localisation signal. NLS: nuclear localisation signal. ZF: zinc finger. PKA: PKA-RII binding site. Image generated using DOG2.0 software.

4.3 Discussion

The replication of the HPV18 genome in primary HFKs was associated with increased activity of the PKA holoenzyme. Bearing in mind that many viruses modulate signal transduction pathways by targeting individual components of the pathway, it was important to determine if HPV interacts with factors associated with PKA signalling, including pathway regulators. Scrutiny of publicly available databases for HPV protein (E2, E6 and E7)-protein interactions highlighted a potential interaction between diverse E6 proteins, including HPV18, and the nuclear PKA-anchoring protein AKAP95.

After first expressing and ensuring that the GST fusions of AKAP95 and HPV18 E6 were functional, this novel virus-host interaction was then confirmed through both *in vitro* and *in vivo* approaches. Using lysates derived from immortalised cervical cancer cells as well as primary HFK cells maintaining HPV18 genomes, GST pull-downs and co-immunoprecipitation experiments confirmed the presence of an AKAP95-HPV18 E6 complex in cells.

While this is, at least to our knowledge, the first description of an HPV oncoprotein interacting with a cellular AKAP, viruses such as HIV and adenovirus, also interact with AKAPs.

For HIV-1, viral reverse transcriptase, the protein responsible for converting viral RNA to DNA, directly interacts with AKAP194 (Lemay et al., 2008), a cellular AKAP that binds to both PKA-RI and-RII holoenzymes and targets them to various subcellular locales, including the outer mitochondrial membrane, endoplasmic reticulum and nuclear membrane (Herberg et al., 2000; Huang et al., 1999). Functional analysis using siRNA knockdown experiments showed that the AKAP was involved in HIV-1 infection of HeLa cells. In addition, loss of the AKAP impaired the reverse transcription steps of the viral

replicative cycle; siAKAP194-transfected cells had 40-50% of early and late reverse transcriptase products, resulting in lower levels of viral protein expression. A mutant reverse transcriptase protein that could not bind to AKAP149 showed major defects in early and late stages of reverse transcription, further confirming a role for the AKAP in HIV-1 transcriptional control (Lemay et al., 2008). How the AKAP regulates these functions is unclear however it can bind to various proteins that may influence viral transcription (Warren et al., 2009). For example, AKAP149 anchors both PKA and PDE4 to mitochondria, both of which have been implicated in viral replication (Rabbi et al., 1998; Sun et al., 2000). In addition, PKA is thought to be involved in viral reactivation from latently infected cells (Rabbi et al., 1998) and is also incorporated into the HIV-1 capsid, which may be important for viral infectivity (Cartier et al., 2003). Therefore, PKA signalling, at least in part mediated by AKAPs, is likely to be a key regulator of the HIV-1 life cycle.

In addition, the adenovirus (Ad) type 12 E1A12S oncoprotein acts as a viral AKAP and redistributes PKA-RII holoenzymes to the nuclei of infected cells where it activates the viral E2 promoter, whose products are essential for viral replication (Fax et al., 2001). The Ad type 5 E1A protein was later shown to bind to both PKA-RI and -RII subunits through an AKAP-like domain in the protein's amino terminus (King et al., 2016). In contrast to Ad12, Ad5, despite binding both regulatory subunits, only redistributed PKA-RI subunits during infection. Knockdown of the individual PKA subunits (RI, RII, Cα) only affected expression of viral proteins from the E3 and E4 transcriptional units, which are early transcribed regions whose products regulate the immune response of infected cells (E3) metabolism of viral mRNAs, viral DNA replication and modulation of host protein synthesis (E4). Furthermore, knockdown of PKA subunits reduced viral titre. Together, the

data suggest that the E1A-PKA axis was involved in regulating viral transcription, protein expression and production of viral progeny (King et al., 2016). Further work from the same group showed that this PKA targeting ability was shared between other E1A proteins from diverse Ad species (Ads 3, 9, 12 and 40), all of which contain the AKAP-like motif in the proteins' amino terminus previously identified for Ad5. Despite this conserved motif, the E1A proteins displayed type-specific interactions with the PKA regulatory subunits, with Ad9 relocalising RI and Ad3 relocalising RII from the cytoplasm to the nucleus. Interestingly, however, these apparent preferences can be modulated by changes in expression of the regulatory subunits; loss of PKA-RI in cells expressing Ad5 E1A resulted in its interaction with PKA-RII instead. Finally, knockdown of the PKA subunits, similar to Ad5, resulted in reductions in viral genome replication and viral titre, indicating that the viral AKAP played an important role in the viral life cycle (King et al., 2018). Together, these data highlight the important role that AKAPs play in the life cycle of different viruses, which indicate a precedent for the E6-AKAP95 interaction playing a functional role in the life cycle of HPV.

Following on from the confirmation that AKAP95 bound HPV18 E6 *in vitro* and *in vivo*, whether AKAP95 was a common binder of diverse E6 proteins was then examined. The mass spectrometry analysis described in **Table 4.1** highlighted a potential interaction with E6 proteins from a number of high-risk types in the alpha genera, but not HPV16 which is the most prevalent HPV type in cancers. In fact, a GST-HPV16 E6 protein, when assayed for its ability to bind to AKAP95, only showed a very faint interaction with AKAP95, suggesting that HPV16 E6 was not a major binder of the protein. Interestingly, E6 proteins of several HPV types of the beta genera were identified as AKAP95 binders in the mass spectrometry analysis. These E6 proteins were from virus types linked to skin

carcinogenesis. Furthermore, the mass spectrometry analysis did not report an interaction between the E6 protein of HPV6b, a low-risk alphavirus and AKAP95, and the data presented here did not show any apparent binding of the low-risk HPV11 E6 to AKAP95 in GST pull-downs. The fact that the E6-AKAP95 interaction appears to be restricted to those virus types linked to cancer development may suggest that it plays an important role in HPV associated carcinogenesis. Furthermore, the E6-AKAP95 interaction is maintained in HeLa cervical cancer cells, which may again suggest it is relevant for HPV associated cancer. Recently, AKAP95 has been shown to be required for cellular transformation in primary mouse embryonic fibroblasts, whereby its loss impedes cellular transformation by the oncogenes H-RAS^{G12V} and c-MYC in oncogene co-operation assays in tissue culture and *in vivo* tumorigenicity assays in nude mice. These data suggest that AKAP95 is required for the oncogene-induced transformation of normal cells to cancer cells (Wei et al., 2019), giving further weight to the possibility that the E6-AKAP95 interaction is relevant for HPV carcinogenesis.

A surprising result was the requirement for an intact E6 PBM for AKAP95 binding and this was shown to occur *in vitro* by GST-AKAP95 pull-down of E6 mutants with a disrupted PBM, but also *in vivo* in HFKs harbouring intact HPV18 genomes that express a mutant ΔPDZE6 protein. Supporting a role for an active E6 PBM in AKAP95 binding was the finding that E6-AKAP95 binding was unaffected by a mutation in the PKA recognition sequence that overlaps with the PBM, suggesting that E6-PDZ targeting and not PKA regulation of the PBM was important for the interaction.

AKAP95 does not contain any appreciable PDZ domain structure so, given that AKAPs often form multiprotein signalling hubs, we next questioned whether the HPV18 E6-AKAP95 interaction required a cellular PDZ protein that is a target of the E6

PBM. Scrutiny of AKAP95 protein-protein interaction databases highlighted potential interactions with the host PDZ proteins hScrib, ZO-1 and ZO-2. This was interesting given that hScrib binds to ZO-2 via its PDZ domains and ZO-2 interacts with ZO-1, suggesting that AKAP95 may be interacting with a multiprotein complex composed of these proteins (Bauer et al., 2010; Itoh et al., 1999; Métais et al., 2005).

In vitro GST pull-down experiments confirmed that GST-AKAP95 interacted with hScrib in the absence of HPV18 E6. The function of this novel protein-protein interaction is unclear, especially as AKAP95 is mainly nuclear and cytoskeletal in localisation and hScrib has been reported to largely localise to sites of cell to cell contact, although subcellular fractionation experiments have revealed a significant proportion of the protein in keratinocyte nuclear fractions (Kranjec et al., 2016). Nuclear hScrib is also seen in hepatocellular carcinoma, albeit the functional relevance is unclear (Kapil et al., 2017). This raises the possibility that AKAP95 binds to a subpopulation of hScrib protein for an as yet unidentified nuclear function. To confirm the exact subcellular fraction of hScrib that interacts with AKAP95, proximity ligation assay could be carried out using antibodies against both proteins; this technique allows for visualisation of protein interactions in fixed cell and/or tissue samples (Klaesson et al., 2018).

This is not the first report of a PDZ protein associating with a cellular AKAP. Trafficking of the β_1-adrenergic receptor (β_1-AR) back to the cell membrane after agonist-promoted internalisation is important for re-sensitisation of β_1-AR signalling. This recycling mechanism requires the binding of AKAP79 to the carboxyl terminus of β_1-AR, leading to AKAP79-bound PKA-dependent phosphorylation of the receptor, which is important for receptor recycling (Gardner et al., 2006). Subsequent work from the same group showed that the AKAP79-β_1-AR receptor interaction was mediated by the PDZ protein Dlg1. In

addition, the Dlg1-AKAP79 interaction was responsible for targeting PKA to the β_1-AR, creating a PDZ-signalosome important for PKA phosphorylation of β_1-AR at serine 312 and subsequent receptor recycling (Gardner et al., 2007).

Co-immunoprecipitation experiments in HFKs maintaining either wild type or ΔPDZE6 genomes showed that only wild type E6 interacted with both AKAP95 and hScrib and this interaction was lost in cells maintaining ΔPDZE6 genomes. These data suggest that the E6-AKAP95 interaction requires an intact PBM as well as the presence of hScrib. This experimental approach cannot, however, exclude that other PDZ domain-containing proteins that are the targets of the E6 PBM also play a part in mediating the E6-AKAP95 interaction. To examine whether this is the case, siRNA knockdown of cellular PDZ domain-containing proteins in the context of the wild type E6 protein, combined with either GST pull-down or co-immunoprecipitation experiments to examine the E6-AKAP95 interaction, would provide further proof of the identity of the PDZ domain-containing protein responsible for mediating the E6-AKAP95 interaction. In addition, while the co-immunoprecipitation experiments suggested a multiprotein complex of E6-hScrib-AKAP95, they cannot confirm the presence of this tertiary complex in cells. To provide evidence for this complex, affinity purification techniques such as two-step co-immunoprecipitation could be employed. This technique involves sequential co-immunoprecipitations using antibodies against two members of the protein complex under study and results in the highly selective enrichment of stable protein complexes from cell lysates, which is thought to exclude non-specific binders and transient low abundance complex proteins (Sciuto et al., 2019).

What remains unclear is, given that both HPV16 and HPV18 interact (as well as the other alpha HPV types defined as type I carcinogens) and degrade hScrib *in vitro* (Nakagawa

and Huibregtse, 2000), why AKAP95 binding appears to be restricted to HPV18 E6 and from the mass spectrometry data, HPV52 and 45, but not HPV16 and 33. The ability of these E6 proteins to target AKAP95 does not appear to be species specific, with the mass-spectrometry identified binders HPV18 and 45 in species 7 and 52 in species 9 and the non-binders HPV16 and 33 in species 9 (Bernard et al., 2010). Interestingly, analysis of the PBM sequence of the high-risk types identified in the mass spectrometry screen suggested two common features; the AKAP95 binders all contained a terminal valine residue (HPV18 E6: ETQV, HPV45 E6: ETQV, HPV52 E6: VTQV) and the non-binders contained a terminal leucine residue (HPV16 E6: ETQL, HPV33 E6: ETAL). As this terminal E6 PBM residue is important for dictating substrate specificity, with a valine residue preferring interaction with Dlg1 and leucine with hScrib (Thomas et al., 2005), perhaps the fact that all the AKAP95 binders contain a terminal valine residue suggests that this is an additional targeting mechanism for the virus to interact with hScrib. In addition to these carboxyl-terminal sequences, differences in other sequences, such as those upstream of the PBM, may also be relevant for this binding (Luck et al., 2012). However, for the beta HPV E6 proteins identified in the mass spectrometry screen, there is no evidence that these proteins encode PBMs. If these are true interacting partners of AKAP95 then this interaction must occur via a different mechanism. It is possible that for these E6 proteins, their interaction with AKAP95 is direct and not mediated by a cellular PDZ domain-containing proteins. Alternatively, E6 may bind to AKAP95 through a non-PDZ domain-containing protein; re-interrogation of both the E6- and AKAP95-mass spectrometry data identified eight proteins common to both the beta E6- and AKAP95-immunoprecipitates, including regulators of actin-dependent ATPase activity, cytoskeletal protein and RNA binding processes.

Extending this approach, we next determined the E6-binding region on AKAP95. Using various AKAP95 mutant expression constructs, these experiments showed that amino acids 1-100 and the PKA-RII binding site were involved in mediating the HPV18 E6-AKAP95 interaction. AKAP95 through these amino-terminal residues interacts with a variety of proteins known to be involved in RNA processing and transcription, including several hnRNP proteins and RNA polymerase II (Hu et al., 2016), although what influence this has on mediating the E6-AKAP95 interaction is at present unclear. The finding that the PKA binding site was required for this interaction was interesting given that hScrib is a known substrate of PKA. Therefore, one possible function of this hScrib-AKAP95-PKA complex may be to regulate phosphorylation either of hScrib itself or other downstream substrates. In addition, phosphorylation of hScrib by PKA alters hScrib interactions with its major binding partner, protein phosphatase 1γ (PP1γ; Kawana et al., 2013; Nagasaka et al., 2010), and therefore this complex may modulate the hScrib interactome. The change in the hScrib-PP1γ interaction mediated by PKA likely results in the formation of a feedback loop to control hScrib phosphorylation, although what effect this has on other hScrib functions (such as its ability to downregulate ERK activation and regulate oncogenic-associated cell transformation) is unclear (Kawana et al., 2013).

Overall, the data presented in this chapter identified a novel interaction between HPV18 E6 and the nuclear PKA-anchoring protein AKAP95. Domain mapping experiments showed that this interaction was dependent on the integrity of the E6 PBM. Analysis of AKAP95-PDZ interactions highlighted a novel interaction between AKAP95 and hScrib, which may mediate the binding of E6 to AKAP95. The reverse domain mapping experiments showed that the first 100 amino acids and the PKA-RII binding site of AKAP95 is required for its interaction with E6. Taken together, these data suggest the

presence of a multiprotein complex composed of HPV18 E6, hScrib, AKAP95 and PKA-RII, which is illustrated in **Figure 4.22** below.

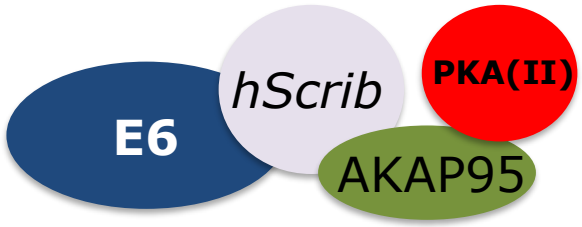

Figure 4.22: Schematic of the proposed E6-AKAP95 complex. The data presented in this chapter identified E6 complexes containing hScrib and AKAP95, with a requirement for PKA-RII binding to the AKAP, in HFK-18 cells.

CHAPTER 5 FUNCTIONAL CHARACTERISATION OF THE HPV18 E6-AKAP95 INTERACTION

5.1 Introduction

While the full repertoire of signal transduction pathways targeted by E6 is not known, what is clear is that these E6 interactions with the host signalosome make significant contributions to the completion of the viral life cycle. Thus, the use of HPV life cycle models has been very insightful into understanding the role of specific E6-host interactions in the infectious life cycle of the virus. One of the best researched E6 interactions is the ability of E6 to target the tumour suppressor p53, which is upregulated in response to unscheduled cell cycle re-entry in E7-expressing cells.

As described in section 1.2.4 in the introduction of this thesis, the ability of E6 to target p53 is important during the virus life cycle where it contributes to replication of viral DNA and episomal maintenance (Flores et al., 2000; Kho et al., 2013; Lorenz et al., 2013; Park and Androphy, 2002; Thomas et al., 1999; Wang et al., 2009). Other E6 interactions are also important however in regulating viral genome and DNA amplification.

In an HPV18 life cycle model in primary foreskin keratinocytes in which viral episomal establishment is not dependent on E6 immortalizing functions, an E6 null mutant genome displayed high levels of p53, a less hyperproliferative phenotype, loss of late protein expression and amplified poorly on organotypic raft culture compared to the wild type genome. Knockdown of p53 or expression of a wild type E6 protein partially restored viral genome amplification in raft culture. In the same study, the effect of various E6 missense mutants was also tested. These mutant E6 proteins contained either substitution of the

phenylalanine at position 4 to a valine (F4V; unable to destabilise p53) or leucine (F4L; partial degrader of p53). Another mutant containing a substitution of F45, F47 and aspartic acid (D) 49, to tyrosine (Y), Y and histidine, the corresponding residues in low-risk E6 proteins, was used, which does not destabilise p53. Expression of these missense mutants could not restore the phenotype of the wild type protein. Unexpectedly, two of these missense mutants (F4L, F4V) amplified in raft culture, albeit to a lesser extent than the wild type protein, and only in cells lacking p53. Together, these observations indicate that additional virus-host interactions are important for viral DNA amplification (Kho et al., 2013).

One such host interaction critical for viral DNA amplification is STAT3. HPV18 replication in monolayer primary HFKs induces the dual phosphorylation of STAT3 at Y705 and S727 residues, compared to control cells. In addition, this enhanced STAT3 phosphorylation is maintained throughout differentiation only in HFK-18 cells. Overexpression experiments using the viral oncoproteins E5, E6 and E7 in C33A cells showed that E6 could promote this dual phosphorylation and activation of STAT; this dependency on E6 for STAT3 phosphorylation was also confirmed in the primary HPV18 life cycle model. In addition, expression of E6 in C33A cells, but not E5 nor E7, induced the activation of two STAT3-dependent reporter plasmids (β-casein, pro-opiomelanocortin), and this was reduced in E6-expressing cells treated with STAT3 inhibitors. Furthermore, E6 also induced the transcription of the STAT3-dependent genes, including Bcl-$_X$L and cyclin D1. The same study also analysed the effect of several E6 mutants on STAT3 phosphorylation, with STAT3 phosphorylation increased by E6 in a p53 and PDZ-independent manner through the actions of Janus kinases and members of the MAPK family. Loss of STAT3, either through siRNA knockdown, use of a

phosphorylation site dominant-negative form of the protein or STAT3 inhibitor, showed that it was involved in cell cycle progression and maintenance of the viral genome in undifferentiated keratinocytes as well as viral genome amplification during differentiation. Finally, transduction of keratinocytes with lentiviruses expressing either control or the dominant-negative mutant grown in 3D showed that STAT3 was required for expansion of the suprabasal compartment and delayed differentiation in cells maintaining HPV18 genomes (Morgan et al., 2018). Overall, the data indicate that the E6-STAT3 interaction is critical for both viral DNA maintenance and genome amplification on keratinocyte differentiation.

In addition to the above E6 interactors, other E6-host interactions such as the PDZ domain-containing proteins Dlg1 and hScrib are also relevant for HPV DNA replication. Studies in cells harbouring high-risk HPV genomes showed that this PDZ targeting ability contributes to the establishment, maintenance and amplification of viral episomes for several oncogenic HPV types (Delury et al., 2013; Lee and Laimins, 2004; Nicolaides et al., 2011). Furthermore, there is some co-operation between the E6 p53 and PDZ targeting functions, with knockdown of p53 by siRNA rescuing episomal maintenance in cells lacking the E6 PBM (Brimer and Vande Pol, 2014). E6-PDZ interactions such as hScrib are important for regulating E6 oncoprotein expression (Kranjec et al., 2016; Nicolaides et al., 2011).

In the previous chapter, a novel interaction between HPV18 E6 and the nuclear PKA-anchoring protein AKAP95 was identified. Given that E6 functions play crucial roles at many stages of the virus life cycle, it was of interest to determine the functional consequence(s) of the E6-AKAP95 interaction in cells.

5.2 Results

5.2.1 Influence of HPV18 E6 on AKAP95 expression and localisation

5.2.1.1 E6 does not direct the degradation of AKAP95

One of the best-characterised features of high-risk E6 is to induce degradation of a subset of host proteins by association with E6-AP, including the tumour suppressor p53 (Huibregtse et al., 1991) and cellular PDZ domain-containing proteins such as Dlg1 (Gardiol *et al*., 1999; Kiyono et al., 1997). Therefore, whether E6 could direct degradation of AKAP95 was investigated in transient overexpression experiments. HPV negative cervical cancer C33A cells were transfected with HPV18 E6 and AKAP95 (Myc-AKAP95) expression vectors, individually or in combination and then residual AKAP95 expression determined by Western blotting 48 hours later. In **Figure 5.1 A**, expression of E6 did not significantly alter levels of endogenous (cf. vector and E6) or overexpressed AKAP95 (cf. E6 and E6 and Myc-AKAP95). To ensure that the overexpressed E6 was functional in the degradation of known targets, lysates used in experiments shown in **Figure 5.1 A** were examined for p53 levels as an indicator of E6 degradation activity. In **Figure 5.1 B**, expression of E6 results in a decrease of endogenous p53 levels by approximately 50% compared to control transfections, suggesting that the exogenously expressed E6 is functional. Quantification of three independent experiments of the data shown in **panel A** is given in **Figure 5.1 C**, indicating that there are no significant differences in the expression of either endogenous or overexpressed AKAP95 in cells expressing HPV18 E6.

Further examination of the data showed that overexpression of AKAP95 did not alter E6 levels, suggesting that the interaction between these two proteins does not lead to stabilization of the oncoprotein, at least in transient transfection experiments (**Figure**

5.1 A). The interaction also did not affect the ability of E6 to degrade p53; in the presence of both E6 and Myc-AKAP95, the level of p53 protein was reduced to a similar level as E6 alone. These data indicate that AKAP95 levels are not affected by E6, suggesting that this E6 interactor is not a degradation target of HPV18 E6.

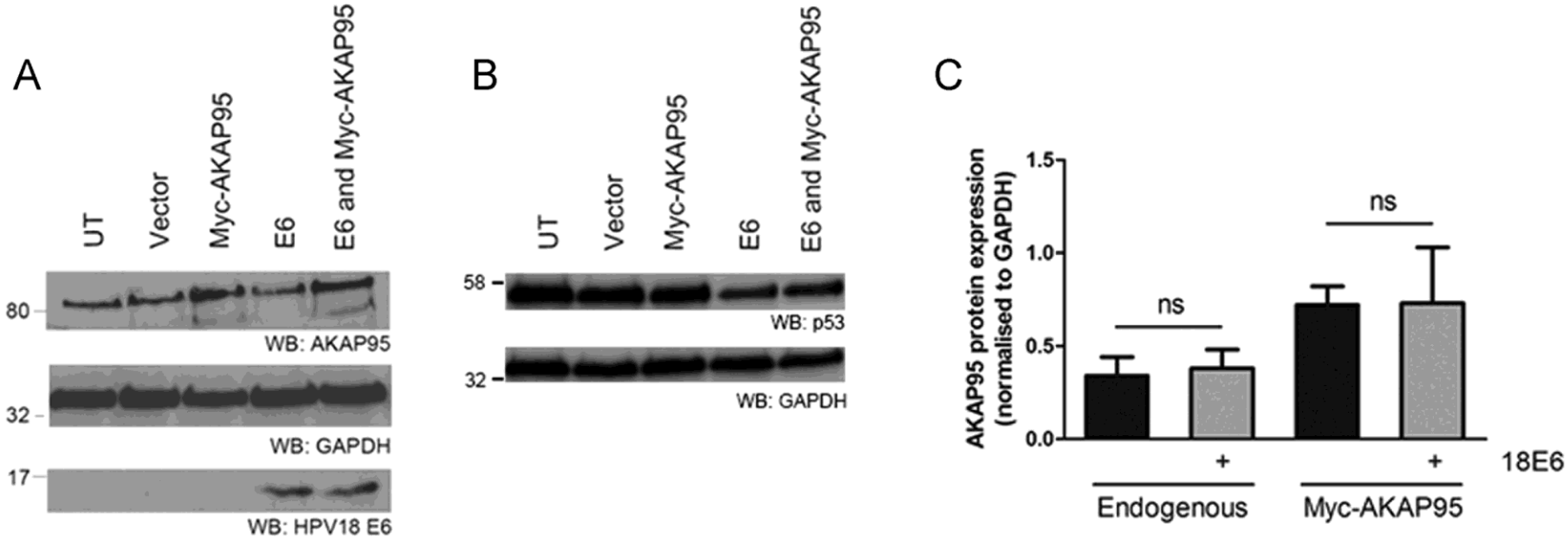

Figure 5.1: HPV18 E6 does not degrade endogenous or overexpressed AKAP95 in transient overexpression experiments. **A**: C33A cells were transfected with the indicated expression vectors and AKAP95 protein levels determined by Western blotting 48 hours later. **B**: Lysates taken from panel A were examined for p53 levels as an indicator for E6 degradation activity. **C**: Quantification of AKAP95 expression from cells expressing HPV18 E6, taken from three independent experiments. Note that endogenous AKAP95 expression represents comparisons between vector and E6 transfections. NS: not significant.

To examine the E6-AKAP95 interaction in a more physiological context, lysates were prepared from donor matched HFK cells or those maintaining HPV18 genomes and levels of AKAP95 were determined by Western blotting. In **Figure 5.2 A**, there was no significant difference in AKAP95 expression between HFK or HFK-18 cells, shown with quantification from two independent foreskin donors in **Figure 5.2 B**. Additionally, HFK-18 cells show no differences in AKAP95 protein expression between vehicle (DMSO) and treatment with the proteasome inhibitor MG132, whereas the p53 protein expression was rescued (**Figure 5.2 C**). Quantification of three independent MG132 experiments is shown in **Figure 5.2 D**, together with levels of p53 as a positive control for MG132 inhibition of the proteasome. These data show that E6 does not direct the degradation of AKAP95 in primary HFK cells maintaining HPV18 genomes. The experiment was repeated using HeLa cells that harbour HPV18 integrants and, as observed in the HFK-18 cells, p53 expression was rescued upon treatment with MG132 but AKAP95 levels were unaffected (data not shown).

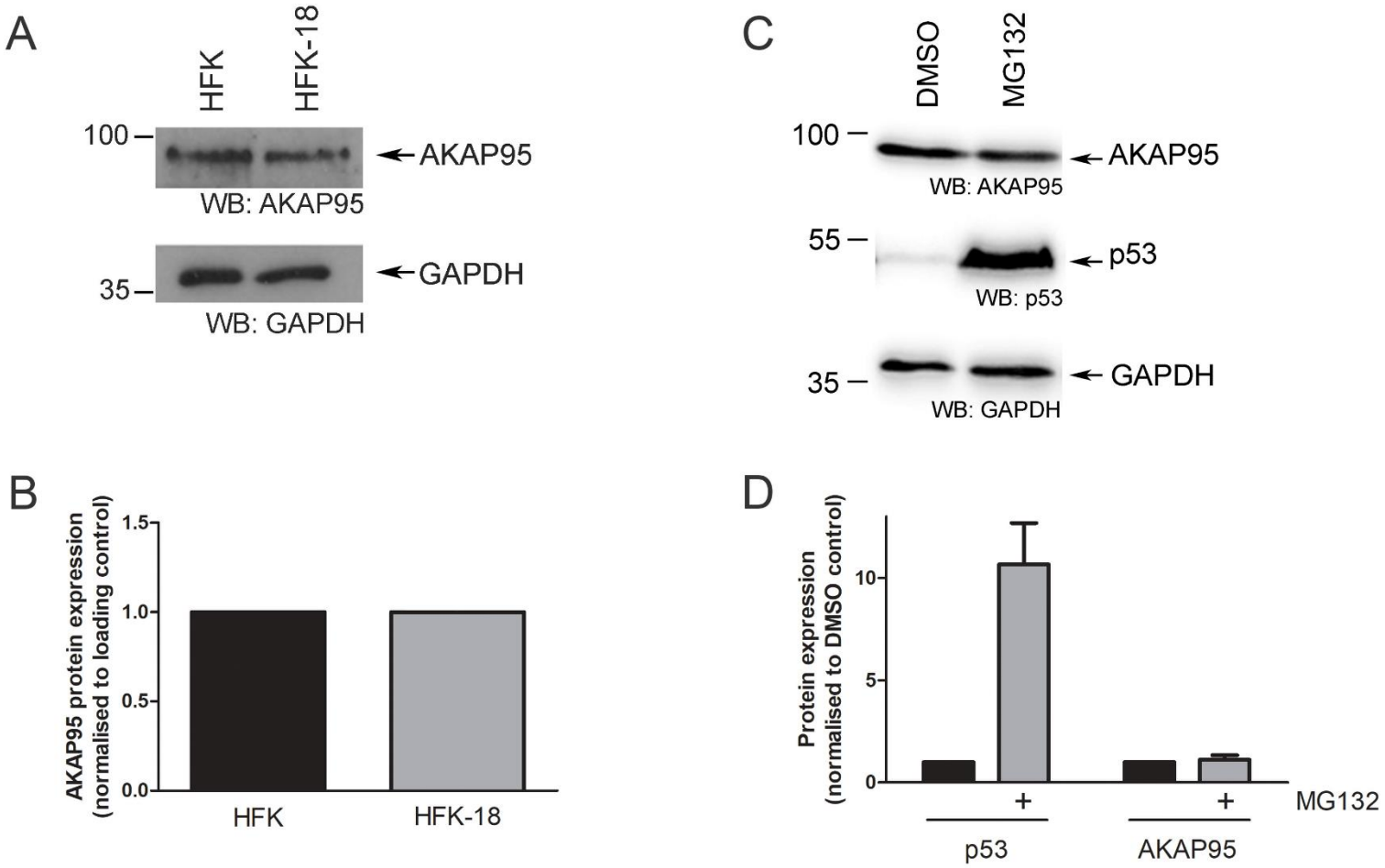

Figure 5.2: Endogenous HPV18 E6 does not direct degradation of AKAP95. A: Donor matched HFK or HFK-18 cells were immunoblotted for AKAP95 expression levels with relative quantification of two donors shown below in panel **B**. **C:** HFK-18 cells were treated with the proteasome inhibitor MG132 for four hours and AKAP95 protein levels determined by Western blotting. Levels of p53 were used as a positive control for proteasome inhibition, with the results of three independent experiments shown in panel **D**.

5.2.1.2 E6 does not induce subcellular relocalisation of AKAP95 in monolayer grown cells

The data presented in **Figures 5.1 and 5.2** indicate that E6 does not direct the degradation of AKAP95 either in transient overexpression studies or in cells immortalised or transformed by HPV18. While E6 can target several host proteins for degradation, it can also induce redistribution of host proteins, such as the PDZ polarity protein Par3 (Facciuto et al., 2014). Whether the expression of HPV18 E6 was associated with subcellular redistribution of endogenous AKAP95 was examined using a combination of overexpression experiments and more physiological experiments using primary keratinocytes maintaining HPV18 genomes.

In **Figure 5.3**, C33A cells were transiently transfected with HPV18 E6 and the subcellular localisation of endogenous AKAP95 determined by indirect immunofluorescence using specific antibodies. In these experiments, cells were also stained for p53 as a surrogate marker for E6 expression as E6 antibodies are poor at detecting E6 by immunostaining. In control C33A cells, AKAP95 was predominantly nuclear with a diffuse uniform localisation pattern and excluded from nucleoli. There was also a low level of staining in the cytoplasm. In cells expressing E6 (C33A-E6: indicated by white arrows and negative for p53 expression), AKAP95 localisation remained nuclear and excluded from nucleoli with a low level of cytoplasmic staining, suggesting that exogenously expressed E6 does not redistribute endogenous AKAP95.

Next, primary HFK or HFK-18 cells were used to examine AKAP95 localisation in a physiological cell system **(Figure 5.4)**. As in C33A cervical cancer keratinocytes, in primary keratinocytes, AKAP95 was largely confined to the nucleus in a uniform staining pattern but excluded from the nucleoli. The subcellular localisation of AKAP95 was

similar in HFK-18 cells except that the nuclear staining was less uniform and more patchy in appearance. A low level of AKAP95 staining occurred in the cytoplasm of both HFK and HFK-18 cells. These data suggest that the subcellular localisation is of the AKAP is not grossly affected by either overexpression of E6 or in cells harbouring intact HPV18 genomes and expressing physiological levels of the E6 oncoprotein. The less uniform nuclear staining pattern (cf. cells indicated by white arrows in HFK and HFK-18 images) may indicate that there is some intranuclear redistribution of the AKAP in cells maintaining HPV18 genomes; however, this requires further investigation.

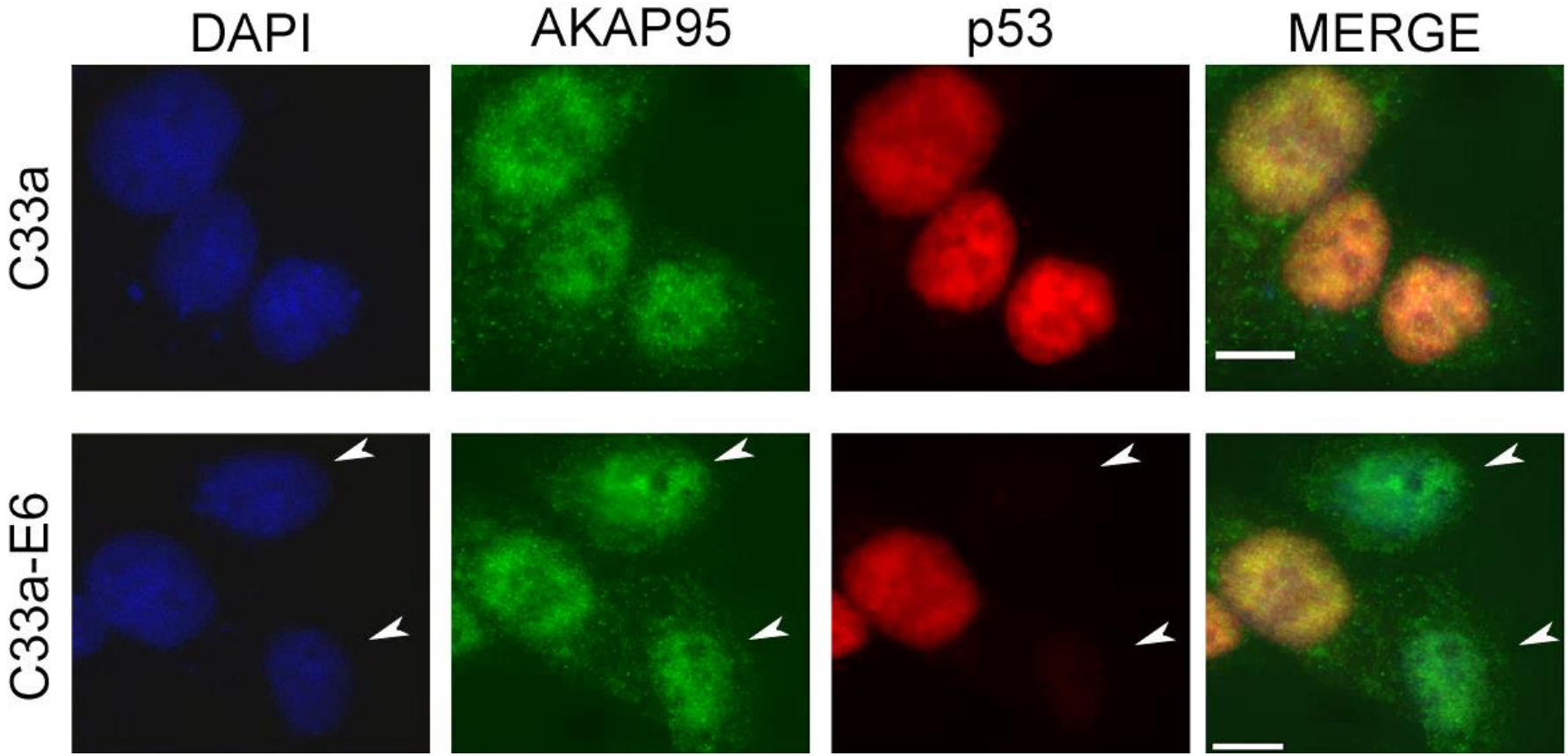

Figure 5.3: Expression of E6 does not induce subcellular redistribution of endogenous AKAP95 in C33A cells. C33A cells either mock transfected or transfected with an expression vector for HPV18 E6 (C33A-E6) were fixed in 4% paraformaldehyde and processed for indirect immunofluorescence, before staining with the indicated antibodies. White arrows in C33A-E6 figures represent C33A cells expressing E6, judged by loss of p53 signal. Scale bar: 10 μM. Merge represents all channels. Identical exposures shown for C33A and C33A-E6 cells. Data representative of three individual experiments.

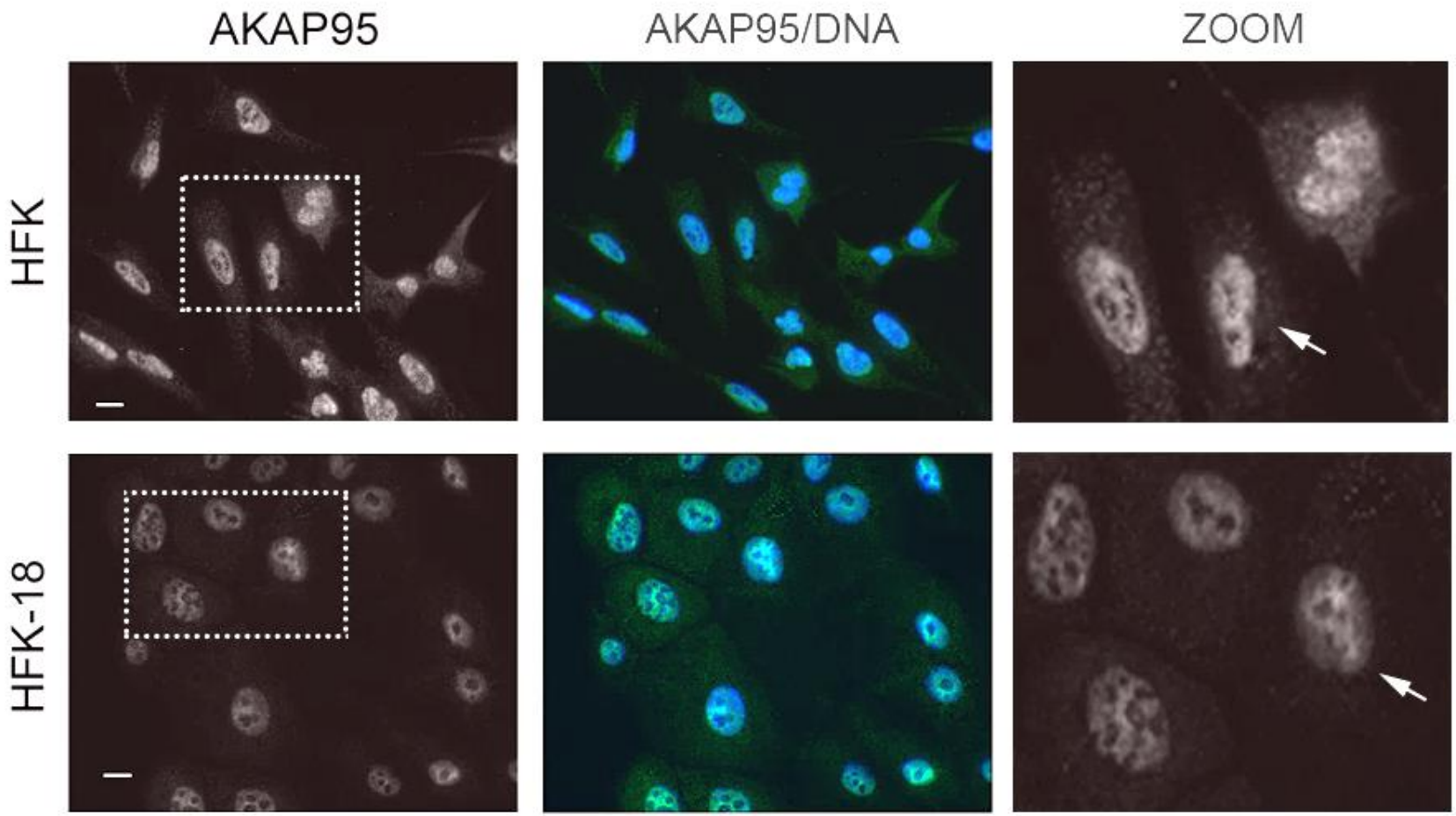

Figure 5.4: AKAP95 subcellular distribution is not grossly altered in HFK cells maintaining HPV18 genomes. Donor matched HFK or HFK cells maintaining HPV18 genomes (HFK-18) were fixed in 4% formaldehyde, permeabilised in 0.1% Triton-X100 incubated with an anti-AKAP95 antibody. Images were taken at identical exposure times. Scale bar represents 10 μm. Note that the zoom panel represents a digital zoom in Adobe Photoshop CS6 based on the cells indicated in the by the dotted panel.

To confirm the lack of clear redistribution of AKAP95 in cells maintaining HPV18 genomes compared to control cells, biochemical fractionation of both HFK and HFK-18 cells was carried out. Markers for specific fractions were used to demonstrate successful fractionation: GRB2 (cytoplasm), E-Cadherin (membrane/organelle associated), p53 (nuclear) and cytokeratin 18 (cytoskeletal). **Figure 5.5** shows that each of the marker proteins was enriched in their expected fraction, demonstrating successful fractionation. Next, lysates were examined for AKAP95 and E6 localisation. In HFK cells, AKAP95 localised to the nuclear (F3) and cytoskeletal (F4) compartments and this was not altered in HFK-18 cells. Note that the buffer used to extract F4 (cytoskeletal fraction) contains SDS, which solubilises both chromatin and the nuclear matrix; AKAP95 is known to associate with both of these structures (Akileswaran et al., 2001; Eide et al., 1998). E6 was present in all fractions in HFK-18 cells, but with an apparent preference for the cytosolic and cytoskeletal fractions. Taken together, these data suggest that HPV18 E6 expressed from intact HPV18 genomes does not redistribute endogenous AKAP95 in primary keratinocytes. In addition, the data show that E6 and AKAP95 are both present in nuclear and cytoskeletal compartments, suggesting that the E6-AKAP95 complex may occur in either or both of these fractions.

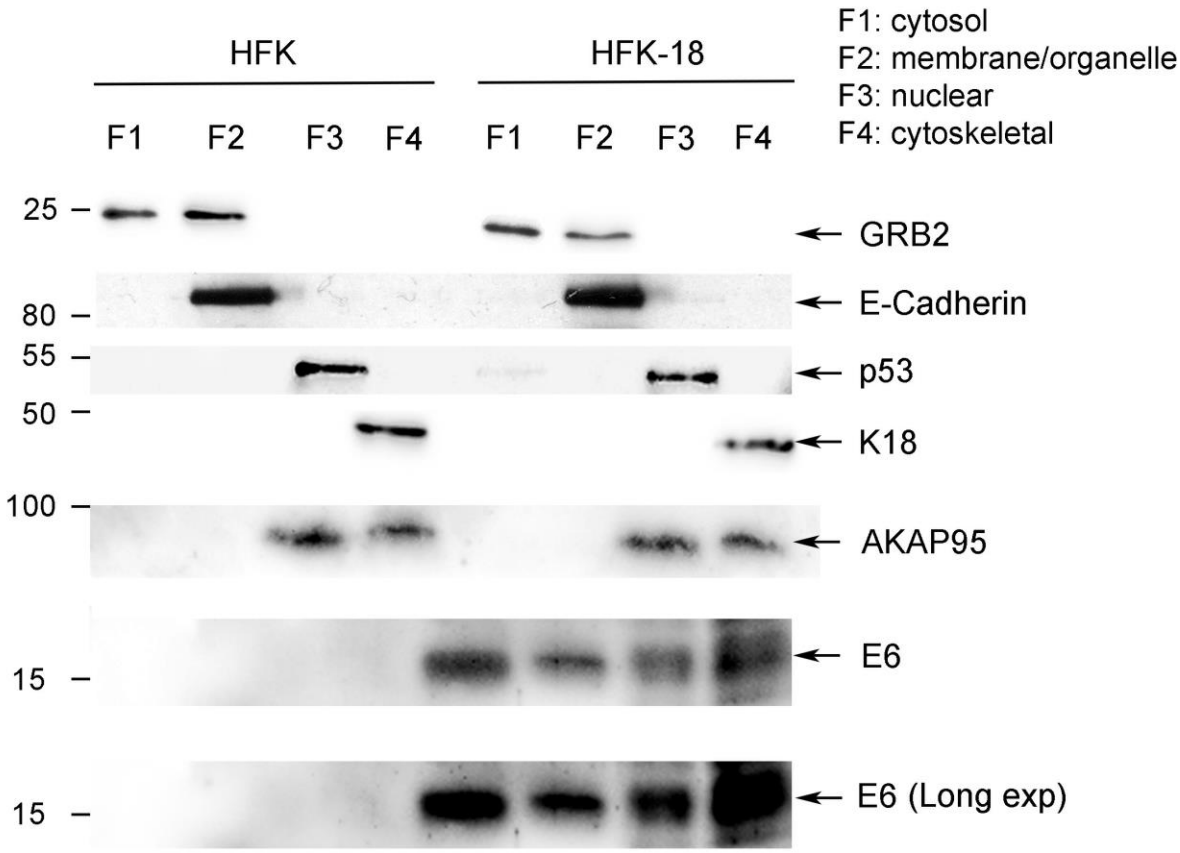

Figure 5.5: HPV18 E6 does not redistribute AKAP95 in primary human foreskin keratinocytes maintaining HPV18 genomes. Donor matched HFK or HFK-18 cells were fractionated using the ProteoExtract Subcellular Proteome Extraction Kit from monolayer grown cells and each fraction examined by Western blotting for the indicated target protein. F1: cytosol, F2: membrane/organelle associated, F3: nuclear and F4: cytoskeletal. Data representative of fractionation of two foreskin donors. Long exp: long exposure.

5.2.1.3 AKAP95 localisation is not altered by HPV18 replication in differentiating epithelium

The data presented so far showed that E6, either overexpressed in isolation or expressed from the complete viral genome, does not redistribute AKAP95 in monolayer grown cells. However, it was important to determine whether there was any effect on AKAP95 expression or localisation during the complete viral life cycle. The productive stages of the viral life cycle are dependent upon keratinocyte differentiation and therefore HFK and HPV18-HFK cells were grown in 3D organotypic raft culture, which accurately recapitulates epithelial differentiation and supports the complete HPV18 life cycle (Knight et al., 2011; Wilson et al., 2007).

As shown in **Figure 5.6**, raft cultures of parental HFKs (**top panel**) showed the typical pattern of keratinocyte differentiation, with each layer clearly identifiable. These layers feature the cuboidal cells that make up the basal layer (stratum basal), slightly larger cells of the lower suprabasal (stratum spinosum) and upper suprabasal (stratum granulosum) layers along with cells of a granular appearance that make up the stratum granulosum. The most superficial layer contains the enucleated cells that make up the cornifying layer (stratum corneum). In cells containing HPV18 genomes (**lower panel**), a similar morphological appearance is apparent except that there is a significant expansion of the suprabasal compartment and retention of cell nuclei throughout the layers.

Formalin-fixed sections were immunostained for AKAP95 (**Figure 5.7**). In HFK cells, AKAP95 localised to bright nuclear foci throughout all layers of the differentiating epithelium and there was no marked difference in localisation in HFK-18 cells, suggesting that activation of the productive cycle of HPV18 does not affect AKAP95 localisation in differentiating epithelium.

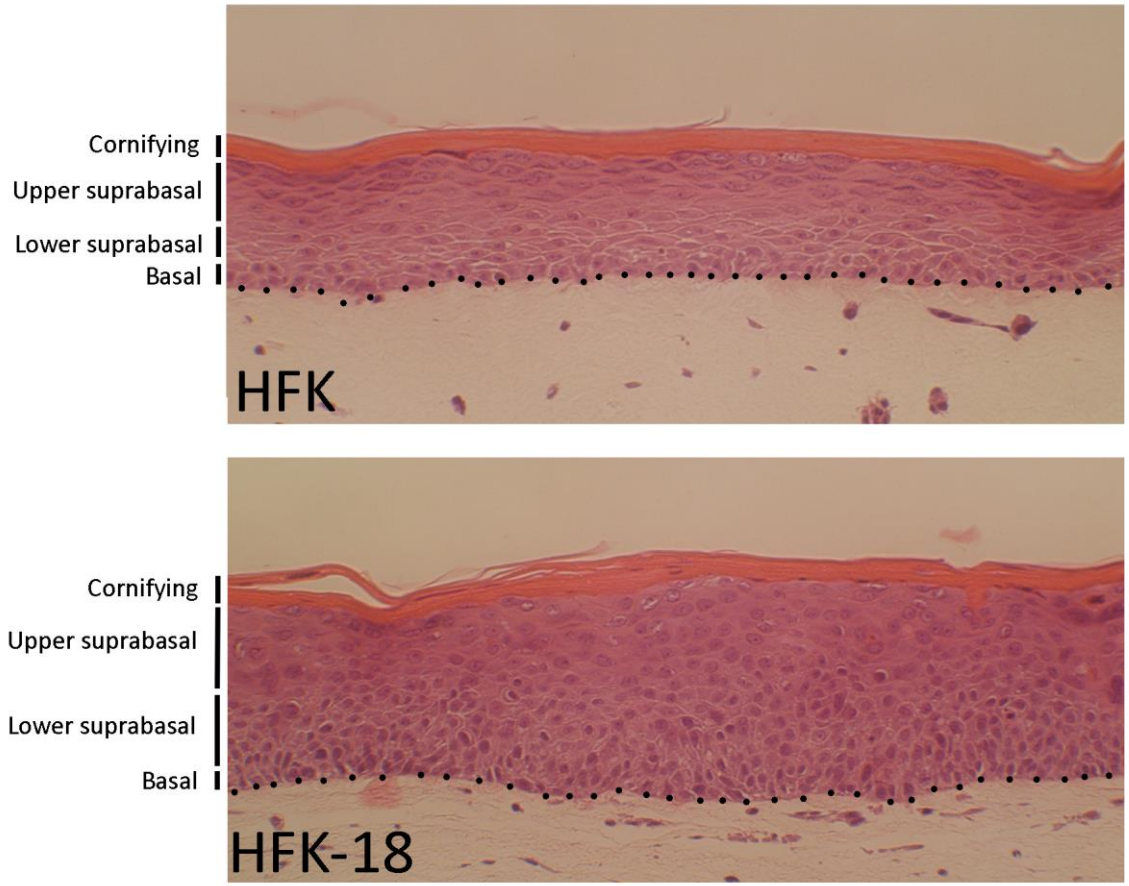

Figure 5.6: Morphology of HPV18 genome containing cells on organotypic raft culture. Donor matched HFK (top panel) or HFK cells maintaining HPV18 genomes (HPV18; bottom panel) were grown in organotypic raft culture for 13 days before fixation and sectioning. Raft sections were then stained with haematoxylin and eosin to show differences in morphology. The black dotted line represents the basal layer. The individual epithelial layers are identified on the left.

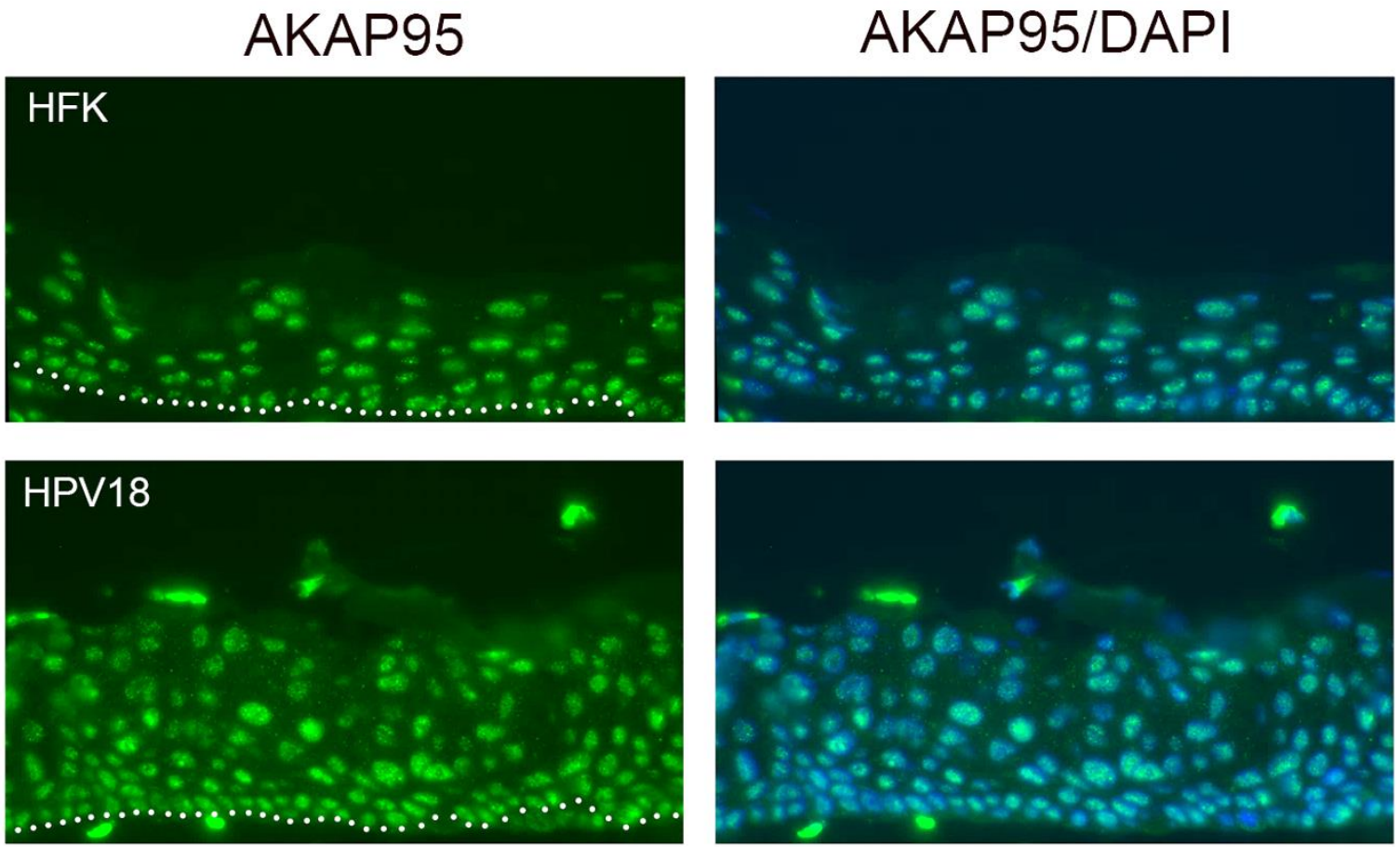

Figure 5.7: AKAP95 expression and localisation are not affected by the late stages of the viral life cycle. Donor matched HFK or HFK cells maintaining HPV18 genomes (HPV18) were grown in organotypic raft culture for 13 days before fixation and sectioning. After epitope retrieval, sections were stained for AKAP95 expression and DAPI was used to highlight cell nuclei. All images were taken at identical exposures. Representative of staining gathered from two donor backgrounds. The white dotted line represents the basal layer.

5.2.2 Functional analysis of loss of AKAP95 in the HPV18 life cycle model

5.2.2.1 Generation of shAKAP95-containing HFK-18 cells

Having shown that AKAP95 is not degraded or relocalised during the virus life cycle, it was then necessary to determine a functional role for this novel E6 interacting partner. For this, human keratinocytes maintaining episomal HPV18 genomes were infected with lentiviruses expressing both single and pooled shRNA constructs against AKAP95 under the control of a doxycycline-inducible promoter. After drug selection, stable cell lines were generated where expression of the shRNA could be activated by adding doxycycline into the cell culture media. **Figure 5.8** shows AKAP95 knockdown following induction of shRNA expression in these cells over a 96-hour experimental time course. The success of AKAP95 knockdown varied at 48 hours between the different shAKAP95 constructs (~40-60% reduction in AKAP95 expression compared to uninduced cells), but by 72 and 96 hours knockdown was >80% compared to uninduced cells for all shAKAP95 constructs tested, indicating that the shAKAP95 constructs successfully reduced protein expression of the AKAP at these time points.

Unfortunately, during this analysis, the HFK-18 shRNA cells developed a mycoplasma infection and so were destroyed. We were not able to repeat these experiments due to time constraints and so the data presented here in the HFK-18 shRNA cells should be considered preliminary until further experiments in additional foreskin donors and/or using additional methods of AKAP95 knockdown are carried out.

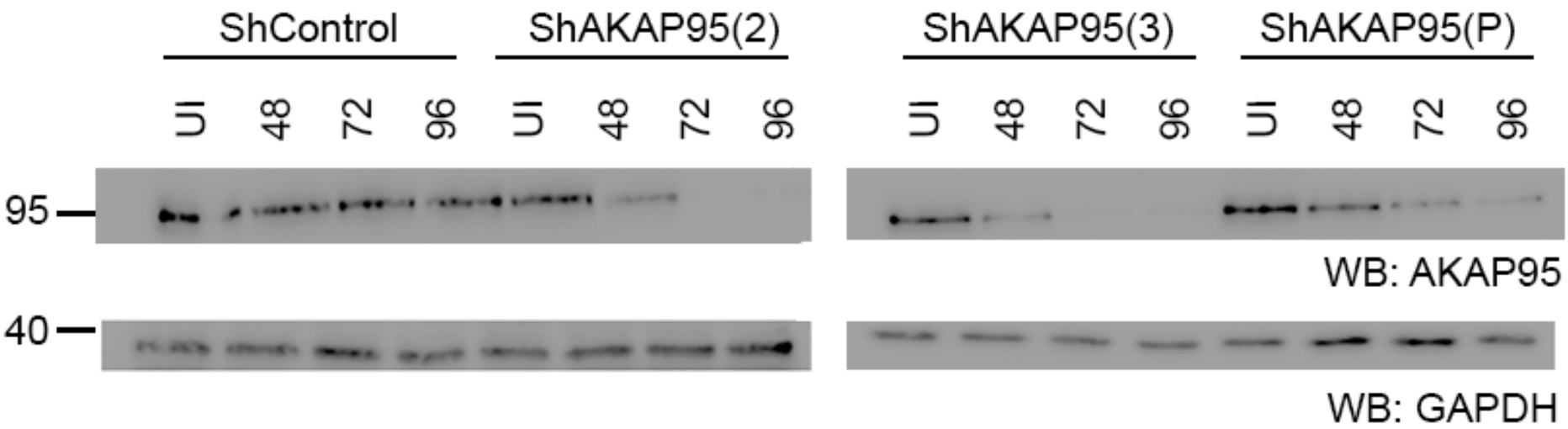

Figure 5.8: AKAP95 expression in HFK-18 cells maintaining shControl or shAKAP95 constructs. HFK-18 cells transduced with the indicated shRNA constructs were uninduced (UI) or induced with doxycycline for the indicated times and levels of AKAP95 protein determined by Western blotting. ShAKAP95(P): pool of shRNA constructs.

5.2.3 Silencing of AKAP95 leads to changes in expression of E6 and E6-PDZ targets

As several viral-host targets are important for regulating the expression of the oncoproteins (Kranjec et al., 2016; Nicolaides et al., 2011), the effect of loss of AKAP95 on E6 and E7 expression, as well as several E6 targets, was examined in HFK-18 cells maintaining the shRNA constructs after a 96 hour induction period with doxycycline (**Figure 5.9**).

Lysates derived from the cells expressing two of the most effective shRNA AKAP95 constructs displayed a significant reduction in AKAP95 protein levels compared to control cells, showing successful induction of the shRNA. Analysis of viral oncoprotein expression in these cells showed that there was a small increase (1.6-fold compared to control cells) in E6 protein but no change in E7 protein levels.

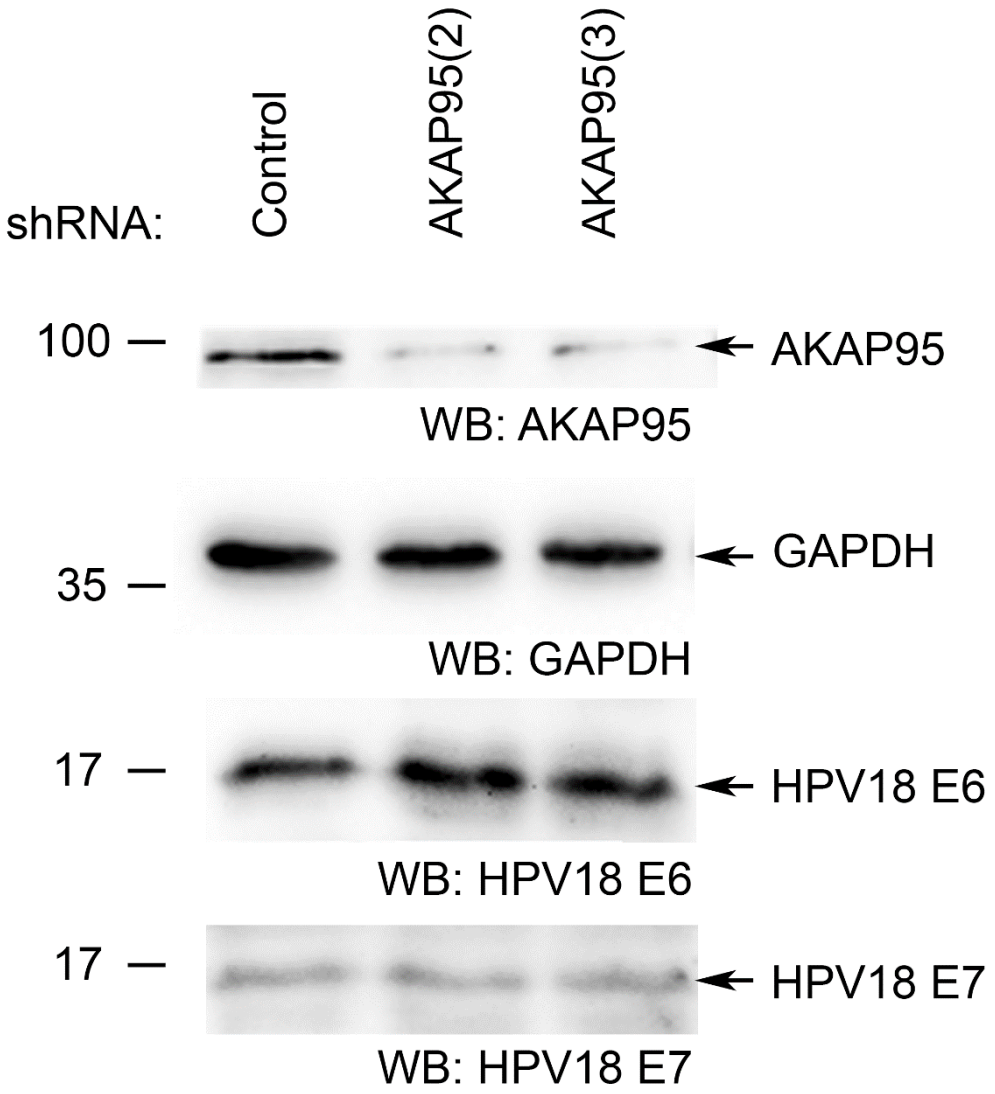

Figure 5.9: Loss of AKAP95 resulted in a slight increase in E6 oncoprotein expression. Lysates prepared from HFK-18 cells expressing the indicated shRNA constructs were examined for E6 and E7 oncoprotein expression by Western blotting. AKAP95(2) and AKAP95(3) represent two independent shRNA constructs.

Even though the increase in E6 protein upon AKAP95 silencing was slight, there might be a biological effect. Therefore, to determine whether these changes in E6 levels were biologically relevant, the expression of known E6 targets, p53, and PDZ proteins Dlg1 and hScrib was determined in shRNA-expressing cells.

The results (**Figure 5.10**) show that silencing of AKAP95 in HFK-18 cells is associated with increased expression of both Dlg1 (2-fold) and hScrib (4-fold), both targets of the E6 PBM, compared to cells expressing the control shRNA. In addition, there was almost a complete loss of p53 protein in AKAP95-shRNA expressing cells. These data show that in HFK-18 cells, silencing AKAP95 expression correlates with changes in expression levels of E6 targets.

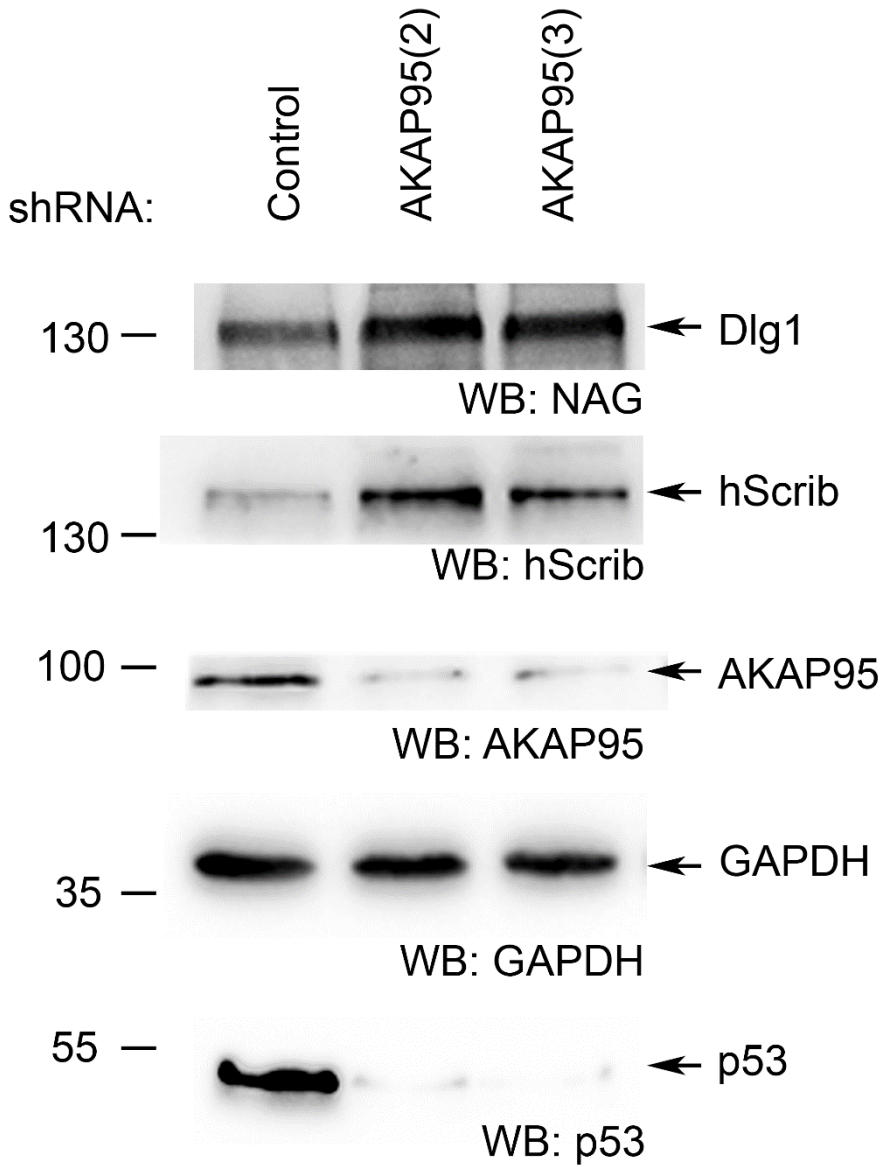

Figure 5.10: Changes in protein expression of hScrib, Dlg1 and p53 in AKAP95-shRNA expressing cells. Lysates prepared from HFK-18 cells expressing the indicated shRNA constructs were examined for E6 target protein expression by Western blotting. AKAP95(2) and AKAP95(3) represent two independent shRNA constructs.

5.2.4 E6 binds to PKA-RII via the E6 PBM

AKAPs provide a high level of specificity to cAMP-PKA signalling by localising the PKA holoenzyme to specific subcellular sites, conveying tight spatiotemporal control to these signalling events. The majority of AKAPs (including AKAP95) interact with PKA-RII; however, some bind to the RI subunit and some are dual specific (Eide et al., 1998; Pidoux and Taskén, 2010). To understand whether E6 binds to the same PKA isoform as AKAP95, E6-IP experiments were carried out from HFK-18 cell lysate expressing epitope-tagged PKA-RI or -RII holoenzymes. The holoenzymes used were tagged with *Renilla* luciferase as the endogenous proteins run close to the molecular weight of the antibody heavy chain, which would obscure detection by Western blotting.

The data shown in **Figure 5.11** shows that E6 binds to specifically to both the PKA-RII regulatory subunit and the PKA-Cα catalytic subunit, suggesting that it can bind to the complete type II holoenzyme. There was no noticeable binding to the PKA-RI regulatory subunit. These data show that E6 binds to specifically to PKA-RII.

Next, whether the interaction with PKA-RII was mediated via the E6 PBM was investigated, reasoning that if E6 interacts with PKA-RII via AKAP95 (which requires the E6 PBM) then disruption of the PBM should result in a defect in E6-PKA-RII binding. Indeed, the data presented in **Figure 5.12**. shows that wild type E6 (as expressed in HFK-18 cells) interacts with PKA-RII and this binding is markedly decreased in cells expressing ΔPDZE6 (HFK cells harbouring mutant HPV18 genomes that lack the E6 PBM; Delury et al. 2013), indicating a requirement of the E6 PBM in mediating the E6-PKA-RII interaction.

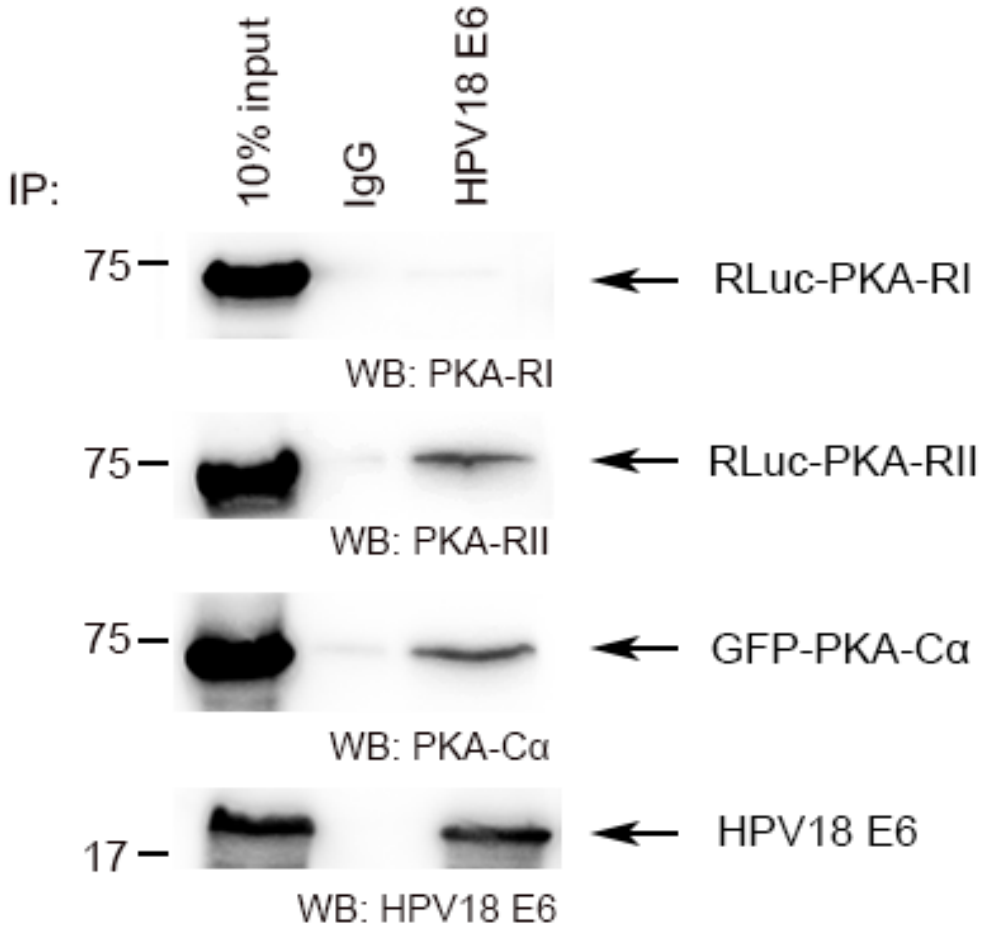

Figure 5.11: HPV18 E6 specifically binds the PKA-RII holoenzyme. E6 was co-immunoprecipitated from lysates prepared from wild type HPV18 genome containing cells expressing the indicated tagged PKA subunits. Data representative of two independent experiments.

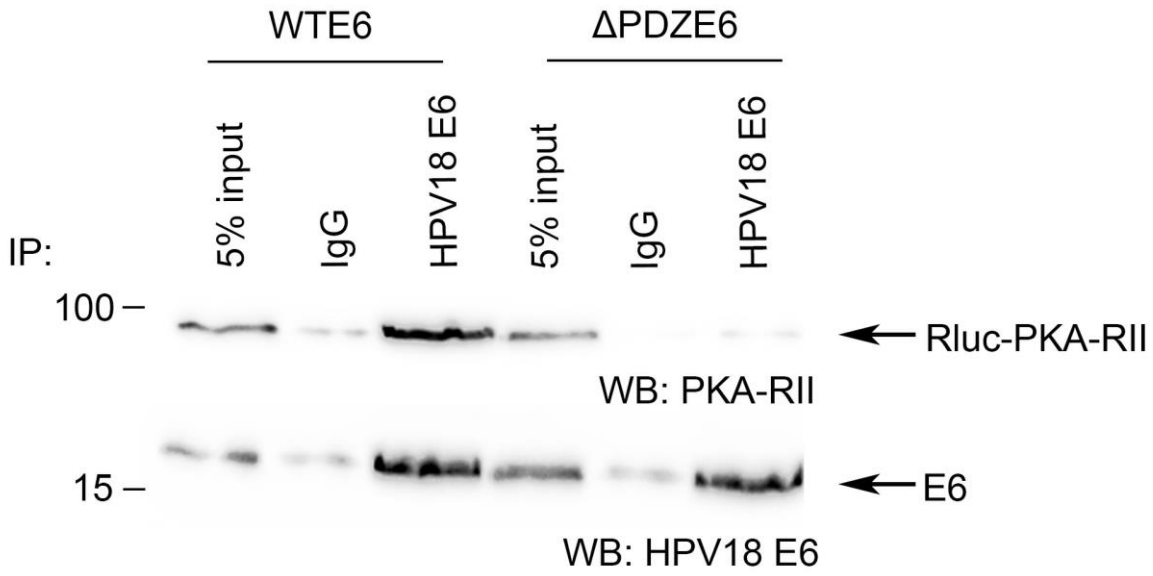

Figure 5.12: HPV18 E6 interacts with PKA-RII through its PBM. E6 was immunoprecipitated from lysates prepared from HFK-18 cells expressing wild type (WT genomes) or ΔPDZE6 (mutant genomes) as well as epitope tagged PKA-RII. Data representative of two independent experiments.

5.2.5 Activation of the PKA catalytic subunit in HFK and HFK-18 cells

Since the data presented thus far suggested the presence of an E6-AKAP95-PKA complex, mediated via the E6 PBM, organotypic rafts sections from HFK and HFK-18 cultures were stained with an antibody that detects the phosphorylated (Thr 197) form of the catalytic subunit of PKA, which is a prerequisite for activation of the kinase (Steinberg et al., 1993; Yonemoto et al., 1993). The data presented in **Figure 5.13** shows that in HFK cells, localisation of the phosphorylated catalytic subunit is present in the cytoplasm and nucleus of cells throughout all layers of the differentiating epithelium, although the intensity of the cytoplasmic signal in the suprabasal layers is somewhat lower than that in the basal and uppermost superficial layers. Of note, in the superficial layers, there are cytoplasmic aggregates of PKA that may represent keratohyalin granules, which are structures that are thought to bind together keratin filaments. In HFK-18 (HFK HPV18) cells, localisation is again seen in the cytoplasm and nuclei of cells throughout all layers of the epithelium, albeit without any major changes in suprabasal signal intensity. The aggregated staining is also present in cells of the uppermost layers. Examination of the nuclei in the HPV18 genome containing cells showed that activated PKA appeared in more intense microdomains compared to HFK cells. Finally, there may be an overall more intense staining throughout the epithelium of HPV18 containing cells compared to HFKs, but this is a little variable between foreskin donors. Together, these data show that the activated PKA catalytic subunit (and hence active PKA signalling) is present in both the cytoplasm and nucleus of HFK and HFK cells maintaining HPV18 genomes.

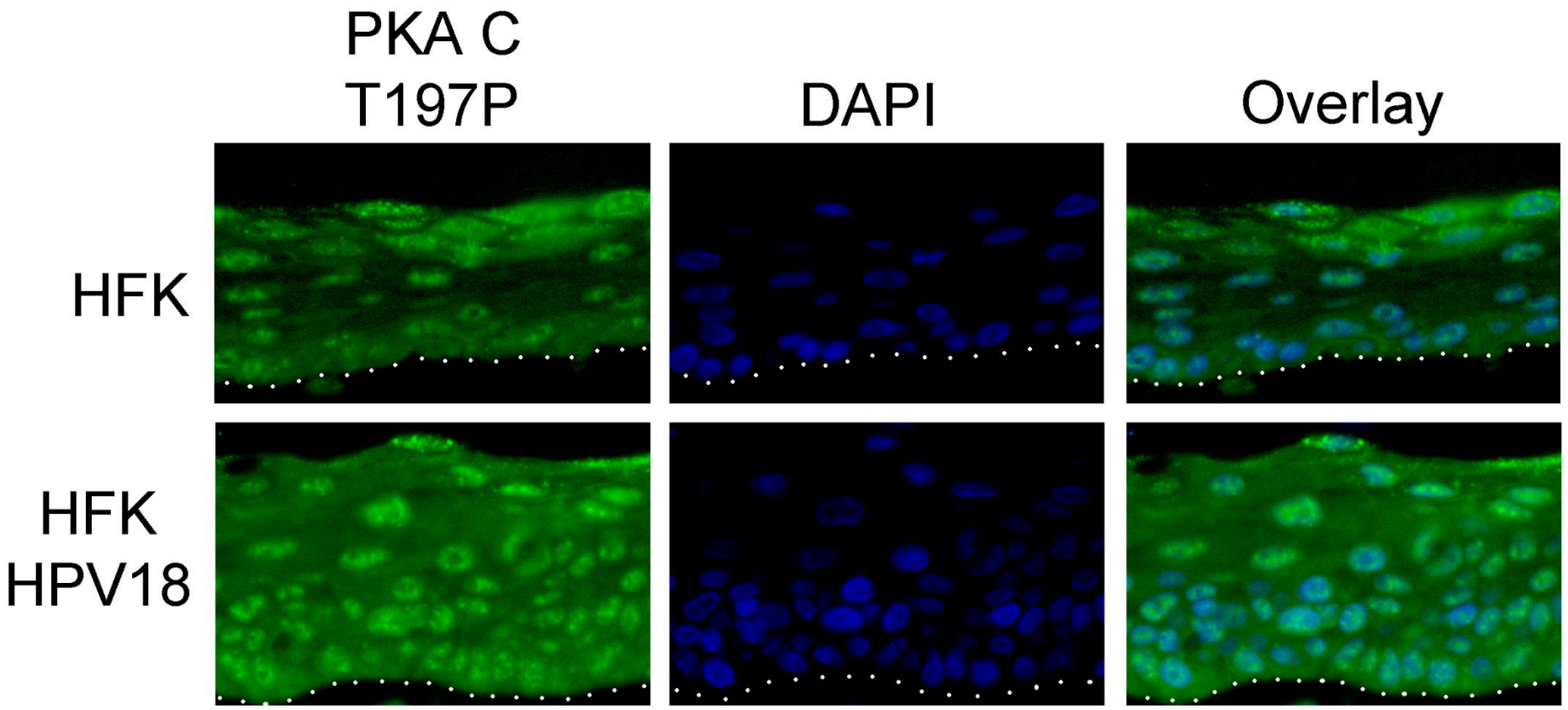

Figure 5.13: Expression of the activated PKA catalytic subunit in HFK and HFK cells maintaining HPV18 genomes. Donor matched HFK or HFK cells maintaining HPV18 genomes (HFK HPV18) were grown in organotypic raft culture for 13 days before fixation and sectioning. After epitope retrieval, sections were stained for the activated PKA catalytic subunit (phospho-T197) and DAPI was used to highlight cell nuclei. All images were taken at identical exposures. The white dotted line represents the basal layer.

5.2.6 E6 modulates AKAP95-PKA-RII interactions

The binding of AKAP95 to its interacting partners is dynamic and expression of different interacting partners in cells leads to alternative AKAP95-complexes (Arsenijevic et al., 2006). Given that E6 binds to PKA-RII specifically, the same PKA isoform that binds to AKAP95, the next logical question was whether E6 can regulate AKAP95 binding to PKA-RII. To investigate this, AKAP95-immunoprecipitates were examined for the presence of tagged PKA-RII subunits in C33A cells expressing vector or HPV18 E6 (+HPV18 E6). The interaction data in **Figure 5.14** show that in the absence of E6, AKAP95 binds to the complete PKA-type two holoenzyme (as indicated by binding of PKA-RII and PKA-Cα), as expected. However, when E6 is co-expressed in these cells, there is a substantial loss of PKA-RII and PKA-Cα bound by AKAP95, suggesting that E6 negatively regulates the ability of AKAP95 to bind to the RII holoenzyme.

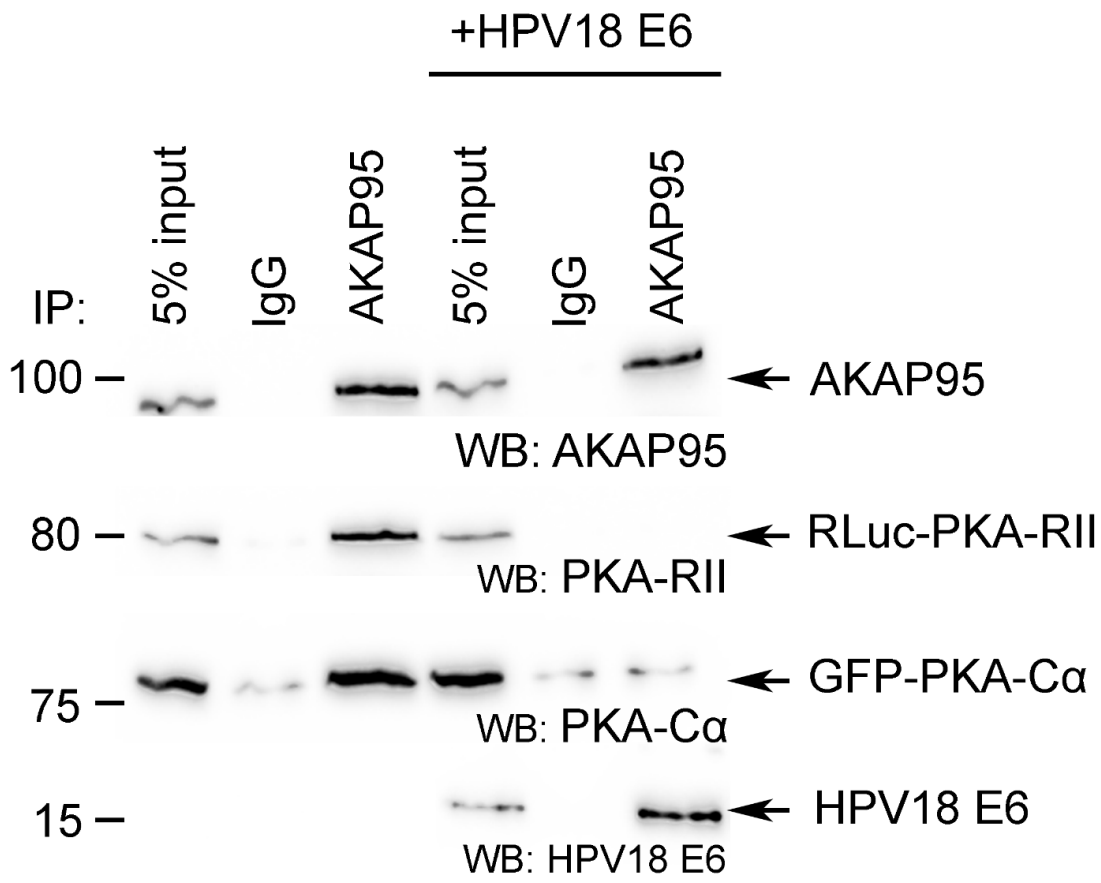

Figure 5.14: HPV18 E6 regulates the AKAP95-PKA-RII interaction. AKAP95-immunoprecipitates were isolated from C33A cells expressing tagged PKA subunits as well as HPV18 E6 (+HPV E6), where indicated, prior to Western blotting for AKAP-interaction partners. Data representative of two independent experiments .

5.3 Discussion

Multiple studies have outlined the important role of E6 interactions for the regulation of both replication and maintenance of viral DNA in undifferentiated cells as well as viral genome amplification in differentiating epithelium. In addition, these interactions play key roles in regulating viral oncoprotein expression and growth of HPV genome containing cells. Therefore, examining how exactly the virus interacts with the host cell is critical for our understanding of the viral life cycle. The previous chapter demonstrated a novel virus-host interaction between the HPV18 E6 oncoprotein and the cellular PKA anchoring protein AKAP95, which was mediated by the E6 PBM. In this chapter, the functional consequence of this interaction was examined in a mixture of immortalised cells expressing HPV18 E6 and primary cells harbouring viral genomes.

Several HPV18 E6 interacting partners, including p53 and several PDZ domain-containing proteins, are targeted for degradation via its association with the cellular E3 ubiquitin ligase E6-AP. Using both immortalised and primary cells expressing E6, either in isolation in overexpression experiments or from complete HPV18 genomes in physiologically relevant cell models, there was no evidence that E6 directed the degradation of AKAP95. In addition, other viral targets, such as the PDZ protein Par3, are mislocalised in cells expressing E6. In analogous experiments, we found no evidence of a gross redistribution of AKAP95 in cells in immortalised cells expressing HPV18 E6, although in the HPV18 life cycle model the nuclear staining of AKAP95 was more patchy in appearance than the donor matched HFKs, which may suggest some intranuclear redistribution in the presence of the complete viral genome. In cells grown in 3D organotypic raft culture, which recapitulates the full differentiation-dependent viral life cycle, there was no convincing

evidence of virus-induced redistribution of AKAP95, with its nuclear localisation in these cells identical to control HFKs.

Of note, rafts from both HFK and HFK-18 cultures had bright nuclear AKAP95 foci and, since AKAP95 is linked to regulation of splicing and transcription (Hu et al., 2016; Jiang et al., 2013), organotypic raft sections were stained with markers of various nuclear domains to ask whether there was any change in virus-induced AKAP95 relocalisation in these nuclear subdomains. Staining of raft sections with markers of PML bodies, splicing factories (SRP20) or DNA damage (γH_2AX) showed no obvious colocalisation (data not shown) so it was not possible to fully examine this possibility. Future experiments using additional nuclear markers, such as UBF, RPA43 and fibrillarin, which would indicate an association with the nucleolus (Marstad et al. 2016) as well as markers of viral replication factories (Swindle et al., 1999), would be useful to determine the identity of these AKAP95 nuclear foci. Once the identity of these nuclear foci is known, additional experiments could be carried out to investigate whether there is any virally-induced redistribution of AKAP95 in these nuclear microdomains.

Next, to examine the function of this novel E6 interactor, HFK-18 cells maintaining shRNA constructs against AKAP95 were developed. Loss of AKAP95 in these cells was associated with a slight increase in protein expression of E6 but not E7. In addition, silencing of AKAP95 was associated with increased protein expression of the E6 targets Dlg1 and hScrib, and an almost complete loss of p53. While the loss of p53 protein expression may be due to the increased expression of E6, it is likely that, at least for Dlg1 and hScrib (whose expression increased in shAKAP95 cells, rather than decreased, which was unexpected in the light of increased E6), but also for p53, these changes relate to an HPV-independent effect mediated solely by changes in expression of the AKAP. As

AKAP95 has a known role in regulating gene expression and alternative splicing of its targets, the changes in protein expression may relate to alterations at the level of RNA processing. To understand whether this is possible, analysis of publicly available splicing data from MDA-MB-231 cells showed that loss of AKAP95 was associated with increased alternative splicing of Dlg1, which may account for changes in protein expression (Wei et al., 2019). As MDA-MB-231 cells are triple-negative breast cancer cells, these results may not be representative of the changes in the HPV18 life cycle model established in primary HFKs, but these data do give an indication of the potential for AKAP95 to control Dlg1 gene expression. There was no information on p53 or hScrib in this database, although this may represent alterations in gene splicing inherent in these cancer cells. Alternative explanations would be that, for hScrib, that the increase in protein expression is post-transcriptional and so would not be captured in the alternative splicing data and, for p53, that the loss is due to protein degradation. Future experiments using quantitative real-time polymerase chain reaction to measure changes in RNA transcript levels and proteasome inhibition using MG132 coupled with Western blotting in the HPV18 life cycle model will provide further insight into the mechanism underlying these changes in AKAP95-depleted cells. In addition, knockdown of AKAP95 expression in HFK cells will provide information as to whether there is any influence of the HPV18 genome on the changes seen here.

As the data presented in chapter 4 highlighted the importance of the RII binding site for the E6-AKAP95 interaction, we wished to determine whether PKA-RII, the PKA holoenzyme that associates with AKAP95, was physically associated with HPV18 E6 in HFK-18 cells. Using epitope-tagged PKA holoenzymes, these experiments indicated that PKA-RII, but not PKA-RI, holoenzymes were complexed with HPV18 E6 in HFK-18 cells. Taking this

one step further, experiments using viral genomes expressing a mutant E6 protein that no longer binds to cellular PDZ domain-containing proteins (ΔPDZE6) showed that this interaction, like the E6-AKAP95 interaction, was mediated by the E6 PBM. Together, these data suggest the presence of an E6-hScrib-PKA-AKAP95 complex in cells maintaining HPV18 genomes. The function of this signalling complex was not explored due to time constraints but it is plausible that it would regulate PKA phosphorylation of downstream substrates. This would be consistent with the work on the β_1-adrenergic receptor, which showed that a complex composed of Dlg1-AKAP79-PKA was required for phosphorylation of the third intracellular loop of the receptor, regulating receptor recycling back to the cell membrane (Gardner et al., 2007). Identifying the targets of this E6-hScrib-PKA-AKAP95 complex is key to understanding the impact of this signalling complex. As the E6 PBM mediates the E6-AKAP95 interaction, E6 immunoprecipitations from cells maintaining wild type or mutant (ΔPDZE6) genomes followed by identification of PKA phosphoproteins by phosphopeptide enrichment prior to mass spectrometry should give an indication of what proteins are phosphorylated by this complex (Shohag et al., 2015).

One interesting target to examine would be CREB. Analysis of chromatin immunoprecipitation data from the papillomavirus genome database showed CREB binding to the early promoter in HeLa cells (data not shown). As CREB is phosphorylated on serine 133 by PKA (and other kinases such as MAPK; Alberini 2009) and this phosphorylation event is critical for recruitment of CREB binding protein and subsequent activation of transcription, changes in PKA phosphorylation may, therefore, be relevant for CREB-dependent transcription from the viral early promoter.

An alternative hypothesis is that E6 regulates the function of the hScrib-AKAP95-PKA complex. AKAP95 interactions have been shown to be dynamic, with the expression of

various interacting partners leading to alternative AKAP95-complexes in cells (Arsenijevic et al., 2004), thus E6 may regulate the formation of AKAP95 protein complexes. As E6 binds to PKA-RII, the same PKA isoform that binds to AKAP95, E6 may recruit PKA-RII from AKAP95-PKA complexes. Consistent with this idea, transient overexpression experiments combined with co-immunoprecipitation showed that E6 negatively regulated the ability of AKAP95 to interact with PKA-RII. This is consistent with data from Pirson group who showed that expression of CDK4 recruited cyclin D3 from AKAP95-cyclin D3 complexes (Arsenijevic et al., 2004). Thus, E6 may destabilise AKAP95-PKA complexes to downregulate nuclear PKA signalling in the HPV genome containing cells. Similar to the experiments outlined above, identifying changes in AKAP95-bound PKA phosphosubstrates in cells expressing either empty vector or an E6 expressing construct would allow for the identification of differentially regulated phosphosubstrates in the presence of E6.

Whether the E6-AKAP95 interaction regulated E6 phosphorylation by virtue of AKAP95's PKA binding ability was investigated. The interaction data presented in the previous chapter suggested that this was not the case, as phosphorylation of the E6 PBM would inhibit its interaction with hScrib through steric hindrance and, as the data shown indicated a requirement for the E6 PBM in mediating this binding, this would, therefore, inhibit E6-AKAP95 binding. To demonstrate this directly, E6 was co-immunoprecipitated from cells either expressing empty vector or AKAP95 and binding to the known PDZ target Dlg1 as well as 14-3-3 (which only recognises the phosphorylated form of the E6 PBM) investigated. This preliminary data showed no difference in E6-Dlg1 binding in the presence of overexpressed AKAP95 and no enrichment of 14-3-3ζ bound by E6, implying that AKAP95 does not induce E6 phosphorylation (data not shown).

Overall, the data presented in this chapter showed that HPV18 E6 did not direct degradation or induced gross mislocalisation of AKAP95, either in E6 transient overexpression experiments or when expressed from the complete viral genome in a physiologically relevant model of HPV18 replication. Instead, there is a signalling complex composed of E6-hScrib-AKAP95-PKA in HFK-18 cells, which may regulate the phosphorylation of cellular and/or viral PKA substrates. Interestingly, E6 can also negatively regulate the interaction of AKAP95 with PKA-RII, which may have profound consequences for PKA-RII signalling in HFK-18 cells.

CHAPTER 6 DISCUSSION

6.1 Overview of findings

The work presented in this thesis sought to address the hypothesis that HPV18 interacted with and modulated the activity of the host cell signalling pathway mediated by the cAMP-dependent PKA. Here, using BRET technology in two model systems of HPV18 replication, there was a consistent activation of the type two PKA holoenzyme (PKA-RII) in cells maintaining HPV18 genomes. Transient overexpression experiments found that HPV18 E5 regulated PKA-RI signalling in C33A cells and this negatively affected the ability of PKA-RI to activate CRE-dependent luciferase transcription. Whether the virus interacted with regulators of the PKA pathway was also examined. Using publicly available virus-host interaction data, a potential interaction between diverse HPV E6 proteins, including HPV18 E6, was found with the nuclear PKA anchoring protein, AKAP95. This interaction was confirmed *in vitro* and *in vivo* using a variety of cell systems, including a physiologically relevant model of HPV18 replication in primary human keratinocytes and HPV18 cancer cells, suggesting a physiologically relevant interaction. Intriguingly, this interaction was mediated by the E6 PBM and, consistent with this, we identified a novel interaction between AKAP95 and hScrib that may mediate the E6-AKAP95 interaction. In addition, domain mapping experiments showed that the amino-terminal 100 amino acids and the PKA-RII binding site on the AKAP were important for its interaction with E6. Initial functional analysis of this interaction in cells expressing HPV18 E6, either in transient overexpression experiments or in the HPV18 life cycle model, showed that E6 did not degrade or induce gross relocalisation of AKAP95, although a subtle intranuclear redistribution cannot be excluded at this stage. Using shRNA

constructs against AKAP95 in HFK cells maintaining HPV18 genomes, silencing of the AKAP was associated with a slight increase in E6 oncoprotein expression, without changes in E7. This was associated with changes in E6 target expression; Dlg1 and hScrib expression were increased in cells maintaining shAKAP95 constructs compared to control and there was almost a complete loss of p53 in addition in these cells. Furthermore, using HFK-18 cells, E6 was found to bind to the same PKA isoform as AKAP95, PKA-RII, and this too occurred via the E6 PBM, suggesting a signalling complex of E6-hScrib-AKAP95-PKA in these cells. Consistent with this, we saw the activation of the PKA catalytic subunit, which is a prerequisite for kinase activation, in cells maintaining HPV18 genomes. Interestingly, however, E6 was also found to modulate AKAP95-PKA interactions. Therefore, the function of this complex may be either for phosphorylation of cellular and/or viral PKA substrates or the virus may modulate AKAP95-PKA interactions to control the phosphorylation status of host substrates that are relevant for the viral life cycle.

6.2 Regulation of PKA activity by HPV18

Given that PKA regulates multiple facets of the HPV life cycle through modification of HPV and/or host protein function, the activity of the pathway was determined in cells harbouring HPV18 genomes.

The BRET data showed consistent activation of PKA-RII, occurring concomitantly with increased levels of cAMP, in HPV18 genome containing cells in two model systems of viral replication, which are not due to changes in PKA regulatory subunit expression or localisation. As PKA is activated by cAMP, it would first be prudent to examine whether the virus induces the activity of the enzymes that produce it, the ACs. There are various

methods to examine cAMP levels in cells, including fluorometric enzyme-linked immunosorbent assay based methodologies that can quantify cAMP in cell lysates. Using assays such as these, whether the virus can induce cAMP could be examined. In addition, as cAMP and PKA signalling are compartmentalised within cells, the data may suggest that the virus modulates the cAMP dynamic at a specific site (or sites) within infected cells, forming an HPV-specific cAMP-PKA-RII microdomain for local regulation of PKA substrates. A key experiment, therefore, would be to identify the exact subcellular site(s) where this alteration in PKA-RII activity occurs. For this, additional sensors that take advantage of the targeting ability of AKAPs (termed A-Kinase Activity Reporters) could be used. These sensors have been successfully used to measure the cAMP landscape at several subcellular locales, including the plasma membrane, mitochondria, cytoplasm and nucleus (reviewed in Paramonov et al., 2015). Alternatively, the fact that the virus appears to specifically targets the RII isoform may suggest that manipulation of PKA-RII dependent signalling is important for the virus life cycle. Unfortunately, studies examining the role of PKA in HPV18 life cycle events do not clarify the exact PKA isoform involved and so it is difficult to hypothesize which viral events specifically require PKA-RII over PKA-RI. Nevertheless, the use of isoform-specific PKA inhibitors combined with analysis of known PKA-dependent processes in the HPV18 life cycle model, such as PKA phosphorylation of E6, would be important in delineating the function of PKA isoforms for HPV18; Rp-8-Br-cAMPS preferentially inhibits PKA-RI whereas Rp-CAMPS inhibits both PKA-RI and -RII holoenzymes (Gjertsen et al., 1995).

As the BRET data were gathered only in cells grown in monolayer, which represent basally infected keratinocytes, it would be interesting to determine whether the same regulation of PKA activity was evident after inducing the late stages of the viral life cycle

through suspension of cells in methylcellulose (Wilson and Laimins, 2005). An alternative method to differentiate cells would be through supplementation of cell media with calcium (Yuspa et al., 1989). Initial attempts to carry out the BRET assay in calcium-differentiated cells, however, were unsuccessful in our hands.

Experiments to determine the viral protein responsible for the observed PKA alterations did not recapitulate the BRET results; however, they did show that the HPV18 E5 protein specifically increased PKA-RI and cAMP sensor activity only in cells pre-treated with the AC inducing agent forskolin. These data disagree with that of Oh et al., 2009 who showed higher basal cAMP levels in E5-expressing cells, although this may reflect differences in the sensitivities of the assays used (BRET versus direct measurement of cAMP). Nevertheless, these data are consistent with the ability of E5 to active cAMP and PKA in C33A cells. Furthermore, the same study showed that E5 induced expression of the EP4 receptor via a variant CRE site in its promoter via PKA and CREB. In this study, experiments using complete PKA holoenzymes showed that PKA-RI activated transcription of a CRE-dependent luciferase reporter which, surprisingly, was inhibited by co-expression of HPV18 E5. The negative regulation of HPV18 E5 on CRE-dependent luciferase transcription occurs via an unknown mechanism and was not explored further due to time constraints. Key experiments would be to identify whether the same effect of E5 is evident in a more physiological cell system, including HPV18 E5 knockout cells, and to identify differentially expressed CREB target genes in cells expressing HPV18 E5.

6.3 Identification and validation of a novel HPV-host interaction

At the same time as exploring whether HPV18 replication affected PKA signalling, a novel interaction between diverse E6 proteins, including HPV18, and the PKA anchoring protein

AKAP95 was identified through publicly available HPV-host interaction data. This interaction was confirmed both *in vitro* and *in vivo* using lysates derived from both E6-expressing immortalised and primary cells and was found to be mediated by the E6 PBM. Furthermore, we identified a novel AKAP95 interactor in the form of hScrib, suggesting that the interaction between E6 and AKAP95 is not direct and instead is mediated by the polarity protein.

The binding of hScrib to AKAP95 is particularly interesting given that the two proteins are thought to occupy different subcellular locales; AKAP95 is predominantly nuclear and cytoskeletal associated and hScrib is thought to primarily localise to sites of cell to cell contact. Biochemical fractionation experiments, however, revealed that a significant proportion of hScrib protein is in the nucleus of keratinocytes (Kranjec et al., 2016) and in liver cancer (Kapil et al., 2017). There is limited information on the function of nuclear hScrib; however, one possible nuclear function involves the orientation of the mitotic spindle.

In HPV18 genome containing cells expressing the ΔPDZE6 protein, there is an increase in spindle-associated abnormalities in late mitosis (Marsh et al., 2017). As AKAP95 is known to form multiprotein scaffolds for the regulation of diverse cellular processes, PKA is important for mitotic spindle formation (Matyakhina et al., 2002), and hScrib is involved in spindle positioning in mitosis (Zigman et al., 2011), it would be worthwhile examining whether the hScrib-PKA-AKAP95 complex was important in maintaining correct spindle orientation in the presence of replicating viral DNA. For this, identification of a mutant hScrib protein that cannot bind to AKAP95 would be instrumental in establishing whether the integrity of this complex plays a role in the regulation of the mitotic spindle.

Work on the β_1-adrenergic receptor showed that another PDZ protein, Dlg1, is crucial in organising AKAP-PKA complexes (Gardner et al., 2007). Therefore, it would be interesting to examine the effect of loss of hScrib on the integrity of the complete E6-AKAP95 complex identified here, reasoning that if hScrib is key for E6 binding to AKAP95 then the loss of hScrib will disrupt this complex as well as possibly E6 binding to PKA, which may occur via the AKAP.

The E6 mass spectrometry database suggested that one determinant of E6-AKAP95 binding, at least for the high-risk types, may be the precise sequence of the E6 PBM, with sequence alignment of the mass spectrometry predicted AKAP95 binders showing two common features. All predicted AKAP95 binders (HPV18, 45 and 52) contained a terminal valine residue while the non-binders contained a terminal leucine residue (HPV16, 33). There is currently no data on whether HPV45 and HPV52 E6 proteins bind to hScrib so it would be interesting to determine whether these proteins are capable of doing so, although a recent report identified hScrib binding as a marker of oncogenicity, suggesting that these high-risk E6 proteins do interact with hScrib (Thomas et al., 2016). In addition, as additional sequences outside of the E6 PBM are also important for regulating E6-PDZ interactions, a key experiment would be to test all predicted AKAP95 binders, which not only will help identify whether E6-AKAP95 is a conserved binding event among all alpha HPVs, but also whether differences in sequences upstream of the PBM are relevant for this novel interaction (Luck et al., 2012; Thomas et al., 2016).

6.4 Functional analysis of the E6-AKAP95 interaction

Functional analysis showed that HPV18 E6 did not degrade or induce a gross mislocalisation of the AKAP in either cells grown in monolayer or 3D raft culture (which

recapitulates the productive phase of the viral life cycle), which is unusual given that E6 generally targets its substrates through one of these mechanisms. To characterise this interaction in HFK-18 cells, cell lines maintaining shRNA constructs against AKAP95 were developed. Silencing of the AKAP was associated with a slight change in E6 expression, as well as changes in E6 targets Dlg1, hScrib and p53. The data presented here is preliminary and therefore should be repeated using additional methods of AKAP95 knockdown, such as siRNA, as well as in additional foreskin donors. Furthermore, whether these changes are specific to HPV18 genome containing cells needs to be determined. For this, knockdown of the AKAP in donor matched HFK cells followed by expression analysis of Dlg1, hScrib and p53 needs to be carried out.

As AKAP95 plays a key role in regulating cellular DNA synthesis through its interaction with MCM2 (Eide et al., 2003), it would be interesting to examine whether changes in AKAP95 expression are relevant for viral DNA replication and/or amplification during keratinocyte differentiation, especially as multiple host proteins are required for efficient replication of viral DNA (McBride, 2017).

An alternative hypothesis is that E6 modulates the activity of the AKAP towards its substrates, possibly regulating viral and/or cellular proteins that are phosphorylated by PKA. The totality of the data presented in this thesis suggested a multiprotein complex composed of E6-hScrib-AKAP95-PKA in HFK-18 cells. While the function of this complex is unclear at present, it is likely that it functions as a signalling complex for the regulation of viral and/or cellular PKA substrates, akin to the Dlg1-AKAP79-PKA complex identified through work on the β_1-adrenergic receptor (Gardner et al., 2007). Therefore, identifying the substrates of the E6-AKAP95 complex will be key experiments.

In addition, the data showed that E6 physically interacted with the same PKA isoform that binds to AKAP95, PKA-RII, and in doing so removes PKA from AKAP95-PKA complexes. The functional importance of this modification of AKAP95 behaviour is not known; however, a likely consequence would be the downregulation of PKA signalling in AKAP95 mediated signalosomes. Indeed, recent evidence has shown that AKAP95 coordinates a signalling hub composed of AKAP95, PKA and PDEs in the nucleus for the regulation of nuclear cAMP. Thus, E6 may disrupt the integrity of this complex, resulting in alternations in nuclear PKA signalling, such as those involving the transcriptional regulator CREB (Clister et al., 2019).

Consistent with this newly identified role for AKAP95 in mediating nuclear PKA signalling, staining of raft sections using an antibody that detects the activated form of the PKA catalytic subunit showed that active PKA was present in both the cytoplasm and nucleus of HFK and HFK-18 cells throughout the differentiating epithelium. As the nuclear active PKA staining may indicate AKAP95-PKA complexes, and the staining results in the rafts show bright nuclear microdomains in the HPV genome containing cells compared to HFKs, it would be interesting to examine whether the virus is able to modulate these complexes during infection. For this, changes in PKA activation could be examined by staining raft sections derived from HFK-18 cultures expressing the ΔPDZE6, which no longer binds to AKAP95 nor PKA, compared to the wild type E6 protein. Furthermore, similar to the experiments suggested above, identification of PKA substrates bound by AKAP95 in cells expressing vector or E6 constructs would be instrumental in identifying the consequence of this E6-AKAP modification.

CHAPTER 7 PRESENTATION OF WORK

The work contained within this thesis has been presented at the following conferences.

Oral presentations

- 'Human papillomavirus type 18 E6 oncoprotein interacts with the protein kinase A-anchoring protein AKAP95'. DNA Tumour Virus Conference (July 2018)

- 'High risk HPV18 E6 interacts with the A-Kinase Anchoring Protein AKAP95' Microbiology Society Conference (April 2018)

- 'High risk HPV18 interacts with multiple components of the protein kinase A pathway during viral infection' HPV UK, Rydall Hall, Lake District (November 2016)

Poster presentations

- 'High risk HPV18 E6 interacts with the protein kinase A binding protein AKAP95' DNA Tumour Virus Conference (July 2017)

- 'Oncogenic HPV18 interacts with multiple components of the host protein Kinase A pathway' Microbiology Society Conference (April 2017)

- 'The use of cell based models to probe HPV-PKA dynamics during the virus life cycle' More than Mice: Alternative models in Biological Research, University of Birmingham (July 2016)

LIST OF REFERENCES

Adams, S., Harootunian, A., Buechler, Y., Taylor, S., and Tsien, R. (1991). Fluorescence ratio imaging of cyclic AMP in single cells. Nature *349*, 649–7.

Akileswaran, L., Taraska, J.W., Sayer, J.A., Gettemy, J.M., and Coghlan, V.M. (2001). A-kinase-anchoring Protein AKAP95 Is Targeted to the Nuclear Matrix and Associates with p68 RNA Helicase. J. Biol. Chem. *276*, 17448–17454.

Akram, N., Imran, M., Noreen, M., Ahmed, F., Atif, M., Fatima, Z., and Bilal Waqar, A. (2017). Oncogenic Role of Tumor Viruses in Humans. Viral Immunol. *30*, 20–27.

Alberini, C.M. (2009). Transcription Factors in Long-Term Memory and Synaptic Plasticity. Physiol. Rev. *89*, 1–7.

Allen-Hoffmann, B.L., Schlosser, S.J., Ivarie, C.A.R., Sattler, C.A., Meisner, L.F., and O'Connor, S.L. (2000). Normal growth and differentiation in a spontaneously immortalized near- diploid human keratinocyte cell line, NIKS. J. Invest. Dermatol. *114*, 444–455.

Anacker, D.C., Gautam, D., Gillespie, K.A., Chappell, W.H., and Moody, C.A. (2014). Productive Replication of Human Papillomavirus 31 Requires DNA Repair Factor Nbs1. J. Virol. *88*, 8528–8544.

Aoubala, M., Holt, J., Clegg, R.A., Rowlands, D.J., and Harris, M. (2001). The inhibition of cAMP-dependent protein kinase by full-length hepatitis C virus NS3/4A complex is due to ATP hydrolysis. J. Gen. Virol. *82*, 1637–1646.

Arsenijevic, T., Degraef, C., Dumont, J.E., Roger, P.P., and Pirson, I. (2004). A novel partner for D-type cyclins: protein kinase A-anchoring protein AKAP95. Biochem. J. *378*, 673–679.

Arsenijevic, T., Degraef, C., Dumont, J.E., Roger, P.P., and Pirson, I. (2006). G1/S cyclins interact with regulatory subunit of PKA via A-kinase anchoring protein, AKAP95. Cell Cycle *5*, 1217–1222.

Ashman, D., Lipton, R., Melicow, M., and Price, T. (1963). Isolation of adenosine 3', 5'-monophosphate and guanosine 3', 5'-monophosphate from rat urine. Biochem Biophys Res Communi *22*, 330–334.

Aydin, I., Villalonga-Planells, R., Greune, L., Bronnimann, M.P., Calton, C.M., Becker, M., Lai, K.Y., Campos, S.K., Schmidt, M.A., and Schelhaas, M. (2017). A central region in the minor capsid protein of papillomaviruses facilitates viral genome tethering and membrane penetration for mitotic nuclear entry. PLoS Pathog. *13*, 1–31.

Azevedo, M.F., Faucz, F.R., Bimpaki, E., Horvath, A., Levy, I., De Alexandre, R.B., Ahmad, F., Manganiello, V., and Stratakis, C.A. (2014). Clinical and molecular genetics of the phosphodiesterases (PDEs). Endocr. Rev. *35*, 195–233.

Barber, R., and Butcher, R. (1981). The Quantitative Relationship between Intracellular Concentration and Egress of Cyclic AMP from Cultured Cells. Mol. Pharmacol. *19*, 38–43.

Bauer, H., Zweimueller-Mayer, J., Steinbacher, P., Lametschwandtner, A., and Bauer,

H.C. (2010). The dual role of zonula occludens (ZO) proteins. J. Biomed. Biotechnol. *2010*.

Beavo, J.A., and Brunton, L.L. (2002). Cyclic nucleotide research — still expanding after half a century. Nat. Rev. Mol. Cell Biol. *3*, 710–717.

Beebe, S., Oyen, O., Sandberg, M., Froysa, A., Hansson, V., and Jahnsen, T. (1990). Molecular cloning of a tissue-specific protein kinase (C gamma) from human testis--representing a third isoform for the catalytic subunit of cAMP-dependent protein kinase. Mol. Endocrinol. *4*, 465–475.

Belotti, E., Polanowska, J., Daulat, A.M., Audebert, S., Thomé, V., Lissitzky, J.-C., Lembo, F., Blibek, K., Omi, S., Lenfant, N., et al. (2013). The Human PDZome: A Gateway to PSD95-Disc Large-Zonula Occludens (PDZ)-mediated Functions. Mol. Cell. Proteomics *12*, 2587–2603.

Bernard, B.A., Bailly, C., Lenoir, M.C., Darmon, M., Thierry, F., and Yaniv, M. (1989). The human papillomavirus type 18 (HPV18) E2 gene product is a repressor of the HPV18 regulatory region in human keratinocytes. J. Virol. *63*, 4317–4324.

Bernard, H.U., Burk, R.D., Chen, Z., van Doorslaer, K., zur Hausen, H., and de Villiers, E.-M. (2010). Classification of papillomaviruses (PVs) based on 189 PV types and proposal of taxonomic amendments. Virology *401*, 70–79.

Bernard, X., Robinson, P., Nominé, Y., Masson, M., Charbonnier, S., Ramirez-Ramos, J.R., Deryckere, F., Travé, G., and Orfanoudakis, G. (2011). Proteasomal degradation of p53 by human papillomavirus E6 oncoprotein relies on the structural integrity of p53 core domain. PLoS One *6*, e25981.

Bienkowska-Haba, M., Williams, C., Kim, S.M., Garcea, R.L., and Sapp, M. (2012). Cyclophilins Facilitate Dissociation of the Human Papillomavirus Type 16 Capsid Protein L1 from the L2/DNA Complex following Virus Entry. J. Virol. *86*, 9875–9887.

Bilder, D., and Perrimon, N. (2000). Localization of apical epithelial determinants by the basolateral PDZ protein Scribble. Nature *403*, 676–680.

Bilder, D., Li, M., and Perrimon, N. (2000). Cooperative Regulation of Cell Polarity and Growth by Drosophila Tumor Suppressors. Science (80-.). *289*, 113–116.

Bird, G., O'Donnell, M., Moroianu, J., and Garcea, R.L. (2008). Possible Role for Cellular Karyopherins in Regulating Polyomavirus and Papillomavirus Capsid Assembly. J. Virol. *82*, 9848–9857.

Biryukov, J., Myers, J.C., McLaughlin-Drubin, M.E., Griffin, H.M., Milici, J., Doorbar, J., and Meyers, C. (2017). Mutations in HPV18 E1ˆE4 impact virus capsid assembly, infectivity competence, and maturation. Viruses *9*, pii: E385.

Boon, S.S., and Banks, L. (2012). High-Risk Human Papillomavirus E6 Oncoproteins Interact with 14-3-3ζ in a PDZ Binding Motif-Dependent Manner. J. Virol. *87*, 1586–1595.

Bordeaux, J., Forte, S., Harding, E., Darshan, M.S., Klucevsek, K., and Moroianu, J. (2006). The L2 Minor Capsid Protein of Low-Risk Human Papillomavirus Type 11 Interacts with Host Nuclear Import Receptors and Viral DNA. J. Virol. *80*, 8259–8262.

Borges, A., Dubrow, R., and Silverberg, M. (2014). Factors contributing to risk for cancer among HIV-infected individuals and evidence that earlier cART will alter risk. Curr.

Opion. HIV AIDS *9*, 34–40.

Bouvard, V., Matlashewski, G., Gu, Z.-M., Storey, A., and Banks, L. (1994). The Human Papillomavirus Type 16 E5 Gene Cooperates with the E7 Gene to Stimulate Proliferation of Primary Cells and Increases Viral Gene Expression. Virology *203*, 73–80.

Boyer, S.N., Wazer, D.E., and Band, V. (1996). E7 protein of human papilloma virus-16 induces degradation of retinoblastoma protein through the ubiquitin-proteasome pathway. Cancer Res. *56*, 4620–4624.

Brimer, N., and Vande Pol, S.B. (2014). Papillomavirus E6 PDZ Interactions Can Be Replaced by Repression of p53 To Promote Episomal Human Papillomavirus Genome Maintenance. J. Virol. *88*, 3027–3030.

Broniarczyk, J., Massimi, P., Bergant, M., and Banks, L. (2015). Human Papillomavirus Infectious Entry and Trafficking Is a Rapid Process. J. Virol. *89*, 8727–8732.

Brown, D.R., and Bryan, J.T. (2000). Abnormalities of cornified cell envelopes isolated from human papillomavirus type 11-infected genital epithelium. Virology *271*, 65–70.

Brown, D.R., Kitchin, D., Qadadri, B., Neptune, N., Batteiger, T., and Ermel, A. (2006). The human papillomavirus type 11 E1∧E4 protein is a transglutaminase 3 substrate and induces abnormalities of the cornified cell envelope. Virology *345*, 290–298.

Bruni, L., Diaz, M., Castellsagué, X., Ferrer, E., Bosch, F.X., and de Sanjosé, S. (2010). Cervical Human Papillomavirus Prevalence in 5 Continents: Meta-Analysis of 1 Million Women with Normal Cytological Findings. J. Infect. Dis. *202*, 1789–1799.

Bryan, J.T., Han, A., Fife, K.H., and Brown, D.R. (2000). The human papillomavirus type 11 E1/\E4 protein is phosphorylated in genital epithelium. Virology *268*, 430–439.

Buck, C.B., Pastrana, D. V., Lowy, D.R., and Schiller, J.T. (2004). Efficient Intracellular Assembly of Papillomaviral Vectors. J. Virol. *78*, 751–757.

Buck, C.B., Cheng, N., Thompson, C.D., Lowy, D.R., Steven, A.C., Schiller, J.T., and Trus, B.L. (2008). Arrangement of L2 within the papillomavirus capsid. J. Virol. *82*, 5190–5197.

Buck, J., Sinclair, M., Schapal, L., Cann, M., and Levin, L. (1999). Cytosolic adenylyl cyclase defines a unique signaling molecule in mammals. Proc. Natl. Acad. Sci. *96*, 79–84.

Bulk, S., Berkhof, J., Bulkmans, N.W.J., Zielinski, G.D., Rozendaal, L., Van Kemenade, F.J., Snijders, P.J.F., and Meijer, C.J.L.M. (2006). Preferential risk of HPV16 for squamous cell carcinoma and of HPV18 for adenocarcinoma of the cervix compared to women with normal cytology in The Netherlands. Br. J. Cancer *94*, 171–175.

Burgers, P.P., van der Heyden, M.A.G., Kok, B., Heck, A.J.R., and Scholten, A. (2015). A Systematic Evaluation of Protein Kinase A–A-Kinase Anchoring Protein Interaction Motifs. Biochemistry *54*, 11–21.

Burk, R.D., Chen, Z., Saller, C., Tarvin, K., Carvalho, A.L., Scapulatempo-Neto, C., Silveira, H.C., Fregnani, J.H., Creighton, C.J., Anderson, M.L., et al. (2017). Integrated genomic and molecular characterization of cervical cancer. Nature *543*, 378.

Burkitt, D. (1962). A children's cancer dependent on climatic factors. Nature *21*, 232–234.

Calton, C.M., Bronnimann, M.P., Manson, A.R., Li, S., Chapman, J.A., Suarez-Berumen,

M., Williamson, T.R., Molugu, S.K., Bernal, R.A., and Campos, S.K. (2017). Translocation of the papillomavirus L2/vDNA complex across the limiting membrane requires the onset of mitosis. PLoS Pathog. *13*, 1–29.

Carnegie, G.K., and Scott, J.D. (2003). A-kinase anchoring proteins and neuronal signaling mechanisms. Genes Dev. *17*, 1557–1568.

Carr, D.W., Hausken, Z.E., Fraser, I.D., Stofko-Hahn, R.E., and Scott, J.D. (1992). Association of the type II cAMP-dependent protein kinase with a human thyroid RII-anchoring protein. Cloning and characterization of the RII- binding domain. J Biol Chem *267*, 13376-82.

Cartier, C., Hemonnot, B., Gay, B., Bardy, M., Sanchiz, C., Devaux, C., and Briant, L. (2003). Active cAMP-dependent protein kinase incorporated within highly purified HIV-1 particles is required for viral infectivity and interacts with viral capsid protein. J. Biol. Chem. *278*, 35211–35219.

Castello, A., Fischer, B., Eichelbaum, K., Horos, R., Beckmann, B.M., Strein, C., Davey, N.E., Humphreys, D.T., Preiss, T., Steinmetz, L.M., et al. (2012). Insights into RNA Biology from an Atlas of Mammalian mRNA-Binding Proteins. Cell *149*, 1393–1406.

Cerqueira, C., Samperio Ventayol, P., Vogeley, C., and Schelhaas, M. (2015). Kallikrein-8 Proteolytically Processes Human Papillomaviruses in the Extracellular Space To Facilitate Entry into Host Cells. J. Virol. *89*, 7038–7052.

Cerqueira, C., Pang, Y.-Y.S., Day, P.M., Thompson, C.D., Buck, C.B., Lowy, D.R., and Schiller, J.T. (2016). A Cell-Free Assembly System for Generating Infectious Human Papillomavirus 16 Capsids Implicates a Size Discrimination Mechanism for Preferential Viral Genome Packaging. J. Virol. *90*, 1096–1107.

Cesareni, G., Ausiello, G., Zanzoni, A., Helmer-Citterich, M., Quondam, M., and Montecchi-Palazzi, L. (2002). MINT: a Molecular INTeraction database. FEBS Lett. *513*, 135–140.

Chalopuka, J., Bullock, S., Iourgenko, V., Levin, L., and J, B. (2006). Autoinhibitory regulation of soluble adenylyl cyclase. Mol Reprod Dev *73*, 361–368.

Chappell, W.H., Gautam, D., Ok, S.T., Johnson, B.A., Anacker, D.C., and Moody, C.A. (2016). Homologous Recombination Repair Factors Rad51 and BRCA1 Are Necessary for Productive Replication of Human Papillomavirus 31. J. Virol. *90*, 2639–2652.

Cheadle, C., Nesterova, M., Watkins, T., Barnes, K.C., Hall, J.C., Rosen, A., Becker, K.G., and Cho-Chung, Y.S. (2008). Regulatory subunits of PKA define an axis of cellular proliferation/differentiation in ovarian cancer cells. BMC Med. Genomics *1*, 1–14.

Cheau-Feng, L., Huang, J., Tsai, S., Nfor, O., Chou, M., Wu, M., Lee, C., Jan, C., and Liaw, Y. (2016). The association between human papillomavirus infection and female lung cancer. Med. *95*, e3856.

Chellappan, S., Kraus, V., Kroger, B., Munger, K., Howley, P., Phelps, W., and Nevins, J. (1992). Adenovirus ElA, simian virus 40 tumor antigen, and human papillomavirus E7 protein share the capacity to disrupt the interaction between transcription factor E2F and the retinoblastoma gene product. Proc. Natl. Acad. Sci. *89*, 4549–4553.

Chen, S.L., and Mounts, P. (1990). Transforming activity of E5a protein of human papillomavirus type 6 in NIH 3T3 and C127 cells. J. Virol. *64*, 3226–3233.

Chen, C., Hsu, W., Yang, H., Lee, M., Chen, H., Chien, Y., and You, S. (2014). Epidemiology of virus infection and human cancer. Recent Results Cancer Res *193*, 11–32.

Cheng, D., Rin, J., and Jackson, E. (2010). Multidrug Resistance Protein 4 Mediates 3',5,-cAMP Efflux From Rat Preglomerular Vascular Smooth Muscle Cells. Clin Exp Pharmacol Physiol *37*, 205–207.

Cheng, S., Schmidt-Grimminger, D., Murant, T., Broker, T., and Chow, L. (1995). Differentiation-dependent up-regulation of the human papillomavirus E7 gene reactivates cellular DNA replication in suprabasal differentiated keratinocytes. Genes Dev. *9*, 2335–2349.

Chhetri, G., Kalita, P., and Tripathi, T. (2015). An efficient protocol to enhance recombinant protein expression using ethanol in Escherichia coli. MethodsX *2*, 385–391.

Chiang, C.M., Ustav, M., Stenlund, A., Ho, T.F., Broker, T.R., and Chow, L.T. (1992). Viral E1 and E2 proteins support replication of homologous and heterologous papillomaviral origins. Proc. Natl. Acad. Sci. U. S. A. *89*, 5799–5803.

Choi, E.J., Ren, Y., Chen, Y., Liu, S., Wu, W., Ren, J., Wang, P., Garofalo, R.P., Zhou, J., and Bao, X. (2018). Exchange Proteins Directly Activated by cAMP and Their Roles in Respiratory Syncytial Virus Infection. J. Virol. *92*, 1–17.

Chojnacki, M., and Melendy, T. (2018). The human papillomavirus DNA helicase E1 binds, stimulates, and confers processivity to cellular DNA polymerase epsilon. Nucleic Acids Res. *46*, 229–241.

Chrivia, J.C., Kwok, R.P.S., Lamb, N., Hagiwara, M., Montminy, M.R., and Goodman, R.H. (1993). Phosphorylated CREB binds specifically to the nuclear protein CBP. Nature *365*, 855–859.

Classon, M., and Dyson, N. (2001). p107 and p130: Versatile Proteins with Interesting Pockets. Exp. Cell Res. *264*, 135–147.

Clegg, C., Cadd, G., and McKnight, G. (1988). Genetic characterization of a brain-specific form of the type I regulatory subunit of cAMP-dependent protein kinase. Proc. Natl. Acad. Sci. *85*, 3703–3707.

Clister, T., Greenwald, E.C., Baillie, G.S., and Zhang, J. (2019). AKAP95 Organizes a Nuclear Microdomain to Control Local cAMP for Regulating Nuclear PKA. Cell Chem. Biol. *26*, 885-891.e4.

Close, P., East, P., Dirac-Svejstrup, A.B., Hartmann, H., Heron, M., Maslen, S., Chariot, A., Söding, J., Skehel, M., and Svejstrup, J.Q. (2012). DBIRD complex integrates alternative mRNA splicing with RNA polymerase II transcript elongation. Nature *484*, 386.

Collas, P., Le Guellec, K., and Taskén, K. (1999). The A-kinase-anchoring protein AKAP95 is a multivalent protein with a key role in chromatin condensation at mitosis. J. Cell Biol. *147*, 1167–1179.

Collins, A.S., Nakahara, T., Do, A., and Lambert, P.F. (2005). Interactions with Pocket Proteins Contribute to the Role of Human Papillomavirus Type 16 E7 in the Papillomavirus Life Cycle. J. Virol. *79*, 14769–14780.

Conrad, M., Bubb, V.J., and Schlegel, R. (1993). The human papillomavirus type 6 and 16 E5 proteins are membrane-associated proteins which associate with the 16-kilodalton pore-forming protein. J. Virol. *67*, 6170–6178.

Conway, M.J., Alam, S., Ryndock, E.J., Cruz, L., Christensen, N.D., Roden, R.B.S., and Meyers, C. (2009). Tissue-Spanning Redox Gradient-Dependent Assembly of Native Human Papillomavirus Type 16 Virions. J. Virol. *83*, 10515–10526.

Corbin, J.D., Keely, S.L., and Park, C.R. (1975). The distribution and dissociation of cyclic adenosine 3':5' monophosphate dependent protein kinases in adipose, cardiac, and other tissues. J. Biol. Chem. *250*, 218–225.

Costa, T., Ogino, Y., Munson, P.J., Onaran, H.O., and Rodbard, D. (1992). Drug efficacy at guanine nucleotide-binding regulatory protein-linked receptors: thermodynamic interpretation of negative antagonism and of receptor activity in the absence of ligand. Mol. Pharmacol. *41*, 549–560.

Crusius, K., Auvinen, E., and Alonso, A. (1997). Enhancement of EGF- and PMA-mediated MAP kinase activation in cells expressing the human papillomavirus type 16 E5 protein. Oncogene *15*, 1437–1444.

Crusius, K., Auvinen, E., Steuer, B., Gaissert, H., and Alonso, A. (1998). The Human Papillomavirus Type 16 E5-Protein Modulates Ligand-Dependent Activation of the EGF Receptor Family in the Human Epithelial Cell Line HaCaT. Exp. Cell Res. *241*, 76–83.

Cummings, D.E., Brandon, E.P., Planas, J. V, Motamed, K., Idzerda, R.L., and McKnight, G.S. (1996). Genetically lean mice result from targeted disruption of the RIIβ subunit of protein kinase A. Nature *382*, 622–626.

Cuschieri, K.S., Cubie, H.A., Whitley, M.W., Gilkison, G., Arends, M.J., Graham, C., and McGoogan, E. (2005). Persistent high risk HPV infection associated with development of cervical neoplasia in a prospective population study. J. Clin. Pathol. *58*, 946–950.

Daniel, B., Mukherjee, G., Rangarajan, A., Krishna, S., and Vallikad, E. (1997). The link between integration and expression of human papillomavirus type 16 genomes and cellular changes in the evolution of cervical intraepithelial neoplastic lesions. J. Gen. Virol. *78*, 1095–1101.

Darnell, G.A., Schroder, W.A., Antalis, T.M., Lambley, E., Major, L., Gardner, J., Birrell, G., Cid-Arregui, A., and Suhrbier, A. (2007). Human papillomavirus E7 requires the protease calpain to degrade the retinoblastoma protein. J. Biol. Chem. *282*, 37492–37500.

David, M.-P., Van Herck, K., Hardt, K., Tibaldi, F., Dubin, G., Descamps, D., and Van Damme, P. (2009). Long-term persistence of anti-HPV-16 and -18 antibodies induced by vaccination with the AS04-adjuvanted cervical cancer vaccine: Modeling of sustained antibody responses. Gynecol. Oncol. *115*, S1–S6.

Davy, C.E., Jackson, D.J., Wang, Q., Raj, K., Masterson, P.J., Fenner, N.F., Southern, S., Cuthill, S., Millar, J.B.A., and Doorbar, J. (2002). Identification of a G2 Arrest Domain in the E1 E4 Protein of Human Papillomavirus Type 16. J. Virol. *76*, 9806–9818.

Day, P.M., Gambhira, R., Roden, R.B.S., Lowy, D.R., and Schiller, J.T. (2008). Mechanisms of Human Papillomavirus Type 16 Neutralization by L2 Cross-Neutralizing and L1 Type-Specific Antibodies. J. Virol. *82*, 4638–4646.

Day, P.M., Thompson, C.D., Pang, Y.Y., Lowy, D.R., and Schiller, J.T. (2015).

Involvement of nucleophosmin (NPM1/B23) in assembly of infectious HPV16 capsids. Papillomavirus Res. *1*, 74–89.

Delury, C.P., Marsh, E.K., James, C.D., Boon, S.S., Banks, L., Knight, G.L., and Roberts, S. (2013). The role of protein kinase A regulation of the E6 PDZ-binding domain during the differentiation-dependent life cycle of human papillomavirus type 18. J. Virol. *87*, 9463–9472.

Demeret, C., Yaniv, M., and Thierry, F. (1994). The E2 transcriptional repressor can compensate for Sp1 activation of the human papillomavirus type 18 early promoter. J. Virol. *68*, 7075–7082.

Demeter, L., Stoler, M., Broker, T., and Chow, L. (1994). Induction of proliferating cell nuclear antigen in differentiated keratinocytes of human papillomavirus-infected lesions. Hum. Pathol. *25*, 343–348.

Dempsey, A.F. (2008). Human Papillomavirus : The Usefulness of Risk Factors in Determining Who Should Get Vaccinated. Rev. Obstet. Gynecol. *1*, 122–128.

DiGiuseppe, S., Bienkowska-Haba, M., Hilbig, L., and Sapp, M. (2014). The nuclear retention signal of HPV16 L2 protein is essential for incoming viral genome to transverse the trans-Golgi network. Virology *458–459*, 93–105.

DiMaio, D., and Petti, L.M. (2013). The E5 proteins. Virology *445*, 99–114.

DiPilato, L.M., Cheng, X., and Zhang, J. (2004). Fluorescent indicators of cAMP and Epac activation reveal differential dynamics of cAMP signaling within discrete subcellular compartments. Proc. Natl. Acad. Sci. U. S. A. *101*, 16513–16518.

Disbrow, G.L., Sunitha, I., Baker, C.C., Hanover, J., and Schlegel, R. (2003). Codon optimization of the HPV-16 E5 gene enhances protein expression. Virology *311*, 105–114.

Dodge, K., and Scott, J.D. (2000). AKAP79 and the evolution of the AKAP model. FEBS Lett. *476*, 58–61.

Dohrman, D.P., Diamond, I., Gordon, A.S., and by David Kipnis, C.M. (1996). Ethanol causes translocation of cAMP-dependent protein kinase catalytic subunit to the nucleus (signal transduction/phosphorylation/localization). Cell Biol. *93*, 10217–10221.

Donaldson, M.M., Boner, W., and Morgan, I.M. (2007). TopBP1 Regulates Human Papillomavirus Type 16 E2 Interaction with Chromatin. J. Virol. *81*, 4338–4342.

Dooley, K.E., Warburton, A., and McBride, A.A. (2016). Tandemly integrated HPV16 can form a brd4-dependent super-enhancer-like element that drives transcription of viral oncogenes. MBio *7*, 1–10.

Doorbar, J., Campbell, D., Grand, R., and Gallimore, P. (1986). Identification of the human papilloma virus-1a E4 gene products. EMBO J. *5*, 355–362.

Doorbar, J., Ely, S., McLean, C., and Crawford, L. (1991). Specific interaction between HPV-16 E1-E4 and cytokeratins results in collapse of the epithelial cell intermediate filament network. Nature *352*, 824–827.

Doorbar, J., Egawa, N., Griffin, H., Kranjec, C., and Murakami, I. (2015). Human papillomavirus molecular biology and disease association. Rev. Med. Virol. *25*, 2–23.

Van Doorslaer, K., DeSalle, R., Einstein, M.H., and Burk, R.D. (2015). Degradation of

Human PDZ-Proteins by Human Alphapapillomaviruses Represents an Evolutionary Adaptation to a Novel Cellular Niche. PLoS Pathog. *11*, 1–14.

Dostmann, W.R.G., Taylor, S.S., Genieser, H.G., Jastorff, B., Doskeland, S.O., and Ogreid, D. (1990). Probing the cyclic nucleotide binding sites of cAMP-dependent protein kinases I and II with analogs of adenosine 3',5'-cyclic phosphorothioates. J. Biol. Chem. *265*, 10484–10491.

Dow, L.E., Brumby, A.M., Muratore, R., Coombe, M.L., Sedelies, K.A., Trapani, J.A., Russell, S.M., Richardson, H.E., and Humbert, P.O. (2003). hScrib is a functional homologue of the Drosophila tumour suppressor Scribble. Oncogene *22*, 9225–9230.

Dreer, M., van de Poel, S., and Stubenrauch, F. (2017). Control of viral replication and transcription by the papillomavirus E8^E2 protein. Virus Res. *231*, 96–102.

Duensing, S., and Münger, K. (2002). Duensing S, Munger K. The human papillomavirus type 16 E6 and E7 oncoproteins independently induce numerical and structural chromosome instability. Cancer Research 2002;62:7075–7082. Cancer Res. *62*, 7075–7082.

Dyson, N., Howley, P., Munger, K., and Harlow, E. (1989). The human papilloma virus-16 E7 oncoprotein is able to bind to the retinoblastoma gene product. Science (80-.). *243*, 934–937.

Eckstein, F., Romaniuk, P.J., Heideman, W., and Storm, D.R. (1981). Stereochemistry of the mammalian adenylate cyclase reaction. J. Biol. Chem. *256*, 9118–9120.

Egawa, N., and Doorbar, J. (2017). The low-risk papillomaviruses. Virus Res. *231*, 119–127.

Egawa, N., Wang, Q., Griffin, H.M., Murakami, I., Jackson, D., Mahmood, R., and Doorbar, J. (2017). HPV16 and 18 genome amplification show different E4-dependence, with 16E4 enhancing E1 nuclear accumulation and replicative efficiency via its cell cycle arrest and kinase activation functions.

Eide, T., Coghlan, V., Ørstavik, S., Holsve, C., Solberg, R., Skålhegg, B.S., Lamb, N.J.C., Langeberg, L., Fernandez, A., Scott, J.D., et al. (1998). Molecular cloning, chromosomal localization, and cell cycle-dependent subcellular distribution of the A-kinase anchoring protein, AKAP95. Exp. Cell Res. *238*, 305–316.

Eide, T., Carlson, C., Taskén, K.A., Hirano, T., Taskén, K., and Collas, P. (2002). Distinct but overlapping domains of AKAP95 are implicated in chromosome condensation and condensin targeting. EMBO Rep. *3*, 426–432.

Eide, T., Taskén, K.A., Carlson, C., Williams, G., Jahnsen, T., Taskén, K., and Collas, P. (2003). Protein kinase A-anchoring protein AKAP95 interacts with MCM2, a regulator of DNA replication. J. Biol. Chem. *278*, 26750–26756.

Elson, D.A., Riley, R.R., Lacey, A., Thordarson, G., Talamantes, F.J., and Arbeit, J.M. (2000). Sensitivity of the Cervical Transformation Zone to Estrogen-induced. Cancer *2*, 1267–1275.

Enemark, E.J., and Joshua-Tor, L. (2006). Mechanism of DNA translocation in a replicative hexameric helicase. Nature *442*, 270–275.

Epstein, M., Achong, B., and Barr, Y. (1964). Virus particles in cultured lymphoblasts

from Burkitt's lymphoma. Lancet (London, England) *1*, 702–703.

European Medicines Agency (2007). European public assessment report - Cervarix - Scientific discussion. 1–56.

European Medicines Agency (2017a). European public assessment report - Gardasil. 2017.

European Medicines Agency (2017b). European public assessment report - Gardasil9. 2017.

Evander, M., Frazer, I.H., Payne, E., Qi, Y.M., Hengst, K., and McMillan, N.A. (1997). Identification of the alpha6 integrin as a candidate receptor for papillomaviruses. J. Virol. *71*, 2449–2456.

Facciuto, F., Bugnon Valdano, M., Marziali, F., Massimi, P., Banks, L., Cavatorta, A.L., and Gardiol, D. (2014). Human papillomavirus (HPV)-18 E6 oncoprotein interferes with the epithelial cell polarity Par3 protein. Mol. Oncol. *8*, 533–543.

Farquhar, M.J., Harris, H.J., Diskar, M., Jones, S., Mee, C.J., Nielsen, S.U., Brimacombe, C.L., Molina, S., Toms, G.L., Maurel, P., et al. (2008). Protein Kinase A-Dependent Step(s) in Hepatitis C Virus Entry and Infectivity. J. Virol. *82*, 8797–8811.

Fast, L.A., Mikuličić, S., Fritzen, A., Schwickert, J., Boukhallouk, F., Hochdorfer, D., Sinzger, C., Suarez, H., Monk, P.N., Yáñez-Mó, M., et al. (2018). Inhibition of tetraspanin functions impairs human papillomavirus and cytomegalovirus infections. Int. J. Mol. Sci. *19*.

Fax, P., Carlson, C.R., Collas, P., Taskén, K., Esche, H., and Brockmann, D. (2001). Binding of PKA-RIIα to the adenovirus E1A12S oncoprotein correlates with its nuclear translocation and an increase in PKA-dependent promoter activity. Virology *285*, 30–41.

Della Fazia, M.A., Servillo, G., and Sassone-Corsi, P. (1997). Cyclic AMP signalling and cellular proliferation: Regulation of CREB and CREM. FEBS Lett. *410*, 22–24.

Fehrmann, F., Klumpp, D.J., and Laimins, L.A. (2003). Human papillomavirus Type 31 E5 Protein Supports Cell Cycle Progression and Activates Late Viral Functions upon Epithelial Differentiation. J. Virol. *77*, 2819–2831.

Feng, H., Shuda, M., Chang, Y., and Moore, P. (2009). Clonal Integration of a Polyomavirus in Human Merkel Cell Carcinoma. Science (80-.). *319*, 1096–1100.

Finnen, R.L., Erickson, K.D., Chen, X.S., and Garcea, R.L. (2003). Interactions between papillomavirus L1 and L2 capsid proteins. J. Virol. *77*, 4818–4826.

Flemington, E.K., Speck, S.H., and Kaelin, W.G. (1993). E2F-1-mediated transactivation is inhibited by complex formation with the retinoblastoma susceptibility gene product. Proc. Natl. Acad. Sci. *90*, 6914–6918.

Flores, E.R., Allen-Hoffmann, B.L., Lee, D., Sattler, C.A., and Lambert, P.F. (1999). Establishment of the Human Papillomavirus Type 16 (HPV-16) Life Cycle in an Immortalized Human Foreskin Keratinocyte Cell Line. Virology *262*, 344–354.

Flores, E.R., Allen-Hoffmann, B.L., Lee, D., and Lambert, P.F. (2000). The Human Papillomavirus Type 16 E7 Oncogene Is Required for the Productive Stage of the Viral Life Cycle. J. Virol. *74*, 6622–6631.

Florin, L., Schäfer, F., Sotlar, K., Streeck, R.E., and Sapp, M. (2002a). Reorganization of

nuclear domain 10 induced by papillomavirus capsid protein l2. Virology *295*, 97–107.

Florin, L., Sapp, C., Streeck, R.E., and Sapp, M. (2002b). Assembly and Translocation of Papillomavirus Capsid Proteins. J. Virol. *76*, 10009–10014.

Florin, L., Becker, K.A., Sapp, C., Lambert, C., Sirma, H., Muller, M., Streeck, R.E., and Sapp, M. (2004). Nuclear Translocation of Papillomavirus Minor Capsid Protein L2 Requires Hsc70. J. Virol. *78*, 5546–5553.

Francis, S.H., Blount, M.A., and Corbin, J.D. (2011). Mammalian cyclic nucleotide phosphodiesterases: Molecular mechanisms and physiological functions. Physiol. Rev. *91*, 651–690.

Freedman, D.A., and Levine, A.J. (1998). Nuclear Export Is Required for Degradation of Endogenous p53 by MDM2 and Human Papillomavirus E6. Mol. Cell. Biol. *18*, 7288–7293.

De Freitas, A.C., De Oliveira, T.H.A., Barros, M.R., and Venuti, A. (2017). HrHPV E5 oncoprotein: Immune evasion and related immunotherapies. J. Exp. Clin. Cancer Res. *36*, 1–15.

Gancedo, J.M. (2013). Biological roles of cAMP: variations on a theme in the different kingdoms of life. Biol. Rev. *88*, 645–668.

Gao, X., Chaturvedi, D., and Patel, T.B. (2012). Localization and retention of p90 ribosomal S6 kinase 1 in the nucleus: Implications for its function. Mol. Biol. Cell *23*, 503–515.

Gardiol, D., Kühne, C., Glaunsinger, B., Lee, S.S., Javier, R., and Banks, L. (1999a). Oncogenic human papillomavirus E6 proteins target the discs large tumour suppressor for proteasome-mediated degradation. Oncogene *18*, 5487–5496.

Gardiol, D., Kühne, C., Glaunsinger, B., Lee, S.S., Javier, R., and Banks, L. (1999b). Oncogenic human papillomavirus E6 proteins target the discs large tumour suppressor for proteasome-mediated degradation. Oncogene *18*, 5487–5496.

Gardner, L.A., Tavalin, S.J., Goehring, A.S., Scott, J.D., and Bahouth, S.W. (2006). AKAP79-mediated targeting of the cyclic AMP-dependent protein kinase to the β1-adrenergic receptor promotes recycling and functional resensitization of the receptor. J. Biol. Chem. *281*, 33537–33553.

Gardner, L.A., Naren, A.P., and Bahouth, S.W. (2007). Assembly of an SAP97-AKAP79-cAMP-dependent protein kinase scaffold at the type 1 PSD-95/DLG/ZO1 motif of the human β1-adrenergic receptor generates a receptosome involved in receptor recycling and networking. J. Biol. Chem. *282*, 5085–5099.

Genther, S.M., Sterling, S., Duensing, S., Münger, K., Sattler, C., and Lambert, P.F. (2003). Quantitative role of the human papillomavirus type 16 E5 gene during the productive stage of the viral life cycle. J. Virol. *77*, 2832–2842.

Genther Williams, S.M., Disbrow, G.L., Schlegel, R., Lee, D., Threadgill, D.W., and Lambert, P.F. (2005). Requirement of epidermal growth factor receptor for hyperplasia induced by E5, a high-risk human papillomavirus oncogene. Cancer Res. *65*, 6534–6542.

Geppetti, P., Veldhuis, N.A., Lieu, T.M., and Bunnett, N.W. (2015). G Protein-Coupled Receptors: Dynamic Machines for Signaling Pain and Itch. Neuron *88*, 635–649.

Gerlt, J.A., Coderre, J.A., and Wolin, M.S. (1980). Mechanism of the adenylate cyclase reaction. Stereochemistry of the reaction catalyzed by the enzyme from Brevibacterium liquefaciens. J. Biol. Chem. *255*, 331–334.

Geuens, T., Bouhy, D., and Timmerman, V. (2016). The hnRNP family: insights into their role in health and disease. Hum. Genet. *135*, 851–867.

Gillison, M.L., Akagi, K., Xiao, W., Jiang, B., Pickard, R.K., Li, J., Swanson, B.J., Agrawal, A.D., Zucker, M., Stache-Crain, B., et al. (2019). Human papillomavirus and the landscape of secondary genetic alterations in oral cancers. Genome Res. *29*, 1–17.

Girault, J.-A., and Greengard, P. (2004). The Neurobiology of Dopamine Signaling. Arch. Neurol. *61*, 641.

Gjertsen, B.T., Mellgren, G., Otten, A., Maronde, E., Genieser, H.G., Jastorff, B., Vintermyr, O.K., McKnight, G.S., and Døskeland, S.O. (1995). Novel (Rp)-cAMPS analogs as tools for inhibition of cAMP-kinase in cell culture: Rasal cAMP-kinase activity modulates interleukin-1β action. J. Biol. Chem. *270*, 20599–20607.

Gofman, Y., Schärfe, C., Marks, D.S., Haliloglu, T., and Ben-Tal, N. (2014). Structure, Dynamics and Implied Gating Mechanism of a Human Cyclic Nucleotide-Gated Channel. PLOS Comput. Biol. *10*, e1003976.

Gold, M.G., Lygren, B., Dokurno, P., Hoshi, N., McConnachie, G., Taskén, K., Carlson, C.R., Scott, J.D., and Barford, D. (2006). Molecular Basis of AKAP Specificity for PKA Regulatory Subunits. Mol. Cell *24*, 383–395.

Gonzalez, G., and Montminy, M. (1989). Cyclic AMP stimulates somatostatin gene transcription by phosphorylation of CREB at serine 133. Cell *59*, 675–680.

Goulding, E., Tibbs, G., and Siegelbaum, S. (1994). Molecular mechanism of cyclic-nucleotide-gated channel activation. Nature *372*, 369–374.

Graham, S. V., and Faizo, A.A.A. (2017). Control of human papillomavirus gene expression by alternative splicing. Virus Res. *231*, 83–95.

Grand, R.J.A., Doorbar, J., Smith, K.J., Coneron, I., and Gallimore, P.H. (1989). Phosphorylation of the human papillomavirus type 1 E4 proteins in Vivo and in Vitro. Virology *170*, 201–213.

Grandoch, M., Roscioni, S.S., and Schmidt, M. (2010). The role of Epac proteins, novel cAMP mediators, in the regulation of immune, lung and neuronal function. Br. J. Pharmacol. *159*, 265–284.

Griffin, L.M., Cicchini, L., and Pyeon, D. (2013). Human papillomavirus infection is inhibited by host autophagy in primary human keratinocytes. *437*, 12–19.

Gu, Z., and Matlashewski, G. (1995). Effect of human papillomavirus type 16 oncogenes on MAP kinase activity. J. Virol. *69*, 8051–8056.

Gulbahce, N., Yan, H., Dricot, A., Padi, M., Byrdsong, D., Franchi, R., Lee, D.-S., Rozenblatt-Rosen, O., Mar, J.C., Calderwood, M.A., et al. (2012). Viral Perturbations of Host Networks Reflect Disease Etiology. PLoS Comput. Biol. *8*, e1002531.

Gunasekharan, V., Hache, G., and Laimins, L. (2012). Differentiation-Dependent Changes in Levels of C/EBP Repressors and Activators Regulate Human Papillomavirus Type 31 Late Gene Expression. J. Virol. *86*, 5393–5398.

Guo, C., and Zhou, H.X. (2016). Unidirectional allostery in the regulatory subunit RIα facilitates efficient deactivation of protein kinase A. Proc. Natl. Acad. Sci. U. S. A. *113*, E6776–E6785.

Hamaguchi, T., Nakamuta, S., Funahashi, Y., Takano, T., Nishioka, T., Shohag, M.H., Yura, Y., Kaibuchi, K., and Amano, M. (2015). In vivo screening for substrates of protein kinase a using a combination of proteomic approaches and pharmacological modulation of kinase activity. Cell Struct. Funct. *40*, 1–12.

Harper, D.M., and DeMars, L.R. (2017). HPV vaccines – A review of the first decade. Gynecol. Oncol. *146*, 196–204.

Harris, L., McFarlane-Majeed, L., Campos-León, K., Roberts, S., and Parish, J.L. (2017). The Cellular DNA Helicase ChlR1 Regulates Chromatin and Nuclear Matrix Attachment of the Human Papillomavirus 16 E2 Protein and High-Copy-Number Viral Genome Establishment. J. Virol. *91*, 1–16.

Hayes, J.S., Brunton, L.L., and Mayer, S.E. (1980). Selective activation of particulate cAMP-dependent protein kinase by isoproterenol and prostaglandin E1. J. Biol. Chem. *255*, 5113–5119.

Heck, D. V., Yee, C.L., Howley, P.M., and Munger, K. (1992). Efficiency of binding the retinoblastoma protein correlates with the transforming capacity of the E7 oncoproteins of the human papillomaviruses. Proc. Natl. Acad. Sci. U. S. A. *89*, 4442–4446.

Herberg, F., Maleszka, A., Eide, T., Vossebein, L., and Tasken, K. (2000). Analysis of A-kinase anchoring protein (AKAP) interaction with protein kinase A (PKA) regulatory subunits: PKA isoform specificity in AKAP binding. J. Mol. Biol. *298*, 329–339.

Herfs, M., Yamamoto, Y., Laury, A., Wang, X., Nucci, M.R., McLaughlin-Drubin, M.E., Münger, K., Feldman, S., McKeon, F.D., Xian, W., et al. (2012). A discrete population of squamocolumnar junction cells implicated in the pathogenesis of cervical cancer. Proc. Natl. Acad. Sci. U. S. A. *109*, 10516–10521.

Herfs, M., Vargas, M., Yamamoto, Y., Howitt, B., Nucci, M., Hornick, J., McKeon, F., Xian, W., and Crum, C. (2013). A novel blueprint for 'top down' differentiation defines the cervical squamocolumnar junction during development, reproductive life, and neoplasia. J Pathol *229*, 460–468.

Hermeking, H., and Benzinger, A. (2006). 14-3-3 proteins in cell cycle regulation. Semin. Cancer Biol. *16*, 183–192.

Hernández-Ramírez, R.U., Shiels, M.S., Dubrow, R., and Engels, E.A. (2017). Cancer risk in HIV-infected people in the USA from 1996 to 2012: a population-based, registry-linkage study. Lancet HIV *4*, e495–e504.

Hofmann, B., Nishanian, P., Nguyen, T., Insixiengmay, P., and Fahey, J. (1993). Human immunodeficiency virus proteins induce the inhibitory cAMP/protein kinase A pathway in normal lymphocytes. Proc. Natl. Acad. Sci. *90*, 6676–6680.

Hong, S., and Laimins, L.A. (2013). The JAK-STAT Transcriptional Regulator, STAT-5, Activates the ATM DNA Damage Pathway to Induce HPV 31 Genome Amplification upon Epithelial Differentiation. PLoS Pathog. *9*.

Hong, S., Mehta, K.P., and Laimins, L.A. (2011). Suppression of STAT-1 Expression by Human Papillomaviruses Is Necessary for Differentiation-Dependent Genome

Amplification and Plasmid Maintenance. J. Virol. *85*, 9486–9494.

Hong, S., Cheng, S., Iovane, A., and Laimins, L.A. (2015). STAT-5 Regulates transcription of the topoisomerase IIβ-Binding protein 1 (TopBP1) gene to activate the ATR pathway and promote human papillomavirus Replication. MBio *6*, 1–9.

Hoppe-Seyler, F., and Butz, K. (1994). Cellular control of human papillomavirus oncogene transcription. Mol. Carcinog. *10*, 134–141.

Hoshi, N., Zhang, J.-S., Omaki, M., Takeuchi, T., Yokoyama, S., Wanaverbecq, N., Langeberg, L.K., Yoneda, Y., Scott, J.D., Brown, D.A., et al. (2003). AKAP150 signaling complex promotes suppression of the M-current by muscarinic agonists. Nat. Neurosci. *6*, 564–571.

Hoshi, N., Langeberg, L.K., and Scott, J.D. (2005). Distinct enzyme combinations in AKAP signalling complexes permit functional diversity. Nat. Cell Biol. *7*, 1066–1073.

Hough, C.D., Woods, D.F., Park, S., and Bryant, P.J. (1997). Organizing a functional junctional complex requires specific domains of the Drosophila MAGUK Discs large. Genes Dev. *11*, 3242–3253.

Hu, J., Khodadadi-jamayran, A., Mao, M., Shah, K., Yang, Z., Nasim, T., Wang, Z., and Jiang, H. (2016). AKAP95 regulates splicing through scaffolding RNAs and RNA processing factors. Nat. Commun. *7*, 1–12.

Huang, L.J.S., Wang, L., Ma, Y., Durick, K., Perkins, G., Deerinck, T.J., Ellisman, M.H., and Taylor, S.S. (1999). NH2-terminal targeting motifs direct dual specificity A-kinase-anchoring protein 1 (D-AKAP1) to either mitochondria or endoplasmic reticulum. J. Cell Biol. *145*, 951–959.

Huibregtse, J.M., Scheffner, M., and Howley, P.M. (1991). A cellular protein mediates association of p53 with the E6 oncoprotein of human papillomavirus types 16 or 18. EMBO J. *10*, 4129–4135.

Hurley, J.H. (1999a). Structure, mechanism, and regulation of mammalian adenylyl cyclase. J. Biol. Chem. *274*, 7599–7602.

Hurley, J.H. (1999b). Structure, mechanism, and regulation of mammalian adenylyl cyclase. J. Biol. Chem. *274*, 7599–7602.

Iaquinta, P.J., and Lees, J.A. (2007). Life and death decisions by the E2F transcription factors. Curr. Opin. Cell Biol. *19*, 649–657.

IARC Working Group (2012). IARC Monographs on the Evaluation of Carcinogenic Risks to Humans, No. 100B. (Lyon: IARC).

Imamura, H., Wagih, O., Niinae, T., Sugiyama, N., Beltrao, P., and Ishihama, Y. (2017). Identifications of Putative PKA Substrates with Quantitative Phosphoproteomics and Primary-Sequence-Based Scoring. J. Proteome Res. *16*, 1825–1830.

International Agency for Research on Cancer (2007). Human Papillomaviruses.

Isensee, J., Kaufholz, M., Knape, M.J., Hasenauer, J., Hammerich, H., Gonczarowska-Jorge, H., Zahedi, R.P., Schwede, F., Herberg, F.W., and Hucho, T. (2018). PKA-RII subunit phosphorylation precedes activation by cAMP and regulates activity termination. J. Cell Biol. *217*, 2167–2184.

Itoh, M., Morita, K., and Tsukita, S. (1999). Characterization of ZO-2 as a MAGUK family member associated with tight as well as adherens junctions with a binding affinity to occludin and alpha catenin. J. Biol. Chem. *274*, 5981–5986.

Jahnsen, T., Hedlin, L., Kidd, V., Beattie, W., Lohmann, S., Walter, U., Durica, J., Schulz, T., Schiltz, E., and Browner, M. (1986). Molecular cloning, cDNA structure, and regulation of the regulatory subunit of type II cAMP-dependent protein kinase from rat ovarian granulosa cells. J Biol Chem *261*, 12352–12361.

Jaiswal, B.S., and Conti, M. (2001). Identification and Functional Analysis of Splice Variants of the Germ Cell Soluble Adenylyl Cyclase. J. Biol. Chem. *276*, 31698–31708.

James, C., and Roberts, S. (2016). Viral Interactions with PDZ Domain-Containing Proteins—An Oncogenic Trait? Pathogens *5*, 8.

James, M.A., Lee, J.H., and Klingelhutz, A.J. (2006). Human Papillomavirus Type 16 E6 Activates NF- B, Induces cIAP-2 Expression, and Protects against Apoptosis in a PDZ Binding Motif-Dependent Manner. J. Virol. *80*, 5301–5307.

Jarnæss, E., Stokka, A.J., Kvissel, A.K., Skålhegg, B.S., Torgersen, K.M., Scott, J.D., Carlson, C.R., and Taskén, K. (2009). Splicing factor arginine/serine-rich 17A (SFRS17A) is an A-kinase anchoring protein that targets protein kinase A to splicing factor compartments. J. Biol. Chem. *284*, 35154–35164.

Javier, R.T., and Butel, J.S. (2012). The History of Tumor Virology. *68*, 7693–7706.

Jeon, S., Allen-Hoffmann, B.L., and Lambert, P.F. (1995). Integration of human papillomavirus type 16 into the human genome correlates with a selective growth advantage of cells. J. Virol. *69*, 2989–2997.

Jewers, R.J., Hildebrandt, P., Ludlow, J.W., Kell, B., and McCance, D.J. (1992). Regions of human papillomavirus type 16 E7 oncoprotein required for immortalization of human keratinocytes. J. Virol. *66*, 1329–1335.

Jiang, H., Lu, X., Shimada, M., Dou, Y., Tang, Z., and Roeder, R.G. (2013). Regulation of transcription by the MLL2 complex and MLL complex-associated AKAP95. Nat. Struct. Mol. Biol. *20*, 1156–1163.

Johansson, C., and Schwartz, S. (2013). Regulation of human papillomavirus gene expression by splicing and polyadenylation. Nat. Rev. Microbiol. *11*, 239–251.

Joyce, J.G., Tung, J.S., Przysiecki, C.T., Cook, J.C., Lehman, E.D., Sands, J.A., Jansen, K.U., and Keller, P.M. (1999). The L1 major capsid protein of human papillomavirus type 11 recombinant virus-like particles interacts with heparin and cell-surface glycosaminoglycans on human keratinocytes. J. Biol. Chem. *274*, 5810–5822.

Kapil, S., Sharma, B.K., Patil, M., Elattar, S., Yuan, J., Hou, S.X., Kolhe, R., and Satyanarayana, A. (2017). The cell polarity protein Scrib functions as a tumor suppressor in liver cancer. Oncotarget *8*, 26515–26531.

Kaupp, U.B., and Seifert, R. (2002). Cyclic Nucleotide-Gated Ion Channels. Physiol. Rev. *82*, 769–824.

Kawana, K., Fujii, T., Nakagawa, S., Yano, T., Taketani, Y., Thomas, M., Subbaiah, V.K., Yamashita, A., Kozuma, S., Nagasaka, K., et al. (2013). A Novel Interaction between hScrib and PP1γ Downregulates ERK Signaling and Suppresses Oncogene-Induced Cell

Transformation. PLoS One *8*, e53752.

Kawasaki, H., Springett, G., Mochizuki, N., Toki, S., Nakaya, M., Matsuda, M., Housman, D., and Graybiel, A. (1998). A family of cAMP-binding proteins that directly activate Rap1. Science (80-.). *282*, 2275–2279.

Khanal, S., and Galloway, D.A. (2019). High-risk human papillomavirus oncogenes disrupt the Fanconi anemia DNA repair pathway by impairing localization and de-ubiquitination of FancD2. PLoS Pathog. *15*, 1–27.

Kho, E.-Y., Wang, H.-K., Banerjee, N.S., Broker, T.R., and Chow, L.T. (2013). HPV-18 E6 mutants reveal p53 modulation of viral DNA amplification in organotypic cultures. Proc. Natl. Acad. Sci. *110*, 7542–7549.

Kim, K.M., Kwon, S.N., Kang, J. Il, Lee, S.H., Jang, S.K., Ahn, B.Y., and Kim, Y.K. (2007). Hepatitis C virus NS2 protein activates cellular cyclic AMP-dependent pathways. Biochem. Biophys. Res. Commun. *356*, 948–954.

Kinderman, F.S., Kim, C., von Daake, S., Ma, Y., Pham, B.Q., Spraggon, G., Xuong, N.H., Jennings, P.A., and Taylor, S.S. (2006). A Dynamic Mechanism for AKAP Binding to RII Isoforms of cAMP-Dependent Protein Kinase. Mol. Cell *24*, 397–408.

Kines, R.C., Thompson, C.D., Lowy, D.R., Schiller, J.T., and Day, P.M. (2009). The initial steps leading to papillomavirus infection occur on the basement membrane prior to cell surface binding The data are consistent with a dynamic model of in vivo HPV infection in which a conformational change and PC cleavage on the BM allows tran. 2–7.

King, C.R., Cohen, M.J., Fonseca, G.J., Dirk, B.S., Dikeakos, J.D., and Mymryk, J.S. (2016). Functional and Structural Mimicry of Cellular Protein Kinase A Anchoring Proteins by a Viral Oncoprotein. PLoS Pathog. *12*, e1005621.

King, C.R., Gameiro, S.F., Tessier, T.M., Zhang, A., and Mymryk, J.S. (2018). Mimicry of Cellular A Kinase-Anchoring Proteins Is a Conserved and Critical Function of E1A across Various Human Adenovirus Species. J. Virol. *92*.

Kirschner, L.S., Carney, J.A., Pack, S.D., Taymans, S.E., Giatzakis, C., Cho, Y.S., Cho-Chung, Y.S., and Stratakis, C.A. (2000). Mutations of the gene encoding the protein kinase A type I-α regulatory subunit in patients with the Carney complex. Nat. Genet. *26*, 89–92.

Kivi, N., Greco, D., Auvinen, P., and Auvinen, E. (2008). Genes involved in cell adhesion, cell motility and mitogenic signaling are altered due to HPV 16 E5 protein expression. Oncogene *27*, 2532–2541.

Kiyono, T., Hiraiwa, A., Fujita, M., Hayashi, Y., Akiyama, T., and Ishibashi, M. (1997). Binding of high-risk human papillomavirus E6 oncoproteins to the human homologue of the Drosophila discs large tumor suppressor protein. Proc. Natl. Acad. Sci. U. S. A. *94*, 11612–11616.

Kjaer, S.K., Brule, A.J.C. Van Den, Paull, G., Svare, E.I., Sherman, M.E., Thomsen, B.L., Suntum, M., Bock, J.E., Poll, P.A., and Meijer, C.J.L.M. (2002). Type specific persistence of high risk human papillomavirus (HPV) as indicator of high grade cervical squamous intraepithelial lesions in young women: population based prospective follow up study. BMJ *325*, 1–7.

Klaesson, A., Grannas, K., Ebai, T., Heldin, J., Koos, B., Leino, M., Raykova, D., Oelrich, J., Arngården, L., Söderberg, O., et al. (2018). Improved efficiency of in situ protein

analysis by proximity ligation using UnFold probes. Sci. Rep. *8*, 1–13.

Klingelhutz, A.J., Foster, S.A., and McDougall, J.K. (1996). Telomerase activation by the E6 gene product of human papillomavirus type 16. Nature *380*, 79–82.

Knight, G.L., Pugh, A.G., Yates, E., Bell, I., Wilson, R., Moody, C.A., Laimins, L.A., and Roberts, S. (2011). A cyclin-binding motif in human papillomavirus type 18 (HPV18) E1^E4 is necessary for association with CDK-cyclin complexes and G2/M cell cycle arrest of keratinocytes, but is not required for differentiation-dependent viral genome amplification or L1 cap. Virology *412*, 196–210.

Konjević, G., Radenković, S., Vuletić, A., Martinović, K., Jurišić, V., and Srdic, T. (2013). STAT Transcription Factors in Tumor Development and Targeted Therapy of Malignancies.

Koster, M., and Roop, D. (2007). Mechanisms regulating epithelial stratification. Annu. Rev. Cell Dev. Biol. *23*, 93–113.

Kranjec, C., Tomaić, V., Massimi, P., Nicolaides, L., Doorbar, J., and Banks, L. (2016). The high-risk HPV E6 target scribble (hScrib) is required for HPV E6 expression in cervical tumour-derived cell lines. Papillomavirus Res. *2*, 70–77.

Kuballa, P., Matentzoglu, K., and Scheffner, M. (2007). The role of the ubiquitin ligase E6-AP in human papillomavirus E6-mediated degradation of PDZ domain-containing proteins. J. Biol. Chem. *282*, 65–71.

Kühne, C., Gardiol, D., Guarnaccia, C., Amenitsch, H., and Banks, L. (2000). Differential regulation of human papillomavirus E6 by protein kinase A: conditional degradation of human discs large protein by oncogenic E6. Oncogene *19*, 5884–5891.

Kundu, K., Mann, M., Costa, F., and Backofen, R. (2014). MoDPepInt: An interactive web server for prediction of modular domain-peptide interactions. Bioinformatics *30*, 2668–2669.

Lace, M.J., Anson, J.R., Klussmann, J.P., Wang, D.H., Smith, E.M., Haugen, T.H., and Turek, L.P. (2011). Human Papillomavirus Type 16 (HPV-16) Genomes Integrated in Head and Neck Cancers and in HPV-16-Immortalized Human Keratinocyte Clones Express Chimeric Virus-Cell mRNAs Similar to Those Found in Cervical Cancers. J. Virol. *85*, 1645–1654.

Lacey, C.J.N., Lowndes, C.M., and Shah, K. V. (2006). Chapter 4: Burden and management of non-cancerous HPV-related conditions: HPV-6/11 disease. Vaccine *24*, S35–S41.

Landsverk, H.B., Carlson, C.R., Steen, R.L., Vossebein, L., Herberg, F.W., Taskén, K., and Collas, P. (2001). Regulation of anchoring of the RIIa regulatory subunit of PKA to AKAP95 by threonine phosphorylation of RIIa: Implications for chromosome dynamics at mitosis. J. Cell Sci. *114*, 3255–3264.

Lang, K., Schmid, F.X., and Fischer, G. (1987). Catalysis of protein folding by prolyl isomerase. Nature *329*, 268–270.

Langeberg, L.K., and Scott, J.D. (2015). Signalling scaffolds and local organization of cellular behaviour. Nat. Rev. Mol. Cell Biol. *16*, 232–244.

Lazarczyk, M., Cassonnet, P., Pons, C., Jacob, Y., and Favre, M. (2009). The EVER

Proteins as a Natural Barrier against Papillomaviruses: a New Insight into the Pathogenesis of Human Papillomavirus Infections. Microbiol. Mol. Biol. Rev. *73*, 348–370.

Lazzeroni, G., Benicchi, T., Heitz, F., Magnoni, L., Diamanti, D., Rossini, L., Massai, L., Federico, C., Fecke, W., Caricasole, A., et al. (2013). A phenotypic screening assay for modulators of huntingtin-induced transcriptional dysregulation. J. Biomol. Screen. *18*, 984–996.

Leavesley, S.J., and Rich, T.C. (2018). Overcoming Limitations of FRET Measurements. Cytom. A *98*, 325–327.

Lechner, M.S., and Laimins, L.A. (1994a). Inhibition of p53 DNA binding by human papillomavirus E6 proteins. J. Virol. *68*, 4262–4273.

Lechner, M.S., and Laimins, L.A. (1994b). Inhibition of p53 DNA binding by human papillomavirus E6 proteins. J. Virol. *68*, 4262–4273.

Lee, C., and Laimins, L.A. (2004). Role of the PDZ Domain-Binding Motif of the Oncoprotein E6 in the Pathogenesis of Human Papillomavirus Type 31. J. Virol. *78*, 12366–12377.

Lee, D., Carmichael, D., Krebs, E., and McKnight, G. (1983). Isolation of a cDNA clone for the type I regulatory subunit of bovine cAMP-dependent protein kinase. Proc. Natl. Acad. Sci. *80*, 3608–3612.

Lee, J.-O., Russo, A.A., and Pavletich, N.P. (1998). Structure of the retinoblastoma tumour-suppressor pocket domain bound to a peptide from HPV E7. Nature *391*, 859–865.

Leechanachai, P., Banks, L., Moreau, F., and Matlashewski, G. (1992). The E5 gene from human papillomavirus type 16 is an oncogene which enhances growth factor-mediated signal transduction to the nucleus. Oncogene *7*, 19–25.

Lemay, J., Maidou-Peindara, P., Cancio, R., Ennifar, E., Coadou, G., Maga, G., Rain, J.C., Benarous, R., and Liu, L.X. (2008). AKAP149 Binds to HIV-1 Reverse Transcriptase and Is Involved in the Reverse Transcription. J. Mol. Biol. *383*, 783–796.

Lesch, K.P., and Manji, H.K. (1992). Signal-transducing G proteins and antidepressant drugs: evidence for modulation of alpha subunit gene expression in rat brain. Biol. Psychiatry *32*, 549–579.

Leung, T., Liu, S., Leung, R., Chu, M., Cheung, A., and Ngan, H. (2015). HPV 16 E2 binding sites 1 and 2 become more methylated than E2 binding site 4 during cervical carcinogenesis. J Med Virol *87*, 1022–1033.

Li, X., and Coffino, P. (1996). High-risk human papillomavirus E6 protein has two distinct binding sites within p53, of which only one determines degradation. J. Virol. *70*, 4509–4516.

Li, H., Adamik, R., Pacheco-Rodriguez, G., Moss, J., and Vaughan, M. (2003). Protein kinase A-anchoring (AKAP) domains in brefeldin A-inhibited guanine nucleotide-exchange protein 2 (BIG2). Proc. Natl. Acad. Sci. U. S. A. *100*, 1627–1632.

Li, N., Franceschi, S., Howell-Jones, R., Snijders, P.J.F., and Clifford, G.M. (2011). Human papillomavirus type distribution in 30,848 invasive cervical cancers worldwide: Variation by geographical region, histological type and year of publication. Int. J. Cancer *128*, 927–935.

Liao, J.B. (2006). Cancer Issue: Viruses and Human Cancer. Yale J. Biol. Med. *79*, 115.

Litvin, T.N., Kamenetsky, M., Zarifyan, A., Buck, J., and Levin, L.R. (2003). Kinetic properties of "soluble" adenylyl cyclase: Synergism between calcium and bicarbonate. J. Biol. Chem. *278*, 15922–15926.

Litwin, T.R., Clarke, M.A., Dean, M., and Wentzensen, N. (2017). Somatic host cell alterations in HPV carcinogenesis. Viruses *9*.

Liu, S., Minaguchi, T., Lachkar, B., Zhang, S., Xu, C., Tenjimbayashi, Y., Shikama, A., Tasaka, N., Akiyama, A., Sakurai, M., et al. (2018). Separate analysis of human papillomavirus E6 and E7 messenger RNAs to predict cervical neoplasia progression. PLoS One *13*, 6–17.

Liu, W., Hua, S., Dai, Y., Yuan, Y., Yang, J., Deng, J., Huo, Y., Chen, X., Teng, B., Yu, X., et al. (2015). Roles of Cx43 and AKAP95 in ovarian cancer tissues in G1/S phase. Int. J. Clin. Exp. Pathol. *8*, 14315–14324.

Liu, X., Dakic, A., Zhang, Y., Dai, Y., Chen, R., and Schlegel, R. (2009). HPV E6 protein interacts physically and functionally with the cellular telomerase complex. Proc. Natl. Acad. Sci. U. S. A. *106*, 18780–18785.

Lodish, H., Berk, A., Kaiser, C., Krieger, M., Scott, M.P., Bretscher, A., Ploegh, H., and Matsudaira, P. (2007). Molecular Mechanisms for Regulating Mitotic Events. In Molecular Cell Biology, p.

Logothetis, D.E., Kurachi, Y., Galper, J., Neer, E.J., and Clapham, D.E. (1987). The βγ subunits of GTP-binding proteins activate the muscarinic K+ channel in heart. 321–326.

Lohmanntt, S.M., Decamilli, P., Einigt, I., and Waltertt, U. (1984). High-affinity binding of the regulatory subunit (RI,) of cAMP- dependent protein kinase to microtubule-associated and other cellular proteins (cytoplasmic organization/microtubule-associated protein 2/R1l binding proteins/affinity chromatography/immunoblotting). Cell Biol. *81*, 6723–6727.

Longworth, M.S., and Laimins, L.A. (2004). Pathogenesis of human papillomaviruses in differentiating epithelia. Microbiol. Mol. Biol. Rev. *68*, 362–372.

Loo, Y.-M., and Melendy, T. (2004). Recruitment of Replication Protein A by the Papillomavirus E1 Protein and Modulation by Single-Stranded DNA. J. Virol. *78*, 1605–1615.

López-Soop, G., Rønningen, T., Rogala, A., Richartz, N., Blomhoff, H.K., Thiede, B., Collas, P., and Küntziger, T. (2017). AKAP95 interacts with nucleoporin TPR in mitosis and is important for the spindle assembly checkpoint. Cell Cycle *16*, 947–956.

Lorenz, L.D., Rivera Cardona, J., and Lambert, P.F. (2013). Inactivation of p53 Rescues the Maintenance of High Risk HPV DNA Genomes Deficient in Expression of E6. PLoS Pathog. *9*.

Luck, K., Charbonnier, S., and Travé, G. (2012). The emerging contribution of sequence context to the specificity of protein interactions mediated by PDZ domains. FEBS Lett. *586*, 2648–2661.

Lue, R., SM, M., Branton, D., and Chishti, A. (1994). Cloning and characterization of hdlg: the human homologue of the Drosophila discs large tumor suppressor binds to

protein 4.1. PNAS *91*, 9818–9822.

Luo, R.X., Postigo, A.A., and Dean, D.C. (1998). Rb interacts with histone deacetylase to repress transcription. Cell *92*, 463–473.

Madamanchi, A. (2007). Beta-adrenergic receptor signaling in cardiac function and heart failure. Mcgill J. Med. *10*, 99–104.

Maglennon, G.A., McIntosh, P., and Doorbar, J. (2011). Persistence of viral DNA in the epithelial basal layer suggests a model for papillomavirus latency following immune regression. Virology *414*, 153–163.

Mantovani, F., Massimi, P., and Banks, L. (2001). Proteasome-mediated regulation of the hDlg tumour suppresor protein. J. Cell Sci. *114*, 4285–4292.

Mariani, L., and Venuti, A. (2010). HPV vaccine: An overview of immune response, clinical protection, and new approaches for the future. J. Transl. Med. *8*, 105.

Marsh, E., Delury, C., Davies, N., Weston, C., Miah, M.A.L., Banks, L., Parish, J., Higgs, M., and Roberts, S. (2017a). Mitotic control of human papillomavirus genome-containing cells is regulated by the function of the PDZ-binding motif of the E6 oncoprotein. Oncotarget *8*.

Marsh, E.K., Delury, C.P., Davies, N.J., Weston, C.J., Miah, M.A.L., Banks, L., Parish, J.L., Higgs, M.R., and Roberts, S. (2017b). Mitotic control of human papillomavirus genome-containing cells is regulated by the function of the PDZ-binding motif of the E6 oncoprotein. Oncotarget *8*, 19491–19506.

Marstad, A., Landsverk, O.J.B., Strømme, O., Otterlei, M., Collas, P., Sundan, A., and Brede, G. (2016). A-kinase anchoring protein AKAP95 is a novel regulator of ribosomal RNA synthesis. FEBS J. *283*, 757–770.

de Martel, C., Plummer, M., Vignat, J., and Franceschi, S. (2017). Worldwide burden of cancer attributable to HPV by site, country and HPV type. Int. J. Cancer *141*, 664–670.

Martinez-Contreras, R., Cloutier, P., Shkreta, L., Fisette, J., Revil, T., and Chabot, B. (2007). hnRNP proteins and splicing control. Adv Exp Med Biol *623*, 123–147.

Martins, S.B., Eide, T., Steen, R.L., Jahnsen, T., Skalhegg, B.S., and Collas, P. (2000). HA95 is a protein of the chromatin and nuclear matrix regulating nuclear envelope dynamics. J. Cell Sci. *113*, 3703–3713.

Masci, A., Galgani, M., Cassano, S., De Simone, S., Gallo, A., De Rosa, V., Zappacosta, S., and Racioppi, L. (2003). HIV-1 gp120 induces anergy in naive T lymphocytes through CD4-independent protein kinase-A-mediated signaling. J Leukoc Biol *74*, 1117–1124.

Matulef, K., and Zagotta, W.N. (2003). Cyclic Nucleotide-Gated Ion Channels. Annu. Rev. Cell Dev. Biol. *19*, 23–44.

Matyakhina, L., Lenherr, S., and Stratakis, C. (2002). Protein kinase A and chromosomal stability. Ann. N. Y. Acad. Sci. 148–157.

McBride, A.A. (2009). The Papillomavirus E2 Proteins. Nat Rev Mol Cell Biol. *10 (2)*, 116–125.

McBride, A.A. (2017). Mechanisms and strategies of papillomavirus replication. Biol. Chem. *398*, 919–927.

McBride, A.A., and Warburton, A. (2017). The role of integration in oncogenic progression of HPV-associated cancers. PLoS Pathog. *13*, 1–7.

McCance, D.J., Patel, D., Huang, S.-M., and Baglia, L.A. (1999). The E6 protein of human papillomavirus type 16 binds to and inhibits co-activation by CBP and p300. EMBO J. *18*, 5061–5072.

McDonough, K.A., and Rodriguez, A. (2011). The myriad roles of cyclic AMP in microbial pathogens: from signal to sword. Nat. Rev. Microbiol. *10*, 27–38.

McGraw, D.W., and Liggett, S.B. (2005). Molecular mechanisms of beta2-adrenergic receptor function and regulation. Proc. Am. Thorac. Soc. *2*, 292–296; discussion 311-2.

McLaughlin-Drubin, M.E., Bromberg-White, J.L., and Meyers, C. (2005). The role of the human papillomavirus type 18 E7 oncoprotein during the complete viral life cycle. Virology *338*, 61–68.

Melar-New, M., and Laimins, L.A. (2010). Human Papillomaviruses Modulate Expression of MicroRNA 203 upon Epithelial Differentiation to Control Levels of p63 Proteins. J. Virol. *84*, 5212–5221.

Melendy, T., Sedman, J., and Stenlund, A. (1995). Cellular factors required for papillomavirus DNA replication. J Virol *69*, 7857–7867.

Métais, J.Y., Navarro, C., Santoni, M.J., Audebert, S., and Borg, J.P. (2005). hScrib interacts with ZO-2 at the cell-cell junctions of epithelial cells. FEBS Lett. *579*, 3725–3730.

Mirkovic, J., Howitt, B.E., Roncarati, P., Demoulin, S., Suarez-Carmona, M., Hubert, P., McKeon, F.D., Xian, W., Li, A., Delvenne, P., et al. (2015). Carcinogenic HPV infection in the cervical squamo-columnar junction. J. Pathol. *236*, 265–271.

Moody, C.A., and Laimins, L.A. (2009). Human papillomaviruses activate the ATM DNA damage pathway for viral genome amplification upon differentiation. PLoS Pathog. *5*.

Moorthy, B.S., Gao, Y., and Anand, G.S. (2011). Phosphodiesterases catalyze hydrolysis of cAMP-bound to regulatory subunit of protein kinase A and mediate signal termination. Mol. Cell. Proteomics *10*, 1–15.

Morales-Sánchez, A., and Fuentes-Pananá, E.M. (2014). Human viruses and cancer. Viruses *6*, 4047–4079.

Moreno-Fernandez, M.E., Rueda, C.M., Velilla, P.A., Rugeles, M.T., and Chougnet, C.A. (2011). cAMP During HIV Infection: Friend or Foe? AIDS Res. Hum. Retroviruses *28*, 49–53.

Morgan, E.L., and Macdonald, A. (2019). Autocrine STAT3 activation in HPV positive cervical cancer through a virus-driven Rac1—NFκB—IL-6 signalling axis.

Morgan, E.L., Wasson, C.W., Hanson, L., Kealy, D., Pentland, I., McGuire, V., Scarpini, C., Coleman, N., Arthur, J.S.C., Parish, J.L., et al. (2018). STAT3 activation by E6 is essential for the differentiation-dependent HPV18 life cycle.

Muller, M., Jacob, Y., Jones, L., Weiss, A., Brino, L., Chantier, T., Lotteau, V., Favre, M., and Demeret, C. (2012). Large scale genotype comparison of human papillomavirus E2-host interaction networks provides new insights for E2 molecular functions. PLoS Pathog. *8*.

Müller, M., Prescott, E.L., Wasson, C.W., and MacDonald, A. (2015). Human papillomavirus E5 oncoprotein: Function and potential target for antiviral therapeutics. Future Virol. *10*, 27–39.

Münger, K., Werness, B.A., Dyson, N., Phelps, W.C., Harlow, E., and Howley, P.M. (1989). Complex formation of human papillomavirus E7 proteins with the retinoblastoma tumor suppressor gene product. EMBO J. *8*, 4099–4105.

Murdoch, J.N., Henderson, D.J., Doudney, K., Gaston-Massuet, C., Phillips, H.M., Paternotte, C., Arkell, R., Stanier, P., and Copp, A.J. (2003). Disruption of scribble (Scrb1) causes severe neural tube defects in the circletail mouse. Hum. Mol. Genet. *12*, 87–98.

Nadella, K.S., and Kirschner, L.S. (2005). Disruption of protein kinase A regulation causes immortalization and dysregulation of D-type cyclins. Cancer Res. *65*, 10307–10315.

Nagasaka, K., Pim, D., Massimi, P., Thomas, M., Tomaić, V., Subbaiah, V., Kranjec, C., Nakagawa, S., Yano, T., Taketani, Y., et al. (2010). The cell polarity regulator hScrib controls ERK activation through a KIM site-dependent interaction. Oncogene *29*, 5311–5321.

Nakagawa, S., and Huibregtse, J.M. (2000). Human Scribble (Vartul) Is Targeted for Ubiquitin-Mediated Degradation by the High-Risk Papillomavirus E6 Proteins and the E6AP Ubiquitin-Protein Ligase. Mol. Cell. Biol. *20*, 8244–8253.

Nakagawa, S., Yano, T., Nakagawa, K., Takizawa, S., Suzuki, Y., Yasugi, T., Huibregtse, J.M., and Taketani, Y. (2004). Analysis of the expression and localisation of a LAP protein, human scribble, in the normal and neoplastic epithelium of uterine cervix. Br. J. Cancer *90*, 194–199.

Nakahara, T., and Lambert, P.F. (2007). Induction of promyelocytic leukemia (PML) oncogenic domains (PODs) by papillomavirus. Virology *366*, 316–329.

Nakahara, T., Nishimura, A., Tanaka, M., Ueno, T., Ishimoto, A., and Sakai, H. (2002). Modulation of the Cell Division Cycle by Human Papillomavirus Type 18 E4. J. Virol. *76*, 10914–10920.

Naud, P.S., Roteli-Martins, C.M., De Carvalho, N.S., Teixeira, J.C., de Borba, P.C., Sanchez, N., Zahaf, T., Catteau, G., Geeraerts, B., and Descamps, D. (2014). Sustained efficacy , immunogenicity , and safety of the HPV-16 / 18 AS04-adjuvanted vaccine Final analysis of a long-term follow-up study up to 9 . 4 years. Hum Vaccin Immunother *10*, 2147–2162.

Navratil, V., De chassey, B., Meyniel, L., Delmotte, S., Gautier, C., André, P., Lotteau, V., and Rabourdin-Combe, C. (2009). VirHostNet: A knowledge base for the management and the analysis of proteome-wide virus-host interaction networks. Nucleic Acids Res. *37*, 661–668.

Neal, C.L., and Yu, D. (2010). 14-3-3Z As a Prognostic Marker and Therapeutic Target for Cancer. Expert Opin. Ther. Targets *14*, 1343–1354.

Neary, C.L., Nesterova, M., Yee, S.C., Cheadle, C., Becker, K.G., and Cho-Chung, Y.S. (2004). Protein kinase A isozyme switching: Eliciting differential cAMP signaling and tumor reversion. Oncogene *23*, 8847–8856.

Nelson, L., Rose, R., LeRoux, L., Lane, C., Bruya, K., and Moroianu, J. (2000). Nuclear import and DNA binding of human papillomavirus type 45 L1 capsid protein. J Cell

Biochem *79*, 225–238.

Newlon, M., Roy, M., Morikis, D., Carr, D., Westphal, R., Scott, J., and Jennings, P. (2001). A novel mechanism of PKA anchoring revealed by solution structures of anchoring complexes. EMBO J. *20*, 1651–1662.

Nguyen, M.L., Nguyen, M.M., Lee, D., Griep, A.E., and Lambert, P.F. (2003). The PDZ Ligand Domain of the Human Papillomavirus Type 16 E6 Protein Is Required for E6's Induction of Epithelial Hyperplasia In Vivo. J. Virol. *77*, 6957–6964.

Nicolaides, L., Davy, C., Raj, K., Kranjec, C., Banks, L., and Doorbar, J. (2011). Stabilization of HPV16 E6 protein by PDZ proteins, and potential implications for genome maintenance. Virology *414*, 137–145.

Nikolaev, V.O., Bünemann, M., Hein, L., Hannawacker, A., and Lohse, M.J. (2004). Novel single chain cAMP sensors for receptor-induced signal propagation. J. Biol. Chem. *279*, 37215–37218.

Nishimura, A., Ono, T., Ishimoto, A., Dowhanick, J.J., Frizzell, M.A., Howley, P.M., and Sakai, H. (2000). Mechanisms of Human Papillomavirus E2-Mediated Repression of Viral Oncogene Expression and Cervical Cancer Cell Growth Inhibition. J. Virol. *74*, 3752–3760.

Nokta, M., and Pollard, R. (1991). Human immunodeficiency virus infection: association with altered intracellular levels of cAMP and cGMP in MT-4 cells. Virology *181*, 211–217.

Nominé, Y., Ristriani, T., Laurent, C., Lefèvre, J.-F., Weiss, É., and Travé, G. (2001). A strategy for optimizing the monodispersity of fusion proteins: application to purification of recombinant HPV E6 oncoprotein. Protein Eng. Des. Sel. *14*, 297–305.

Nominé, Y., Masson, M., Charbonnier, S., Zanier, K., Ristriani, T., Deryckère, F., Sibler, A.P., Desplancq, D., Atkinson, R.A., Weiss, E., et al. (2006). Structural and functional analysis of E6 oncoprotein: Insights in the molecular pathways of human papillomavirus-mediated pathogenesis. Mol. Cell *21*, 665–678.

Norris, R.P., Ratzan, W.J., Freudzon, M., Mehlmann, L.M., Krall, J., Movsesian, M.A., Wang, H., Ke, H., Nikolaev, V.O., and Jaffe, L.A. (2009). Cyclic GMP from the surrounding somatic cells regulates cyclic AMP and meiosis in the mouse oocyte. Development *136*, 1869–1878.

Oh, J.M., Kim, S.H., Lee, Y. Il, Seo, M., Kim, S.Y., Song, Y.S., Kim, W.H., and Juhnn, Y.S. (2009). Human papillomavirus E5 protein induces expression of the EP4 subtype of prostaglandin E2 receptor in cyclic AMP response element-dependent pathways in cervical cancer cells. Carcinogenesis *30*, 141–149.

Oh, J.M., Kim, S.H., Cho, E.A., Song, Y.S., Kim, W.H., and Juhnn, Y.S. (2010). Human papillomavirus type 16 E5 protein inhibits hydrogen peroxide-induced apoptosis by stimulating ubiquitin-proteasome-mediated degradation of Bax in human cervical cancer cells. Carcinogenesis *31*, 402–410.

Oh, S.T., Kyo, S., and Laimins, L.A. (2001). Telomerase Activation by Human Papillomavirus Type 16 E6 Protein: Induction of Human Telomerase Reverse Transcriptase Expression through Myc and GC-Rich Sp1 Binding Sites. J. Virol. *75*, 5559–5566.

Ørstavik, S., Eide, T., Collas, P., Han, I., Taskén, K., Kieff, E., Jahnsen, T., and Sklhegg, B.S. (2000). Identification, cloning and characterization of a novel nuclear protein, HA95, homologous to A-kinase anchoring protein 95*. Biol. Cell *92*, 27–37.

Ozbun, M.A. (2002). Human papillomavirus type 31b infection of human keratinocytes and the onset of early transcription. J. Virol. *76*, 11291–11300.

Palmer, T., Wallace, L., Pollock, K.G., Cuschieri, K., Robertson, C., Kavanagh, K., and Cruickshank, M. (2019). Prevalence of cervical disease at age 20 after immunisation with bivalent HPV vaccine at age 12-13 in Scotland: Retrospective population study. BMJ *365*, 1–10.

Paramonov, V.M., Mamaeva, V., Sahlgren, C., and Rivero-Müller, A. (2015). Genetically-encoded tools for cAMP probing and modulation in living systems. Front. Pharmacol. *6*, 1–21.

Parish, J.L., Bean, A.M., Park, R.B., and Androphy, E.J. (2006). ChlR1 Is Required for Loading Papillomavirus E2 onto Mitotic Chromosomes and Viral Genome Maintenance. Mol. Cell *24*, 867–876.

Park, R.B., and Androphy, E.J. (2002). Genetic Analysis of High-Risk E6 in Episomal Maintenance of Human Papillomavirus Genomes in Primary Human Keratinocytes. J. Virol. *76*, 11359–11364.

Park, D.-W., Kim, S.-S., Nam, M.-K., Kim, G.-Y., Kim, J., and Rhim, H. (2011). Improved recovery of active GST-fusion proteins from insoluble aggregates: solubilization and purification conditions using PKM2 and HtrA2 as model proteins. BMB Rep. *44*, 279–284.

Peh, W.L., Middleton, K., Christensen, N., Nicholls, P., Egawa, K., Sotlar, K., Brandsma, J., Percival, A., Lewis, J., Liu, W.J., et al. (2002). Life Cycle Heterogeneity in Animal Models of Human Papillomavirus-Associated Disease. J. Virol. *76*, 10401–10416.

Pentland, I., Campos-León, K., Cotic, M., Davies, K.J., Wood, C.D., Groves, I.J., Burley, M., Coleman, N., Stockton, J.D., Noyvert, B., et al. (2018). Disruption of CTCF-YY1-dependent looping of the human papillomavirus genome activates differentiation-induced viral oncogene transcription. PLoS Biol. *16*, e2005752.

Pidoux, G., and Taskén, K. (2010). Specificity and spatial dynamics of protein kinase a signaling organized by A-kinase-anchoring proteins. J. Mol. Endocrinol. *44*, 271–284.

Pim, D., Thomas, M., Javier, R., Gardiol, D., and Banks, L. (2000). HPV E6 targeted degradation of the discs large protein: evidence for the involvement of a novel ubiquitin ligase. Oncogene *19*, 719–725.

Pim, D., Tomaic, V., and Banks, L. (2009). The Human Papillomavirus (HPV) E6* Proteins from High-Risk, Mucosal HPVs Can Direct Degradation of Cellular Proteins in the Absence of Full-Length E6 Protein. J. Virol. *83*, 9863–9874.

Plummer, M., de Martel, C., Vignat, J., Ferlay, J., Bray, F., and Franceschi, S. (2016). Global burden of cancers attributable to infections in 2012: a synthetic analysis. Lancet Glob. Heal. *4*, e609–e616.

Ponsioen, B., Zhao, J., Riedl, J., Zwartkruis, F., van der Krogt, G., Zaccolo, M., Moolenaar, W.H., Bos, J.L., and Jalink, K. (2004). Detecting cAMP-induced Epac activation by fluorescence resonance energy transfer: Epac as a novel cAMP indicator.

EMBO Rep. *5*, 1176–1180.

Porter, S.E., Dwyer-Nield, L.D., and Malkinson, A.M. (2001). Regulation of lung epithelial cell morphology by cAMP-dependent protein kinase type I isozyme. Am. J. Physiol. - Lung Cell. Mol. Physiol. *280*, 1282–1289.

Prescott, E.L., Brimacombe, C.L., Hartley, M., Bell, I., Graham, S., and Roberts, S. (2014). Human Papillomavirus Type 1 E1^E4 Protein Is a Potent Inhibitor of the Serine-Arginine (SR) Protein Kinase SRPK1 and Inhibits Phosphorylation of Host SR Proteins and of the Viral Transcription and Replication Regulator E2. J. Virol. *88*, 12599–12611.

Prinz, A., Diskar, M., Erlbruch, A., and Herberg, F.W. (2006). Novel, isotype-specific sensors for protein kinase A subunit interaction based on bioluminescence resonance energy transfer (BRET). Cell. Signal. *18*, 1616–1625.

Rabbi, M.F., Al-Harthi, L., Saifuddin, M., and Roberts, K.A. (1998). The cAMP-Dependent Protein Kinase A and Protein Kinase C-β Pathways Synergistically Interact to Activate HIV-1 Transcription in Latently Infected Cells of Monocyte/Macrophage Lineage. Virology *245*, 257–269.

Ramoz, N., Rueda, L.-A., Bouadjar, B., Montoya, L.-S., Orth, G., and Favre, M. (2002). Mutations in two adjacent novel genes are associated with epidermodysplasia verruciformis. Nat. Genet. *32*, 579–581.

Rehmann, H., Arias-Palomo, E., Hadders, M.A., Schwede, F., Llorca, O., and Bos, J.L. (2008). Structure of Epac2 in complex with a cyclic AMP analogue and RAP1B. Nature *455*, 124.

Reimann, E., Walsh, D., and Krebs, E. (1971). Purification and Properties of Rabbit Skeletal Muscle Adenosine 3',5'-Monophosphate-dependent Protein Kinases. J. Biol. Chem. *246*, 1986–1995.

Rezaee, F., Harford, T.J., Linfield, D.T., Altawallbeh, G., Midura, R.J., Ivanov, A.I., and Piedimonte, G. (2017). cAMP-dependent activation of protein kinase A attenuates respiratory syncytial virus-induced human airway epithelial barrier disruption. PLoS One *12*, 1–22.

Rich, T.C., Webb, K.J., and Leavesley, S.J. (2014). Can we decipher the information content contained within cyclic nucleotide signals? J. Gen. Physiol. *143*, 17–27.

Richards, K.F., Bienkowska-Haba, M., Dasgupta, J., Chen, X.S., and Sapp, M. (2013). Multiple Heparan Sulfate Binding Site Engagements Are Required for the Infectious Entry of Human Papillomavirus Type 16. J. Virol. *87*, 11426–11437.

Roberts, S. (2015). Papillomaviruses. In ELS, (Chichester, UK: John Wiley & Sons, Ltd), pp. 1–11.

Roberts, S., Ashmole, I., Johnson, G.D., Kreider, J.W., and Gallimore, P.H. (1993). Cutaneous and Mucosal Human Papillomavirus E4 Proteins Form Intermediate Filament-like Structures in Epithelial Cells. Virology *197*, 176–187.

Roberts, S., Calautti, E., Vanderweil, S., Nguyen, H.O., Foley, A., Baden, H.P., and Viel, A. (2007). Changes in localization of human discs large (hDlg) during keratinocyte differentiation is associated with expression of alternatively spliced hDlg variants. Exp. Cell Res. *313*, 2521–2530.

Roberts, S., Delury, C., and Marsh, E. (2012). The PDZ protein discs-large (DLG): the "Jekyll and Hyde" of the epithelial polarity proteins. FEBS J. *279*, 3549–3558.

Roman, A. (2006). The human papillomavirus E7 protein shines a spotlight on the pRB family member, p130. Cell Cycle *5*, 567–568.

Roman, A., and Munger, K. (2013). The papillomavirus E7 proteins. Virology *445*, 138–168.

Rondard, P., Iiri, T., Srinivasan, S., Meng, E., Fujita, T., and Bourne, H.R. (2001). Mutant G protein α subunit activated by Gβγ: A model for receptor activation? PNAS *98*, 6150–6155.

de Rooij, J., Zwartkruis, F.J.T., Verheijen, M.H.G., Cool, R.H., Nijman, S.M.B., Wittinghofer, A., and Bos, J.L. (1998). Epac is a Rap1 guanine-nucleotide-exchange factor directly activated by cyclic AMP. Nature *396*, 474–477.

De Rooij, J., Rehmann, H., Van Triest, M., Cool, R.H., Wittinghofer, A., and Bos, J.L. (2000). Mechanism of regulation of the Epac family of cAMP-dependent RapGEFs. J. Biol. Chem. *275*, 20829–20836.

Rosano, G.L., and Ceccarelli, E.A. (2009). Rare codon content affects the solubility of recombinant proteins in a codon bias-adjusted Escherichia coli strain. Microb. Cell Fact. *8*, 41.

Rosenbaum, D.M., Søren, G.R., and Kobilka, B.K. (2009). The structure and function of G-protein-coupled receptors. Nature *459*, 356–363.

Rous, P. (1911). A Sarcoma of the Fowl Transmissible by an Agent Separable from the Tumor Cells. Am. J. Med. Sci. *142*, 312.

Rozenblatt-Rosen, O., Deo, R.C., Padi, M., Adelmant, G., Calderwood, M.A., Rolland, T., Grace, M., Dricot, A., Askenazi, M., Tavares, M., et al. (2012). Interpreting cancer genomes using systematic host network perturbations by tumour virus proteins. Nature *487*, 491–495.

Sadana, R., and Dessauer, C.W. (2009). Physiological roles for G protein-regulated adenylyl cyclase isoforms: Insights from knockout and overexpression studies. NeuroSignals *17*, 5–22.

Sakakibara, N., Mitra, R., and McBride, A.A. (2011). The Papillomavirus E1 Helicase Activates a Cellular DNA Damage Response in Viral Replication Foci. J. Virol. *85*, 8981–8995.

Sarabia-Vega, V., and Banks, L. (2019). Acquisition of a phospho-acceptor site enhances HPV E6 PDZ-binding motif functional promiscuity. J. Gen. Virol. 0–9.

Schaper, I.D., Marcuzzi, G.P., Weissenborn, S.J., Kasper, H.U., Dries, V., Smyth, N., Fuchs, P., and Pfister, H. (2005). Development of Skin Tumors in Mice Transgenic for Early Genes of Human Papillomavirus Type 8. Cancer Res. *65*, 1394–1400.

Scheffer, K.D., Gawlitza, A., Spoden, G. a, Zhang, X. a, Lambert, C., Berditchevski, F., and Florin, L. (2013). Tetraspanin CD151 mediates papillomavirus type 16 endocytosis. J. Virol. *87*, 3435–3446.

Scheffner, M., Werness, B.A., Huibregtse, J.M., Levine, A.J., and Howley, P.M. (1990). The E6 oncoprotein encoded by human papillomavirus types 16 and 18 promotes the

degradation of p53. Cell *63*, 1129–1136.

Scheffner, M., Takahashi, T., Huibregtse, J.M., Minna, J.D., and Howley, P.M. (1992). Interaction-of the human papillomavirus type 16 E6 oncoprotein with wild- type and mutant human p53 proteins. J. Virol. *66*, 5100–5105.

Scheffner, M., Huibregtse, J.M., Vierstra, R.D., and Howley, P.M. (1993). The HPV-16 E6 and E6-AP complex functions as a ubiquitin-protein ligase in the ubiquitination of p53. Cell *75*, 495–505.

Schelhaas, M., Shah, B., Holzer, M., Blattmann, P., Kühling, L., Day, P.M., Schiller, J.T., and Helenius, A. (2012). Entry of human papillomavirus type 16 by actin-dependent, clathrin- and lipid raft-independent endocytosis. PLoS Pathog. *8*.

Schoneberg, T., Schulz, A., Biebermann, H., Hermsford, T., Rompler, H., and Sangkuhl, K. (2004). Mutant G-protein-coupled receptors as a cause of human diseases. Pharmacol Ther *104*, 173–206.

Schütz, W., and Freissmuth, M. (1992). Reverse intrinsic activity of antagonists on G protein-coupled receptors. Trends Pharmacol. Sci. *13*, 376–380.

Sciuto, M.R., Coppola, V., Iannolo, G., De Maria, R., and Haas, T.L. (2019). Two-Step Co-Immunoprecipitation (TIP). Curr. Protoc. Mol. Biol. *125*.

Scott, J. (1991). Cyclic nucleotide-dependent protein kinases. Pharmacol. Ther. *50*, 123–145.

Scott, J., Glaccum, M., Zoller, M., Uhler, M., Helfman, D., McKnight, G., and Krebs, E. (1987). The molecular cloning of a type II regulatory subunit of the cAMP-dependent protein kinase from rat skeletal muscle and mouse brain. Proc. Natl. Acad. Sci. *84*, 5192–5196.

Sedman, J., and Stenlund, A. (1998). The papillomavirus E1 protein forms a DNA-dependent hexameric complex with ATPase and DNA helicase activities. J. Virol. *72*, 6893–6897.

Sekhar, V., and McBride, A.A. (2012). Phosphorylation Regulates Binding of the Human Papillomavirus Type 8 E2 Protein to Host Chromosomes. J. Virol. *86*, 10047 LP – 10058.

Sekhar, V., Reed, S.C., and McBride, A.A. (2010). Interaction of the Betapapillomavirus E2 Tethering Protein with Mitotic Chromosomes. J. Virol. *84*, 543–557.

Selinka, H.-C., Giroglou, T., and Sapp, M. (2002). Analysis of the infectious entry pathway of human papillomavirus type 33 pseudovirions. Virology *299*, 279–287.

Shafti-Keramat, S., Handisurya, A., Kriehuber, E., Meneguzzi, G., Slupetzky, K., and Kirnbauer, R. (2003). Different heparan sulfate proteoglycans serve as cellular receptors for human papillomaviruses. J. Virol. *77*, 13125–13135.

Shai, A., Brake, T., Somoza, C., and Lambert, P.F. (2007). The human papillomavirus E6 oncogene dysregulates the cell cycle and contributes to cervical carcinogenesis through two independent activities. Cancer Res. *67*, 1626–1635.

Shohag, M.H., Nishioka, T., Ahammad, R.U., Nakamuta, S., Yura, Y., Hamaguchi, T., Kaibuchi, K., and Amano, M. (2015). Phosphoproteomic analysis using the WW and FHA domains as biological filters. Cell Struct. Funct. *40*, 95–104.

Simoes, P., Medeiros, L., Simoes Pires, P., Edelweiss, M., Rosa, D., Silva, F., Silva, B., and Rosa, M. (2012). Prevalence of human papillomavirus in breast cancer: a systematic review. Int J Gynecol Cancer *22*, 343–347.

Sims, R.J., and Reinberg, D. (2006). Histone H3 Lys 4 methylation: Caught in a bind? Genes Dev. *20*, 2779–2786.

Skoyles, J., and Sherry, K. (1992). Pharmacology, Mechanisms of Action and Uses of Selective Phosphodiesterase Inhibitors. Br J Anaesth *68*, 293–302.

Smith, J.L., Campos, S.K., and Ozbun, M.A. (2007). Human Papillomavirus Type 31 Uses a Caveolin 1- and Dynamin 2-Mediated Entry Pathway for Infection of Human Keratinocytes. J. Virol. *81*, 9922–9931.

Song, S., Gulliver, G.A., and Lambert, P.F. (2002). Human papillomavirus type 16 E6 and E7 oncogenes abrogate radiation-induced DNA damage responses in vivo through p53-dependent and p53-independent pathways. Proc. Natl. Acad. Sci. *95*, 2290–2295.

Spanos, W.C., Geiger, J., Anderson, M.E., Harris, G.F., Bossler, A.D., Smith, R.B., Klingelhutz, A.J., and Lee, J.H. (2008). Immortalization and Anchorage-Independent Growth. Growth (Lakeland) *30*, 139–147.

Spoden, G., Freitag, K., Husmann, M., Boller, K., Sapp, M., Lambert, C., and Florin, L. (2008). Clathrin- and caveolin-independent entry of human papillomavirus type 16--involvement of tetraspanin-enriched microdomains (TEMs). PLoS One *3*, e3313.

Stauffer, Y., Raj, K., Masternak, K., and Beard, P. (1998). Infectious human papillomavirus type 18 pseudovirons. J Mol Biol *283*, 529–536.

Steen, R.L., Cubizolles, F., Le Guellec, K., and Collas, P. (2000). A kinase-anchoring protein (AKAP)95 recruits human chromosome-associated protein (hCAP)-D2/Eg7 for chromosome condensation in mitotic extract. J. Cell Biol. *149*, 531–536.

Steger, G., and Corbach, S. (1997). Dose-dependent regulation of the early promoter of human papillomavirus type 18 by the viral E2 protein. J. Virol. *71*, 50–58.

Steinberg, R.A., Cauthron, R.D., Symcox, M.M., and Shuntoh, H. (1993). Autoactivation of catalytic (C alpha) subunit of cyclic AMP-dependent protein kinase by phosphorylation of threonine 197. Mol. Cell. Biol. *13*, 2332–2341.

Stenlund, A. (2003). E1 initiator DNA binding specificity is unmasked by selective inhibition of non-specific DNA binding. EMBO J. *22*, 954–963.

Stephen, C.W., Helminen, P., and Lane, D.P. (1995). Characterisation of Epitopes on Human p53 using Phage-displayed Peptide Libraries: Insights into Antibody-Peptide Interactions. J. Mol. Biol. *248*, 58–78.

Stepp, W.H., Meyers, J.M., and McBride, A.A. (2013). Sp100 provides intrinsic immunity against human papillomavirus infection. MBio *4*, 1–13.

Sterlinko Grm, H., and Banks, L. (2004). Degradation of hDlg and MAGIs by human papillomavirus E6 is E6-AP-independent. J. Gen. Virol. *85*, 2815–2819.

Stewart, D., Ghosh, A., and Matlashewski, G. (2005). Involvement of Nuclear Export in Human Papillomavirus Type 18 E6-Mediated Ubiquitination and Degradation of p53. J. Virol. *79*, 8773–8783.

Stöppler, M.C., Straight, S.W., Tsao, G., Schlegel, R., and McCance, D.J. (1996). The E5 gene of HPV-16 enhances keratinocyte immortalization by full-length DNA. Virology *223*, 251–254.

Straight, S.W., Hinkle, P.M., Jewers, R.J., and McCance, D.J. (1993). The E5 oncoprotein of human papillomavirus type 16 transforms fibroblasts and effects the downregulation of the epidermal growth factor receptor in keratinocytes. J. Virol. *67*, 4521–4532.

Straight, S.W., Herman, B., and McCance, D.J. (1995). The E5 oncoprotein of human papillomavirus type 16 inhibits the acidification of endosomes in human keratinocytes. J. Virol. *69*, 3185–3192.

Straub, E., Fertey, J., Dreer, M., Iftner, T., and Stubenrauch, F. (2015). Characterization of the Human Papillomavirus 16 E8 Promoter. J. Virol. *89*, 7304–7313.

Stünkel, W., and Bernard, H.U. (1999). The chromatin structure of the long control region of human papillomavirus type 16 represses viral oncoprotein expression. J. Virol. *73*, 1918–1930.

Sugihara, T., Nakagawa, S., Sasajima, Y., Ichinose, T., Hiraike, H., Kondo, F., Uozaki, H., Fukusato, T., and Ayabe, T. (2016). Loss of the cell polarity determinant human Discs-large is a novel molecular marker of nodal involvement and poor prognosis in endometrial cancer. Br. J. Cancer *114*, 1012–1018.

Sun, Y., Li, L., Lau, F., Beavo, J.A., and Clark, E.A. (2000). Infection of CD4 + Memory T Cells by HIV-1 Requires Expression of Phosphodiesterase 4 . J. Immunol. *165*, 1755–1761.

Suryavanshi, S., Jadhav, S., and McConnell, B. (2018). Polymorphisms/Mutations in A-Kinase Anchoring Proteins (AKAPs): Role in the Cardiovascular System. J. Cardiovasc. Dev. Dis. *5*, 7.

Sutherland, E.W., Robison, G.A., and Reginald, W. (1968). Some Aspects of the Biological Role of. World Wide Web Internet Web Inf. Syst. 279–306.

Suzuki, K., Bose, P., Leong-quong, R.Y.Y., Fujita, D.J., and Riabowol, K. (2010). REAP : A two minute cell fractionation method.

Swindle, C.S., Zou, N., Van Tine, B.A., Shaw, G.M., Engler, J.A., and Chow, L.T. (1999). Human papillomavirus DNA replication compartments in a transient DNA replication system. J. Virol. *73*, 1001–1009.

Tan, S.H., Leong, L.E., Walker, P.A., and Bernard, H.U. (1994). The human papillomavirus type 16 E2 transcription factor binds with low cooperativity to two flanking sites and represses the E6 promoter through displacement of Sp1 and TFIID. J. Virol. *68*, 6411–6420.

Tao, H., Liu, W., Simmons, B.N., Harris, H.K., Cox, T.C., and Massiah, M.A. (2010). Purifying natively folded proteins from inclusion bodies using sarkosyl, Triton X-100, and CHAPS. Biotechniques *48*, 61–64.

Tarocchi, M., Polvani, S., Marroncini, G., and Galli, A. (2014). Molecular mechanism of hepatitis B virus-induced hepatocarcinogenesis. World J. Gastroenterol. *20*, 11630–11640.

Tasken, K., Skalhegg, B.S., Solberg, R., Andersson, K.B., Taylor, S.S., Lea, T., Blomhoff, H.K., Jahnsen, T., and Hansson, V. (1993). Novel isozymes of cAMP-dependent protein

kinase exist in human cells due to formation of RIα-RIβ heterodimeric complexes. J. Biol. Chem. *268*, 21276–21283.

Taylor, S., Buechler, J., and Yonemoto, W. (1990). cAMP-dependent protein kinase: framework for a diverse family of regulatory enzymes. Annu Rev Biochem *59*, 971–1005.

Thatte, J., Massimi, P., Thomas, M., Boon, S.S., and Banks, L. (2018). The Human Papillomavirus E6 PDZ Binding Motif Links DNA Damage Response Signaling to E6 Inhibition of p53 Transcriptional Activity. J. Virol. *92*, 1–14.

Thierry, F. (2009). Transcriptional regulation of the papillomavirus oncogenes by cellular and viral transcription factors in cervical carcinoma. Virology *384*, 375–379.

Thomas, J.G., and Baneyx, F. (1996). Protein misfolding and inclusion body formation in recombinant Escherichia coli cells overexpressing Heat-shock proteins. J. Biol. Chem. *271*, 11141–11147.

Thomas, J.T., Hubert, W.G., Ruesch, M.N., and Laimins, L.A. (1999). Human papillomavirus type 31 oncoproteins E6 and E7 are required for the maintenance of episomes during the viral life cycle in normal human keratinocytes. Proc. Natl. Acad. Sci. *96*, 8449–8454.

Thomas, M., Massimi, P., Jenkins, J., and Banks, L. (1995). HPV-18 E6 mediated inhibition of p53 DNA binding activity is independent of E6 induced degradation. Oncogene *10*, 261-8.

Thomas, M., Massimi, P., Navarro, C., Borg, J.-P., and Banks, L. (2005). The hScrib/Dlg apico-basal control complex is differentially targeted by HPV-16 and HPV-18 E6 proteins. Oncogene *24*, 6222–6230.

Thomas, M., Myers, M.P., Massimi, P., Guarnaccia, C., and Banks, L. (2016). Analysis of Multiple HPV E6 PDZ Interactions Defines Type-Specific PDZ Fingerprints That Predict Oncogenic Potential. PLoS Pathog. *12*, 1–21.

Thomsen, P., Van Deurs, B., Norrild, B., and Kayser, L. (2000). The HPV16 E5 oncogene inhibits endocytic trafficking. Oncogene *19*, 6023–6032.

Tian, R., Cui, Z., He, D., Tian, X., Gao, Q., Ma, X., Yang, J., Wu, J., Das, B.C., Severinov, K., et al. (2019). Risk stratification of cervical lesions using capture sequencing and machine learning method based on HPV and human integrated genomic profiles. Carcinogenesis 1–9.

Torres-Quesada, O., Mayrhofer, J., and Stefan, E. (2017). Adenylyl cyclase signalling complexes – Pharmacological challenges and opportunities. Pharmacol. Ther. *172*, 171–180.

Tresguerres, M., Levin, L., and Buck, J. (2011). Intracellular cAMP signaling by soluble adenylyl cyclase. Kidney Int *79*, 1277–1288.

Trimarchi, J.M., and Lees, J.A. (2002). Sibling rivalry in the E2F family. Nat. Rev. Mol. Cell Biol. *3*, 11–20.

Tsalkova, T., Blumenthal, D.K., Mei, F.C., White, M.A., and Cheng, X. (2009). Mechanism of Epac activation. Structural and functional analyses of Epac2 hinge mutants with constitutive and reduced activities. J. Biol. Chem. *284*, 23644–23651.

Tulay, P., and Serakinci, N. (2016). The role of human papillomaviruses in cancer

progression. J. Cancer Metastasis Treat. *2*, 201.

Tuteja, N. (2009). Signaling through G protein coupled receptors. Plant Signal Behav *4*, 942–947.

Ustav, M., Ustav, E., Szymanski, P., and Stenlund, A. (1991). Identification of the origin of replication of bovine papillomavirus and characterization of the viral origin recognition factor E1. EMBO J. *10*, 4321–4329.

Vaccarella, S., Herrero, R., Dai, M., Snijders, P.J.F., Meijer, C.J.L.M., Thomas, J.O., Anh, P.T.H., Ferreccio, C., Matos, E., Posso, H., et al. (2006). Reproductive factors, oral contraceptive use, and human papillomavirus infection: Pooled analysis of the IARC HPV prevalence surveys. Cancer Epidemiol. Biomarkers Prev. *15*, 2148–2153.

Valle, G.F., and Banks, L. (1995). The human papillomavirus (HPV)-6 and HPV-16 E5 proteins co-operate with HPV-16 E7 in the transformation of primary rodent cells. J. Gen. Virol. *76*, 1239–1245.

Vallee, R.B., DiBartolomeis, M.J., and Theurkauf, W.E. (1981). A protein kinase bound to the projection portion of MAP 2 (microtubule-associated protein 2). J. Cell Biol. *90*, 568–576.

Velfhuijzen, N., Snijders, P., Reiss, P., Meijer, C., and van de Wijgert, J. (2010). Factors affecting transmission of mucosal human papillomavirus. Lancet Infect Dis *12*, 862–874.

Verma, R.R., Sriraman, R., Rana, S.K., Ponnanna, N.M., Rajendar, B., Ghantasala, P., Rajendra, L., Matur, R. V., and Srinivasan, V.A. (2013). E6 protein of human papillomavirus 16 (HPV16) expressed in Escherichia coli sans a stretch of hydrophobic amino acids, enables purification of GST-ΔE6 in the soluble form and retains the binding ability to p53. Protein Expr. Purif. *92*, 41–47.

Viarisio, D., Mueller-Decker, K., Kloz, U., Aengeneyndt, B., Kopp-Schneider, A., Gröne, H.J., Gheit, T., Flechtenmacher, C., Gissmann, L., and Tommasino, M. (2011). E6 and E7 from beta hpv38 cooperate with ultraviolet light in the development of actinic keratosis-like lesions and squamous cell carcinoma in mice. PLoS Pathog. *7*, e1002125.

Viarisio, D., Mueller-Decker, K., Kloz, U., Aengeneyndt, B., Kopp-Schneider, A., Gröne, H.-J., Gheit, T., Flechtenmacher, C., Gissmann, L., and Tommasino, M. (2016). Correction: E6 and E7 from Beta Hpv38 Cooperate with Ultraviolet Light in the Development of Actinic Keratosis-Like Lesions and Squamous Cell Carcinoma in Mice. PLoS Pathog. *12*, e1006005.

Vigil, D., Blumenthal, D., Bornw, S., Taylor, S., and Trewhella, J. (2004). Differential Effects of Substrate on Type I and Type II PKA Holoenzyme Dissociation. Biochemistry *43*, 5629–5636.

Villa, L.L., Ault, K.A., Giuliano, A.R., Costa, R.L.R., Petta, C.A., Andrade, R.P., Brown, D.R., Ferenczy, A., Harper, D.M., Koutsky, L.A., et al. (2006). Immunologic responses following administration of a vaccine targeting human papillomavirus Types 6, 11, 16, and 18. Vaccine *24*, 5571–5583.

De Villiers, E.M., Fauquet, C., Broker, T.R., Bernard, H.U., and Zur Hausen, H. (2004). Classification of papillomaviruses. Virology *324*, 17–27.

Vousden, K.H., and Prives, C. (2009). Blinded by the Light: The Growing Complexity of p53. Cell *137*, 413–431.

Wallace, N.A., and Galloway, D.A. (2015). Novel Functions of the Human Papillomavirus E6 Oncoproteins. Annu. Rev. Virol. *2*, 403–423.

Wallin, K.-L., Wiklund, F., Angstrom, T., Bergman, F., Stendahl, U., Wadell, G., Hallmans, G., and Dillner, J. (1999). Type-Specific Persistence of Human Papillomavirus DNA before the Development of Invasive Cervical Cancer. Lancet *341*, 1633–1638.

Wang, H.K., Duffy, A.A., Broker, T.R., and Chow, L.T. (2009a). Robust production and passaging of infectious HPV in squamous epithelium of primary human keratinocytes. Genes Dev. *23*, 181–194.

Wang, Q., Kennedy, A., Das, P., McIntosh, P.B., Howell, S.A., Isaacson, E.R., Hinz, S.A., Davy, C., and Doorbar, J. (2009b). Phosphorylation of the Human Papillomavirus Type 16 E1^E4 Protein at T57 by ERK Triggers a Structural Change That Enhances Keratin Binding and Protein Stability. J. Virol. *83*, 3668–3683.

Warren, K., Warrilow, D., Meredith, L., and Harrich, D. (2009). Reverse transcriptase and cellular factors: Regulators of HIV-1 reverse transcription. Viruses *1*, 873–894.

Wasson, C.W., Morgan, E.L., Müller, M., Ross, R.L., Hartley, M., Roberts, S., and Macdonald, A. (2017). Human papillomavirus type 18 E5 oncogene supports cell cycle progression and impairs epithelial differentiation by modulating growth factor receptor signalling during the virus life cycle. Oncotarget *8*, 103581–103600.

Watson, R., Rollason, T., Reynolds, G., Murray, P., Banks, L., and Roberts, S. (2002). Changes in expression of the human homologue of the Drosophila discs large tumour suppressor protein in high-grade premalignant cervical neoplasias. Carcinogenesis *23*, 1791–1796.

Watson, R., Thomas, M., Banks, L., and Roberts, S. (2003). Activity of the human papillomavirus E6 PDZ-binding motif correlates with an enhanced morphological transformation of immortalized human keratinocytes. J. Cell Sci. *116*, 4925–4934.

Wei, L., Hu, J., Shi, B., and Jiang, H. (2019). Protein Condensates with Appropriate Material Properties Regulate Tumorigenesis. BioRxiv 1–19.

Wetherill, L.F., Holmes, K.K., Verow, M., Muller, M., Howell, G., Harris, M., Fishwick, C., Stonehouse, N., Foster, R., Blair, G.E., et al. (2012). High-Risk Human Papillomavirus E5 Oncoprotein Displays Channel-Forming Activity Sensitive to Small-Molecule Inhibitors. J. Virol. *86*, 5341–5351.

Wetherill, L.F., Wasson, C.W., Swinscoe, G., Kealy, D., Foster, R., Griffin, S., and Macdonald, A. (2018). Alkyl-imino sugars inhibit the pro-oncogenic ion channel function of human papillomavirus (HPV) E5. Antiviral Res.

White, E.A., Kramer, R.E., Tan, M.J.A., Hayes, S.D., Harper, J.W., and Howley, P.M. (2012a). Comprehensive analysis of host cellular interactions with human papillomavirus E6 proteins identifies new E6 binding partners and reflects viral diversity. J. Virol. *86*, 13174–13186.

White, E.A., Sowa, M.E., Tan, M.J.A., Jeudy, S., Hayes, S.D., Santha, S., Munger, K., Harper, J.W., and Howley, P.M. (2012b). Systematic identification of interactions between host cell proteins and E7 oncoproteins from diverse human papillomaviruses. Proc. Natl. Acad. Sci. *109*, E260–E267.

Wilson, R., and Laimins, L. (2005a). Differentiation of HPV-containing cells using

organotypic “raft” culture or methylcellulose. Methods Mol. Med. *119*, 157–169.

Wilson, R., and Laimins, L.A. (2005b). Differentiation of HPV-containing cells using organotypic “raft” culture or methylcellulose. Methods Mol. Med. *119*, 157–169.

Wilson, R., Fehrmann, F., and Laimins, L.A. (2005). Role of the E1 E4 Protein in the Differentiation-Dependent Life Cycle of Human Papillomavirus Type 31. J. Virol. *79*, 6732–6740.

Wilson, R., Ryan, G.B., Knight, G.L., Laimins, L.A., and Roberts, S. (2007). The full-length E1E4 protein of human papillomavirus type 18 modulates differentiation-dependent viral DNA amplification and late gene expression. Virology *362*, 453–460.

Wong, W., and Scott, J.D. (2004). AKAP signalling complexes: focal points in space and time. Nat. Rev. Mol. Cell Biol. *5*, 959–970.

Woods, D., and Bryant, P. (1991). The discs-large tumor suppressor gene of Drosophila encodes a guanylate kinase homolog localized at septate junctions. Cell *66*, 451–464.

Woods, D.F., Hough, C., Peel, D., Callaini, G., and Bryant, P.J. (1996). Dlg protein is required for junction structure, cell polarity, and proliferation control in Drosophila epithelia. Dev. Biol. *134*, 1469–1482.

Xie, Q., Soutto, M., Xu, X., Zhang, Y., and Johnson, C.H. (2011). Bioluminiscence Resonance Energy Transfer (BRET) imaging in Plant Seedlings and Mammalian Cells. Methods Mol. Biol. *680*, 3–28.

Yang, Y., Mahaffey, C.L., Bérubé, N., and Frankel, W.N. (2006). Interaction between fidgetin and protein kinase A-anchoring protein AKAP95 is critical for palatogenesis in the mouse. J. Biol. Chem. *281*, 22352–22359.

Yeo-Teh, N.S.L., Ito, Y., and Jha, S. (2018). High-risk human papillomaviral oncogenes E6 and E7 target key cellular pathways to achieve oncogenesis. Int. J. Mol. Sci. *19*.

Yonemoto, W., Garrod, S.M., Bell, S.M., and Taylor, S.S. (1993). Identification of phosphorylation sites in the recombinant catalytic subunit of cAMP-dependent protein kinase. J. Biol. Chem. *268*, 18626–18632.

Yoon, C.S., Kim, K.D., Park, S.N., and Cheong, S.W. (2001). α 6 integrin is the main receptor of human papillomavirus type 16 VLP. Biochem. Biophys. Res. Commun. *283*, 668–673.

Yoshimatsu, Y., Nakahara, T., Tanaka, K., Inagawa, Y., Narisawa-Saito, M., Yugawa, T., Ohno, S.I., Fujita, M., Nakagama, H., and Kiyono, T. (2017). Roles of the PDZ-binding motif of HPV 16 E6 protein in oncogenic transformation of human cervical keratinocytes. Cancer Sci. *108*, 1303–1309.

You, J., Croyle, J.L., Nishimura, A., Ozato, K., and Howley, P.M. (2004). Interaction of the bovine papillomavirus E2 protein with Brd4 tethers the viral DNA to host mitotic chromosomes. Cell *117*, 349–360.

Yu, T., Peng, Y.-C., and Androphy, E.J. (2007). Mitotic Kinesin-Like Protein 2 Binds and Colocalizes with Papillomavirus E2 during Mitosis. J. Virol. *81*, 1736–1745.

Yuspa, S.H., Kilkenny, A.E., Steinert, P.M., and Roop, D.R. (1989). Expression of murine epidermal differentiation markers is tightly regulated by restricted extracellular calcium concentrations in vitro. J. Cell Biol. *109*, 1207–1217.

Zaccolo, M., and Pozzan, T. (2002). Discrete Microdomains with High Concentration of cAMP in Stimulated Rat Neonatal Cardiac Myocytes. Science (80-.). *295*, 1711–1715.

Zaccolo, M., Giorgi, F. De, Cho, C.Y., Feng, L., Knapp, T., Paul, A., Taylor, S.S., Tsien, R.Y., and Pozzan, T. (2000). A genetically encoded, fluorescent indicator for cyclic AMP in living cells. *2*, 25–29.

Zhang, B., Chen, W., and Roman, A. (2006). The E7 proteins of low- and high-risk human papillomaviruses share the ability to target the pRB family member p130 for degradation. Proc. Natl. Acad. Sci. U. S. A. *103*, 437–442.

Zhang, Y., Dasgupta, J., Ma, R.Z., Banks, L., Thomas, M., and Chen, X.S. (2007). Structures of a Human Papillomavirus (HPV) E6 Polypeptide Bound to MAGUK Proteins: Mechanisms of Targeting Tumor Suppressors by a High-Risk HPV Oncoprotein. J. Virol. *81*, 3618–3626.

Zhao, S., Yi, M., Yuan, Y., Zhuang, W., Zhang, D., Yu, X., Chen, X., Teng, B., Guan, Z., and Zhang, Y. (2015). Expression of AKAP95, Cx43, cyclinE1 and cyclinD1 in esophageal cancer and their association with the clinical and pathological parameters. Int. J. Clin. Exp. Med. *8*, 7324–7332.

Zhao, Z., Xia, J., Tastan, O., Singh, I., Kshirsagar, M., Carbonell, J., and Seetharaman, J.K. (2011). Virus interactions with human signal transduction pathways. Int. J. Comput. Biol. Drug Des. *4*, 83.

Zigman, M., Trinh, L., Fraser, S., and Moens, C. (2011). Zebrafish Neural Tube Morphogenesis Requires Scribble- Dependent Oriented Cell Divisions. Curr. Biol. *21*, 79–86.

Zimmermann, H., Degenkolbe, R., Bernard, H.U., and O'Connor, M.J. (1999). The human papillomavirus type 16 E6 oncoprotein can down-regulate p53 activity by targeting the transcriptional coactivator CBP/p300. J. Virol. *73*, 6209–6219.

Zippin, J.H., Farrell, J., Huron, D., Kamenetsky, M., Hess, K.C., Fischman, D.A., Levin, L.R., and Buck, J. (2004). Bicarbonate-responsive "soluble" adenylyl cyclase defines a nuclear cAMP microdomain. J. Cell Biol. *164*, 527–534.